University of Reading

Quantifying Responses to Abrupt Climate Change in the Andes, South America

PhD

Department of Geography and Environmental Science

School of Archaeology, Geography and Environmental Science

Daniel Lee Alexander Teeling

October 2022

Declaration

I confirm that this is my own work and that use of all material from other sources has been properly and fully acknowledged.

Daniel Lee Alexander Teeling.

Abstract

This thesis provides new palaeoenvironmental data from two basins in the Peruvian Andes, and helps the understanding of vegetational, environment, and land-use changes as well as human responses to abrupt climate changes through the Holocene. The basins in Antaycocha and Huarca provide a transect across the Andes region to better understand environmental responses in different climatic zones, as well as aid in the understanding of social responses in different regions across the Peruvian Andes. By using a multi-proxy approach to analysing the wetland archives (stable isotopes, *n*-alkanes, pXRF, Rock-Eval Pyrolysis), we can better understand how past societies responded to major periods of climate change, such as the Medieval Climate Anomaly (MCA) and the Little Ice Age (LIA); but also how the environment responded to periods of pre-historic change through the Holocene, such as at the mid-Holocene drought period and the pluvial phase thereafter. The results of these analyses have shown that pre-Columbian civilisations were able to adapt to the climatic conditions by constructing reservoirs, terraces, and completely changing their agricultural practices during times of abrupt change. This study has also demonstrated that the basins have the potential to undertake high-precision analysis of environmental change and have been able to detect large scale regional climate changes such as the MCA and LIA, but also the short-lived climatic changes such as that of El Niño. This study has also shown the potential of how Rock-Eval pyrolysis might be used in the future, to detect sources of old carbon within sequences. This will have huge impacts on the field of radiocarbon, if proved to be true, as this would enable the field to create more robust chronologies based on better selected age samples.

Acknowledgements

First and foremost, I'd like to thank my wife, Jess. Without you, your love and support I don't think I'd have managed to put myself forward for this degree, never mind finishing it. You have always been there for me, in my corner cheering me on when I need you the most.

To my supervisors, Dr. Stuart Black, Prof. Nick Branch and Dr. Chris Vane. Your guidance and support over the last 4 years has been brilliant. I can't thank you enough for answering all the inane questions I have come up with!

This research project was funded by the SCENARIO DTP and CASE sponsored by the British Geological Survey (BGS) and my thanks goes to them for allowing me to carry out this research.

Dr. Alex Herrera (Universidad de los Andes, Bogotá, Colombia) and Dr. Carlos Farfán (Universidad Nacional Federico Villareal, Lima, Peru) for aiding in the identification of suitable field sites, and for their invaluable knowledge of the local archaeological remains. Thank you also to Dr. Frank Meddens, Prof. Andrew Wade, Dr. Josie Handley (all University of Reading) and Douglas Walsh (Cusichaca S.A.C, Cusco, Peru), all for their help on fieldwork and their great company during the trip.

Radiocarbon dating in this project was supported by the NEIF Radiocarbon application (allocation number 2505.0422 – This project) (2339.0221 and 2196.1019 – Handley, 2022). The Rock-Eval and *n*-alkane extractions were obtained at the Organic Geochemistry department, British Geological Survey and special thanks go to Vicky Moss-Hayes and Alex Kim for their assistance in collecting and assisting with the data.

Finally, I'd like to thank all my family and friends that have stood by me over the last 4 years. To Mum, Dad, Sean, and Callum for always believing in me and sending your love and support throughout. To Lorna, Ian, Gina, Charlie, and Nick, all your help throughout the years and for keeping me going. To Josie, Row, Nerea, Becky for the many coffee chats which have kept me going throughout, even though I've been that "grumpy northern man" for the last 4 years.

Contents

List of Figures

List of Tables

1. Introduction

1.1 Introduction to Themes

This project provides new insights into the palaeoenvironment through the Holocene, from two regions of the Peruvian Andes and gives new information on human responses to climate changes over the last 2,500 years. The climatic history suggests that there have been several abrupt climatic events during the Holocene that have had profound influences upon the environment and, in the context of the cultural horizons, the human civilisations living within them. The cultural and archaeological histories suggest that the large empires of the Early Intermediate Period to the Late Horizon (418 to 2,150 cal yr BP) adapted to these abrupt climatic events by constructing highly innovative agricultural systems, irrigation networks, and reservoirs. Despite the wealth of knowledge from palaeoclimate records, there is still a paucity in knowledge pertaining to climatic changes and the resilience of pre-Columbian societies.

Figure 1.1: Photograph taken of modern agriculture systems at Huarca. Nevado Huascarán can be seen in the background.

There is a growing number of high-resolution records from the Central Andes (See Chapter 2 for more information), that cover the Holocene from lakes, speleothems, ice-cores and the tropical oceans (e.g., Thompson et al., 1992, 1995, 2013; Rein et al., 2004, 2005; Bird et al., 2011b, Kanner et al., 2013), but gaps in the knowledge remain. This becomes especially apparent when relating impacts of abrupt climate change to societal changes in the Late-

Holocene. Chronology is of the upmost importance when trying to relate the two together, there are a lot of older chronologies based on ceramic stratigraphy that are not robust enough and are too rigid, to compare any of the developments of the different cultures through the horizons; or the palaeoclimatic records that exist are not dated at a high enough resolution to ratify the short-lived events that have occurred across the cultural horizons. There are also knowledge gaps documenting changes in land-use patterns and vegetational changes, especially from areas that are proximal to sites of known human occupation. Palaeoenvironmental information from basins close to archaeological remains may provide a valuable insight into the sensitivity of the surrounding landscape and human occupations to periods of abrupt climate changes. Therefore, this study aims to use a multi-proxy analysis of intermontane wetlands, from sites proximal to known sites of occupation, to provide new high temporal resolution records of palaeoenvironmental change.

Even though the study aims to ratify abrupt climate changes across the Holocene, the focus is on the last 2,500 years of history. This is of huge significance for Peru, as it encompasses major societal developments such as that of the large empire states of the Wari (950-1,450 cal yr BP) and the Inca (418-512 cal yr BP), as well as smaller scale developmental stages where nucleated populations prevailed. There are also two major climatic events that occur during this period: the Medieval Climate Anomaly (MCA) and the Little Ice Age (LIA), allowing for the study of the timings of these events, socio-economic changes, land-use practices and responses to climate changes over these periods in each of the study sites.

1.2 Geographical Context

The Peruvian Andes were created due to the uplift caused from the subduction zone created between the Nasca and South American plates (Lau, 2016). The nature of the Andes themselves creates a set of vertical environmental zones, which can be travelled between over a short time period by gaining or decreasing altitude (Handley, 2022). Altitudinal location is key in determining the available resources in the Andes. Below 3000m asl, temperatures rarely drop below freezing, but above 4000m frosts can occur up to 25 days per month during the winter (Quilter, 2013). There are also varying temperature and precipitation gradients throughout each zonation and leads to a variety of settlements and production regimes (Handley, 2022).

The most productive of the zones are traditionally located on the western flanks of the Andes mountain range and consist of the *Yunga, Quechua* and *Suni*. The *Yunga* zone generally consists of the zone between 1000-3000m asl and is made up of forested slopes and riverine valleys. This zone is generally considered to be one of the most fertile zones for agriculture, as the precipitation and the climate combine to create almost perfect growing conditions for cultivars such as chilli, avocado, beans, and assorted fruits (Quilter, 2013).

The *Quechua* zone covers the area between 2500-3500m asl, which remains relatively frost free throughout the year. The zone receives the most precipitation throughout the year due to

its altitudinal range. Due to the precipitation and altitude the climate is generally mild and, as such, means that it agriculturally productive with a lot of growth of potato, mashua, maize, cotton, squashes and oca occurring in this zone (Quilter, 2013). Huarca sits within this environmental zone, meaning it is well placed to analyse past agricultural practices pertaining to the environment during the Holocene changes of this zone.

The last major ecological zone is the *Suni* zone which occupies the area between 3500-4000m asl, where there is still a low enough risk of frost that it is still low enough to permit crop farming (Swinton et al., 1999). Crop production is still limited to those that are frost and drought resistant, due to the lower precipitation at higher elevations, such as quinoa, some tuber species, and seed crops of barley, wheat and rye (Aguilar and Jacobsen, 2006). The basin of Antaycocha sits within this zone and as such, gives us insights into how humans may have interacted within this zone during the late-Holocene.

1.3 Site Selection

In order to meet the aims and objectives, set out below, the study sites of Huarca and Antaycocha were chosen (see fig 1.2). As mentioned previously both sites sit within different climatic zones in the Andes and allow for comparisons of socio-economic impacts pertaining to a varied environmental zonation. Within the chosen valleys each basin was chosen due to

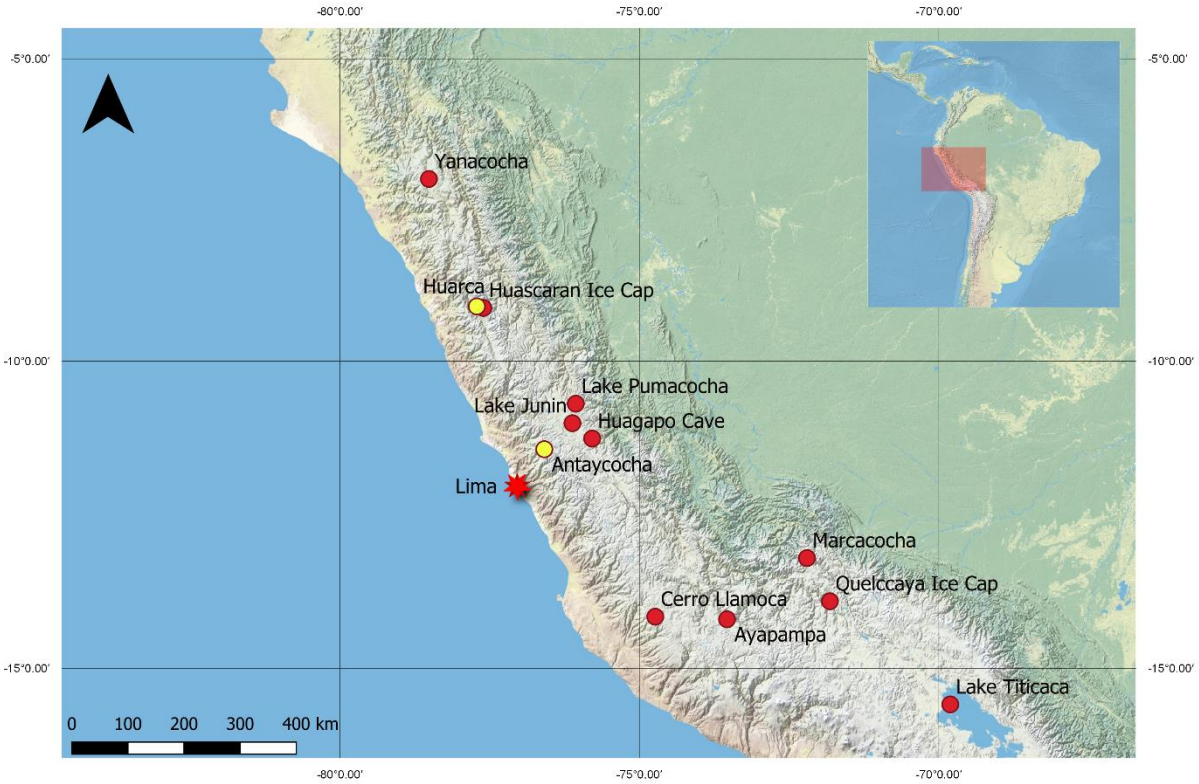

Figure 1.2: Map of Peru containing the study sites (in Yellow) along with other sites within the wider literature (Red). Map created in QGIS 3.10 with the ESRI standard TMS plugins

it being known that there was known to be an active agricultural practise nearby and that there was some archaeological remains nearby also. This too allowed for comparisons of human

interferences in the basins and allowed studies into environmental changes and the impacts they have had on human societies living in close proximity. Details of each specific site can be found in the site chapters.

1.4 Aims and Objectives

Aim:

1. Reconstruct the impact of prehistoric and historic agro-pastoral land-use and climate change on the environment of the Peruvian Andes.

Objectives and Research Questions:

1. To determine the relationship between cultural change and agro-pastoral land-use in the Peruvian Andes during the Late Holocene.
    a. What do the new (this study) and published palaeoenvironmental records tell us about agro-pastoral land-use change?
    b. Is there a relationship between cultural change and agro-pastoral land-use change?
    c. Did past climate change drive any of the agro-pastoral land-use changes observed?
2. To determine the relationship between climate change and environmental change in the Peruvian Andes during the Late Holocene.
    a. What do the new (this study) and published palaeoenvironmental records tell us about environmental change?
3. To undertake organic geochemical analyses of all core materials to provide information on depositional processes and detailed sedimentological record.
    a. Can the *n*-alkane data identify dietary information, by way of identifying chains of key cultivars (e.g. Zea Mays, Chenopodium quinoa, Oxalis tuberosa, Solanum tuberosum)?
4. Evaluate the application of RockEval data for radiocarbon dating of palaeoenvironmental records.
5. Evaluate the application of trace elemental data to quantify sources of sediment input.
    a. What are the timings of arid events, which lead to periods of greater sediment accumulation and what can this tell us about land-use changes?
6. To construct robust chronologies, for each of the identified field sites.
    a. What are the timings of climatic and environmental changes, in relation to the cultural horizons and do they alter the current narrative?

b. How can all the new records (from this project) be combined temporally, and how do they fit in with established palaeo-records?

1.5 Structure of Thesis

The thesis is split into 7 chapters. The first, sets out the rationale for the study, the research aim and research questions that it hopes to address. **Chapter 2** is a critique of the literature, which outlines the climatic context of South America and Peru in more detail. It also details the archaeological context of Peru, with the need for more chronological testing of the archaeological remains and outlines the requirement for more palaeoenvironmental studies from intermontane basins and more robust chronologies that span the late Holocene in general. **Chapter 3** outlines the methodologies used in this project. **Chapter 4** and **Chapter 5** focus on the study areas in this project and are presented each with their own introductions, site specific methods, results and interpretations. **Chapter 6** discusses the findings of the study and ties the work together, with **Chapter 7** concluding the findings and recommending future work.

2. Literature Review

2.1 Introduction

During the Holocene, there has been global-scale climatic variability which have induced complex environmental responses in the central Andes, with clear evidence supporting these changes (Jansen et al., 2007; Bird et al., 2011b). These climatic events have all, in some way, led to short-lived oscillations in temperature, precipitation and circulation regimes (Jansen et al., 2007; Bird et al., 2011a). The central Andes region is characterised by several climatic parameters, of varying gradients, making it very sensitive to short-term climatic events (Schittek et al., 2015). As a result, there are many local microclimates and environments, that have all varied differently, resulting in significant responses in the zonation and type of vegetation, land-use, geomorphology as well as other system changes (Grosjean et al., 2001; Garreaud, Vuille and Clement, 2003; Grosjean and Veit, 2005).

There have been several studies, that have significantly impacted our understanding of South American climate change and the mechanisms behind these changes (Hansen, Wright and Bradbury, 1984; Hansen, Seltzer and Wright, 1994; Ekdahl et al., 2008; Garreaud et al., 2009; Bird et al., 2011b; 2011a). However, there are still several parameters that are poorly defined or those that are not yet fully understood, despite the considerable efforts to resolve them (Grosjean, 2001; Schittek et al., 2015).

Of particular interest are the series of oscillations between humid/dry phases, which have appeared markedly throughout the Holocene (van Breukelen et al., 2008; Fornace et al., 2014). These changes often affect the resolution at which these short-term climatic events can be defined (Schittek et al., 2015). Detailed knowledge of the spread, magnitude and timings of these events, in the Central Andes, are severely lacking regarding how they relate to the climatic regimes for the rest of the Southern Hemisphere (Haug et al., 2001; Baker et al., 2005). The drivers of these changes have been described in relation to the El Niño Southern Oscillation (ENSO), and the Intertropical Convergence Zone (ITCZ).

2.2 Modern and Past Climate Drivers Affecting Peru

2.2.1 El Niño Southern Oscillation

The Pacific coast of northern Peru is a key area of ENSO activity (Sandweiss et al., 2001), which are seen to be recurrent in many long-term proxy records. These proxies resolve the variable nature of ENSO; however, some have been limited to short records of change (Thompson, Mosley-Thompson and Thompson, 1992; Apaéstegui et al., 2018) or have been undertaken at a very coarse resolution (Sandweiss et al., 1996, Tudhope et al., 2001). There are a variety of records to suggest that the current climatic conditions, of Peru, did not form until ~3.2 ka (Veit, 1996; Marchant, Hebbeln and Wefer, 1999; Sandweiss et al., 2001; Moreno et al., 2007). There were some marked periods of lake level rise, from Peru and Northern

Chile, which all show a similar trend – rising rapidly at ~3.5 ka approaching modern levels by ~2.9 ka (Abbott et al., 1997; Cross et al., 2000; Rowe et al., 2003; Moreno et al., 2007).

ENSO itself is made up of two parts, El Niño and La Niña. Both of these systems denote sea-surface temperature (SST) conditions in the tropical Pacific Ocean (Cai et al., 2020). El Niño was first described by Peruvian fisherman in the 19th Century, who described a pattern of warmer ocean conditions, around Christmas time, which would disrupt the local fishing communities and bring in torrential rain patterns along the, usually arid, coastal regions of Peru and Ecuador (Cai et al 2020). The effects of ENSO can be observed across the entire South American continent, with regional variations in strength and pattern (Grimm et al. 2000, 2002).

Under non-El Niño conditions, the upwelling of cold currents interacts with the sea air, causing more rain over the highlands. During El Niño years, the temperature gradients between the sea and the coast are closer together and results in an increase in coastal precipitation – leading to large-scale flooding events (Garreaud et al., 2003). The opposite is true for La Niña years, which sees very dry conditions on the coast and higher precipitation in the highlands. SSTs during this cycle are colder than normal in the Eastern Pacific (Maasch, 2008). However, dry La Niña years and wet El Niño years are not entirely uncommon occurrences, which means the relationships between SST and precipitation in the Central Andes, is not as simple as it sounds (Garreaud et al., 2003).

The large-scale teleconnections throughout South America (and indeed the Central Andes) mean that the dynamics of the SASM are greatly affected by changes in ENSO conditions, however the decadal and centennial variations in the systems are still not fully understood (Henke *et al.,* 2017). It is a possibility that, due to its proximity to the Pacific coast, that one of the study sites Antaycocha may have experienced more ENSO influence than the other site at Huarca. This may also be due, in part, to it's positioning on the western flank of the Andes. Recent studies have identified that precipitation, on this position in the Andes, is primarlily sourced from the Pacific Ocean – which may also have been true of the past (Aron, 2021; Handley, 2022).

2.2.2 South American Summer Monsoon (SASM)

The SASM was only first discussed by Lau and Zhou (1998), but since then there have been further discussions that have made significant progress in understanding the dynamics and variability of the SASM (Raia and Cavalcanti, 2008; Vuille *et al.,* 2012). The SASM has some cyclicity, with a distinct start in October (maturing between DJF) and then declining by April. The precipitation in the Peruvian Andes is sourced from deep within the Amazon basin, and ultimately the tropical Atlantic Ocean, and is carried by the prevailing easterly trade winds during the austral summer (Kanner *et al.* 2013). It is during this time that the Peruvian Andes receives the most amount of precipitation, due to this westerly moisture transport, with ~60% of the mean average rainfall occurring between the rainy season from December to March (Garreaud *et al.,* 2003; Kanner *et al.,* 2013). Over the modern period, the SASM system is

affected by other modes of variability chief of which is ENSO. There are other smaller systems that relate to the SASM variability which include Pacific Decadal Oscillation (PDO), tropical Atlantic variations, colder air from mid-latitudes and Atlantic Multidecadal Oscillation (AMO) (Vuille *et al.,* 2012). Garreaud *et al.,* 2009 writes that the effect on ENSO, on the SASM, varies throughout the year, but generally the El Niño years tend to be drier than normal conditions with La Niña years essentially the reverse.

Little is known about how the SASM varied in the past, but to some extent there is some confusion in the literature relating to the relationship between the SASM and ITCZ (Vuille *et al.,* 2012). However, there are some good correspondences between the different proxy records in the late-Holocene; despite this the regional-scale and sub-orbital fluctuations over the last 2000 years are not well established (Kanner *et al.,* 2013). Of a particular note, are the forces on the SASM variability on sub-orbital timescales throughout the Holocene which have not been fully explained. Climate variations originating in the North Atlantic can partially explain the centennial-scale fluctuations over the last 2000 years (Vuille *et al.,* 2012, Kanner *et al.,* 2013). As mentioned above one of the major drivers behind the SASM is ENSO, some of its influences have can be observed within some proxy data amongst interannual isotope reconstructions (e.g. Vuille and Werner, 2005) and Andean ice cap accumulation records (e.g. Bradley *et al.,* 2003). With this, where there are some high resolution records it could be possible to detect El Niño and La Niña cycles outside of the last 2000 years, and thus relating them to variability in the SASM.

2.2.3 Intertropical Convergence Zone

The ITCZ is zone that appears near to the equator where the northeastern and southeastern trade winds converge with one another, providing a vast area of convective storms. The iTCZ itself is not a stationary and moves throughout the year to where the surface areas are the warmest. The austral summer is a time, in the Southern hemisphere, that is where the solar radiation is the strongest (Maasch, 2008). Therefore, this then creates a southern displacement of the ITCZ, which coincides with the timing of South American Summer Monsoon (SASM); in turn bringing an increased amount of precipitation into the Southern hemisphere and indeed the Peruvian Andes – with the more intense rainfall resulting from a more southern position of the ITCZ (figure 2.2) (Vuille *et al.,* 2012). The opposite conditions are true during the austral winter, as the ITCZ moves further north bringing areas of high pressure resulting in dry conditions across Peru (Maasch, 2008) (figure 2.2). These drier conditions according to Moreno et al. (2007), were not a constant occurrence but rather a series of short-lived oscillations. The dry spells were interceded by other wetter periods, which have been noted in sediment records across the Andes (Grosjean et al., 2001; Schittek et al., 2015). Therefore, the ITCZ is mostly recognised as the main driver behind the seasonality changes throughout Peru, with the resulting winter-summer switch regarded to be most like

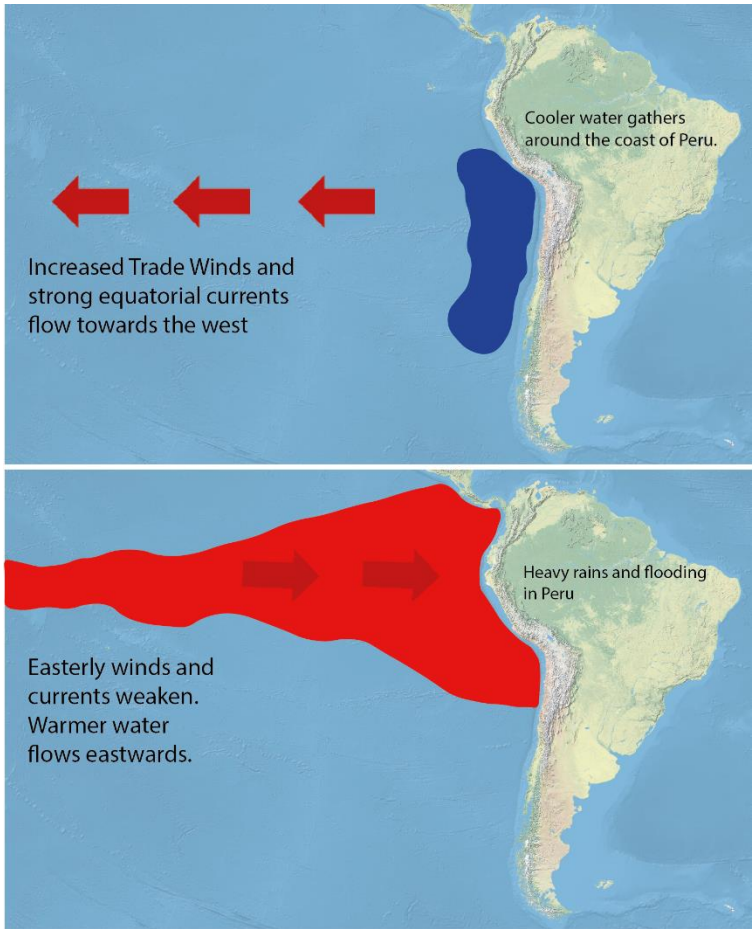

Figure 2.1: Basic map of ENSO conditions for South America, during "normal" conditions (top) and during an El Nino year (bottom)

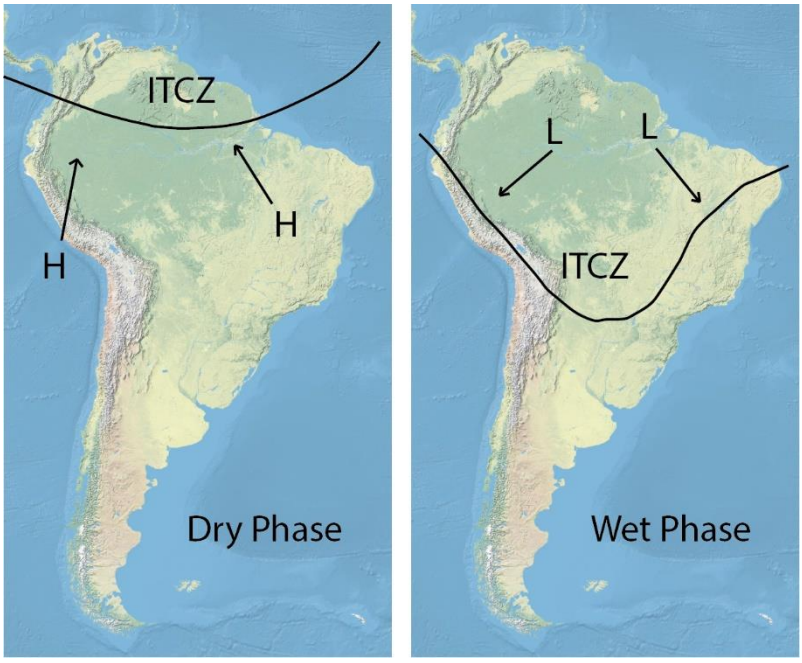

Figure 2.2: Positional changes of the ITCZ, over South America, during Dry and Wet phases. Base map taken from ESRI plugin used in QGIS 3.10

monsoon conditions due to the extreme weather conditions that it causes (Garreaud *et al.,* 2009).

Nonetheless, the proxy records that are available for the mid to late-Holocene are generally sparse and are not a fully continuous indicator of change in the Central Andes (Holmgren and Scheffer, 2001; Kuentz, Ledru and Thouret, 2012; Schittek et al., 2015). The methods, and the amount of sediment examined, has meant that there are discrepancies in the timing, magnitude, and interpretation of key indicators of change. It is concerning that many Andean records do not indicate any centennial to millennial scale variability needed to make comparisons to global/regional proxy records (Lamy et al., 2001; Cardozo et al., 2014).

2.4 Culture, chronology, and climate impacts on Andean civilisations

Chronology is a high priority for paleoenvironmental and archaeological investigations. This has been the main issue when reconstructing the history of the South America since the inception of studies into historical civilisations. During the early 20th Century, the main ways to track cultural shifts, was to look at the stratigraphy of ceramic materials from the Inca and work back in time (Unkel et al., 2012). It wasn't until the work of Willard Libby, who determined the use of high energy radiation in the upper atmosphere (Libby, 1955), that archaeologists could advance their field with the use of radiocarbon dating. Radiocarbon dating is not without its flaws, however, there are reversals and plateaus within the radiocarbon calibration curve that are a recognised challenge for dating palaeoenvironmental and archaeological sequences alike. A given set of ^{14}C values, that are calibrated along one of these plateaus will produce calendar ages with probabilities spread across over a long period(s) irrespective of the accuracy of the method or the measurement (Manning et al., 2020). This poses difficulties for resolving short-lived periods of time, such as the Andean cultural horizons – some of which are only a few hundred years in length (See table 2.1). One of these plateaus occurs ~900-800 cal yr BP (see figure 2.3), which occurs around the time of the Medieval Climate Anomaly (MCA) making any ^{14}C age probability occur over a multitude of possible different dates. Another well resolved issue, is a radiocarbon reversal and plateau that occurs during 320-470 cal yr BP (see Taylor, Stuiver and Reimer, 1996 and Manning et al., 2020). This is of particular interest to this study as it coincides with the expansion of the Inca empire and the arrival of the first Europeans to Peru.

With the ever-increasing number of archaeological finds, the older chronologies built in the 1960's are not of a high enough resolution, to compare the developments of different cultures throughout South America (Unkel et al., 2012). This is more apparent when further investigations into the Moche culture of Northern Peru (Chapdelaine, 2011), and the origins of the societies on the central coast of Peru, are carried out (Solis, Haas and Creamer, 2001).

Another example of this lies within the Ayacucho Valley, Peru, and its current chronology of Wari occupation. The original ceramic stratigraphy would suggest that the disappearance of Wari style ceramics occurs around 1000AD and that there was no trace of settlements after

this time. ^{14}C dating of funerary remains by Finucane et al. (2007) would suggest that this is an inflexible view and needs to be reworked. Their research suggests that state authority persisted within the valley until the mid-11th century. Secondly, despite the decline of the Wari state the settlements around the valley continued to persist and create ceramic styles like that of the Wari culture. The findings emphasise that the era of stylistic unity pertaining to the MH persisted well after the collapse of the Wari polity and that the extent and timings of the Wari's political regime cannot be inferred from presence or absence of ceramics (Finucane et al., 2007). Similar studies and findings are increasing with the extension of radiocarbon methodologies. Radiocarbon chronologies from the Callejon de Huaylas (Lau, 2004), Palpa valley (Unkel et al., 2012), and Ica valley (Cadwaller et al., 2018) amongst others are evidence that the original ceramic regimes are too rigid and the preferred method of evaluating cultural decline should be by building a robust chronology based on ^{14}C dates.

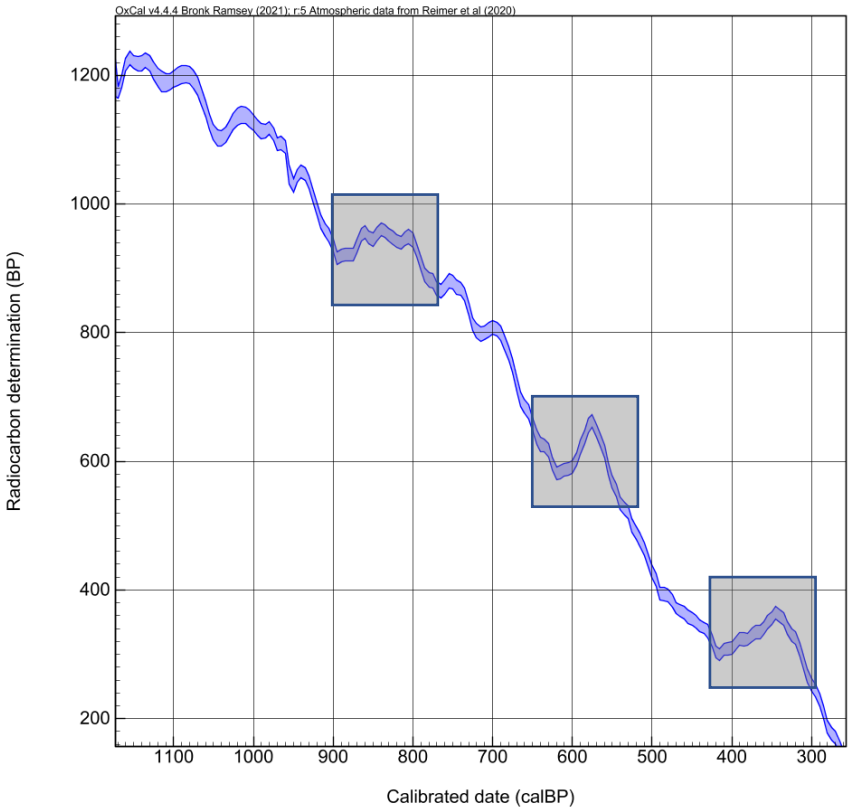

Figure 2.3: An excerpt of the IntCal20 radiocarbon curve (Reimer et al., 2020) of the last 1,100 cal yr BP. 3 major plateaus and reversals in the curve are highlights in grey, these 3 occur within the cultural horizons this study aims to ratify.

The Holocene has been a time of population expansion, with occupation of the Peruvian coast, dating back more than 5 ka (Schittek et al., 2015), and the Peruvian Amazon has been occupied for, at least, the last 11,000 years (Roosevelt et al., 1996; Bush, Silman and Listopad, 2007). The exact scale of human occupation and land-use change is still debated in the literature, with dividing opinions as to how and when these occurred. By the time Europeans encountered South American civilisations, there were an estimated 5–10 million indigenous peoples (Denevan, 1976). There is, however, a good summary of the main

archaeological subdivisions from Peru in Unkel et al. (2012) and Schittek et al. (2015) which are outlined in the below sub-sections.

Table 2.1: Andean Cultural timeline, with approximate chronology and major developments. Adapted from Kemp et al., 2006

Cultural Horizon	Approximate Chronology (BC/AD)	Major developments during horizon
Republic	1826 AD - Present	After many years of struggle, during the early stages of the 19th Century, Peru gains their independence from Spain.
Colonial Period	1532 – 1826 AD	Invasion of the Conquistadors into the Andes region and decline of the existing cultures throughout much of South America.
Late Horizon	1438 – 1532 AD	Expansion of Inca empire throughout much of South America. Able to expand quickly due to already existing framework of roads and agricultural systems from previous empire states.
Late Intermediate Period	1100 – 1438 AD	Decline of major civilisations leads to population decline and nucleation of existing communities.
Middle Horizon	500 – 1100 AD	Inception linked to long term drought. Known mainly for the Wari and Tiwanaku Empires. Expansion of the Wari leads to the wide-spread use of agricultural terrace systems.
Early Intermediate Period	200 BC – 500 AD	Rise of Nasca. Major advancements in agricultural practises, social structures, ceramic and textile manufacture. Populations start to spread onto the valley floors, rather than on mountain slopes.
Early Horizon	800 - 200 BC	Rise of Paracas culture in the coastal regions. Intense immigration into the Western Cordillera leads to increased human activity and camelid herding.

2.4.1 The Early Horizon 800-200 BC

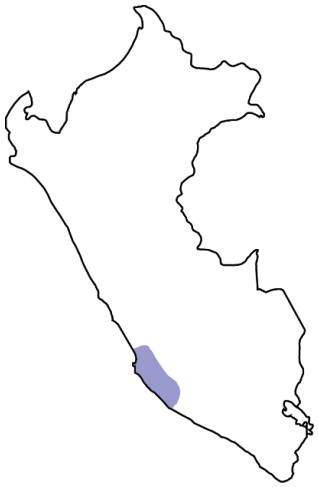

Figure 2.4: Territory of the Paracas culture, during the Early Horizon. Adapted from van Gijsegham et al (2006)

Running from 800 - 200 BC (See Table 2.1), the Early Horizon is known for the rise of the Paracas culture on the south coast of Peru. This culture was first described by Tello (1959), through the subdivision of burial tradition of the Paracas Peninsula (van Gijseghem, 2006). It is estimated by ~400 BC that a considerable amount of immigration, alongside camelid herding and experience of highland farming, led to an increase of human activity on the slopes of the Western Cordillera of Peru (Sossna, 2014). It was during this time that the Paracas were creating sophisticated fabrics of woven cotton. The increased importance of Chavín de Huantar, at this time, may have been related to the demise of other early Horizon ceremonial sites on the coast. Caballo Muerto, Haldas and Garagay all preceded the zenith of Chavín, but had declined by the 4th Century BC (Burger, 1981).

The initial Nasca period (Schittek et al., 2015) runs from 260 BC - AD 80. Settlement in the Southern Nasca Region (SNR) started with the Paracas as a part of important migratory movement (van Gijseghem, 2006; Vaughn and van Gijseghem, 2007). This shift in population appears to occur at a time where the Paracas, in the Ica valley, underwent population nucleation (Vaughn and van Gijseghem, 2007). The origin of the Nasca people occurred quite rapidly, a theory upheld by the literature, suggesting the potential for rapid social innovation (Parker and Rodseth, 2005; Unkel et al., 2007; Sossna, 2014); leading to the dissolution of the Paracas culture, and the start of the Nasca.

2.4.2 The Early Intermediate Period 200BC – 500AD

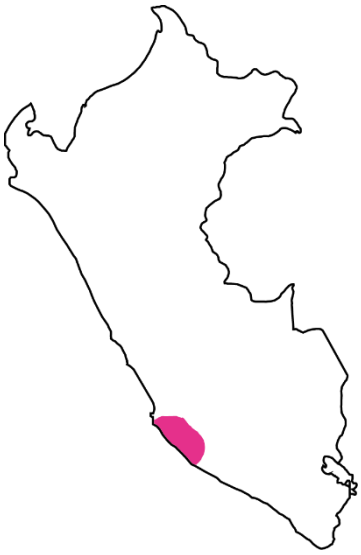

Figure 2.5: Extent of the Nasca culture, during the Early Horizon to the Early Intermediate Period. Adapted from Proulx (2008).

The Early Intermediate Period (200 BC –500AD) followed on and is divided into a further 3 sub-periods: early, middle and late Nasca. The culture and way of life changed during this time, with advances in agriculture, social structure and manufacture of textiles and ceramics (van Gijseghem, 2006). This reconstruction of civilisation also meant a contrast to previous ones, whereby the new settlements evolved and spread into the valley floodplains rather than on the slopes of the mountains (van Gijseghem, 2006; Vaughn and van Gijseghem, 2007; Schittek et al., 2015). The peak of this civilisation came ~AD 200 with the founding of Cahuachi, located towards the south coast of Peru, an important centre of ceremony and pilgrimage (Silverman, 1994), which was later abandoned a century later (Schittek et al., 2015). Due to the population shift into the valley systems, the population fell into decline, towards the end of the middle Nasca Phase and continued to the late Nasca Phase (300 – AD 640) (Unkel et al., 2007; Schittek et al., 2015).

2.4.3 The Middle Horizon 500-1100 AD

The inception of the Middle Horizon (~AD 500-1100) has been linked to a long-term drought event from AD 562-594, with precipitation levels around 20-30% less than normal (Shimada et al., 1991). This period is characterised by the two principal states of the Wari and Tiwanaku. The expansion of the Wari led to the introduction of terraced agriculture in the highlands (Williams, 2002). Although terraced structures had been utilised during the early Horizon, it was the Wari expansion that led to the systems introduction into the higher elevations. Where the more southerly Tiwanaku province, still cultivated crops in the middle valley plains.

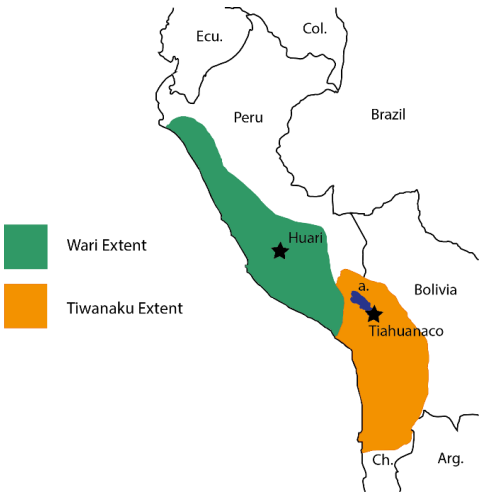

Figure 2.6: Extent of Wari and Tiwanku cultures, during the Middle Horizon, with centres of both civilisations marked. Adapted from Isbell (2008). a. denotes Lake Titicaca – which spans the border of Peru and Bolivia.

The authority of the Tiwanaku began to decline circa AD 1000 and has been attributed to a variety of factors including: drought (Weiss, 2016), internal factionalism (Janusek, 2008), and socio-economic fragmentation and destabilisation during the end of the Middle Horizon (Sutter and Sharratt, 2010). There is evidence of significant drought, towards the end of the Middle Horizon, inferred from the Quelccaya Ice core data and Lake Titicaca sediment record (Thompson *et al*, 1988; Binford *et al.,* 1997). Both records independently track major reductions in precipitation after AD 1100, with a drop in lake levels also observed (Abbott *et al.,* 1997; Weide *et al.*, 2017). This would have caused the shores of the lake to recede, effectively stranding large areas of agricultural systems and rendering irrigation systems inoperable (Thompson, Kolata and Weiss, 2017). The Quelccaya dust particulate record indicates that the maximum period of drought, in the Middle Horizon, persisted into the thirteenth and fourteenth centuries (Thompson and Kolata, 2017).

2.4.4 The Late Intermediate Period 1100 – 1438AD

During the Late Intermediate Period (AD 1100 - 1438), the central Andes region experienced the decline and rise of imperial polities. The decline of the Wari and the Tiwanaku and the end of their influence meant a further nucleation of communities around the Central Andes, with evidence of expansion later; after a depopulation ~AD 1000 (Schreiber, 1987; Covey, 2008). The only civilisations are merely fragments of the Early Intermediate Period, located around Cusco – a precursor to the later Inca state (Covey, 2008).

Figure 2.7: Extent of the Inca Empire during the late Horizon. Adapted from Covey (2008).

2.4.5 The Late Horizon 1438-1532AD

The Inca Empire of the Late Horizon (AD 1438 - 1532) conquered the entire Andean region from Chile to Ecuador (Schreiber, 1987; Covey, 2008). Menzel (1959), was one of the first to evaluate the Inca control based on the archaeological context of the study sites, identified that there were differences within the Inca imperial control, based on the existence of different local politics. The Inca flourished because of already existing construction of roads and administrative centres, left by the Wari and Tiwanaku (Menzel, 1959; Schreiber, 1987; Covey, 2008). The first frameworks of expansion, from Cusco, were developed by Rowe (1944), but are dramatically outdated. A chronology based on the work of Ogburn (2012), provides a more accurate dating method of the Inca Empire – although the use of radiocarbon dates may not provide a high resolution to include the short span of the Inca Empire.

2.5 Existing records in the Central Andes

There are a substantial number of records from the Central Andes region, which have had an array of different proxy analysis performed on them in order to further the knowledge of the climate and environmental shifts that occur in this region. The main proxy analysis, for these records, can be found below.

2.5.1 Speleothems

Speleothems represent a significant series of terrestrial based records and faithfully record climatic and environmental conditions from precipitation and temperature. They provide high-resolution geochemical data (for example $\delta^{18}O_c$, $\delta^{13}C_c$) that can be accurately dating using uranium-series dating methods. The oxygen isotope content of the speleothems is controlled by several factors which include latitude, altitude, and air temperature (McDermott, 2004). The interpretation of $\delta^{18}O_c$ largely depends on the assumption that the carbonates have precipitated in equilibrium with cave drip-water throughout the study period (McDermott, 2004). Whereas the carbon isotope composition of speleothems is controlled by the $\delta^{13}C_c$ of the soil, temperature, and in closed systems, the dissolution of bedrock carbonates. The $\delta^{13}C$ of modern soil CO_2, is mainly controlled by the varying proportions of the vegetative mixing of C_3 and C_4 plants and, thus, large deflections in $\delta^{13}C$ have been attributed to major vegetation changes. There are some cases, however, where degassing of CO_2 from groundwater and precipitation of vadose zone carbonates may lead to erroneous $\delta^{13}C$ values.

Well preserved speleothems can be accurately dating using uranium-thorium series (U-Th) dating in time ranging from a few hundred years to ~650,000. U-Th dating is based upon the ratios of the three nuclides in the ^{238}U decay chain: ^{238}U, ^{234}U, and ^{230}Th (Wendt et al., 2021). The carbonates precipitated from natural springs have a good amount of U, but little Th. It is through time that the decay of the parent isotope that the amount of ^{230}Th increases.

Major breakthroughs in the techniques used for U-Th analysis (e.g., Cheng et al., 2013) have increased the level at which the U-Th atoms can be detected at; samples that are of a few hundred years old can now be dated accurately, within one year (Wendt et al., 2021). With good deposition and preservation, speleothems deposited 10,000 years ago can be dated with an accuracy of ±10 years (with 2σ error) (Wendt et al., 2021).

Speleothems can be found across the Andes, as there us a vast abundance of carbonate rock and evaporite systems (Deininger et al., 2019). The distribution of these records, used in chapter 2.6, can be found in figure 2.8. These studies typically focus on monsoon variability and have revealed insight into the sensitivity of the SASM to insolation forcing (Wang et al., 2007; van Breukelen et al., 2008), abrupt changes in North Atlantic Climate (Wang et al., 2004) and it's relationship with monsoonal activity in the Northern Hemisphere (Wang *et al.,* 2006, Vuille *et al.,* 2012). The shorter records, that span the Holocene, tend to focus on these factors more – as SASM variability is short-lived which these shorter records can define more readily. The Huagapo, Cascayunga, and Palestina cave (all Peru) speleothems, all define these rapid

changes in precipitation and SASM activity well, due to the shorter time-scales they present. Other spelethems, such as Cueva Del Diamante and El Condor (Peru) can reveal insights into Heinrich event, Dansgaard-Oeschger cycles, and other large-scale climatic anomalies, as they are placed on the eastern flank of the Andes where tropical Atlantic moisture is transported, by the monsoon systems, across this portion of the mountains and away from any glacial activity which would hamper the growth of the speleothem.

2.5.2 Lacustrine systems

Environmental information in lacustrine systems is often interpreted as 1) physical 2) biological and 3) chemical and are used to infer changes in past environmental and ecological conditions. Physical properties are often descriptive in nature and are often used for colour, texture, density, magnetism, and particle size analyses (Bell and Blais, 2021). They are rarely used on their own and are best used in multi-proxy analysis (Mills et al., 2017). Biological assemblages are used to make inferences about past species diversity, temperature, moisture, fire frequency, pH, nutrient status, dissolved oxygen and ion concentrations (Mills et al., 2017; Bell and Blais, 2021). Examples of biological indicators include pollen, NPPs, charcoal, plant and animal remains. Many of the biological organisms used have a tolerance range of conditions related to their growth and population maintenance. The relative abundance of these proxies can serve as measures for past changes of conditions that have influenced the population of the organism (Bell and Blais, 2021). The final group are the chemical proxies, which is a large group that includes the use of metals (e.g., Al, Fe, Ti etc.), non-metals (e.g., P, S, N, O, H, C etc.), stable isotopes ($\delta^{13}C$, $\delta^{15}N$, $\delta^{34}S$ etc.) as well as range of molecular compounds and lipids (Bell and Blais, 2021). Chemical proxies have been used to infer a range of different environmental changes, for example metal compounds can be used to track human induced changes from mining and pollution (Rodbell et al, 2014). Macro-nutrient changes can be linked with biological contributions from plant, animal and human life (Mills et al., 2017). Biomarkers are usually organic compounds from biological, anthropogenic, or environmental sources. The chemical proxies can all be used in conjunction with one another, or with a range of other proxies, to infer past climate, pre-human disturbances, and anthropogenic disturbances on their lived environments (Bell and Blais, 2021).

Lacustrine records are lacking, in the Central Andes, and studying palaeolimnology in this region is difficult at best. There are few records that are of a continuous nature as many lakes in the tropics are ephemeral, those lakes that are long records often have a slow sedimentation rate; which makes it difficult to study any rapid changes in climate. The latter is certainly ture of the larger lake systems of Yanacocha, Junín and Titicaca (in Peru) (Fritz et al*.,* 2007; Stansell et al*.,* 2015; Woods et al., 2020) as well as the Laguna La Gaiba sequence in Bolivia (Whitney et al., 2011). These records make for excellent reconstruction of climate changes on timescales deep into the Pleistocene but aren't at a fine enough resolution to study short lived oscillations or make for good comparisons to human induced change. The smaller montane basins, that are accessible, are sensitive recorders of global change, in part due to their

remoteness (Catalan et al, 2013b). But climate also directly influences mountain lake structure and function by exerting controls on water temperature, hydrology and aquatic life (Moser et al., 2019). There are also indirect responses to climate changes that are expressed moreso in montane basins. For example, landscape change through loss of upstream glaciers and snow and shifts in the vegetation type and cover (Adrian et al., 2009; Harsch et al., 2009). Lake Pumacocha is one of these montane basins. It's a small lake situated within a glacial cirque, with precipitation mainly driven by the SASM. It's positioning on the western flank of the Andes may also make this basin sensitive to rapid ENSO events (Bird et al, 2011).

2.5.3 Marine Records

A number of deep-sea cores have been recovered from the Pacific and Atlantic oceans and provide a good record of Late-Holocene sedimentation in pelagic and hemipelagic settings. These records often provide a long continuous record, but temporal resolution is often limited due to slow sedimentation rates of 2-5cm/kyr. There are some areas where sedimentation rate can reach 2m/kyr, but this is usually where turbidites feature as a significant element of the sedimentary regime (Reeder et al., 2002).

A range of palaeoceanographic proxies have been applied to these cores which reveal information about sea-surface temperatures (SSTs), sea-surface salinity (SSS), ENSO events, and continental run-off. At Peru, precipitation run-off erodes fine-grained lithic material from the continental soils, which are flushed into the oceans via rivers and are then dispersed over hundreds of kilometres along the shelf by the northward flowing Peruvian currents (Rein et al, 2004). During strong El Niño periods, there is an increased volume of precipitation along the coastal regions of Peru and so the proxies for ENSO can be derived from key peaks in lithic concentrations from marine cores taken from the shelf sediments (Rein, 2004; 2005).

There is also a paucity of historical marine data coverage that has made it difficult to assess magnitude and patterns of natural and anthropogenic temperature change. Palaeoclimate proxy records from reef-building corals have extended the coverage of the limited instrumental data, providing improved constraints of the internal and external factors of climate variability on tropical and sub-tropical oceans (Thompson, 2021). The changes in the corals growth and geochemistry reflect the oceanic conditions at the time of growth. A few factors make reef corals an important archive of past ocean variability:

1) A high-resolution record of variability as corals have a relatively rapid growth rate (~0.3-2cm/y, Thompson, 2021), combined with fine scale milling techniques to permit analysis to even sub-annual reconstruction.
2) Annual density banding (Knutson et al., 1972) in combination with current radiometric dating methods allows for robust chronologies, with small uncertainties, to allow for short lived events to be well-resolved.
3) Modern and fossil corals samples are well preserved in time and fill a critical gap in the spatial and temporal coverage of climate information for the tropical and sub-tropical regions of the globe (Lough, 2010; Thompson, 2021).

There is a wealth of geochemical reconstructions based on coral growth from the Galapagos Islands, Ecuador (e.g., McConnaughey, 1989; Dunbar et al., 1994; Jiminez et al., 2018; Reed et al., 2021), but no records exist that span the entirety of the 20th Century (Reed et al., 2021). Several of the Galapagos coral records end during the 1982-83 El Niño event (Dunbar et al., 1994), which caused wide-spread mortality across the regions corals which limits the temporal resolution of SST reconstructions with satellite data (Reed et al., 2021).

2.5.4 Tropical ice-core records

As has previously been stated there is a scarcity of continuous long-term climatic records for the Andes. Such histories may be reconstructed from high-elevation tropical ice caps, as they continuously record the chemical and physical properties of the Earth's atmosphere (Thompson, 2000). Cores extracted from these areas can often provide palaeoclimate data that is at a decadal or an annual resolution, making them excellent repositories of continuous change. Andean ice cores are especially unique as a palaeoclimatic archive which is mainly related to their geographic setting and some of their physical properties (Vimeux et al., 2009). Ice cores also provide a unique set of proxy information (water isotopes, dust accumulation, net accumulation, ions, trace elements etc.) which are useful additions to other sources of palaeoclimatic data for interregional comparisons for South America; this is provided that the record sensitivity is understood (Vimeux et al., 2009).

Despite their potential for use as long term indicators of palaeoclimatic change there are some important limitations to their usage. Andean ice-cores have shown to have a high accumulation rate, with the last millennia usually the major part of the ice-core. For example, the last 1000 years is expressed in roughly the top 115m and 70m and Illimani and Sajama respectively (Thompson et al., 1998; Ramirez et al., 2003), with the last few metres containing 10-15,000 years of climate data (Vimeux et al., 2009). Consequently, annual layer counting (ALC) is accurate at the surface and has been estimated to be ±10 years at 100 BP (Knüsel et al., 2003); but the loss of annual resolution after a few centuries, at many of the locations, makes it unsuitable to use the ice-cores as archives unless one follows the approach of Moberg et al. (2005) to merge different archives of varying frequencies and resolutions (Vimeux et al., 2009)

An accurate chronology is crucial to interpreting the climatic signals from the ice-core records. A few methods exist, such as ALC, reference horizons, radionuclides, and comparative proxy archive matching. ALC is the most accurate method and is based on the seasonal variation of the insoluble particles and isotopic composition of the ice. Electric Conductivity Management (ECM) is a technique used to count these annual layers and can deliver a high resolution, (~1mm) continuous profile along the core, with the advantage of being a non-destructive method. This was first applied to polar ice-cores but has also been utilised on the Illimani ice-core record, where it was assumed changes in the ECM are due to variations in H^+ and major ion concentrations (Knüsel et al., 2003).

In order to independently test the robustness of ALC, reference horizons have been used to "anchor" layers to specific points in time. Radioactive fallout from the 1950s and 1970s can be

measured by the detection of tritium peaks, beta activity, or ^{137}Cs (which is used most today) (Vimeux et al., 2009). Tritium peaks occurred, in the southern hemisphere, between 1964-1967 and have been used as a reference point for Huascarán, Quelccaya, Illimani, and Sajama. Large volcanic eruptions can also provide chronological tie-points as they are widespread and occur within distinct time intervals. The Illimani ice core record contains ash layers from Pinatubo (1991AD), Agung (1963AD) and Tambora (1815AD) (Ramirez et al., 2003), the ECM method had also identified volcanic emissions relating to eruptions of El Chichon (1982AD), Krakatoa (1883AD) and another unknown eruption that occurred in 1258AD (Vimeux et al., 2009).

Radioactive isotopes such as ^{210}Pb (which has a half-life of 22.3 years) and has been applied to a handful of ice-core records in South America, including that of Illimani (Knüsel et al., 2003). ^{210}Pb is a decay product of ^{222}Rn, which emanates from the earth's crust ad into the atmosphere, the ^{210}Pb particles attach themselves to aerosol particles and reach the glacier surface through dust accumulation in drier conditions, or though wet deposition in precipitation. ^{14}C dating has also been applied to the Sajama ice-core record (Thompson et al., 1998), but this could only be applied to the core due to the amount of biological material preserved within the layers, which is not normally the case for most ice-core records (Vimeux et al., 2009).

2.6 Quality of existing palaeoclimatic chronologies

As previously alluded to, the existing datasets based on ceramic stratigraphy cannot be relied upon as many of them have been reworked to include new horizons. Radiocarbon dating is an important tool in understanding climatic and environmental pressures impact upon the societies of the central Andes region, given the short timescales of the cultural horizons. Before being used in the analyses and site comparisons, data for the Central Andes region has been quality-checked. Unreliable chronologies may lead to incorrect assumptions, when used for intra-site comparisons. The following criteria was used to refine the list of suitably dated sites for comparison to this study.

1. Dating precision. As this research aims to ratify climatic changes within short time series (i.e., a few hundred years) we must move to exclude sites which include ^{14}C dates, within their final age-model, with a standard deviation (1σ) of more than 50 years. Uncertainties, within radiocarbon dating, arise from a variety of ways including equipment error, measurement stability, and the random nature of radioactive decay (van der Plicht and Bruins, 2005; Flohr et al., 2016). Dates with high 1σ margins are more likely to have had problems in pre-treatment or the material itself may be unsuitable for radiocarbon dating. These error margins may also put the associated proxy data, outside of the cultural horizons the author(s) intend to discuss.
2. Type of material. Dates from shells were omitted due to risk of recrystallisation of giving erroneous ages (Olsson, 2009), as well as with hard-water effects from terrestrial species. Radiocarbon ages from corals must also be used with caution, for similar reasons. Corals original structures can undergo calcite recrystallisation in open

geochemical systems allowing more recent carbon contamination (Chappel and Polach, 1972); there is also some problems with leaching effects with modern CO_2 in deep sea coral systems, as well as the marine reservoir effect (Adkins et al, 2002; Okumura et al., 2021). Coral samples must, therefore, have undergone rigorous pre-treatment methods in order to minimise these factors – if to be used in comparative discussion at all.

3. Length of record. The full length of ages must cover, at least, the last 2,500 years B.P. As this will then cover the major cultural horizons (Table 2.1) and can then be used for inter-site comparisons with societal change due to climatic and environmental pressures. More modern records, such as late-Holocene dendrochronology, have been omitted for this study as they do not go back far enough in time. Cores that extend back through to the early-Holocene, would be favourable as this would enable this study to independently test the robustness of the proxy data, in relation to major changes that occurred further back in time. Records with large gaps in them due to hiatus or, for example, where speleothem records do not continue growth after a certain age have been used sparingly as they may still contain relevant climatic information that can be referenced against.
4. Number of dates. The research community generally regards one ^{14}C date per millennium as sufficient to provide a robust chronology for their site. However, these may fail to capture true sediment accumulation rates and can lead to erroneous age estimations (Blaauw et al., 2018). Upping this to at least two dates per millennium, as per Blaauw et al. (2018), may well provide more precise age-models useful for ratifying the shirt-lived environmental pressures to human societies, in the central Andes region.
5. Samples that had any notes on being problematic were also rejected in this study.

2.6.1 Notes on other dating methods

Strong consideration is given to records that have U-series dates as chronological tie markers but were checked to ensure accurate age modelling had taken place. Tephrochronology is also considered here for its ability to link dating and synchronising, paleoenvironmental and archaeological records together (Lowe, 2011; Abbott et al., 2020). The correlation of these records relies heavily on matching physical characteristics, mineralogy, and geochemical profiles of the tephra shards. Tephrochronology can be used to correlate records over thousands of kilometres away, as they act as geological tie points through time. There is a generally a good understanding of regional volcanic activity for the southernmost part of South America, during the Holocene (e.g., Stern et al., 2015) and the central Andes region (e.g., Thouret et al., 2002; Cobeñas et al., 2012), and thus would give a certain robustness to records containing tephra layers.

2.6.2 Assessment of current chronologies

This study has used the available data from The National Oceanic and Atmospheric Administration (NOAA) palaeoclimatic database, which has a large set of data available from previous published works. It must be noted, however, that not all palaeoclimatic data has been archived in this database, but a large proportion has been which makes it a good summary of the data available to date. The NOAA database has:

1. There were 81 studies in its database for the central Andes region which included Peru, Bolivia, and Ecuador. Some of these studies were carried out on the same sites, after compiling these together, the total number was 44.
2. These records (see Table 2.2), including speleothem, lakes, peat, tree ring, coral, and tropical ice-core records.
3. Studies that had enhanced previous published data. For example, some lake cores had been analysed isotopically in addition to already established pollen stratigraphies. Some speleothem records have trace element data, as well as carbon and oxygen isotopes that enable a better interpretation of the datasets.
4. Many these records also contained useful information about their chronologies, including how many dates are available as well as the dating method applied (i.e., radiocarbon, U/Th etc.)

Using the criteria outlined in section **2.6.1** this study finds that 9 of the original 44 records are useable in comparative work, that attempt to ratify environmental and/or climatic shifts that lead to societal collapses during the late Holocene. The results of which can be found in table 2.2. The major categories that the studies belong to are discussed below. The selected records can be found in figure 2.8)

Table 2.2: The number of records, of each type, that have passed or failed the criteria for comparative studies. The category labelled as other contained records from tree rings, modern boreholes and the Cerro Llamoca record (Schittek et al., 2015).

Type of Record	Number of Studies	Number Passed	Number Failed
Speleothem	6	2	4
Lacustrine	12	2	10
Marine	3	1	2
Tropical Ice-Core	4	3	1
Other	19	1	18

2.6.2.1 Speleothems

Speleothem records that span the last 2,500 years, within the Andes, are rare and only a handful exist. Huagapo cave, Peru (Kanner et al., 2013) contains stable isotope history of the past 7,150 years across 2 speleothems which overlap in age at 1,100-1,400 BP. The combined ages for the P00-H1 and P09-H2 are well ratified, with no age reversals within them

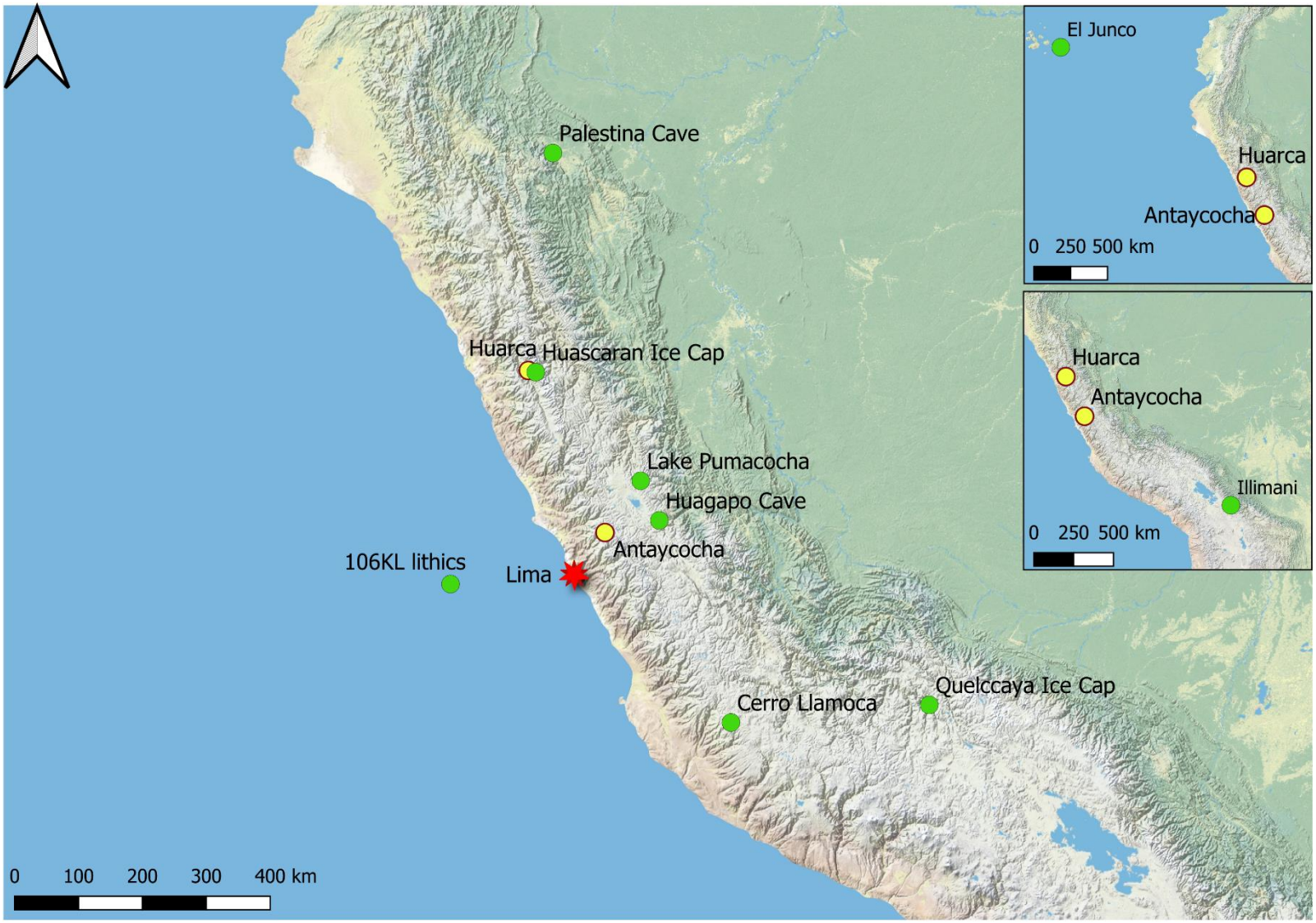

Figure 2.8: Location of the core sites in this study (yellow) with the locations that pass the chronological review (green). Inset are the two records outside of Peru: El Junco (Galapagos Islands, Ecuador) and Illimani tropical ice core (Bolivia).

mad contain low detrital Th concentrations which give low 2σ errors of between ±2 to ±15 years across the entire record (Kanner et al., 2013). This gives a total of 13 dating points within the 2,500-time criteria, which lends a high-precision dataset to be able to make regional comparisons to.

Cueva del Diamante and El Condor records, both Peru, (Cheng et al., 2013) are both long records of palaeoclimate stretching back 250,000 and 50,000 years for Diamante and El Condor respectively. The chronology for these records is based on 197 ^{230}Th ages, which all have a 2σ error of better than 1% (Cheng et al., 2013). However, this project cannot use the Diamante record for use in inter-site comparisons, in this instance, due to the earliest age recorded as 2,513 cal yr BP – which sits outside the timeframe for this study. On the other hand, the El Condor speleothem data contains 13 U-Th ages within the last 2,500 years with the earliest age recorded as 304 cal yr BP making it a candidate for this project to use in comparative studies Palestina cave, Peru (Apaéstegui et al., 2014) is a shorter record of climate history for the Andes. The PAL3 and PAL4 speleothems have 20 U-Th dates attributed to them from 413AD to 1824AD and 1096AD to 1925AD respectively, with errors ranging from ±4 to ±21, the PAL3 record contains a more sporadic error range across its U-Th dates. It has good correlation with other cave records, as well as the Pumacocha and Quelccaya sequences through the MCA and LIA. However, it does not have a continuous record through the 2,500-year time-span that the criteria requires. None the less it is a high-precision record and would be useful in some comparison studies for the Middle Horizon onwards.

Similar to the above, Cascayunga cave (also Peru) (Reuter et al., 2009) sits roughly 20km from the Palestina speleothem record and spans a period of ~1,460 years. There are only 7 U-Th dates associated with the CAS-D speleothem which covers 540AD to ~1900AD. The study by Reuter et al (2009) only covers the top 14cm of the speleothem, covering the last 1,000 years of time. Again, this does not cover the total time period that the study aims to ratify, but it could be useful for covering the time periods after the Middle Horizon, as there are some good correlations through the LIA period.

Pacupahuain Cave, Peru, (Kanner et al., 2012), was formed in an area where glacial landforms are not present and thus presents a longer record of time. The P09-PH2 speleothem, however, stopped growing around 16,610 cal yr BP putting it well outside the timeframe for human occupation of the Andean region. For this reason alone, this study cannot accept it for use in comparative figures.

2.6.2.2 Lacustrine records

A significant challenge, in studying the paleolimnological history of South America is the lack of lacustrine records that are of a continuous nature. In the tropical lowlands lakes are typically ephemeral and older lakes typically have slower sedimentation rates (Seltzer et al., 2000). However, there are a few long records from larger lacustrine systems that span the entire

Holocene with varying sedimentation rates and chronologies (e.g Seltzer et al., 2000; Fritz et al., 2007; Bird et al., 2011a; Stroup et al., 2015), although there are still some difficulties and gaps within their dating programmes.

A great deal of the chronological information for the larger lake basins stretches far a great length of time, but due to the sedimentary depositional rates, many of the ^{14}C dates fail the above criteria. For example, the top age given in the Lake Titicaca record (Fritz, et al., 2007) is recorded at 3,050 cal yr BP, which is before many of the cultural horizons that this study is making comparisons to and will not be well ratified in this sequence. Similarly, the sedimentation at Yanacocha (Stansell et al., 2015) is also very low and, as such, the chronology means that there is 2,180 years within ~40cm of sediment making their study quite a coarse resolution to make comparisons to. Lake Junin (Woods et al., 2020), has an incredibly long and well dated sequence, for the older portions of the sequence. Where it does not excel, is in the upper parts of the basin. Here radiocarbon dates are sparse, with 4 in the last 2500 years that do not have a 1σ error of less than 50 years; with only 1 valid date in the last 1000 years making temporal resolution low. Lake Limon (Parsons et al., 2018) offers a short-range insight into pre-instrumental hydrological regimes, over roughly 2,000 years which puts it just short of the timeframe of this study. It is also located outside of the Andes region, where this study is located, making it problematic for inter-site comparisons to be made, due to its main climate impacts derived from deep within the Amazonian regions of Peru.

The Peruvian record of Laguna Pumacocha is a small lake situated at a very high altitude and has been faithfully recording precipitation variability in the Andes over the last 11,200 years. The decadally resolved has a suite of ^{210}Pb ages, at a 1cm resolution, for 30cm alongside 18 ^{14}C dates across its entire length. The last 2,500 years have been recorded over ~2m of core length, and measured by 12 radiocarbon dates, making this record a great comparative site to use to ratify climatic and environmental shifts seen in this project study sites – due to Pumacochas high resolution record.

There are 2 lake records from Ecuador, in this review, El Junco and Laguna Pallcacocha. The former, sits outside of the Andean region and is in the Galapagos Islands. However, hydroclimatic model simulations suggest that this crater lake responds sensitively to precipitation changes due to ENSO regimes (Conroy et al, 2008). Included in its chronology are 9 ^{210}Pb dates, in the top 18cm of the core, with a ^{137}Cs spike anchoring the ages at 1963AD. For the radiocarbon chronology there are 23 radiocarbon ages (of which, 5 are post-bomb), 8 of these dates have ranges within the last 2,500 years making this site a reasonable comparative study for ENSO activity in the study sites.

The Laguna Pallcacocha sequence, which was first dated in the 1990s, has large 1σ errors associated with it (Rodbell et al., 1999). This was added to in recent years with the addition of several ^{210}Pb dates and 5 new ^{14}C dates, all within the last millennium (Mark et al, 2022). These new dates, however, reveal that the sedimentation rate if the lake is low and that the new top age is ~870 BP at 15cm of depth. The new ages have been spliced into the

chronological record with the older ^{14}C ages from the 1990s, with the advances in radiocarbon techniques these could be further ratified now and may need reanalysing.

Both of the Bolivian lacustrine systems, from the NOAA database, will be excluded from any comparative work in this project. The Salar de Uyuni (Fritz et al., 2001) dataset, within NOAA, has the top age as 9,370 cal yr BP at 4.38m, leaving a large amount of sediment to be modelled from these ages. This is due to the nature of the sediments in the study, as they were retrieved from paleolakes which have since stopped accumulating any sediment – making them unusable on the time scale this project is based on. The chronology from Laguna La Gaiba (Whitney et al., 2011) also leaves a little to be desired. The shallow lake has a top age of 2,701 cal yr BP at 44cm with a second date of 6,298 cal yr BP at 92cm, this means that there is an estimated sedimentation rate of 0.013cm per year making it a coarse resolution record and one that is modelling modern dates based on a date of 2,701 years. With this modelling strategy and the 1σ errors of over 50 for the earliest radiocarbon ages, this cannot be used to accurately ratify the short-lived cultural horizons that this study is interested in.

2.6.2.3 Marine records (including corals)

The 106KL marine core, was gathered 80km off the coast of Lima, Peru (see Rein et al., 2004; 2005) and is located on a small basin on the edge of the continental shelf. It has faithfully recorded ENSO variability for the last ~20,000 years through using material specific absorption features in reflectance spectra to derive lithic matter and photosynthetic pigment concentrations, all conducted at 2mm intervals (Rein et al, 2005). The detailed chronology of the Holocene is measured by 38 ^{14}C dates in total, with the last 2,500 years based on 8 ^{14}C dates with a combination of lead and caesium isotope profiles of the topmost sediments (Rein et al., 2004). It is concluded in the study by Rein et al (2004; 2005), that an early maxima of ENSO activity was rapidly followed by weakened El Niño activity during the mid-Holocene period (8-5.6 ka). El Niño flooding that produced the thickest deposits of lithic material occurred during the second and third millennium BP. During the last millennium, ENSO activity tracks changes in global temperature; thus, major Holocene ENSO weaknesses during late medieval period implies that the climate during these times may only be of limited use when used to discuss modern climate changes (Rein et al., 2005).

Unfortunately, there are few sub-annually resolved coral records in the Galapagos as modern coral reefs are rare making comparisons for more modern ENSO variability difficult to undertake (Reed et al., 2021). There are also too few records that resolve the earlier cultural horizons that this study is particularly interested in, with the oldest records starting ~1600 AD (e.g., Dunbar et al., 1994), making any ENSO variability comparisons within the study sites to coral data difficult at best.

2.6.2.4 Tropical Ice-Cores

There are various tropical ice-cores for the Andean region, that this project is interested in. Huascarán, Peru, has a long record that stretches back into the last Glacial maximum

(Thompson et al., 1995). The development of the age model was done by the identification of the dry season (July-October) using elevated measurements of NO_3-, which corresponds to the middle of the dry season (Thompson et al., 1995; Henderson, 1999). Rapid layer thinning below 120m limits annual resolution to the most recent 270 years at Huascarán, but high accumulation and strong preservation of seasonal cycles also makes it possible to have sub-annual resolution between 1884-1993 (the year of coring). Several event horizons have been used to confirm the ALC method, firstly a magnitude 7.7 earthquake in 1970 is recognised by a peak in particulate matter within the layer counts. Secondly, ^{36}Cl profile of a second core confirms a 100-fold increase in concentrations relating to 1952-53 nuclear weapons testing. Finally, both cores taken from the glacier contain the 1883 AD eruption of Krakatoa which is identifiable by anomalous sulfate readings (Thompson et al., 1995; Henderson et al., 1999). Huascarán is dated to a high resolution and has a variety of tie-points that make it a strong candidate to be used in comparative studies. It also lies in close proximity to one of the study sites of this project, giving us the unique opportunity to independently test the reliability of site data.

Quelccaya, Peru, was dated with annual resolution down to 683 AD, the older ages were determined with a polynomial fit model – outlined in Thompson et al. (2013) – which gives a bottom age of 226AD. This is just short of the full 2,500 years that the criteria that this study is aiming to use for comparative studies, however, the high precision of the core and its reliable dataset make it a key record for understanding Holocene climatic shifts in the Andes. There is also a tie-point used to anchor the layer counting, at Quelccaya, with the 1600AD eruption of Huaynaputina recorded by a large spike in insoluble dust concentrations (Thompson et al., 1986).

Two parallel ice-cores were extracted from the cap at Illimani, which contain the climate history of the last ~18,000 years (Knüsel et al., 2003; Ramirez et al., 2003). The ECM method was used to establish the chronology of the cores, using the tritium peak at 1964AD as a reference point. The counting of the layers by the ECM method was conducted over the top 125m (~90% of the core) representing a time period from 1200-1999AD (Knüsel et al., 2003). The rest of the ages are tied in using a combination of ^{210}Pb dating and volcanic eruption tie points. There are also 16 tie points to the Huascarán core (Ramirez et al., 2003). There are also a suite of ^{14}C dates for the Illimani ice-core record, between 89.3m and 113.1m, deduced from water-insoluble organic carbon fractions - which also adds to the robustness of the chronology (Sigl et al., 2009).

The Sajama ice-core record extends back the furthest in time, with the last 25,000 years of climatic history recorded in the sequence (Thompson et al., 1998; 2000). The ice cores, as mentioned previously, contain biological fragments which include: intact insects, insect fragments, and polyepis plant material with sufficient mass for ^{14}C dating (Thompson et al., 1998). Some of these ^{14}C dates, however, have large 1σ errors associated with them (between 70-370 years) and so the reliability of them must be questioned. The top of the sequence has

annual layer counts calibrated using a tritium peak at 1963AD for the most recent 100 years. One ash horizon (Huaynaputina, 1600AD) is also used as a chronological tie point. For the glacial portion of the record, matching to the GISP2 record was carried out on associated $\delta^{18}O_{atm}$ and $\delta^{18}O_{ice}$ peaks. The large errors used in the ^{14}C dating programme make this a record that is not as reliable for use in comparative studies, over the time periods this study is interested in – as some of the radiocarbon ages are within the last 2,500 years of time.

2.7 Summary of Late-Holocene climate changes and the need for further research

There has only been the suggestion of North Atlantic climate forcing in the Andes, but the mechanisms linking the North Atlantic climate changes with the Andes is still lacking (Urrego, Bush and Silman, 2000; Schiferl et al., 2018). Major climate fluctuations such as the Medieval Climate Anomaly (MCA) and the Little Ice Age (LIA), have been shown to have their origins in the Atlantic with initial suggestion that they had some influence in the Southern Hemisphere; although the evidence is not robust enough (Mann et al., 2009).

Many palaeoecological records agree that the MCA was a period of weaker monsoons and short-lived aridity events (Kuentz, Ledru and Thouret, 2012; Apaéstegui et al., 2018). However, there is some debate within similar studies, with some indication that there was a time of prolonged aridity during the MCA – as shown in depleted $\delta^{18}O$ values, in diatoms, at Lake Pumacocha (Bird et al., 2011b). Similarly for the LIA, records show an increase in monsoon activity and precipitation (Thompson et al., 1995; Bird et al., 2011a, b; Apaéstegui et al., 2018), again there are only a few records that correlate with one another. From these examples, it is easily identifiable that there is still much more work to be done before the mechanisms and timings of these events can be correlated with other regional records. With a distinct lack of chronology, this will be difficult to achieve which, as previously mentioned, will be vital to underpinning major fluctuations in climate and why certain Andean civilisations have disappeared through time. There have been recent advancements in building a chronology in Peru (Unkel et al., 2007, 2012; Unkel and Kromer, 2009; Ogburn, 2012), but there is still a lack of a robust chronology based on radiocarbon dating of archaeological remains/site.

A significant challenge in studying the palaeoclimatology of the Central Andes, is the distinct lack of lacustrine records that span the Holocene (Seltzer, Rodbell and Burns, 2000). This review has found that many of the lake systems from the tropical lowland but are often lacking in a continuous record, or one that is only a short-term sequence such as that at Lake Limon. Larger lake systems, such as Yanacocha, Lake Junin, and Lake Titicaca, that have records that span over longer timescales (some extending through to the Pleistocene) have low sedimentation rates which makes any age-depth modelling problematic to be able best constrain the environmental changes that occur within the short-lived cultural horizons. For example, the top age for Lake Titicaca lies outside of the time period of interest (the last 2,500 years) and thus any modelling through to the modern era becomes unreliable based on these

older ages. Other large lake systems either have stopped accumulating sediments after a certain point in time, as seen at Salar de Uyuni, or have chronologies based on older radiocarbon dates (as at Laguna Pallacocha).

Smaller basins, such as those within montane valleys may offer the chance of studying records that contain a long sedimentary history. This can be seen from the Pumacocha sequence, which spans the last 11,200 years of history. It has a very well ratified sequence due to its high accumulation rate, allowing for the application of 12 ^{14}C ages over the last 2,500 years (alongside ^{210}Pb ages along the top 30cm). Similarly, the sequence at El Junco provides another high-precision dataset which has a reliably dated sequence from a small crater basin. It is these smaller basins that are accumulating sediment over a shorter time frame that make them sensitive to rapid climatic events, such as ENSO, which are not picked up in the longer sediment records of the larger basins.

There is currently a wealth of information of stable isotopic records from tropical glaciers (Thompson et al., 1995, 1998, 2000; Knüsel et al., 2003; Ramirez et al., 2003; Davis and Thompson, 2006; Sigl et al., 2009), monsoon records of cave speleothems (Vuille et al., 2012; Kanner et al., 2013; Bustamante et al., 2016; Apaéstegui et al., 2018), that are all very well ratified and well dated. They allow for decadal resolution, in the very least, with most records offering annual and even sub-annual records of climatic change.

More work is needed in the smaller montane valley basins of the Andean region. The tropical lowlands, as mentioned previously do not offer the chance of analysing a continual record of Holocene climatic change; or where it is possible to analyse such sediments, the sedimentation rate is often too low to ratify the short-lived climatic events that occur during the Holocene. These smaller basins also offer a key chance to analyse local and regional changes in relation to archaeological evidence found in proximity to the basins, which will also give the opportunity to test outstanding hypotheses surrounding decline of populations – for instance the collapse of the Wari after the middle horizon. Or questions of changes of agricultural practices, from terraced agriculture to more pastoralism and were these brought on by changes in climate? There is a scarcity of records from sites adjacent to archaeological regions, within the Andes, while the larger international records offer the chance of studying circulation patterns such as the ITCZ and SASM, we still do not know how these patterns have affected the local human populations. We can only use the information from these regional records to infer what the impacts may have been, but without proximal data from archaeological sites we cannot be certain of the impacts of climate change on the Andean cultures during the late-Holocene.

2.8 Application of methods

Below is a brief explanation of the use of the methods in this study. These are further expanded upon in chapter 3.

2.8.1 Stable Isotopes

The use of stable carbon and nitrogen isotopes in soils (and palaeosols) is a powerful indicator of palaeoenvironmental conditions. A great number of studies have used these to reconstruct past vegetation communities in South America (e.g., Powell et al., 2009, 2012; Novello et al., 2019). The use of carbon isotopes is particularly effective in the semi-arid climates where the plant communities have undergone changes in the ratio of species that are C_3 and C_4 (Nordt, 2001). Similarly with nitrogen, as enriched measurements of $\delta^{15}N$ are often associated with cycling of N caused by decreased amounts of rainfall.

Organic matter from pedogenic sources are desirable for the use of palaeoenvironmental reconstructions, as the isotopic values derived from these are direct measurements of the organic matter source and will reflect the isotopic values of the plants growing directly in the soil (Nordt, 2001).

While there are a number of key studies, in South America, that utilise C-N ratios for defining the type of vegetation there are very few studies from within Peru itself. There is one key quaternary site, however, which has used C isotopes to determine past environmental controls. Lake Titicaca use δ13C ratios to infer lake levels from the organic material that were present throughout the sequence (Fritz et al., 2007). The δ13C measurements inferred that periods of high lake level, from planktonic sources, is dominated by low δ13C values. Conversely, higher δ13C values are indicative of lower lake levels derived from littoral macrophytes (Fritz et al., 2007).

Stable isotopes of sulphur, in palaeoenvironmental reconstructions include, but are not limited to, pollution (Derda et al., 2006), plant physiology (Trust and Fry, 1992), bacterial formation, archaeological studies (Kinaston et al., 2014) and a range of mining histories. There are only a handful of studies within Peru, which have focussed mainly around the human induced environmental changes, through pollutants (Cooke and Abbot, 2008).

2.8.2 Portable XRF (pXRF)

pXRF is a reliable and rapid way of gaining information pertaining to environmental studies. These include mining histories, soil chemistry, metallurgy, and agronomy (Weindorf et al., 2014a; Ribeiro et al., 2017). The elements of phosphorous (P), sulphur (S), copper (Cu), Lead (Pb), and Zinc (Zn) can be isolated to determine impacts of human-induced environmental patterns and pollutants within the soil. The key indicators here are Cu, Pb, and Zn, as these have been shown to be key indicators of mining history within Peru. These are all common elements in polymetallic deposits across the country and have been used since ancient times. For example, Pb, lends itself as the basis of many Peruvian mining histories, where argentiferous galena was the main ore in the productions of silver (Cooke et al., 2007). The study by Ogburn et al., (2013) studies the use of pXRF to examine the effects of surface contamination and the effects of weathering processes on building stones around the Cusco region, and is another way to utilise this technique in lived environments.

The main limitations for the use of this technique surround the type of sediment used. There are questions surrounding the chemical make up of the soil, which can cause some interference (Peinado et al., 2010). For example, some elements may show as the same peak number in the analyser (e.g. As and Pb). There are other limitations to using this technique and some caution applied when using pXRF. One must consider the moisture content (>20%), the particle size, and the homogeneity of the soil profile.

2.8.3 n-Alkanes

Normal Alkanes (n-alkanes) are a class of leaf wax that is stable and resistant to degradation, and so preserves well. They can be used for both palaeoenvironmental study, as the data produced can give information on the type of vegetation and changes in plant communities (this study) and also through the use of compound specific isotopes (e.g. Schneider et al., 1983; Farrington et al., 1987, Garcin et al., 2014) When used for climate the H isotopes, within the leaf wax can prove useful in these types of studies. The latter point have mainly been used in gaining knowledge into the hydrological processes. For example the study by Kahmen et al (2013) determined the n-alkane δD (Deuterium) values are effected by evaporative D-enrichment of leaf water. Other studies into the climatic controls on leaf wax n-alkanes can be found in Feakins et al., (2016a,b) which focus on South America.

The use of n-alkanes in environmental studies are through the determination of plant type and coverage, which can be indirectly linked to changes in the climate systems. They are, ultimately, dependant on the climate-induced environmental changes such as temperature and CO_2, which have impacts on the plants growth and distribution (Eglinton and Eglinton, 2008). Lipid chain lengths are often used as the main indicator of plant types, within the samples, and can be an indicator of terrestrial plant life (e.g. Chevalier et al., 2015) or aquatic life (Liu and Liu, 2016). There are other indices that can be used in these type of studies to determine the composition of the soil organic matter (SOM). The main one here is the CPI which gives information on the odd/even chain predominance to determine the quality of the SOM and the contribution of external sources of input – such as petroleum hydrocarbons (Bray and Evans, 1961; Chevalier et al., 2015).

There are some limitations of the practise, which relate to their abundance and composition. An example of this is the biomarkers transferred from the land must be considered within the areas that have supplied them, as well as the depositional rate and environment where they are found (Eglinton and Eglinton, 2008). There are also questions surrounding the decomposition and if there are any labile elements that could be exchanged, which change the chemical make-up of the sample.

2.8.4 Rock-Eval Pyrolysis

The use of Rock-eval is still a novel approach in many sedimentary environments and hasn't before been used in Peru. It is a major component of studying the maturity of hydrocarbon bearing rocks (e.g. Könitzer et al., 2016), but recently has had success in tracking sources of

organic matter (OM) and vegetational changes (e.g. Englehart et al., 2013; Lacey et al., 2015; Newell et al., 2016).

The main components of the method, that are used heavily in this study, are as follows. Total Organic Carbon (TOC%), is a descriptor applied to the content of the OM, and can produce information on the different biopolymers and geopolymers in the samples.

T_{MAX} is the measure of the maximum temperature needed to break bound hydrocarbons, in the sample. This is related to the properties of the OM, and determines the content of lignin, cellulose, and xylans in the sample. It can also be used to, in conjunction with TOC%, to ratify the mineral content of the sample – as can the parameter minC (mineral Carbon).

The Hydrogen and Oxygen indices (HI and OI) are usually used in conjunction with one another. The HI gives an indication of the hydrogenation of the sample, and enables researchers to identify depositional effects of the OM input. OI is a descriptor applied to the amount of OM that has undergone aerobic decay. Where there are increased OI values, these samples tend to be more hydrogen poor, labile organics that are more highly decayed. Where the OI:HI ratio favours the OI, we can make inferences on the OM type that has been transported into the basin by other means.

There are also the I and R indices, which can be found in chapter 4. These are of some use as they both refer to the thermal degradation of the OM in the soil. I-index refers to the preservation of thermally labile immature OM with the R-index assessing the contribution of thermally stable SOM (Sebag et al., 2006, 2016). The I and R-indices are useful in this regard as they provide information on the degradation and preservation of the OM in the core sequence.

The limitations of the use of Rock-Eval relate to the mineral matrix and questions surrounding organic enrichment of these matrices. Some studies suggest that this can create variations in the hydrocarbon and CO_2 concentrations, which could have negative consequences to the HI and OI indices.

2.8.5 Non-Pollen Palynomorphs (NPPs)

NPPs include a variety of spores, ferns, seeds, mosses, and invertebrates. NPPs have been used as a means of tracking humans in the landscape, and changes in herbivory. This study, as others, have focussed on coprophilous fungal assemblages, to do so. *Sporormiella* is the chief NPP used in environmental studies, inclusive of herbivores and humans (e.g. Raper and Bush, 2009; Chepstow-Lusty et al., 2019). However, this the relative abundance of *Sporormiella*, in Holocene deposits, is quite rare, and identified spores make up 1% (or less) of the total assemblage (Davis and Shafer, 2006) – a major limitation. It is then advised to use a total assemblage of a variety of different ascomycetes.

One main study of note is the paper by Chepstow-Lusty et al (2019), which is located at Marcacocha in Peru. This paper analyses the use of *Sporormiella*, in conjunction with oribatid mites, to reveal information on herbivore density at the site. The authors then find that the

Sporormiella concentrations do not reflect the major changes in the density of herbivores in the region but does reflect the changes in lake level. It is difficult, then, to provide key information on the density of herbivore and human populations from using NPPs as a sole method. We can, however, make inferences in the land-use changes that are driven by humans as well as infer that human populations (and proceeding abandonment of sites) were within the sites of choice.

2.9 Hypotheses of the study

1. The main proxies used in this research will help determine the environmental shifts that have driven the land-use changes between civilisations.

We can test this hypothesis well, with a multi-proxy approach. Well constrained age modelling will, also help to pin-point the major shifts in relation to these short-term ceramic horizons.

2. The use of Rock-Eval pyrolysis, while a novel approach to South America, can help to untangle the sources of sediment input and the type of vegetation coverage in the basins.

Rock-Eval pyrolysis has been used, over the last two decades, in a variety of other sedimentary environments. These studies have demonstrated the practical use of the method and has shown to be an effective means of tracking organic matter input in these environments.

3. Rock-Eval pyrolysis can generate information relating to old sources of carbon, to enable us to choose the best samples for radiocarbon data.

There are several parameters that the Rock-Eval gives data for, that are primarily used for the maturity of old hydrocarbons. We can use some of these parameters that correlate well with the age discrepancies between bulk and plant ages, to come to a determination of the novelty of this approach.

4. The positioning of the study site at Antaycocha, is such that there is scope to determine the sensitivity of small basins to short-lived climate changes e.g., ENSO.

Antaycocha sits on the western flank of the Andes mountains, facing towards the Pacific Ocean, and has shown to have a rapid accumulation rate. It is not beyond reason that the basin could be sensitive to rapid ENSO events, due to its position and accumulation rate.

5. With the use of trace element data, we can create more robust uses of proxy data. For example, we can use this new data to analyse the periodicity of arid events and determine the sources of organic matter input that are outlined in the RockEval methods.

pXRF studies have been undertaken in a variety of means and has shown that it is capable of tracking sources of sedimentary units. Using both pXRF and Rock-Eval together may make

for a stronger set of results, and could enable researchers to better determine the sources of sediment input.

6. The geochemical analyses of the sediments (isotopic and *n*-alkane) can provide details on the depositional process, and the type of agro-pastoral practices used by the civilisations present during the time periods outlined in this study.

Stable isotopes of carbon, nitrogen, and sulphur have been undertaken in many different locations, and studies, to determine similar results. This study aims to ratify the type of vegetation coverage and if past civilisations have used these basins for agricultural practices. We can use these proxies to understand the presence of C_3 and C_4 plants in the area, as well as if there were any periods of abandonment in the basins.

3. Methodology

Chapter 3 will detail the methodologies used within this thesis. The rationale behind choosing each of them is explained before the outline of each of the methods.

3.1 Field Methodology and Sediment Descriptions

Site selections for Huarca and Antaycocha were based on the following criteria:

1) The sequence would likely return a relatively long, continuous record of sedimentation, which would return a high-resolution age-depth model.
2) Sites located proximal to archaeological remains. E.g., Antaycocha is within the Cantamarca archaeological zone, while Huarca is located next to relic terrace systems.

The site of Huarca was selected with the help of Dr. Alex Herrera (University of Los Andes, Bogotá, Colombia). The site selection of Antaycocha was carried out with the aid of Dr. Carlos Farfán (Federico Villarreal National University, Lima, Peru). The site descriptions, major sedimentary changes, coring co-ordinates, and modern surface plant material etc. were detailed in fieldwork notebooks and photographed as logged.

Cores were gathered using a standard Russian peat sampler (5cm diameter, semi-circular), in 50cm sections (Jowsey, 1966). Two coring holes (labelled A and B) were used, spaced no more than 30cm apart, to allow for 10cm overlaps between cores to lessen the impact of

Figure 3.1: Photographs of core material recovered from 2019 fieldwork left recovered from Huarca with right recovered from Marcapomacocha (not within this project).

potential disturbances from the peat coring. Each core section was labelled with the appropriate site name and depth e.g. Antaycocha 40-90cm (Core B), Antaycocha 80-130cm (Core A) etc. Two duplicate cores were taken at each site using a fresh set of coring holes to provide 'sister cores' for additional material for analytical methods to be carried out on them should the need for additional material be required. The cores were wrapped and sealed in plastic wrap, in the field, and transported back to the University of Reading where they were placed in cold storage at ~5°C.

Each of the cores had their lithostratigraphy described using the Troels-Smith method (1955), following Birks and Birks (1980). This allows for the analysis of composition, physical components, and degree of humification. The physical properties of the sediments also include the colour of the sediments, which are described using a Munsell Colour chart (Munsell, 1994), as well as providing information on the boundaries between the sedimentary units. The composition of the sediments also includes an abbreviated term relating to the type of sediments present in the core. Each of these lithological elements is then given a descriptor based on the proportion of the sediment type within the unit, with each having a value of 1-4 (1=25%, 2=50%, 3=75%, and 4=100%). It is also possible to have a unit with a proportion descriptor of '+' which denotes that the sediment type is "trace", where a specific unit did not add up to 25% of the unit composition.

Loss-On-Ignition (LOI) was carried out to provide an estimation of organic matter content of each of the cores as set out in Bengtsson and Enell (1986). Each of the cores was sampled at 8cm for an, to fit in with the pollen dataset in Handley (2022) but elected to sample the Huarca edge core at every 16cm due to the length of the core. The method involves drying 1cm^3 of sediment overnight at 105°C before cooling in a desiccator, to ensure that no further moisture remained in the sample before weighing. The weight of the furnace crucible and the combined weight of the crucible with the sample was recorded prior to burning at 550°C. To avoid overheating the crucibles were only added to the furnace once it had reached temperature (Heiri et al., 2001). Samples were left in the furnace for a total of 2 hours, before being returned back to the desiccator to cool. The crucible with the ashed samples were then weighed again, the amount of organic matter lost was calculated with the below formula:

$$\% \text{ Organic Matter} = ((\text{Dry-Ash})/(\text{Dry-Crucible})) \times 100$$

3.2 Stable Isotopes

Prior to analysis each of the samples were taken at regular intervals along the sequences, this was undertaken at every 4cm at the Central Basin core for Huarca and then at every 8cm for the Edge core and at Antaycocha. This was mainly to fit in with the pollen analysis to aid in interpretations of the data later. Only organic rich sediments were chosen, as they would contain a detectable ratio of isotope (carbon, nitrogen, sulfur etc.) required for analysis. The samples were taken from the centre of the cores and dried in an oven overnight and then hand ground in an agate pestle and mortar. The dried samples were transferred to micro-centrifuge

Figure 3.2: Photograph of mass spectrometer with Elemental Analyser (Photograph by Stuart Black)

tubes and were then weighed into tin capsules for C-N analysis (0.2-0.3mg). Sulfur was also recorded for Antaycocha, but due to the low amount of organic matter at this site a larger amount of sediment had to be weighed out (0.9-1.0mg).

Analysis of C-N-S isotopes was conducted on a Thermo-fisher DeltaV Advantage, fitted with a Temperature Conversion Elemental Analyser (TC/EA) with smart EA function and a zero-blank auto-sampler at the University of Reading. Standard scale normalisation and quality assurance monitoring was undertaken using internal standards together with USGS42 (Tibetan hair), USGS43 (Indian hair), IAEA-CH-7, (polyethylene), IAEA-601 (benzoic acid), and IAEA-S-4 (Sulfur). Replication of standards was better than 0.14 ‰ and 0.17 ‰ for $\delta^{13}C$ and $\delta^{15}N$, respectively. The data were stretch, and drift corrected following the methods in Carter and Barwick (2011).

3.2.2 Use of carbon, nitrogen, and sulphur stable isotopes in palaeo studies

Stable isotope ratios of carbon ($^{13}C/^{12}C$), nitrogen ($^{15}N/^{14}N$) and sulfur ($^{32}S/^{34}S$) are important proxy of human-induced environmental change. The chemical proxies work well in a multi-proxy approach and can often lead to robust datasets that can be linked to other sites with similar datasets. Stable isotopes are extremely useful as they do not need a large amount of material and can be undertaken at a high resolution along a sequence, being able to pick up short-lived changes in environment and climate is key to understanding human-environment interactions during the cultural horizons in the Andes.

Stable isotopes of carbon ($\delta^{13}C$) and nitrogen ($\delta^{15}N$) are especially important and can provide information, along with other proxies, on vegetation type and coverage. With shifts in the vegetation indicators, often related to periods of climatic change. For instance the $\delta^{13}C$ values of the main two types of terrestrial plants (C_3 and C_4 – named as such by the photosynthetic pathway that these plants follow) are quite distinct from one another, with C_3 plants having a mean $\delta^{13}C$ value of c. -26‰ (which is true of most terrestrial plants), and the C_4 plants mean $\delta^{13}C$ values of c. 12‰ (made up mostly of arid tolerant plants, and grasses) (Smith and Epstein, 1971; Szpak et al., 2014). In the central Andean region, the abundance of C_4 plants remains relatively rare, in the higher altitudes (Szpak et al., 2013) which tend to be cooler and wetter than those areas at lower altitudes and coastal regions.

Plants grown for agriculture, of which this study is interested in, are less susceptible to environmental pressures on isotopic compositions (Szpak et al., 2014). This is specifically because theplants may be supplied by other water through irrigation. This is true of many Peruvian sites, where there are details of vast terraced systems (e.g. Londoño et al., 2017). Effects of this irrigation, and the subsequent water availability, may have limited impacts on

the isotopic composition of $\delta^{13}C$ and $\delta^{15}N$ (Szpak et al., 2014). For example the wild plants sampled in the Moche valley (Peru) had high $\delta^{15}N$ values of ~+17‰ (Szpak et al., 2013), while neigbouring valleys which have large irrigation systems had a highest value of +6‰ (Szpak et al., 2012).

As breifly mentioned above the main bulk of studies, that have utilised carbon and nitrogen stable isotopes, have focussed on characterising the diet of human populations (Knudson et al., 2015) that reveal adaptations and different focusses on agriculture. There are, however, studies that have used bulk C/N ratios of organic matter within the lacustrine deposits, that have revealed important information on the palaeoenvironments of the area, which also serve to compliment the pollen-based palaeovegetation studies on the same matter. One major study where these ratios have been used is at Lake Titicaca. A major part of this study was to use $\delta^{13}C$ ratios to infer lake levels from the organic material that were present throughout the sequence (Fritz et al., 2007). The $\delta^{13}C$ measurements inferred that periods of high lake level, from planktonic sources, is dominated by low $\delta^{13}C$ values. Conversely, higher $\delta^{13}C$ values are indicative of lower lake levels derived from littoral macrophytes (Fritz et al., 2007). The Lake Titicaca seqence has furthered the research, in South America, documenting at least 4 glaical-interglacial cycles within the Andes region.

Sulphur isotopes have been used more readily in a environmental and dietary studies, over the past three decades. Several different aspects of environmental studies have used sulphur analysis, such as in pollution (Derda et al., 2006), plant physiology (Trust and Fry, 1992), bacterial formation, archaeological studies (e.g. Kinaston et al., 2014) and a range of mining histories. The main studies, utilising sulphur isotopes, in Peru are those where there are archaological remains and mainly focus on palaeodiet. The use of sulphur isotopes, within these studies, have focussed on differentiating fauna found in existing habitats (Bishop, 2017), and where these have come from within the large civilisations present in Peru. There are few palaeolimnological studies of sulphur, in Peru, but as mentioned above these studies investigate the pollution inputs as a result of industrial outputs (e.g. Cooke and Abbott, 2008).

Information derived from stable isotopes of carbon, nitrogen and sulphur provide us with a dataset that can give researchers information on the lived environment of the surrounding basin as well as indirect information of the climate, as a result of the changing vegetational cover (e.g. change in composition of C_3 to C_4 plants). However, the use of the above stable isotopes alone cannot give the full picture and is limited to a certain amount of information that they can give, relating to pollutants (in the case of sulphur) and different vegetational coverage. Stable isotopes are an effective means of gathering information, but utilising them as part of a wider multi-proxy analysis is a must, in order to dervie the best analysis of a basin to reveal the entire story.

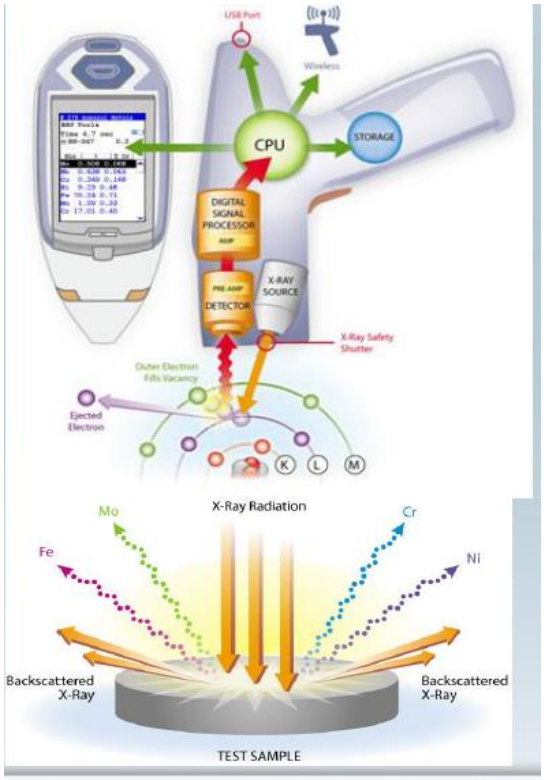

Figure 3.3: Diagram of the pXRF procedure, taken from the manufacturers handbook.

3.3 Portable X-Ray Fluorescence (pXRF)

A small amount of dried and powdered sample is placed onto 4µm propylene film and analysed for 120s on Mining mode (M). The M mode used in the measurement allows the following elements to be detected: Sb, Sn, Cd, Pd, Ag, Mo, Nb, Zr, Sr, Rb, Bi, As, Se, Au, Pb, W, Zn, Cu, Re, Ta, Hf, Ni, Co, Fe, Mn, Cr, V, and Ti.

The x-ray radiation from the analyser strikes the sample, the rays are transferred to the sample (interaction) and the atoms contained within the sample fluoresce a characteristic fingerprint, which is detected and transmitted to the pre-amplifier.

This is then transmitted into the digital signal processor (DSP) which digitises and sums signals. The resulting spectrum is processed in the central processing unit (CPU) and treated to obtain the elemental analysis, the results of the analysis are displayed and stored on the internal memory, which can be transferred to an external source for assimilation.

3.3.1 Application of XRF techniques

pXRF scanning provides a rapid, non-destructive, elemental dataset that can provide the identification and quantification of several elements from Mg to U. XRF spectroscopy is the most widely used X-ray technique used in environmental studies of mining histories, soil chemistry, metallurgy, and agronomy (Weindorf et al., 2014a; Ribeiro et al., 2017). For the purposed of this study, and indeed many environmental studies, the pXRF method allows the determination of trace elements and heavy metals to determine geomorphological, climatological, and anthropological contaminant history of a sequence. The elements of phosphorous (P), sulphur (S), copper (Cu), Lead (Pb), and Zinc (Zn) are used, in this study, to identify sources of pollution. Of particular significance are the elements of Cu, Pb and Zn, as these are the three most common elements in Peruvian deposits which have been utilised, in some way, since pre-Hispanic times and are the foundation of one of the world's largest mining networks. Lead is of a special interest, as it is the basis of silver production in the Incan Empire – where argentiferous galena was the main ore used to derive the silver (Cooke et al., 2007). Other elements of interest are potassium (K), iron (Fe), calcium (Ca), titanium (Ti), silica (Si), rubidium (Rb), and strontium (Sr). These elements are commonly used to indicate the variations in sediment input and may be indicative of erosional activity or where sediments may be of a terrigenous origin.

One study, from Peru, utilising this method can be found in Ogburn et al. (2013). Here the approach of pXRF was to examine the effects of surface contamination and the effects of weathering processes on building stones around the Cusco region. The concluding remarks of this paper are that the contamination and weathering effects were most impactful on the lighter elements (K and Ca) and appear to be the least effective means to test the provenance of the building material. Other elements of Tin, Mn, Fe, Rb, Sr, Zr, and Ba are best used for these studies owing to their greater critical penetration depths (Ogburn et al., 2013).

There are studies that have used other XRF techniques (e.g. ITRAX) to assimilate data based on sources of sediment input into the basin as well as looking for any erosional markers within the basin to determine the depositional environment at the time of the peaks in XRF markers (Handley, 2022).

Other uses of ITRAX, in South America, include characterising dust deposition in ombrotrophic mires (Sapkota et al., 2007). Ti concentrations in bulk peat, in combination with other proxies, were used to calculate mineral accumulation rates within the peat. Ca, Mn, and Ti distributions show that the mineral accumulations were of an atmospheric dust source. Giving weight to using the XRF technique as a basis for sedimentological study. Another use from Campos et al. (2019), is for use in precipitation changes and use in models of precipitation coverage. Here Ti/Ca and Fe/K ratios are utilised to track terrigenous sources of inorganic sediment matter in marine cores – as precipitation levels increase so does the amount of erosional process depositing the land-based sediment into the cores.

XRF techniques, where they are very good at producing datasets rather quickly cannot give the full amount of information on its own. The technique is valuable in understanding sources of sediment input from different processes, but also must be assimilated using mathematic analyses before they are usable with other data sets. They can also be used to give more information that other proxy analyses cannot fully define (as seen in the Huarca chronology reconstruction in chapter 4).

There are also several sources of interference that can occur when using pXRF methods. These include particle-size, homogeneity of the sediments, moisture content of the sediments (where these are greater than 20%), and chemical-matrix effects causing some interference (Peinado et al., 2010). The latter point, for example, there can be some interference with As and Pb as they can have a shared spectral peak (McWhirt et al., 2012).

3.4 Normal Alkanes (*n*-Alkanes)

n-Alkanes are a class of leaf wax that are stable at low temperatures and are resistant to degradation and are often well-preserved in most sedimentary environments (Meyers, 1997). A fraction of the leaf waxes might be remineralised by microbial activity, but the waxes are more resistant to wear than many other biochemicals produced by plants. This means, therefore, that the amount of leaf waxes increases as the other more labile compounds are degraded. The specific compounds from wetlands and peat bogs can provide information of

palaeoenvironment and palaeoclimate in relation to vegetation changes. Because of their resilience in sedimentary records, they have the potential to inform of long-term changes in agricultural practices as well as pre-historic plant community changes through the Holocene. The below extraction was taken place at the British Geological Survey by Dr. Chris Vane and his team in the Organic Geochemistry Department.

3.4.1 Extraction and isolation

Sediments ~2.0 g and vegetation ~0.4 g were spiked with a surrogate standard of n-C24D50 (2000 ng in 100 µL of toluene) and allowed to equilibrate for approximately 16 hours. Samples were extracted in an accelerated solvent extraction system (ASE 350, Dionex, Thermo) using 30mL extraction cells with the sample mixed homogenously in an anhydrous sodium sulphate dispersant containing 1 g of copper powder to remove amorphous elemental sulphur. ASE conditions were: dichloromethane (DCM) and acetone (50:50) operated at 100°C at a pressure of 1500psi, with an oven heat-up time of 5 min and static time of 5 min, the total volume extract was 40mL. Extracts were evaporated to 'dryness' under a stream of dry nitrogen gas using a Turbovap operated at 40°C and reconstituted in a minimal volume of DCM and quantitatively transferred to 0.3g of silica (5% deactivated) and allowed to dry. The n-alkanes and aliphatic hydrocarbons were isolated by mini-column chromatography using a glass Pasteur pipette containing 0.9 g Silica (5% deactivated), conditioned with n-hexane. The analytes were eluted with 5mL of n-hexane. Extracts were reduced to 'dryness' with a gentle flow of dry nitrogen gas.

3.4.2 Urea Adduction

Urea ~10g was washed with n-hexane (3 x 30mL) and allowed to dry. The urea was dissolved in a minimum volume of methanol to produce a saturated solution. The sample extracts were dissolved in 2-3mL of hexane:acetone (2:1) to which the methanolic urea was added dropwise in excess. The resultant crystals were dried with a gentle flow of dry nitrogen gas and washed with n-hexane (3 x 2mL) with centrifuging between each wash, this contained the non-adducted compounds. The washed urea crystals were dissolved in deionised water (3-4mL) and the resulting aqueous solution extracted with n-hexane (3 x 3mL), this contained the adducted n-alkanes. Moisture was removed by passing the n-hexane (containing the n-alkanes) through a glass Pasture pipette containing anhydrous sodium sulphate into 10mL glass vial. The n-hexane was reduced to 0.9mL with a gentle flow of dry nitrogen gas, transferred into 2mL GCMS vial and spiked with an internal standard of squalane (2000ng in 100µL of toluene).

3.4.3 Gas Chromatography - Flame Ionisation Detector (GC-FID) Analysis

GC-FID analysis was performed on a Thermo Scientific Trace 1300 gas chromatograph (GC). Sample application (1 µL) was by split injection mode (1:5, 60°C to 300°C). The GC was fitted with an Agilent Technologies DB-1 capillary column (60 m length × 0.25 mm i.d. × 0.1 µm film thickness). The GC oven-temperature programme was 60°C (1 min. isothermal) to 320°C at

8°C/min (10min. isothermal). Helium was used as the carrier gas (1 mL/min). Data processing was performed using Chromeleon software (version 7.2.10). Chromatograms for all samples can be found in the appendices.

3.4.5 Applications of *n*-Alkanes

The lipid components of the leaf waxes, as briefly mentioned above, remain incredibly resistant to degradation and wear (Eglinton and Eglinton, 2008). This, therefore, means that they are incredibly valuable in understanding past-land uses (through identifying possible cultivation indicators) and lending an aid in determining the vegetational changes through time. There are, however, limitations to using *n*-alkanes as a proxy for environmental change, which relate to the factors resulting in their abundance and composition. For example, the leaves biomarkers transferred from land must be considered within the areas that have supplied them as well as the depositional environment and rates of transfer by the processes that have supplied them (Eglinton and Eglinton, 2008). There are also some questions about if decomposition alters the signals produced by the *n*-alkanes due to the uncertainties about the depositional processes (Thomas et al., 2021) and how this might affect the preservation of the vegetational signals. It is, therefore, desirable to use this proxy alongside other well established proxy data sources, that can give more information on the transport of the organic material, that produces the leaf wax signals.

Both the terrigenous and aquatic sources of *n*-alkanes are, ultimately, dependent on the climate-induced environmental changes (much like the stable isotopes as mentioned above) such as temperature and CO_2 pressure etc (Eglinton and Eglinton, 2008). The vegetation signals, therefore, are directly related to the climatic conditions that control the growth of the plants and the erosion of the landscape that transports the material into the basins. The most notable of these are temperature and aridity.

Lipid chain length is often used as a main indicator of the vegetation type. Odd chain lengths with high number of carbon atoms (for example C_{27} – a molecule with 27 carbon atoms in it's chain), indicate mainly terrigenous sources of plant material (Sikes et al., 2009; Seki et al., 2010, Chevalier et al., 2015), whereas shorter chain lengths (e.g. C_{17}) are characteristic of algal organic matter (Liu and Liu, 2016). There are some mid-length chains that are important to note (C_{21} to C_{25}) that are mainly submerged and aquatic plant life (Ficken et al., 2000). There are then some indices that are based on these chain lengths, which can be used to determine the composition of the soil organic matter (SOM). The principle one used in this study is Carbon Preference Index (CPI), which gives information on the odd/even chain predominance to determine the quality of the SOM and the contribution of external sources of input – such as petroleum hydrocarbons (Bray and Evans, 1961; Chevalier et al., 2015).

n-alkane studies have been conducted in a variety of environments in Peru, and South America ranging from terrestrial organic matter sources in marine sediments (Schneider et al., 1983; Farrington et al., 1987), studies on plant direct plant material in tropical ecosystems (Garcin et al., 2014; Graham et al., 2014; Feakins et al., 2016), analysis of signal preservation

and degradation along transects (Teunissen van Manen et al., 2020) and a variety of compound specific isotope analysis of the leaf waxes themselves (e.g. Fornace et al., 2014). The number, and range, of studies utilising this technique is testament to the flexibility of the proxy, to answer a number of environmental and climatic questions.

3.5 RockEval Pyrolysis

Each of the cores were sampled at a resolution of 8cm, or where irregular boundaries between units were identified. Sediments were first freeze dried and then powdered, using a ball mill, before analysis on the Rock-Eval(6) analyser. The fine powder allows for better and more complete burning. Samples must be freeze dried, as being oven dried may cause there to be some burning of the organic matter content.

The powdered samples (10mg) were heated at 200°C for 3 minutes, and then heated up to 650°C at a rate of 25°C/min, in an inert atmosphere of N_2. The residual carbon is then oxidised at 300°C to 850°C at 20°C/min.

The performance of the instrument was tested, every 8 to 10 samples, by comparison to accepted values of Institute Français du Pétrole standards (IFP 160000, S/N1 5-081840).

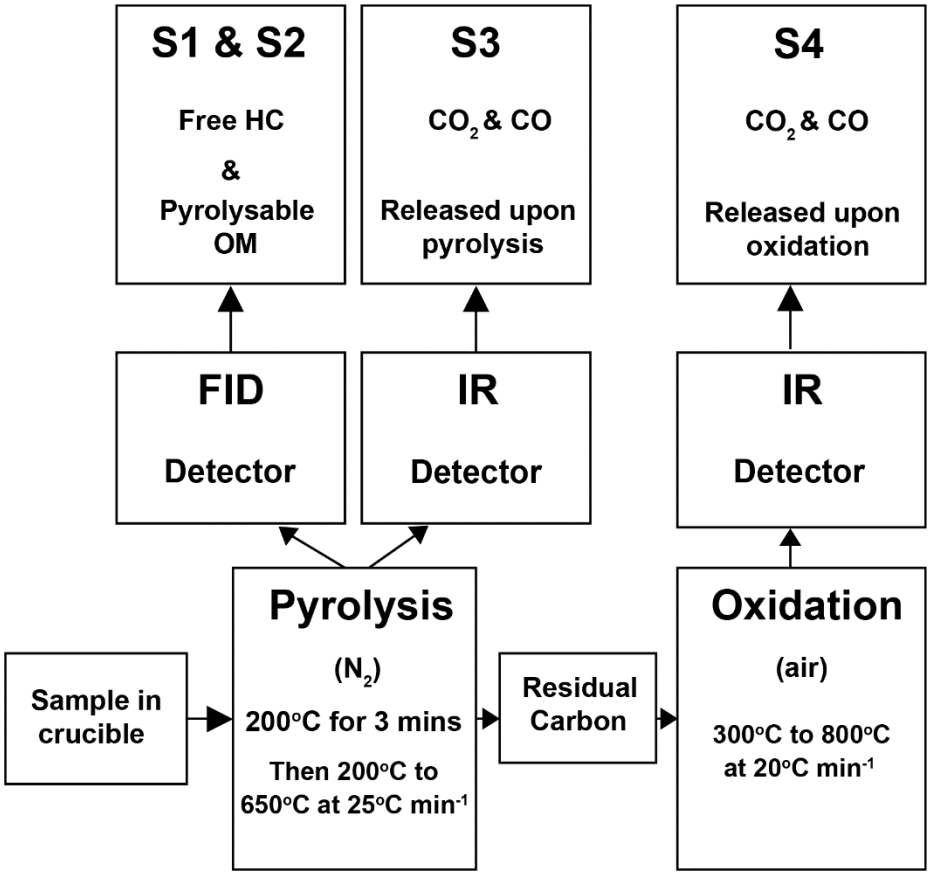

Figure 3.4: Operating procedure of the RockEval pyrolyser. FID = flame Ionisation detector. IR = Infrared. Diagram adapted from Disnar et al (2003).

The parameters of the instrument are determined as the amount of HC (free hydrocarbons) which can be expressed as mg/HC/g (S1), the hydrocarbons released through the thermal cracking of organic sediments (S2), carbon dioxide (CO_2) released during the pyrolysis (S3),

TOC and mineral carbon. The hydrocarbons are given as a proportion of the OM with the HI calculated as HI = S2 x 100/TOC, and the amount of oxygen in respect to the OM also similarly described as OI = S3 x 100/TOC.

The principles of how the analyser works, can be found above.

3.5.1 RockEval Pyrolysis Applications

RockEval pyrolysis is a method that is generally applied to study maturity of hydrocarbon bearing rocks, such as shales (Slowakiewicz et al., 2015; Könitzer et al., 2016), but has had recent success at tracking the changes in vegetation, sources of organic matter (OM), and degradation of unconsolidated sediment within lakes, peats, and coastal systems (Steinmann et al., 2003; Marchand et al., 2008; Englehart et al., 2013; Lacey et al., 2015; Newell et al., 2016; Mills et al., 2018).

One advantage of using RockEval pyrolysis is to provide total organic carbon (TOC%) values without the need for any pre-treatment for carbon mineralisation, to determine the organic carbon content. The TOC% descriptor pertains to the content of the OM and is made up of volatile hydrocarbons and cell wall biopolymers, as well as geopolymers such as humic substances and kerogen (Newell et al., 2016).

The hydrogen index (HI) is calculated using the formula S2 x 100/TOC and is an extent of organic matter hydrogenation as well as an estimation of pre- and post-depositional effects (Newell et al., 2016). In a similar vein, the oxygen index (OI) is calculated S3 x 100/TOC and provides an estimation of the amount of oxygen containing compounds, which increases upon the amount of aerobic decay (Slowakiewicz et al., 2015; Newell et al., 2016).

The last major parameter of note is the thermal maximum (T_{MAX}) which is provides an estimate of changes in OM type, due to the temperature at which bound hydrocarbons are broken is related to the properties of that OM (i.e. cellulose, lignin, xylans etc.) (Marchand et al., 2008).

This is a novel technique to South America, and indeed to palaeoenvironmental studies, so any comparative studies must be made from other sources.

One study, from Steinmann et al. (2003) aim to ratify the OM transport around Lake Neuchâtel. The TOC, HI, and OI parameters effectively trace the changes of the sedimentary OM. Most of the sedimentary changes are where there are well oxygenated sediments, which point to an effective shielding of OM by mineral particles leading to their preservation. The study uses the HI and OI index to point towards the type and origin of the OM within the cores, which have good agreement with terrestrial inputs, due to the ratio of OI and HI.

The study by Newell et al (2016), investigates the use of RockEval in riparian peatlands, to understand the palaeohydrology of the peatland. They point out that the use of RockEval can quickly and ‘cost effectively’ be used to track the organic matter change and subsequent vegetational coverage of a wetland.

There are, as with all proxy analyses, limitations to using the RockEval method. Some studies have shown that variations in the mineral matrix and organic enrichment can affect both the hydrocarbon and CO_2 concentrations; and therefore, has a knock-on effect with the HI and OI ratios (Katz, 1983). This then implies that researchers must apply some caution when expressing the type of vegetation when using this approach. A given characteristic may then give varied OI and HI values, if not used correctly.

3.6 Non-Pollen Palynomorphs (NPPs)

1cm^3 sub samples were taken along a broad horizon of points along the cores, that were driven by large deflections in the geochemistry plots. For example, where signals in the isotope record deviated by a significant amount due to external forcing, it was deemed necessary to identify the NPP assemblages before and during these peaks.

Each sample was left in 25ml of 1% Sodium Pyrophosphate and left on a hotplate for 40 minutes to allow for deflocculation to occur and to remove the humic acid. A tablet of *Lycopodium* was added to each of the samples at this point also.

A 20µm top mesh was used to remove any large mineral and organic matter, with a bottom 5µm mesh to remove the finer material. 20µm was deemed a large enough mesh to allow for any *Sporormiella* and other dung-related spores to pass through, while keeping out any larger inorganic material.

The material left was transferred to individual micro-centrifuge tubes, with 1.5ml of distilled water added to them. They were each centrifuged at 2500rpm for 5 minutes, and the supernatant poured off afterwards.

After this first centrifuge, saffarin was added to each of the samples and topped up with more distilled water. All samples were then centrifuged again at 2500rpm for 5 minutes. The supernatant was poured off again afterwards.

A small amount of glycerol jelly was added to the samples and mixed together with a wooden stick which was then transferred to a glass slide with a cover slip applied. It was felt that there was no need for any heavy separation or acetolysis during the methodology, as the sieving method applied would get rid of most of the organic material and would leave behind the notable NPPs.

3.6.1 NPP applications

Non-Pollen Palynomorphs (NPPs) include a variety of spores, ferns, mosses, cyanobacteria, and invertebrate remains. A large amount of these have been identified and described, but there are a large proportion that have no ecological or taxonomic information associated with them; therefore, are unusable in any study of palaeo vegetation. Fungal spores deposited in peat have been collected more readily than those within lake sediments, due to the localised nature of spore deposition; as often they become fossilised close to their dispersal zone (van Geel, 2001).

NPPs can give details on human activity, herbivory (through the presence of coprophilous fungal remains), vegetation changes and depositional environment (e.g., some can give information on open water systems, others on drier environments etc).

This study tried to focus more on the identification of *Sporormiella* (figure 3.4), as it has often been suggested to offer a proxy measure of herbivore presence and abundance in palaeoenvironments (Davis and Shafer, 2006; Raper and Bush, 2009; Chepstow-Lusty et al., 2019). However, Holocene samples typically do not contain *Sporormiella* spores, and when they are identified they do not usually exceed 1% of the total assemblage (Davis and Shafer, 2006). This then, poses a problem when using one taxon for herbivory identification; therefore this study widened its scope for identification of a wider variety of NPPs and recorded a total assemblage to record changes in vegetation, environmental change, human disturbance, and possible pastoral agricultural practices.

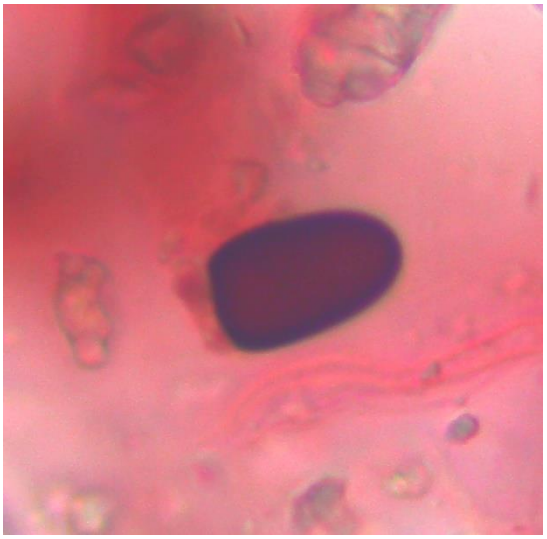

Figure 3.5: Sporormiella spore recovered from the study, photo taken at 40x magnification.

Many coprophilous fungal remains, and indeed many NPP analyses, have been undertaken as part of a wider study utilising pollen or phytoliths within lacustrine and peatland systems. This said, however, the study by Chepstow-Lusty et al (2019) is one of the few studies utilising dung fungi, as a main indicator. Here the authors examine the use of *Sporormiella* spores from Marcacocha (Cusco, Peru). Previous studies, at the same site, reveal that herbivore density reflect the proportion of oribatid mites at this location. The study itself then tests the assumption that the relative proportion of *Sporormiella* would likely respond in a similar way to the mite concentrations. The authors then find that the *Sporormiella* concentrations do not reflect the major changes in the density of herbivores in the region but does reflect the changes in lake level.

3.7 Summary of methods

Below is a short tabular summary of the applications, and limitations for the analytical methods used in this study.

Method	Applications	Limitations
Stable isotopes	- Important proxy to understand human-induced climate change. - Can provide information on vegetation type and coverage. - Indirect evidence of climatic changes, as vegetation coverage comes as a result of climate change. - Scan for cultivars (C_4 plant type) - Sulphur isotopes use as pollutant indicator. - Differentiating types of fauna (e.g., bacteria)	- Cannot be used as a sole indicator of vegetational change, should be used as part of a multi-proxy analysis. - Questions surrounding fractionation may need to be considered before applying the method in environmental research
pXRF	- Rapid datasets gathered from sediments. - Includes lots of different elements in the study. - Can give background information on soil chemistry, mining history, anthropogenic contaminant history. - Adds to stronger PCA testing of other methods (see Chapter 5)	- Invaluable information gathered in a quick time frame although needs to be added as part of a wider network of proxies. - Several sources of interference that can occur, including: moisture, chemical-matrix interaction, particle size, and homogeneity of sediment
n-Alkanes	- Class of leaf wax that are stable at low temperatures and preserve well. - Potential to infer long-term changes in agricultural practices and pre-historic plant community change. - Application to some land-use change (in the form of providing information on plant changes)	- Limitations relate to the abundance and composition (e.g., the leaves biomarkers transferred from land must be considered within the areas that have supplied them as well as the depositional environment and rates of transfer by the processes that have supplied them) - Some questions on if decomposition can affect the makeup of the n-alkanes
Rock-Eval	- Novel method to understand the sources of organic matter. - Has been shown that the method can track sources of OM input and vegetational changes. - Some interesting results when used to track sources of 'old carbon' (see chapter 4).	- Mineral matrix variations and organic matter enrichment can influence the hydrocarbon content and CO_2 concentrations, which could make the HI and OI values unusable to track vegetation change
NPPs	- Track herbivory and humans in the landscape	- Lots of NPPs have no taxonomic details attached to them. - Questions on the dispersal of some of the spores. - Lack of knowledge if Sporormiella can be used to effectively track herbivory

4. Huarca Basin

4.1 Introduction

Chapter 4 sets out the results and analysis of the Huarca wetland, Ancash Region. The first section focusses on the main archaeological history of the region, as a way of introducing the history of the wetland and its surroundings. This is followed by a brief section of the methodology (more can be found in Chapter 3). A full description of the results follows this, including the sedimentology, inorganic and organic geochemistry, and the palaeoecological analysis. Finally, the results are discussed in conjunction with previously published literature, to make some comparisons of where this site fits in with the rest of the South American environmental datasets.

4.4.1 Regional Archaeology

Early Horizon (2,150-2,750 BP)

The Early Horizon (EH), in the Ancash region, was a period of widespread construction, development of religious ideology and adoption of ceramics (Arkush and Tung, 2013). During this period Chavín-related goods and styles reached a peak, with the culture thriving at a time of relative peace (Arkush and Tung, 2013). Interregional exchanges of valuable materials intensified during the EH, between the Chavín and other regional polities, which can be seen through burial sites throughout the northern highlands through this time. It wasn't until ~2,350 BP that defensive structures began to increase as interregional trading lapsed and conflict began to rise (Billman, 1996; Arkush and Tung, 2013).

Towards the end of the EH the Chavín culture civilisation collapsed, which coincided with a widespread disruption of social patterns in the Ancash region (Burger, 1985; Lau, 2007; 2016). There are ceramic changes associated with groups called 'Huaras', which a considered to be a precursor to the Recuay people, as well as differentiations with settlement patterns who had largely rejected the idea of Chavín religious ideology (Lau, 2007; 2016). Some of the Huaras settlements had been built directly on top of the original Chavín structures, which had seen a decline in use from 2,350 BP and had started to fall into disrepair (Arkush and Tung, 2013; Handley, 2022).

Early Intermediate Period (1,250-2,150 BP)

The Early Intermediate Period (EIP) is generally made up of the Recuay culture and is split into four further sub-divisions, which includes the latter stages of the EH and some initial periods of the Middle Horizon (MH): Huaras Phase (1,700-2,150 BP), Recuay Phase (1,350-1,700 BP), Late Recuay (1,250-1,350 BP) and Wilkawain (1,050-1,250 BP). Recuay culture emerged as part of the mass regional developments that occurred during the LIP (Lau, 2004). The time of socio-economic innovations, including the formation of expansionist ideals, urban

centres, technologies, new religious ideals and economic production between regions (Lau, 2004). Many of these centres occupied strategic locations on hilltops, which were often part of vital economic exchange routes, with smaller communities established to make use of the higher altitude pastoral *puna* zone for camelid herding, or the *quechua* zone for agricultural practices (Lau, 2001; 2004).

The creation of hilltop settlements dates to the earlier Huaras phase, which was later implemented by their Recuay counterparts (Lau, 2016). The smaller villages were commonly found at these higher altitudes, between 3,500-4,100m a.s.l. which allowed for access to multiple agricultural zones (Handley, 2022). The early Recuay expansion, through the highlands, may have been aided by favourable climatic conditions between 1,650-1,450 cal yr BP as seen in the Huascarán record (Thompson, 2001; Lau, 2011). Colder conditions prevailed shortly after this, from 1,450-1,250 cal yr BP, and would have brought limitations to the amount of arable land available for agriculture (Thompson, 2001; Lau, 2011). There are some suggestions that temperature decreases of as little of 1°C or 2°C could lower the limits of agricultural lands by 200-400m (Cardich, 1985; Lau, 2007). This reduction in agricultural land may have resulted in the demise of the Recuay culture in the early stages of the 8th Century (Lau, 2007; 2011).

The end of the Recuay was signalled by 1,250 cal yr BP, with the growing influence of Wari culture. The distinctive styles and imagery of the Recuay culture had all been abandoned in favour of the Wari style by this point, which is the definitive end of the Recuay influence in the Ancash region (Lau, 2004).

Middle Horizon – Wilkawain (1,050-1,250 BP)

With the expansion of the Wari and the collapse of the Recuay culture, into the MH, the boundaries between communities become more permeable with greater external influences placed on the region (Lau, 2002, 2004). More Wari style pottery has been recovered from the region, which was of a “non-local” origin in contrast to the Recuay before them, indicative of a wider influence from a larger empire state (Lau, 2002). The presence of the Wari, in Ancash, was not just for an administrative purpose, but as part of the core expansionist ideals of the Wari polity (Lau, 2004). Some settlements show a variation of Wari influence with some sites having little to no evidence of Wari ceramics, textiles or iconography (e.g., Pashash), with others like Chichawas maintaining their local ideals while integrating Wari culture (Handley, 2022).

During the MH settlement location was an important factor, especially for the Wari, with proximity to exchange networks being a critical factor (Lau, 2012). Communities such as Wilkawain and Chinchawas, which were located close to important transport highways, and those located next to bottlenecks like Honcopampa grew increasingly more important (Lau, 2012). These settlements all saw sudden increases in building regimes and population growth, which is not surprising due to their prominent positions and careful management from the central Wari powers (Lau, 2012). Well-located settlements with a multitude of purposes, such

as the ones above, ranging from funerary, public, residential and administrative sectors appear to have been the main contexts for early Wari interactions in Ancash (Lau, 2007; 2012). There is some debate, however, to the validity of the importance of Honcopampa is to the Wari and if it was a Wari site to begin with. The architectural styles don't typify Wari tradition and point towards more of a local focus, with the archaeology suggesting that population interacted with the Wari empire and adopted their customs but did not form part of its state (Lau, 2001; 2012).

The Chinchawas culture, of the MH, is another example of such mixing. The Chinchawas settlement is located in a location of power, along an important trading route through the Casma Valley across the Cordillera Negra (Lau, 2005). The main expansion of the culture took place ~1,150-1,050 cal yr BP and was associated with the expansion of the Wari state. Throughout the occupation of the Chinchawas camelids were the primary goods exchanged between the two peoples, due to the settlement's location, which was situated at high altitude to exploit the *puna* grasslands for camelid pastures (Lau, 2007).

Cultural interactions slowed towards the end of the MH, with Wari influence gradually dwindling by 1,000 cal yr BP. Climate likely played a significant role in shaping access to local resources and subsistence strategies in the highland settlements, such as that of the Chinchawas. Given its location at the upper limits of agriculture, long-term changes in climate would alter production of food resources in these local regions (Lau, 2007). This could be said across vast swathes of similar settlements across northern Peru.

Late Intermediate Period (500-1,050 BP)

The LIP is recorded as a time of increase regional specialism of regional styles, as cultures fragmented after the Wari empire diminished after the MH (Lau, 2016). This opened up more areas of conflict, in the highlands, with an increased reliance and importance of fortifying hilltop settlements (Handley, 2022). The archaeology shows and increased amount of warfare during the LIP, but this was mainly between smaller settlements vying for control of small areas of land (Arkush and Tong, 2013).

The LIP centred around the creation of complex water management complexes, with a suite of silt dams, reservoirs and irrigation systems (Lane, 2009). This type of hydraulic advancement was key for large-scale camelid herding as it provided them with a range of plant life for grazing and as an area for watering (Lane, 2009). The move to pastoral agricultural activities was likely influenced by the settlement locations at the higher altitudes, which were above the key zone for agriculture (Aguilar Diaz, 2019).

Late Horizon (418-500 BP)

Ancash, during the LH, belonged to one of four Inca sectors called Chinchasuyu. In contrast to some of the cultures that had proceeded them, a great deal of settlement development was undertaken on the flat land. These developments were often close to large state roads and were likely more dedicated to administrative functions for the Inca state (Lau, 2016). Pachacamac makes mention of a number of sites along a state road, which makes its way

through Ancash, including that of Choquerecuay (also called Pueblo Viejo) (Bernabé, 2017). There are some indications from religious iconography and construction that the site was repurposed as and administrative centre by the Inca, after periods of occupation dating back to the EIP (Bernabé, 2017, Aguilar Diaz, 2019). Its favourable location between the limits of the *quechua* and *puna* zones, with close proximity to the Santa river, the area would have likely produced a variety of cultivated plants and would have had access to large areas for camelid grazing (Tantaleán and Carmen, 2004; Bernabé, 2017).

The site itself is spreads over some 44ha preserving some Inca influences in its design, such as its stepped square which stands out for its volume and was used mainly as a meeting place for the Incan elite to host ceremonies, for the redistribution of goods (Tantaleán and Carmen, 2004; Bernabé, 2017). It is thought that, however, there is some differentiation in architectural influences that make the site not truly Inca even though Choquerecuay was under direct control of the Inca (Tantaleán and Carmen, 2004). There are similar accounts of this from other sites across the Inca empire, where many of the sites were designed by the Inca but were built by the local labour forces and that the local crafts people could have had some influence over the variation in designs (Tantaleán and Carmen, 2004; Handley, 2022).

4.2 Study Area and Site Description

The village of Huarca, Yungay, Peru (9°5’55” S 77°42’45” W) (Figure 4.1) is situated in the Cordillera Blanca at 3190m above sea level. The large in-filled basin is surrounded by pre-Columbian agricultural terraces, and modern agricultural systems that are cultivating potato, maize, and quinoa. There is also some evidence of modern pig, sheep, cattle alongside more traditional camelid farming within the surrounding area, which is thought to have been the case in pre-Columbian times. Huarca sits in the shadow of both Nevado Huandoy and Huascarán within proximity to the Llanganuco gorge, suggesting that the morphology of the landscape is glacial in origin – most likely being closed off by moraines, giving the basin its shape.

There is also some evidence of mass flow movement into the basin towards its Eastern edge. Lake Keushu is directly above the wetland at 3,800m a.s.l, which is an important archaeological site. The area includes ceremonial, mortuary and domestic architecture spanning from the beginning of the Initial period to the early Colonial Period (c. 2000BC – AD1570) (Gerdau-Radonic and Herrera, 2010). There is very little other archaeology in the regions adjacent to Huarca, other than at Keushu and the terrace systems – which may have been used by the same peoples at Keushu.

Figure 4.1: Map of the basin of Huarca, within the Yungay province. The proximal ice caps at Huandoy and Huascaran can be seen to the right of the map, along with the modern glacial extent. Keushu is also added to this map as it is a site of archaeological significance. Inset is the location of the Huarca basin in relation to major quaternary records in Peru. Map created in QGIS using the ESRI satellite plug-in.

Figure 4.2: Huarca basin with modern agricultural systems, utilising older terrace systems. Nevado Huandoy can be seen in the background.

Figure 4.3: The field site of the Huarca basin with the modern vegetation cover. Some modern buildings of the village can be identified in the background. Nevado Huandoy (left) and Nevado Huascaran (Right) can be seen in the background.

4.3 Methodology

For the main methods used at Huarca, please see the methodology section (Chapter 3).

4.3.1 Field Methods

The sampling site for the central basin core was decided in a coring programme in 2018 with a maximum depth of 4.7m (see Handley, 2022), as it is the most central location suitable for coring. The main idea for this location was that it offered a chance to analyse vegetation signals from the local area, which would include the modern anthropogenic signals from the current farming systems close to the basin – hence the same site was selected for re-coring in 2019 (this study). Three replicate cores of 3.7m were gathered in 2019 using a standard Russian peat corer. Some of the isotopic analysis was carried out on the 2018 core, as this gave a greater depth than the newer core material.

During the 2019 season, a second core (named the Edge core) was gathered near to the northern edge of the basin (see figure 4.1 above), close to relic terraces (09°5’49” S 77°42’45.2” W) at a maximum depth of 8.56m, with two other replicates reaching 2.9m – as this is where we thought this part of the basin was ~2500 years old based on the stratigraphic matching of the core material with the central basin core. Being so close to relic terraces also gives an advantage in understanding human societal changes, due to climatic changes, as well as farming regimes through the use of Zea mays and coprophilous fungal spore counting. Zea mays is a key indicator of pre-Columbian food production throughout South America (Branch et al., 2007; Bush et al., 2007, Whitney et al., 2012). Due to its size (55 – 120µm), however, Zea mays has a poor dispersion rate from the parent plant which has been shown in both field and laboratory studies (Raynor et al., 1972; Aylor, 2002; Jarosz et al., 2003). Similarly, coprophilous fungal spores (such as Sporormiella) have been utilised as a proxy for the density of wild and domesticated animals (Davis and Schafer, 2006). These proxies are more abundant nearer to basin edges and often show a decline in abundance closer to the middle of the basin (e.g., Rapper and Bush 2009). For these reasons taking a core closer to the terraces seemed to be a viable option to pick up these signals.

Figure 4.4: Coring site for the Huarca Central basin core. There are modern artificial channels that have been cut into the surface of the wetland, that the locals use as drainage ditches, close to the coring location.

Figure 4.5: Coring location of the Huarca Edge core (as indicated by the red arrow). This location was picked due to its accessibility closer to the relic terraces (to the right of the image). Photograph by Stuart Black.

4.4 Results

4.4.1 Sedimentary Analysis

Central Basin Core

The 4.7m sequence of the central basin core (made up of a composite of both 2018 and 2019 cores) is detailed below, it comprises of 20 units (fig 4.6). The base of the core is estimated to be, which is rich in fine and coarse sands resulting in a low organic matter content of 3% possibly relating to a more open water system. Units 2 – 4 (443-283cm), which are comprised of organic rich peats more likely due to a slower water flow to the basin, has resulted in a slow accumulation of sediment within the basin. Organic matter rises sharply, as identified in the LOI, at the contact between units 1 and 2 with the values at their highest point here (97%) at 400cm.

LOI remains high throughout unit 2, reaching 83.0% at 368cm, but this declines to 52.9% towards the top of the unit where there is a sharp contact to coarser sediments. Herbaceous peat continues from 283 - 311cm, with a high abundance of plant macrofossils throughout this section. Between 281-283cm, the peat units are punctuated by a return to silty material (unit 5). The LOI still remains high (~70%) here, which relates to more organic silts at this depth. Units 8 – 12 are represented by a large influx of inorganic sediments, made up of fine to coarse sands with some visible gravels through the core. During this time the LOI values are very low (1-5%%). This low point is found in unit 10, where the coarsest of the sand units is found. Peat formation resumes from 167cm, until 140cm, LOI reaches 58.6% at 144cm before falling to 0.9% shortly after. At 140cm (unit 14) there is another intrusion of sands.

The formation of herbaceous peats starts again at 119cm and is punctuated by a thin layer of silty clays (unit 18) at 98 – 102cm and again at 74 – 77cm. LOI values take some time to rise form a low of 0.9% at 128cm to 44.3% at 96cm and increase to 83.0% by 48cm. Values do fluctuate in the top 50cm of the core, but this is due to short lived inputs of silty clays into this part of the basin, like those described above.

Huarca Edge Core

The edge cores relate to one long core (of 8.56m) and two shorter cores (of 2.9m), the main sedimentary units of each are discussed below. Unit 1 begins with gravels at the base of the unit fining upwards into sands of varying coarseness, with a diffuse boundary to unit 2 – which consists of clays and silts. Organic matter is low, as to be expected, with values of 3.5% (Unit 1) and 23.8% (Unit 2) as given by LOI. Unit 3 is made up of mostly organic clays with a sharp contact to Unit 4, which consists of peats, with large plant macrofossils present throughout. The peat units here (Unit 4 and 5) are quite thick (~1m in total).

A thin unit of silty clay material, with sharp upper and lower boundaries, is identified between peat layers at 733cm. Peat formation resumes from 733 to 641cm (Units 7 to 9), which contain some clay within the sediment as well as an abundance of plant macrofossils. LOI values

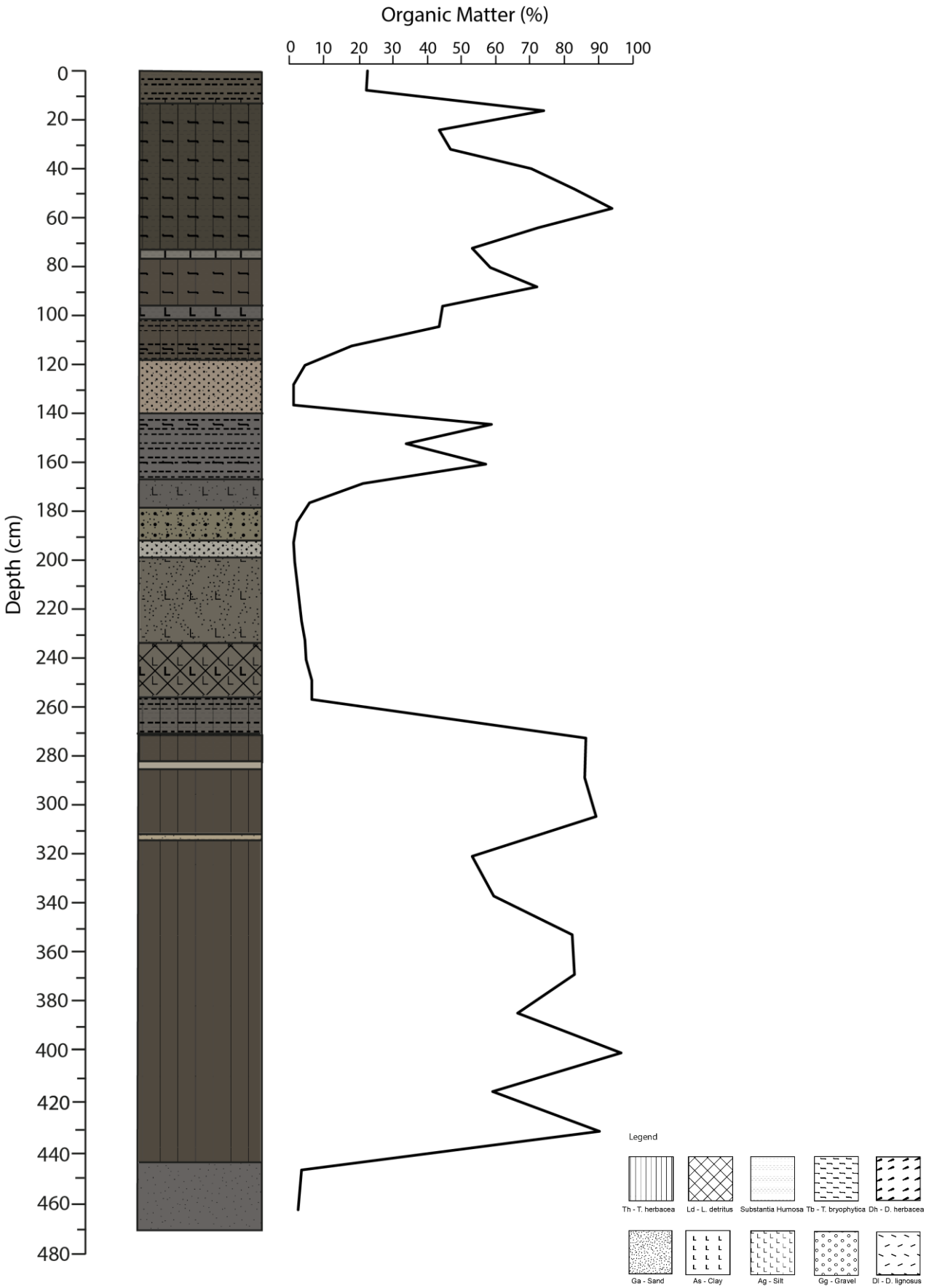

Figure 4.6: Stratigraphic log of the Huarca Central Basin sequence with Loss on Ignition (LOI) values expressed on the right-hand axis.

fluctuate throughout these units, reaching a low of 736cm (12.05%) and 688cm (28.51%), where there are some intrusions of minerogenic sediments within the peat units. There is a diffuse gradient, at the top of unit 9, to fine grained sediment of silty clays. This gradient can be observed in the gradual lower LOI values, reaching 29% at 640cm – during the diffuse gradient into unit 10.

Units 11-13 (491 – 681cm) represent continued peat growth at the edge of the basin, which are punctuated by short periods of silt material. Unit 12 contains more silt material than the units above and below it, which also sees a slight decrease in LOI values from 81.5% to 63.4% as the sediment input becomes less organic. Overlying these units there are several clay units containing organic material from 491-442cm (units 14-18) there are some plant macrofossils throughout these units, but the LOI values start to decrease from 81.2% at the lower contact of unit 14 to 10.9% at the mid-point of unit 18 – where there is some in wash of sediments from an unknown origin. These values start to increase again from 456cm to 84.5% at 448cm. Unit 19 (404-442cm) is a continuation of peat formation, which is punctuated by some banding of clay at 442 – 430cm. Peat formation continues through Units 20-24 (404-354cm), but clay inputs increase through the units which is identified by the LOI%, as organic matter drops from 73.9% at 368cm to 26.8% at 360cm. Organic rich clays continue into unit 25 (352-334cm) as LOI values return to 81.9% before decreasing again, to 48.1%, through the diffuse contact with the unit above.

Units 26 and 27 (334-295cm) represent a large minerogenic input, similar to the one identified in the Central Basin Core (fig 4.7), but the Edge core does not contain any visible clasts. It is a thick silty clay unit, with low organic matter (~13%) throughout. Organic matter formation resumes in unit 28, which is a diffuse contact with the unit it overlies. There is a distinct present of clay sedimentation, but this gradually becomes less the further up the unit. TOC% values point towards this, as LOI values rise from 13.8% at the base of unit 28 to 52.2% at the top end. Peat continues to build-up from units 29 – 32 (258-83cm), with less humified peats during units 29-30 which become more humified through time. There are some clay/silt inclusions at 203cm, 197cm and 150cm. LOI values remain high (~85%) through this part of the sequence, only lowering due to the short minerogenic layers (e.g., 40.2% at ~200cm).

Overlying this layer of peat there are 4 distinct minerogenic units of silty clays (units 33-36; 83-65cm), with some evidence of plant macrofossils in them, the LOI values drop to 5.2% through these units. The finer sediments gradually lessen towards the top end of unit 36, as more organic peats form again from 54cm until the present day – with LOI rising from 24.8% at 64cm to 62.5% at 32cm. There is some evidence of *Phragmites* material within unit 37, another indicator of a lacustrine environment in the near past.

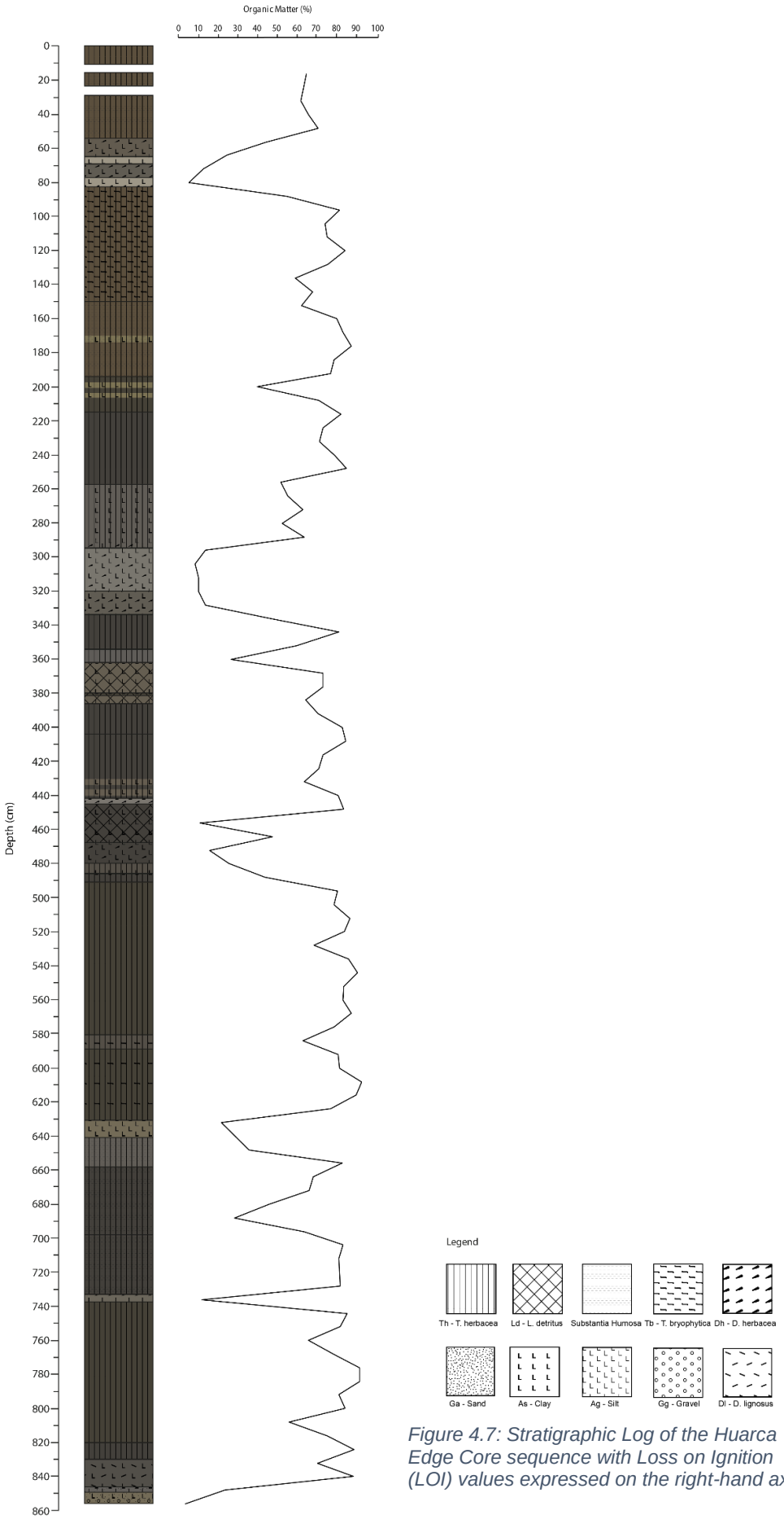

Figure 4.7: Stratigraphic Log of the Huarca Edge Core sequence with Loss on Ignition (LOI) values expressed on the right-hand axis.

4.4.2 Radiocarbon dating programme

Central Basin Core

There are currently 18 radiocarbon samples, taken from the central basin core (see table 4.2 below), which were selected based on the following criteria. All dates can be found in the appendices, along with the modelled ages.

1. High organic matter values or where there was high availability of plant macrofossils.
2. Proximity to environmental shifts, observed in geochemical analyses.
3. Where there is a large amount of sediment input (see section 4.4.2), radiocarbon dates are needed to "bracket" this event.
4. 1 date was taken to test the hypothesis that the Rock-Eval 6 pyrolysis method is able to detect sources of older carbon, within a sedimentary sequence.

The purpose of carrying out this programme was to provide a high-resolution record to constrain major paleoenvironmental shifts recorded in the sedimentary sequences, in order to compare them to existing terrestrial, marine, speleothem, and ice core records which span the length of the cultural horizons. Several of the dates were omitted from the final model, as they had a poor agreement due to causing age reversals or where the output modelled the agreement at less than 60% (see Bronk Ramsey, 2009). There are large age differences between the picked plant material ages and the bulk humic fractions, which will be discussed further in chapter 6. The dates with the code UCIAMS, did not report back the $\delta^{13}C$ measurements and so are missing from the final table.

The age-depth model (Fig 4.8) was created using OxCal 4.4 (Bronk Ramsey, 2009a) and the current IntCal20 calibration curve (Reimer et al., 2020). The model suggests that sediment started accumulating, in this part of the basin, at 11,470 cal yr B.P. (Before Present) possibly because of retreating ice at the end of the last glaciation. This point, however, has been interpolated from the basal radiocarbon date at 433cm and sedimentation could have begun later than this date. The top of the core is more modern, with a modern date of AD 2006.

Table 4.2: Results of the radiocarbon dating programme for the Huarca Central Basin core

Lab No.	Sample ID	Sample Depth (cm)	Radiocarbon Age BP	Calibrated Date Cal yr. BP (95% confidence)	$\delta^{13}C‰$	Material Dated
SUERC-84607	HURC-18-18	18-19	333±34	309-475	-25	Picked Plant Material
SUERC-99698	HURC-1-42	42-43	408±37	320-522	-27.4	Picked Plant Material
SUERC-99699	HURC-2-56	56-57	564±37	521-646	-24.9	Picked Plant Material
SUERC-99700	HURC-3-88	88-89	359±37	314-495	-27.2	Picked Plant Material
SUERC-99701	HURC-4-108	108-109	623±37	548-659	-27.6	Picked Plant Material
SUERC-99702	HURC-5-144	144-145	1001±37	793-960	-26.5	Bulk Organic Sediment

SUERC-99703	HURC-6-165	165-166	1215±37	1008-1270	-24.5	Bulk Organic Sediment
UCIAMS-267787	HURC-7-232	232-233	2009±35	1833-2045	-	Bulk Organic Sediment
SUERC-84608	HURC-18-273	273-274	3011±34	3075-3337	-23.7	Bulk Organic Sediment
UCIAMS-267804	HURC-8-311/1	311-312	2791±35	2783-2991	-	Picked Plant Material
UCIAMS-267788	HURC-8-311/2	311-312	3768±35	3988-4244	-	Bulk Organic Sediment
UCIAMS-267805	HURC-9-350/1	350-351	6416±35	7270-7423	-	Picked Plant Material
UCIAMS-267789	HURC-9-350/2	350-351	8969±35	9916-10231	-	Bulk Organic Sediment
UCIAMS-267806	HURC-10-370/1	370-371	5947±35	6672-6682	-	Picked Plant Material
UCIAMS-267790	HURC-10-370/2	370-371	8158±35	9008-9266	-	Bulk Organic Sediment
UCIAMS-267807	HURC-11-400/1	400-401	7229±35	7964-8170	-	Picked Plant Material
UCIAMS-267791	HURC-11-400/2	400-401	8910±35	9905-10184	-	Bulk Organic Sediment
SUERC-84609	HURC-18-432	432-433	9339±34	10419-10660	-20	Bulk Organic Sediment

Huarca Edge Core

There are a total of 13 radiocarbon dates for the basin edge core (see table 4.9 below). The radiocarbon dating programme was selected on similar criteria as the central basin core but was also needed to create a robust chronology for the whole core, as previously there were no dates associated with it. As with the central basin core, some of the dates were omitted due to poor agreement with the model due to creating age reversals from younger dates from plant material vs bulk humic fractions. A composite age model, which uses both plant and humic dates can be found in figure 4.9.

Table 4.3: Results of the radiocarbon dating programme for the Huarca basin edge core

Lab No.	Sample ID	Sample Depth (cm)	Radiocarbon Age BP	Calibrated Date Cal yr. BP (95% confidence)	Material Dated
UCIAMS-267808	EDGE-1-40/1	40-41	n/a modern	1963-1980AD	Picked Plant Material
UCIAMS-267792	EDGE-1-40/2	40-41	n/a modern	1962-1984AD	Bulk Organic Sediment
UCIAMS-267809	EDGE-2-104/1	104-105	70±35	25-263	Picked Plant Material
UCIAMS-267793	EDGE-2-104/2	104-105	266±35	151-453	Bulk Organic Sediment
UCIAMS-267810	EDGE-3-116/1	116-117	55±35	31-259	Picked Plant Material
UCIAMS-267796	EDGE-3-116/2	116-117	308±35	297-466	Bulk Organic Sediment
UCIAMS-267811	EDGE-4-232/1	232-233	848±35	681-898	Picked Plant Material
UCIAMS-267797	EDGE-4-232/2	232-233	947±35	775-926	Bulk Organic Sediment

UCIAMS-267798	EDGE-5-344	344-345	2512±35	2470-2739	Bulk Organic Sediment
UCIAMS-267813	EDGE-6-624/1	624-325	5794±35	6491-6674	Picked Plant Material
UCIAMS-267799	EDGE-6-624/2	624-325	6361±35	7167-7420	Bulk Organic Sediment
UCIAMS-267800	EDGE-7-656	656-657	7528±35	8206-8408	Bulk Organic Sediment
UCIAMS-267801	EDGE-8-824	824-825	9898±36	11224-11399	Bulk Organic Sediment

4.4.2.1 *Notes on the radiocarbon dating programme*

As mentioned above the radiocarbon programme was designed in order to either directly date or capture the age ranges of sedimentary events, or key deflections in the proxy data. An example of this is sample "SUERC-99703" which was used to target the large deflection in the $\delta^{13}C$ dataset. For a number of these radiocarbon dates, this study selected both bulk and plant samples, from the same depth, in order to test the hypothesis that the RockEval was sensitive enough to detect sources of "old carbon" – this is discussed further in section 4.4.3.1.

The samples that have radiocarbon ages associated with them have small age ranges and are well constrained. The modelled age ranges, in the central basin core, that are before 160cm are also well constrained by the Oxcal program. Where there are large age ranges, are where the material is under the large zone of coarse clasts. These large ranges make it more difficult to be as precise as possible, when making comparisons to other quaternary sites. Where the large ranges are most pronounced, in the central core, is between samples "SUERC-84608" and "UCIAMS-267806" where there is a difference of almost 1m with no dating methods applied to the sediments here. The sigma errors are up to ±833 years, which are the largest margins for this site (see appendix and figure 4.8). To improve on these errors there should be more dating methods applied to them, using a targeted approach backed up by proxy data.

The edge core dates were chosen along the same rationale as the central basin, whereby the dates assigned were driven by the proxy analyses. The full rationale for the UCIAMS dates can be found in the appendices, as these dates were fully funded by NERC for this project. As with the central basin core, the radiocarbon dates are well constrained as are the younger of the modelled age ranges – between UCIAMS-267811 and the basin surface. There are 3 large modelled age ranges in this sequence, the most pronounced of which is between samples UCIAMS-267798 and UCIAMS-267813 where the modelled age ranges reach a maximum of ±824 years (see appendix and figure 4.9). There are only 7 usable dates for this radiocarbon profile, and so this core may benefit from a more expansive dating programme to ratify some of these large margins. As this study uses many of the shorter cores (mentioned above) for the proxy analysis, we can be sure that the inter-site comparisons are robust as these are where the most constrained modelled age ranges are.

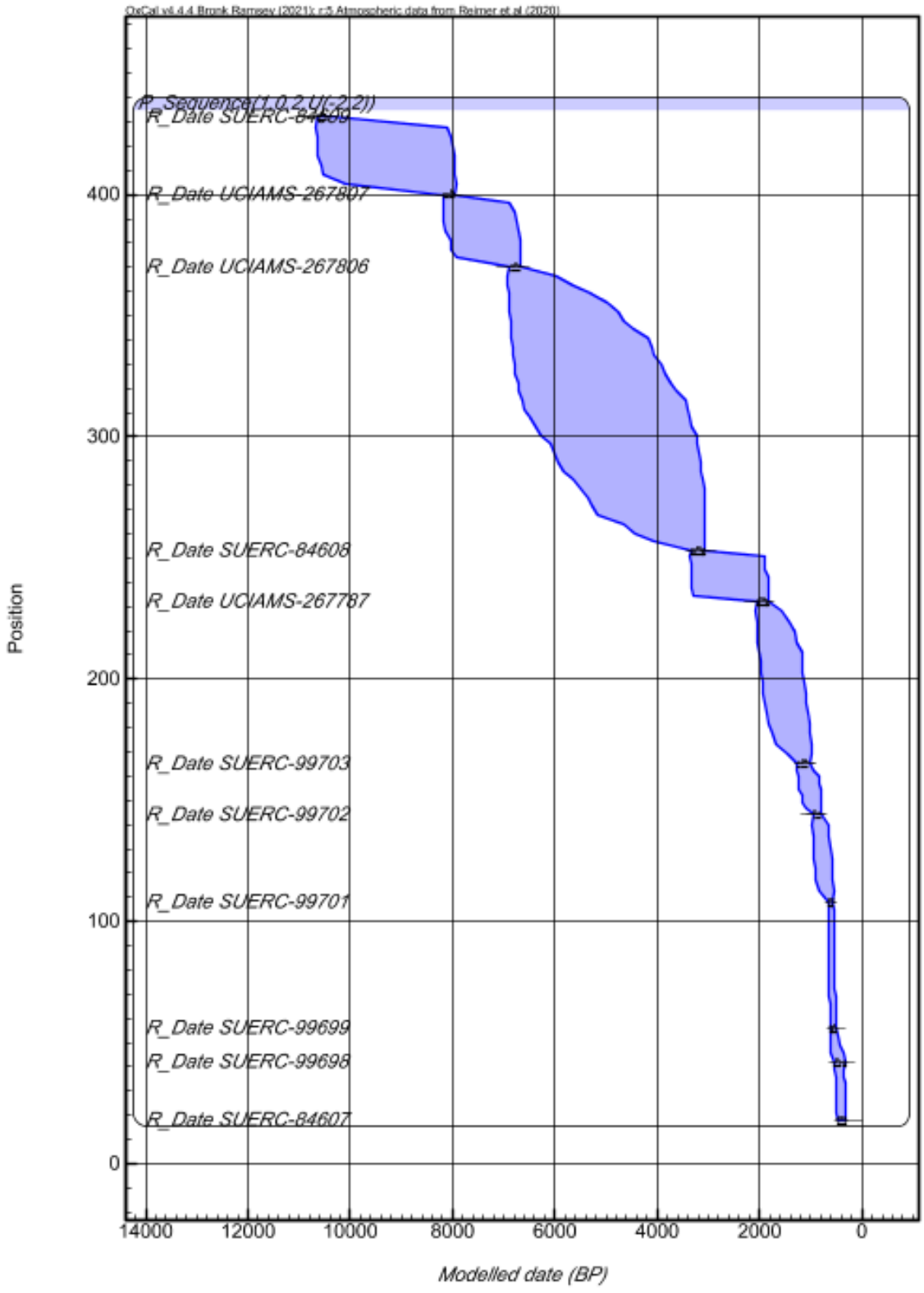

Figure 4.8: Results of the radiocarbon dating programme for the Huarca Central Basin core

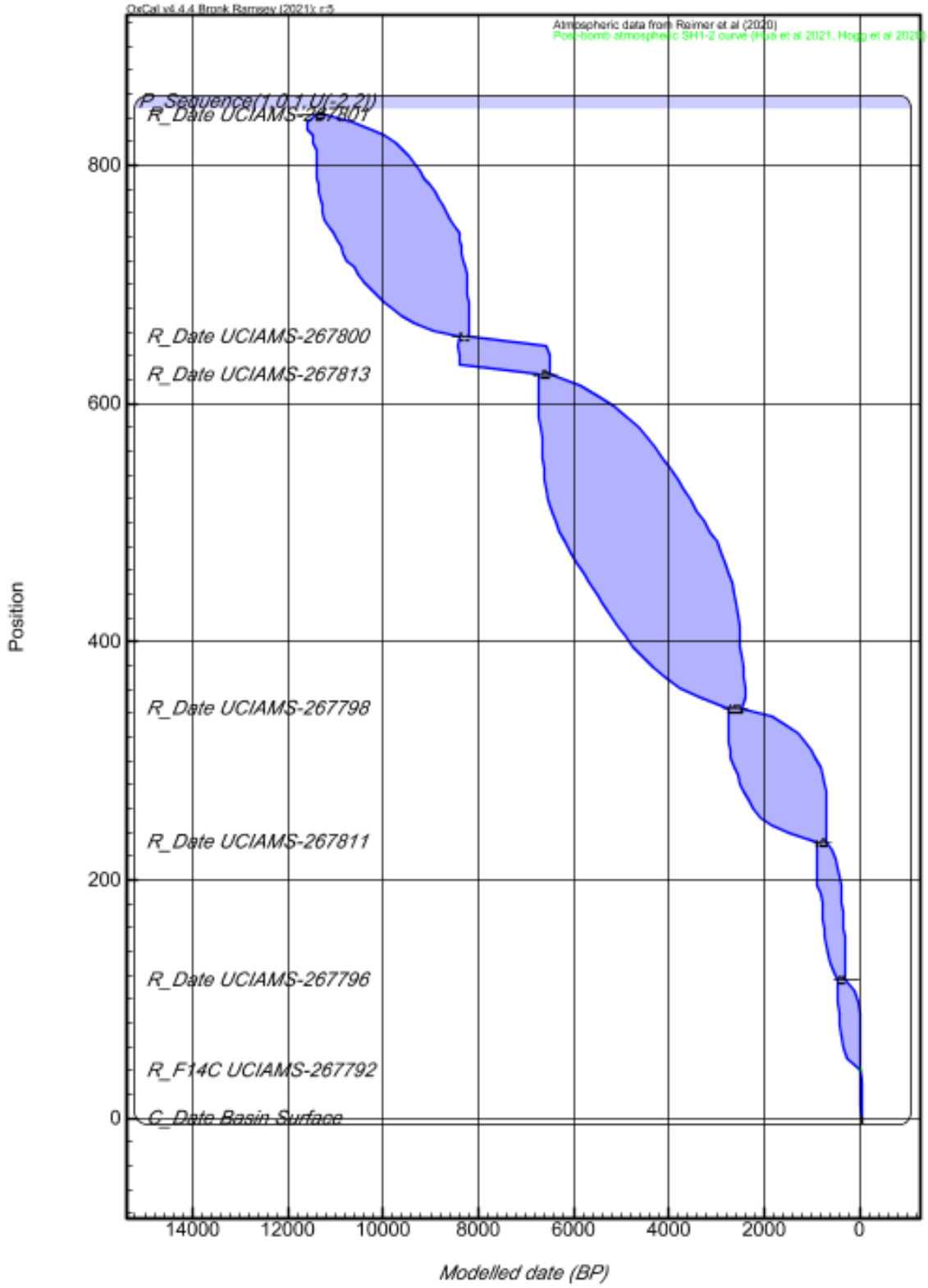

Figure 4.9: Results of the radiocarbon dating programme for the Huarca Edge core.

4.4.3 Bulk Organic Geochemistry

Central Basin Core

The bulk organic geochemistry can be found in figure 4.14, below. At the base of the central basin core, the parameters shown all track on another closely but there are some variations. TOC% remains relatively high throughout most of the central basin core at ~50%. There is a large area of the core that the TOC% does drop to <1% from 1,948 until 846 cal yr BP where the levels rise to 21.7%. A converse relationship occurs when we take T_{MAX} into consideration with TOC% values. This is often observed where there is an in-wash of more inorganic sediments, into the basin and vice versa.

A decrease in TOC% is mapped by a low in the Hydrogen Index (HI), with an increase in the Oxygen Index (OI) 5,018 ± 833 cal yr BP. Between 4,821 to 4,410 cal yr BP there is an 18°C decrease in T_{MAX}, where HI, TOC and Hydrocarbons all increase to their near maximum values, indicative of increased allochthonous organic material accumulation. A large zone of low organic carbon has been discovered between 1,948 and 1,081 cal yr BP. This region is quite distinct in most of the parameters used in this analysis. A gradual “ramping down” of T_{MAX} values from 430°C to 410°C, is observed, within this “barren” zone before increasing sharply to 425°C at the end of the zone. Coupled with the OI curve reaching a high of 248mg HC/TOC and the HI reaching a low of 148mg HC/TOC, within this “barren zone”, could potentially mean that this represents a source of older carbon from a source outside the basin, possibly from a mass movement event.

After this event, TOC% starts to increase again but decreases to 1.7% at 775 ± 99 cal yr BP with OI values overlapping the HI. This short-lived event, unlike the barren zone, is more of an indication of sedimentary source and depositional environment rather than one of older carbon sources. TOC%, T_{MAX} and HI/OI fluctuate from 609 ± 31 cal yr BP to present but remain high throughout this period, reflecting changes in sedimentary environments.

Edge Core

The Rock-Eval method, at the edge core, reveals 3 distinct areas of low T_{MAX} values, each bottoming out at ~160°C, coinciding with herbaceous peat formations or where more modern plant growth has started to accumulate. Generally, TOC% and T_{MAX} remain high throughout, but fluctuate depending on the sediment type it identifies. The HI:OI ratio remains constant for much of the time recorded, however, there are 4 periods where the OI is higher than the HI. At 736 ± 36 cal yr BP, 408 ± 79 cal yr BP, 195 ± 81 cal yr BP and 49 ± 118 cal yr BP. The switches identified at 195 ± 81 cal yr BP and 49 ± 118 cal yr BP also coincide with the lowest TOC% values (each ~4%), which reflect the changes in depositional environments. Here there are very minerogenic units of silty clays which have the possibility of identifying changes in water level as the mire returns to more open water conditions.

4.4.3.1 Notes on Rock-Eval pyrolysis use in radiocarbon dating methods

There are age discrepancies between the bulk and plant radiocarbon ages in the Huarca basin; with some of up to 2,500 years. The age difference is more pronounced in the middle of the sequences (see figure 4.10), which causes problems for the age-depth modelling for the site as it has resulted in various age reversals within the modelled data. The study finds that there must be sources of 'old carbon' from the bulk sediments within the basin, mixing with the 'young carbon' of the vegetative material. It has been postulated that the RockEval pyrolysis methodology may be able to, not only track sources of organic matter (OM) as identified in other publications (Englehart et al., 2013a; Lacey et al., 2015, 2018; Newell et al., 2016) but may also be used to pin-point sources of 'old carbon' (OC) within sequences to better refine radiocarbon methods and chronologies.

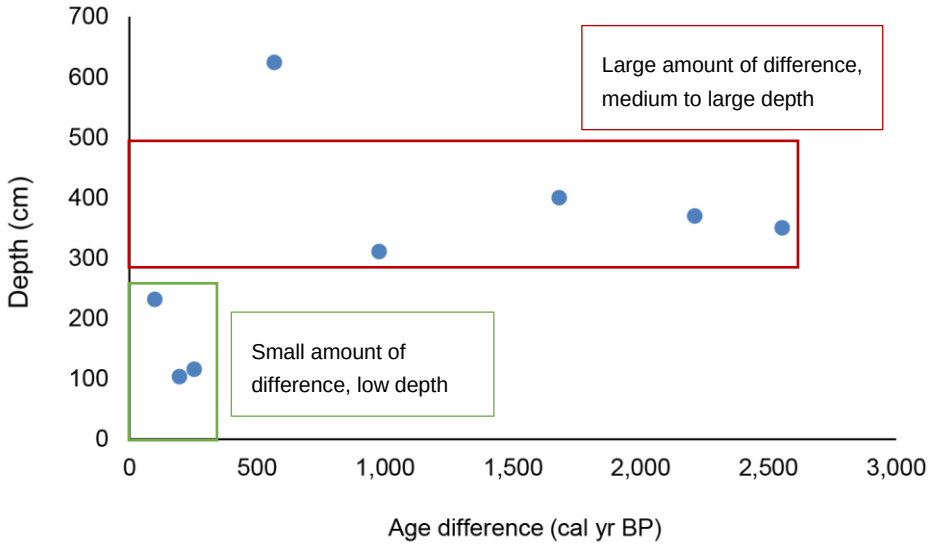

Figure 4.10: Age difference by depth. The difference in age between plant and humic age is more pronounced in the middle of the sequences for the Edge and Central cores.

There are several promising parameters, which are in table 4.4, that could be used to define this OC source within sedimentary sequences, that will be further explained. The Hydrogen Index is a measure of the extent of organic matter hydrogenation as well as a descriptor of alteration during pre- and post-deposition (Newell et al., 2016), in a similar way the Oxygen Index provides an estimate of oxygen containing compounds, with the value increasing upon aerobic biological decay (Slowakiewicz et al., 2015; Newell et al., 2016). The thermal maximum (T_{MAX}) values tend to provide an estimate of changes to OM type input because the maximum temperatures at which it takes to break the bonds between the bound hydrocarbons is related to the proportions of biopolymers (i.e., cellulose, lignin etc.) (Carrie et al., 2012). The

I and R indices are also useful to note, the results of which can be found in figure 4.11 below, both refer to the thermal stability of soil organic matter (SOM). I-index refers to the preservation of thermally labile immature OM with the R-index assessing the contribution of thermally stable SOM (Sebag et al., 2006, 2016).

The I and R-indices are useful in this regard as they provide information on the degradation and preservation of the OM in the core sequence. The datasets for both of the Huarca sites, show strong correlations between the two indices (see figure 4.11 below). Following the work of Sebag et al. (2016) and Ordoñez *et al.* (2019) this suggests that the thermal stability of the

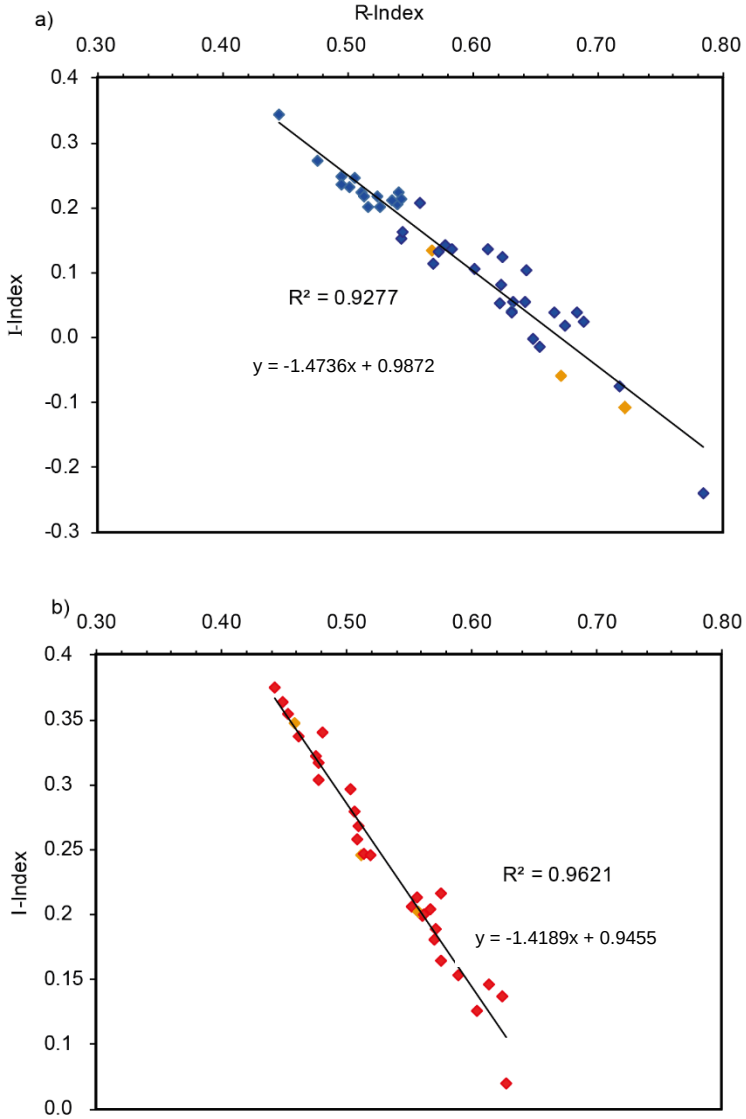

Figure 4.11: I- and R-Index for Huarca Central Basin (Blue), Edge (Red) with the R^2 values. The indices measure the stability and lability of the organic matter in the sediments. Points further to the bottom right are more labile and appear to be more degraded than those in the top left. Orange markers denote samples that were used in radiocarbon dating programmes.

organics within the basins must therefore be controlled by the processes of degradation. This degraded matter is more pronounced in samples that present the lowest I-index values for a given R-index, suggestive of substantial loss of the most labile OM and appear to be more degraded than the matter around it, thus pointing towards it being from an “older” carbon source as it is likely to be more deeply buried.

Correlation tables (see tables 4.3 and 4.4) for the major outputs would suggest that using the I-Index, T_{MAX} and OI, in tandem with each other, would provide the necessary details to start to gather information on older sources of bulk sediment within a sequence. What is surprising is that the parameter oxidised mineral carbon (oxiMINC) is also producing a correlation with both the bulk and plant ages and should also be considered. This parameter is influenced by the organic and inorganic fractions of sediment input, as shown in the PCA test data (figures 6.6abc below). This is also producing a weaker correlation (see figure 4.12 below), which would need more samples the correlation is found to be stronger, but it is promising.

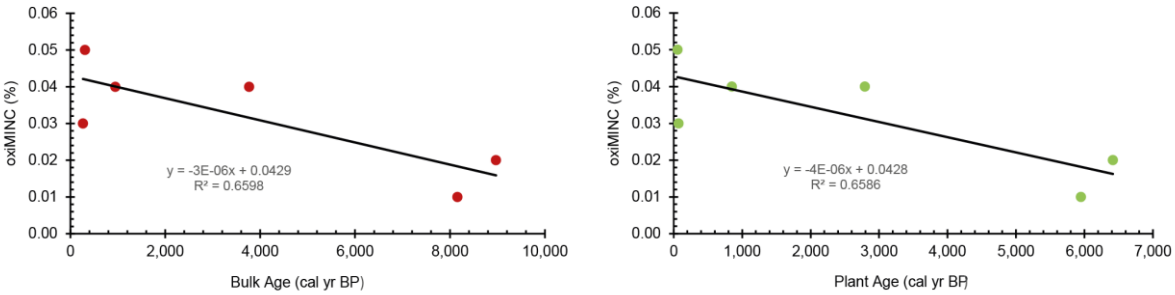

Figure 4.12: Oxidised Mineral Carbon (oxiMINC) correlation diagrams with Bulk humic ages (left) and Plant ages (left)

These Radiocarbon samples for Huarca including the main parameters from the Rock-Eval pyrolysis method that influence degradation of OM parameters, as the PCA outputs would also indicate, are controlled mainly by thermal degradation. This would suggest that the samples appearing in this quadrant would give the largest discrepancies in age between the plant and bulk sediment radiocarbon dates. What is interesting, here, is that the vector for $\delta^{13}C$ also plots amongst the parameters that this study puts forward to use in radiocarbon methodologies. This would suggest, therefore, that the bulk isotope analyses in the lower parts of the sequence are considered “old” signals and may be in the incorrect place temporally. this impact, however, would lessen the younger the sediments were as the age differences seem to lessen the younger the sediments are – possibly as they haven’t undergone further maturation processes as the older sediments would have. More work would need to be done to understand the degradation processes at each site, to better understand the maturity of OM. There are also only a small sample number in this study which provide weak correlations with one another, given more samples with ^{14}C dates on bulk and plant material these correlations might be stronger.

Table 4.4: Radiocarbon samples for Huarca including the main parameters from the Rock-Eval pyrolysis method that influence degradation of OM

Sample	Bulk Age	Plant Age	I-Index	R-Index	S1	S2	T_{MAX}	PC	RC	TOC	HI	OI	PyroMINC	oxiMINC	MINC	LOI
HURC-8-311	3,768	2,791	-0.11	0.72	0.04	7.84	422	0.87	2.57	3.44	228	147	0.25	0.04	0.29	89.36
HURC-9-350	8,969	6,416	-0.06	0.67	0.30	253.69	420	22.73	27.64	50.37	504	74	1.19	0.02	1.21	82.13
HURC-10-370	8,158	5,947	0.13	0.57	0.15	33.15	422	3.11	4.22	7.33	452	108	0.31	0.01	0.32	83.04
HURC-11-400	8,910	7,229	-	-	-	-	-	-	-	-	-	-	-	-	-	96.60
EDGE-2-104	266	70	0.15	0.56	0.23	190.71	404	17.76	25.42	43.18	442	116	0.93	0.03	0.96	74.88
EDGE-3-116	308	55	0.20	0.51	0.18	193.88	407	18.55	26.04	44.59	435	135	1.31	0.05	1.36	85.06
EDGE-4-232	947	848	0.30	0.46	0.19	124.42	325	12.92	38.24	51.16	243	109	1.03	0.04	1.07	72.11
EDGE-6-624	6,361	5,794	-	-	-	-	-	-	-	-	-	-	-	-	-	77.77

Table 4.5: Correlation table for Bulk ages, inclusive of the Rock-Eval parameters. Correlations between bulk ^{14}C ages seem to be with those controls of aerobic and thermal decay i.e. OI, T_{MAX}, I- and R-Indices.

	Bulk Age	*I-Index*	*R-Index*	*S1*	*S2*	*Tmax*	*Pc*	*RC*	*TOC*	*HI*	*OI*	*PyroMINC*	*oxiMINC*	*MINC*	*LOI*
Bulk Age	1														
I-Index	-0.57	1													
R-Index	0.56	-1.00	1												
S1	0.17	0.20	-0.26	1											
S2	-0.10	0.14	-0.21	0.90	1										
Tmax	0.50	-0.72	0.73	-0.12	-0.07	1									
Pc	-0.16	0.21	-0.28	0.89	1.00	-0.14	1								
RC	-0.43	0.58	-0.63	0.70	0.75	-0.71	0.80	1							
TOC	-0.34	0.46	-0.52	0.81	0.89	-0.51	0.92	0.97	1						
HI	0.40	-0.05	0.02	0.70	0.61	0.53	0.57	0.07	0.28	1					
OI	-0.60	0.02	0.02	-0.84	-0.56	0.07	-0.54	-0.41	-0.49	-0.57	1				
PyroMINC	-0.33	0.39	-0.47	0.75	0.92	-0.33	0.94	0.88	0.95	0.38	-0.37	1			
oxiMINC	-0.81	0.24	-0.26	-0.30	0.09	-0.37	0.14	0.35	0.28	-0.52	0.65	0.38	1		
Minc	-0.36	0.40	-0.47	0.73	0.91	-0.34	0.93	0.88	0.95	0.36	-0.35	1.00	0.41	1	
LOI	0.50	-0.70	0.70	-0.53	-0.36	0.76	-0.41	-0.74	-0.65	0.02	0.41	-0.41	0.05	-0.40	1

Table 4.6: Correlation table for Plant ages, inclusive of the Rock-Eval parameters. Correlations between bulk ^{14}C ages seem to be with those controls of organic and thermal decay i.e., OI, I- and R-Indices

	Plant Age	***I-Index***	***R-Index***	***S1***	***S2***	***Tmax***	***Pc***	***RC***	***TOC***	***HI***	***OI***	***PyroMINC***	***oxiMINC***	***MINC***	***LOI***
Plant Age	1														
I-Index	-0.56	1													
R-Index	0.55	-1.00	1												
S1	0.15	0.20	-0.26	1											
S2	-0.13	0.14	-0.21	0.90	1										
Tmax	0.47	-0.72	0.73	-0.12	-0.07	1									
Pc	-0.19	0.21	-0.28	0.89	1.00	-0.14	1								
RC	-0.43	0.58	-0.63	0.70	0.75	-0.71	0.80	1							
TOC	-0.36	0.46	-0.52	0.81	0.89	-0.51	0.92	0.97	1						
HI	0.37	-0.05	0.02	0.70	0.61	0.53	0.57	0.07	0.28	1					
OI	-0.59	0.02	0.02	-0.84	-0.56	0.07	-0.54	-0.41	-0.49	-0.57	1				
PyroMINC	-0.35	0.39	-0.47	0.75	0.92	-0.33	0.94	0.88	0.95	0.38	-0.37	1			
oxiMINC	-0.81	0.24	-0.26	-0.30	0.09	-0.37	0.14	0.35	0.28	-0.52	0.65	0.38	1		
Minc	-0.38	0.40	-0.47	0.73	0.91	-0.34	0.93	0.88	0.95	0.36	-0.35	1.00	0.41	1	
LOI	0.48	-0.70	0.70	-0.53	-0.36	0.76	-0.41	-0.74	-0.65	0.02	0.41	-0.41	0.05	-0.40	1

4.4.3.2 Rock-Eval pyrolysis and PCA testing

Statistical analysis of the Rock-Eval dataset was carried out using Principal Component Analysis (PCA) in order to identify potential OM sources and controls of thermal degradation of that OM. The results of the PCA test reveal that PC1 is mainly influenced by parameters that are controlled by thermal processes of degradation, or those samples that contain more hydrogen poor labile OM i.e., high values of OI and T_{MAX}. These samples often are of an allochthonous origin and therefore do not originate from within the basin itself. For example, at Huarca, most of the samples that plot with these vectors are within the zone of low TOC; of which sediments have been transported into the basin from a different origin. The parameters that lean more to PC2 are those parameters that are defined more as organic rich sediments that are more hydrogenous and do not seem to have undergone aerobic degradation. The parameters of TOC, PC, RC and HI are all the main influencers on these samples (figure 4.13).

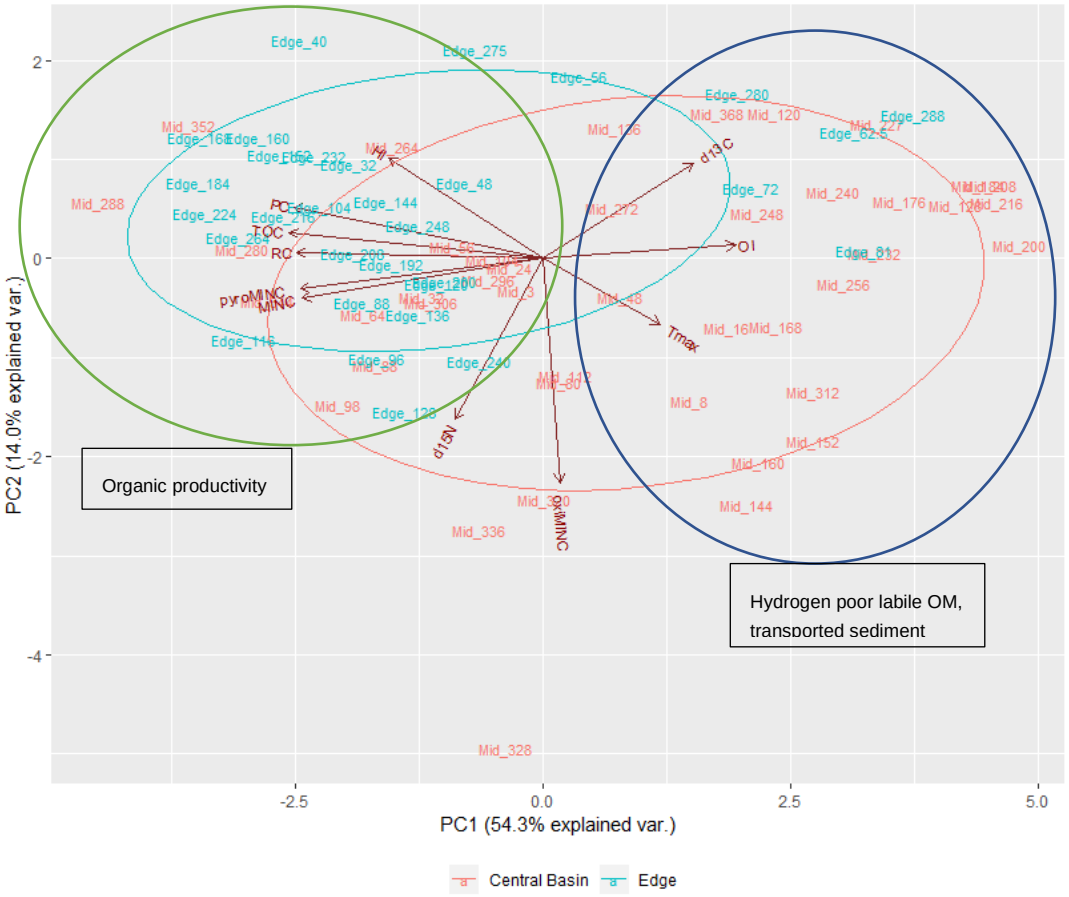

Figure 4.13: PCA plot from Huarca Central Basin (Blue) and Edge (Red) cores, illustrating the PC1 and PC2 groupings

4.4.4 Isotope Geochemistry

Central Basin Core

What is striking is, that unlike the Rock-Eval analysis, there are large hiatuses in both the $\delta^{13}C$ and $\delta^{15}N$ records (see figure 4.14) where the detection limit is too low. Between 8,000 and 6,000 cal yr BP both the $\delta^{13}C$ and the $\delta^{15}N$ curves are variable but show a slight increasing trend from -27.0‰ to -24.8‰. There is one period of lower values in both curves from 6,656 to 6,158 cal yr BP with $\delta^{13}C$ dropping by 2.1 per mil during this time, with $\delta^{15}N$ showing a similar trend with a deviation from the mean of 1.8 per mil. in the same period. These lower values sharply increase by 1.2 per mil in the carbon record, where a mean increase of 6.1 per mil can be identified in the nitrogen curve.

A first peak in $\delta^{13}C$, of +3.1 per mil, at 4,581 ± 815 cal yr BP is met by a sharp decrease to more negative values in the nitrogen curve of -4.6 per mil, which is a stark inverse relationship between the two isotope curves, which isn't observed again in either of the records from both parts of the basin. After a long hiatus, of c. 2,100 years there is a large increase in both values, at 1,053 cal yr BP, +6.5 mil for carbon and +8.9 mil for nitrogen, which is then followed by a mean decline of -0.1 per mil and a small increase of +0.3 per mil for; both carbon and nitrogen values, respectively.

Another short period of low carbon and nitrogen follows, of 315 years, where a two-step trough in the carbon curve can be observed. There is a small peak in $\delta^{13}C$ of +2.2 per mil and a large deflection in the $\delta^{15}N$ curve as values increase from the mean +5.8 per mil at 572 ± 64 cal yr BP. The rest of the core is variable in nature, reflecting possible changes in plant communities and other smaller environmental shifts.

Edge Core

The edge core's $\delta^{13}C$ reconstruction remains variable throughout its history. There are two early peaks in this curve, which show a mean increase of 1.6 per mil at 785 ± 267 cal yr BP and a second with a mean deflection of +2.1 per mil at 673 ± 105 cal yr BP. The second of these peaks is also tracked by a comparable mean deflection in the $\delta^{15}N$ of +5.6 per mil. Both isotope curves deteriorate decline 673 to 477 cal yr BP before an increase of 0.3 per mil at 450 ± 102 cal yr BP for carbon, which is not met by a comparable increase of nitrogen values. There is a mean deviation of -1.3 per mil in $\delta^{13}C$ values at 408 ± 79 cal yr BP with a decrease of -1.2 per mil $_{observed}$ in the $\delta^{15}N$ curve at the same time. A small increase, in the carbon record, of 0.2 per mil that is mapped by a mean deviation of +1.5 per mil in the nitrogen record. Following from this peak there is a sharp deterioration of $\delta^{15}N$ values between 195 to 49 cal yr BP which range from -3.6 per mil to -4.4 per mil, while there is not a comparable shift

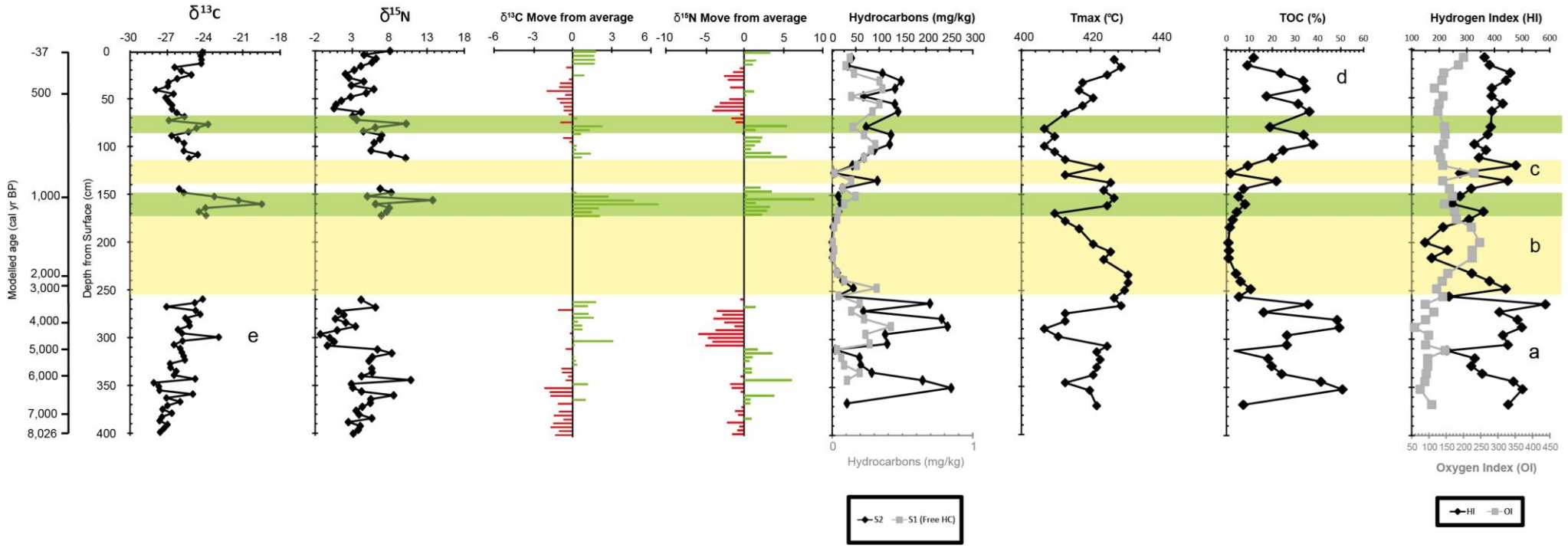

Figure 4.14: Isotope Geochemistry and main Rock-Eval parameters for the Huarca Central Basin core, inclusive of the deviation from the average isotope values (-25.9‰ for $\delta^{13}C$ and +4.66 for $\delta^{15}N$). The large yellow areas denotes the zone of low organic carbon, with the green areas denoting periods of aridity.

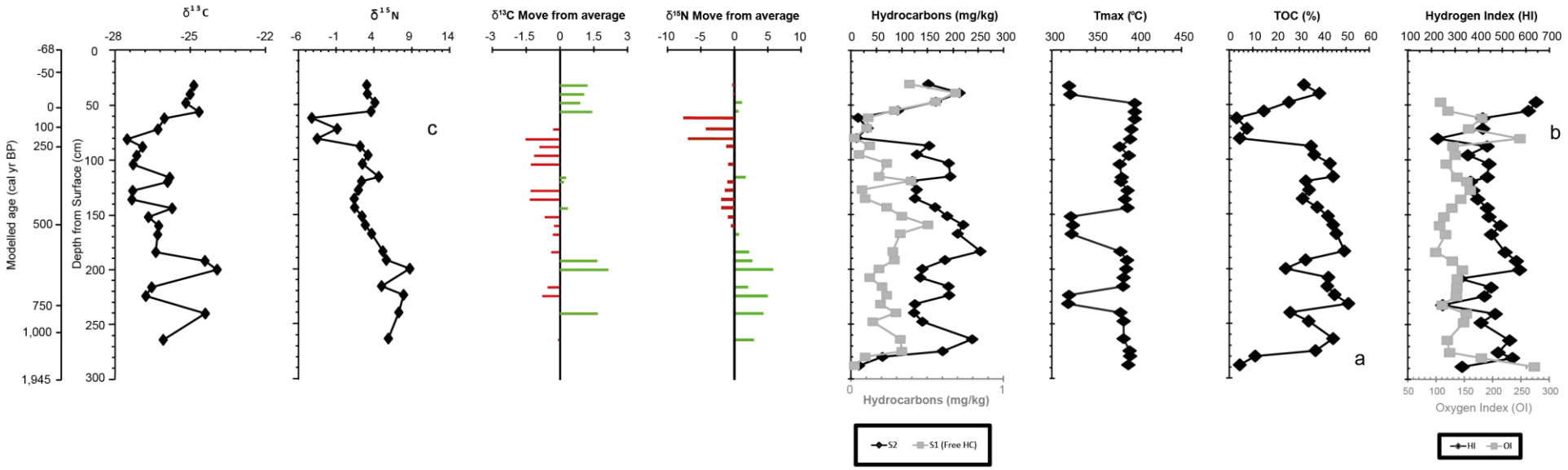

Figure 4.15: Isotope Geochemistry and main Rock-Eval parameters for the Huarca Central Basin core, inclusive of the deviation from the average isotope values (-26.0‰ for $\delta^{13}C$ and +3.08‰ for $\delta^{15}N$).

in the carbon reconstruction values drop to -27.5‰ at the beginning of the same period, before increasing again to -26.0‰ by the end. Values for both carbon and nitrogen return to 'normal' conditions again through until the top of the cores are reached, towards the present day (Figure 4.15)

4.4.5 Non-Pollen Palynomorphs

Non-Pollen Palynomorphs (NPPs) were collected at targeted intervals, and specifically during periods of changeable conditions identified within the geochemical analysis of the core material. This was undertaken on the edge core, only, due to its location close to relic terrace systems and provided the opportunity to reconstruct agropastoral land use, and to test if there is a potential relationship between the climate variability and the recorded land use changes.

Zone 1 (184-206cm) (610-692 cal yr BP)

Zone 1 is dominated by HdV-18 and HdV-16a (*Byssothecium circinnans*), which make up 81.2% of the total of species counted. Both taxa remain in lower counts, in this zone, when compared to the rest of the core; but remain at a relatively similar level through this zone. EMA-25 (*Discomycetes*) (2.4%) and HdV-123 (0.8%) make up the rest of the assemblage of "Other Fungal Remains" (OFR). There are low counts of coprophilous remains during this zone with *Valsaria* type (HdV-263) spores being the most common (5.6%) but were only identified in two of the samples (184cm and 198cm) and are otherwise absent from the rest of the zone. *Sporormiella* (HdV-113) (2.0%) was only present at 190cm in this zone but along with *Podospora* type (HdV-368) (4.4%), *Sordaria* type (HdV-55) (2.0%), *Gelasinospora* (HdV-2) (1.6%), TM-H (1.6%), *Apidosordaria* (HdV-169) (0.4%) and *Podospora polysporus* (TM-110) (0.4%) make up the rest of the dung-related ascomycetes.

Zone 2 (115-118cm) (377-385 cal yr BP)

Low counts of HdV-18 (27.1%) resume into this, short, NPP zone which also contains a marked absence of HdV-16a as well as other taxa of the OFR assemblages in the other zones. The human indicator HdV-351 makes a marked appearance in zone 2, with a total abundance of 31.0%. *Sporormiella* is also absent from this zone, but there is an abundance of other dung-related ascomycetes. *Coniochaeta cf. ligniaria* (HdV-172) is the most abundant coprophilous fungus in this zone, where it reaches its peak in the assemblage making up 14% of this zone. TM-H (17.1%), HdV-55 (7.8%) and HdV-2 (3.1%) have also been identified within this zone.

Zone 3 (70-98cm) (108-309 cal yr BP)

HdV-16a (28.3%) and HdV-18 (35.9%), once again, dominate the assemblage increasing further up the zone – bar at 82cm where HdV-16a peaks within this zone. EMA-25 (6.7%) is absent at the base of this zone but appears again from 82cm to the top of the zone. HdV-351 (3.9%) is a key indicator of human induced changes and is abundant in the 94cm sample but only appears again as single spores at 72cm and 74cm. Coprophilous fungal remains are spread out along the zone but occur more frequently in samples 86-98cm; the most abundant being TM-H (16.8%), which isn't identified from 82cm onwards, peaking at 86cm. Sporormiella

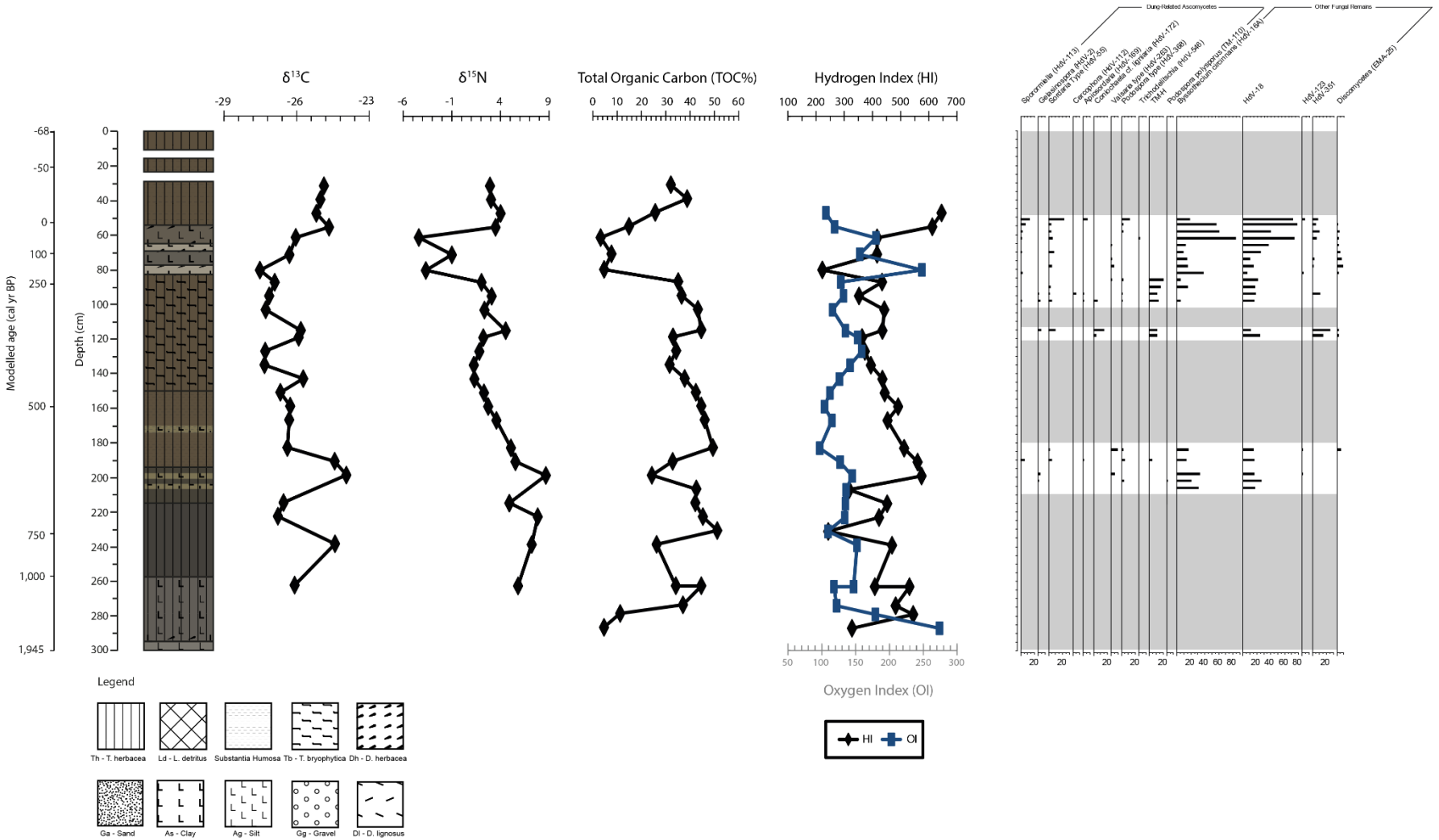

Figure 4.16: Identified NPPs along with the isotope curves and selected Rock-Eval parameters. Grey areas are where there were no identifications carried out. The stratigraphy can be found on the left-hand side of the diagram.

(1.1%) is identified in 3 of the samples 98cm, 82cm and 70cm. The other dung-related ascomycetes identified here are HdV-55 (5.9%), HdV-263 (1.7%), HdV-112 (1.4%), HdV-172 (1.4%), HdV-368 (1.4%), HdV-2 (1.1%), HdV-169 (0.6%).

Zone 4 (51-66cm) (-6-78 cal yr BP)

HdV-16a peaks at the base of this zone (66cm) and gradually lessens towards the top of the zone overall, it accounts for 35.6% of the total assemblage. HdV-18 (46.6%) counts remain high for much of this zone; however, the values lessen at a depth of 58cm before returning to greater levels at the top of the zone. EMA-25 numbers peak at 66cm but gradually wain to the top sample (51cm) and accounts for a total of 1.5% of the total assemblage. In its place HdV-123 is discovered at 51cm, which is the only sample it was identified within and only makes up for 0.6% of the total NPP counts. The key coprophilous fungal remains of *Sporomiella* peak at the top of the zone and have only not appeared in one of the samples (66cm), it makes up for 3.4% of the total assemblage. Other dung-related ascomycetes identified were HdV-55 (5.3%), HdV-368 (2.8%) and HdV-169 (0.9%). There are two rarer fungal remains of *Valsaria* type (HdV-263) and *Trichodelitschia* (HdV-546), but both only total a small number of spores (0.2% for each).

4.4.6 n-Alkane signatures

Huarca central basin core

n-Alkanes for the Huarca central basin core are dominated by longer chain lengths (n-C_{24}-C_{31}) with a high Carbon Preference Index (CPI) (See figures 4.13 to 4.15), for the majority of the samples analysed (3.1 – 7.2). There are two samples that have a CPI of 1.4 and 1.7, but do not typify any significant contamination from oils or fossil carbon sources (Bray and Evans, 1961; Eglinton and Hamilton, 1967). The samples taken at 12cm to 160cm show a higher percentage of n-C_{31}, but all samples show a variety of chain lengths which include some of the shorter *n*-alkane chains between n-C_{16} to n-C_{20}. This results in an Average Chain Length (ACL) of ~28 for all samples, although a higher CPI of 6.4 for 12cm, this quickly drops to 4.0 at 40cm and 3.4 at 76cm. The CPI values rapidly increase again at sample 160cm to a peak of 7.2 – the highest value for Huarca. There is a sharp increase in ACL, to 30.4, where the CPI falls slightly to 6.3 within the 172cm sample. At this depth there is a distinct increase in chain lengths C_{33} and C_{35}, in comparison to the samples above it, which explain this increase in ACL. Both CPI and ACL values drop gradually the further down the core, from 30.4 to 27.2 (ACL) and 6.3 to 1.4 (CPI). There is also an observable difference in the distribution of the *n*-alkane chain lengths, in these samples. Where n-C_{31}, and above, are the more abundant chains these make way for n-C_{27} at 300cm, and n-C_{24} at 324cm and 370cm. The 300cm sample is intriguing as there is a greater abundance of shorter chains, with even dominance, from n-C_{14} to n-C_{26}, when compared to the other samples.

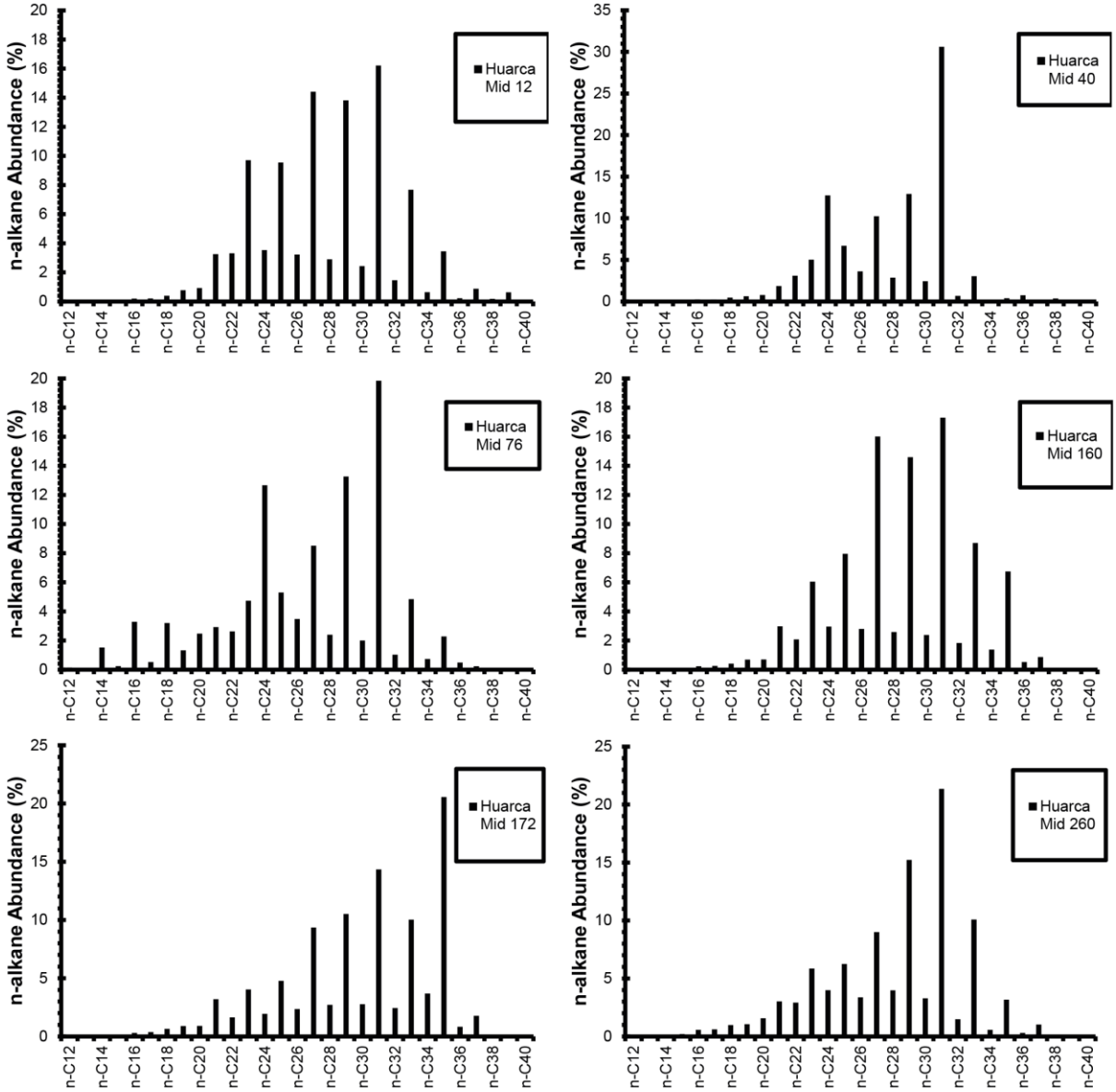

Figure 4.17: n-Alkane abundances for samples 12cm to 260cm for the Central Basin core

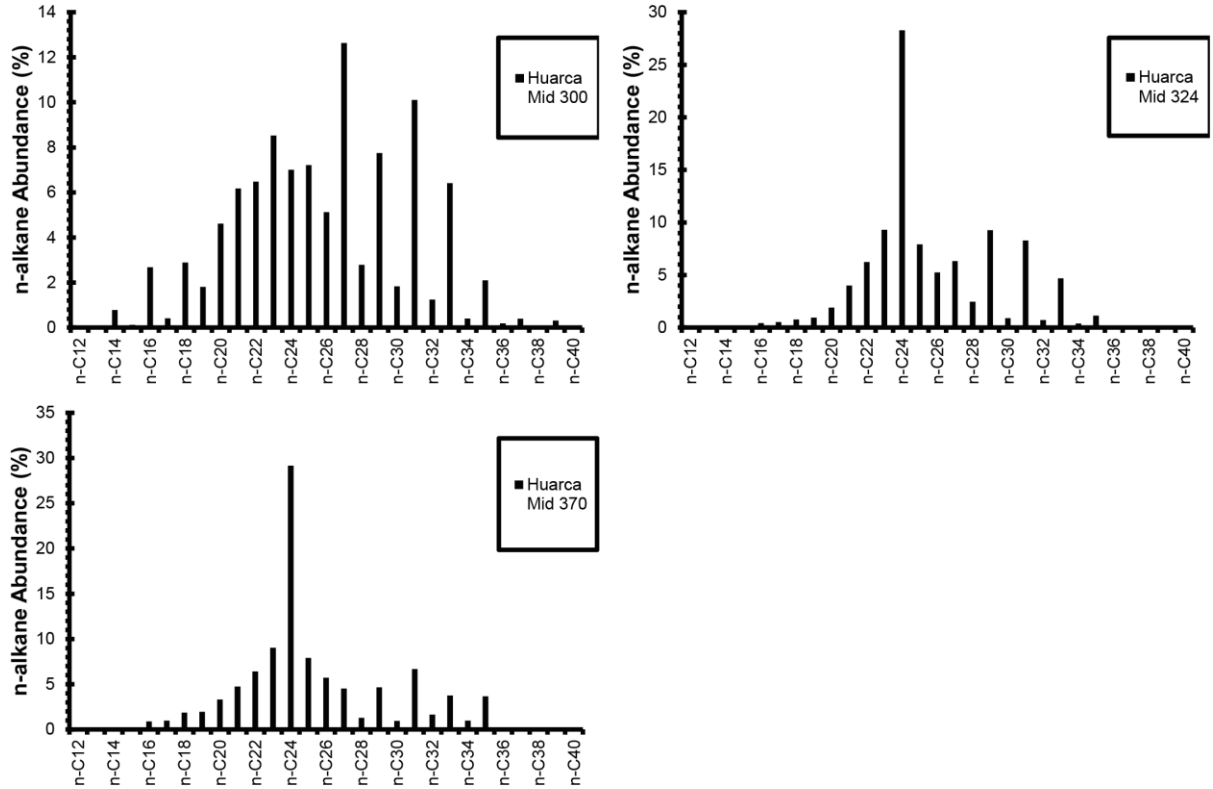

Figure 4.18: n-Alkane abundances for samples 300cm to 370cm for the Huarca Central Basin

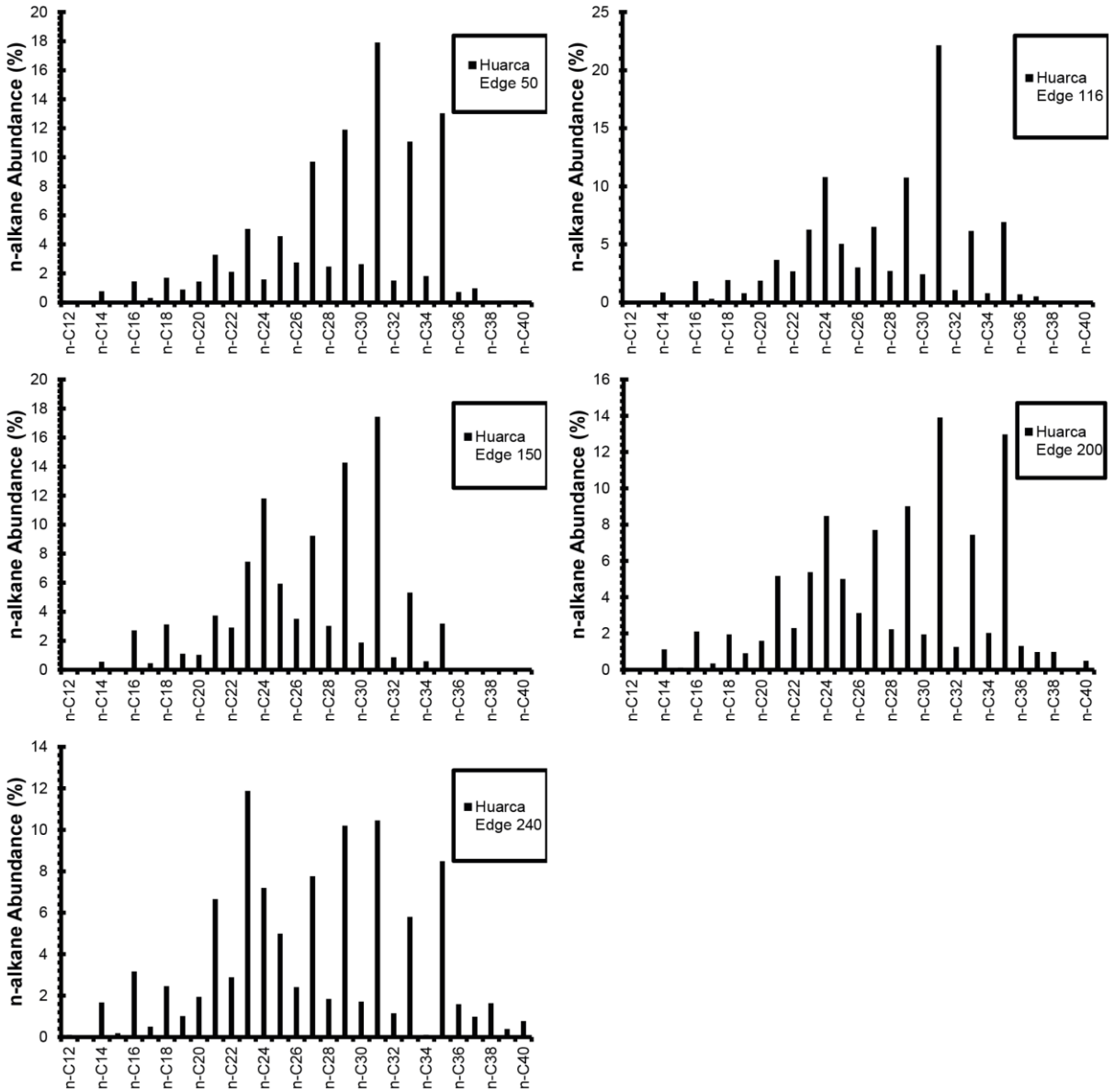

Figure 4.19: n-Alkane abundances for the Huarca Edge samples

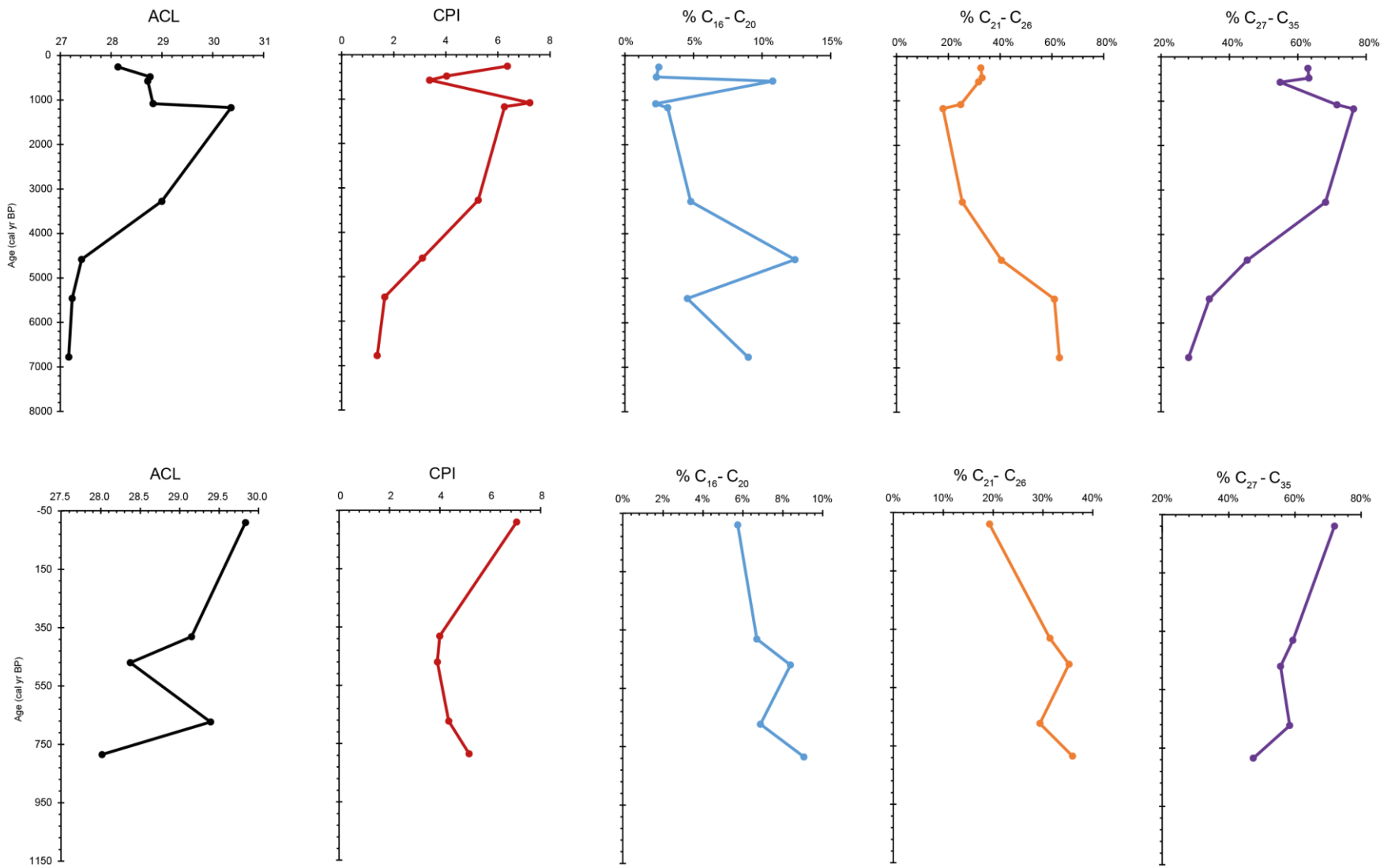

Figure 4.20: n-Alkane measurements for Average Chain Length (ACL) (Black), Carbon Preference Index (CPI) (Red), % abundance of chains C_{16}-C_{20} (Blue), % abundance of chains C_{21}-C_{26} (Orange), and % abundance of chains C_{27}-C_{35} (Purple), for Huarca Central Basin (top) and Edge (bottom) cores)

Huarca edge core

The *n*-alkane distributions, in the edge core (See figures 4.15 and 4.16), appear to be more varied in comparison to the distribution of the chain lengths within the mid-core. The ACL ranges from 29.8 to 28.0, with the CPI remaining high throughout, with a range of 7.0 to 5.2. This distribution is typical of fresh vegetation, rendering any significant input of oils or fossil carbon sources very unlikely (Bray and Evans, 1961; Eglinton and Hamilton, 1967). For the majority of the samples, the most abundant chain length is n-C_{31}, which typifies the higher ACL values, although chain lengths n-C_{27} to n-C_{35} are also abundant. A key area to note are the shorter chain lengths, which are also even dominant, n-C_{14} to n-C_{24} which also make up a large part of the sedimentary signatures. ACL, at the top of the core, remains high at 29.8 but gradually decreases down to 28.4 within the 150cm sample. At this depth, there is an observable increase in the shorter chain lengths, when compared to the samples above them – 9% of lengths n-C_{12} to n-C_{20} at 150cm, with 6.7% and 7.9% for 50cm and 116cm respectively. There is also an increased percentage of n-C_{23} to n-C_{25} at this sample depth, adding to the lower ACL value. ACL increases sharply at the 200cm sample, which contains a 13% abundance of n-C_{35}; unlike the samples towards the top of the core there is a mixture of shorter chain lengths within this sample. The ACL drops again at sample 240cm, which has a greater percentage of n-C_{23} (11.9%) than any other chain length, contributing to the lower ACL than the other samples.

4.4.7 Interpretation of Paleoenvironmental Data

Sedimentary History

Central Basin

The sedimentary sequence at the centre of the basin started to accumulate ~11,468 cal yr BP. With the deposition of coarse and fine sands (unit 1), possibly as a result of glacial retreat (figure 4.21 A). There was then a prolonged period of stabilised conditions that allowed for the accumulation of peat (units 2-4) ~10,807-3,966 cal yr BP with extraordinarily little influence from any anthropogenic sources (Figure 4.21 B). There is a small punctuation of coarser material at 312cm (~5,018 cal yr BP), which is indicated by the HI:OI ratio becoming almost equal (see figure 4.14 point a) and low TOC% values of 3.4%. This is indicative of sediment transport from an allochthonous source, which could originate from the retreating glaciers from the nearby Nevado Huandoy (see figure 4.1). Unit 5 (3,877-3,966 cal yr BP) indicates a short-lived open water system with silts being deposited in between layers of peat. There is no indication from the Rock-Eval, at this depth, that this is similar to the event at unit 3. Therefore, this points towards a lake environment that could have developed as a result of increased precipitation following an arid period during the mid-Holocene (Bird et al., 2011b) (figure 4.21 C). These conditions stabilise again between 3,877-3,237 cal yr BP, with further peat formation indicating dropping of the water levels.

Unit 8 (~1,960-3,237 cal yr BP) indicates the beginning of the transition to coarse material, inclusive of coarse sands and large unsorted clasts. This continues in units 9-11 (~1,250-1,960), with TOC% levels reaching <1% during this time (see figure 4.14 point b). The HI:OI ratio turns in favour of the OI, at ~1,561 cal yr BP, indicative of in washing sediment from an outside source (Figure 4.1 D). A ^{14}C date taken from within this 'barren zone' (UCIAMS-267787 – see table 4.2) would indicate that this is sediment accumulation is washing in over time and is not one large erosional event as indicated by the material identified in the sequence. The allochthonous origin of the sediments is most likely terrigenous in origin and a likely candidate could be from a series of flooding events from Keushu, but more work would need to be completed in order to pin-point the location. These clastic sediments could also be of a glacial origin, as the Huarca basin lies beneath Nevado Huandoy (see figure 4.1). Layers of lake type sediment within the unit 8 and 9 may also indicate an open water system in the basin, as this correlates to a period of wetter conditions shown in other palaeoclimatic records (Rein et al., 2004; Bird et al., 2011b, Kanner et al., 2013) which may have contributed to increased run-off in the basin and formation of lake. Lake sediment accumulation ceases through the transition into unit 11 and there is no indication of any further sediment of this type in unit 12 (~1,139-1,250 cal yr BP), with an increase in sands identified. The HI:OI ratio transitions back in favour of the HI and TOC% increase again as plant macrofossils become more prevalent. This may be due to a dropping of water levels and a decrease in water velocity as the depositional environment stabilises again.

Peat formation in unit 13 (870-1,139 cal yr BP) leads to an increase in TOC% values, from 2.7% at the base of the unit to 21.7% at the top contact of the unit. Humification in the unit is recorded at 4, which would typify that the surface wetness was low. Sand deposition occurs again, in the centre of the basin, from 680-870 cal yr BP (Unit 14). This is also indicated by a decreased TOC% input with values dropping to 1.73% ~775 cal yr BP, which is also mapped by the HI:OI ratio favouring the OI (see figure 4.14 point c). This may indicate a period of increased erosional activity during an arid phase experienced by the Huarca basin, meaning that the wetland is sensitive to changes in the climate. Units 12 to 14, sit within the boundaries for the MCA (~700-1,100 cal yr BP) which is characterised by a decrease in precipitation and possibly increased temperatures (Lüning et al., 2019) (Figure 4.22 E). This may have led to an increase of sediment transportation from fluvial or aeolian processes, which would accommodate the increase in OI values observed in unit 13. Fluvial sediment transport may have come from meltwater from retreating glaciers from the nearby Huandoy ice cap, due to the higher temperatures and lower precipitation that would have occurred during the MCA (Handley, 2022). This is plausible given the proximal location to Huandoy itself (see Figure 4.1).

Peat formation returns during ~257-680 cal yr BP (units 15-19), coinciding with an increase in TOC% values which remain ~33% until 454 cal yr BP where they drop to 9.1% at the top of unit 19. Decreased humification values, during units 17 and 18, indicate increased surface

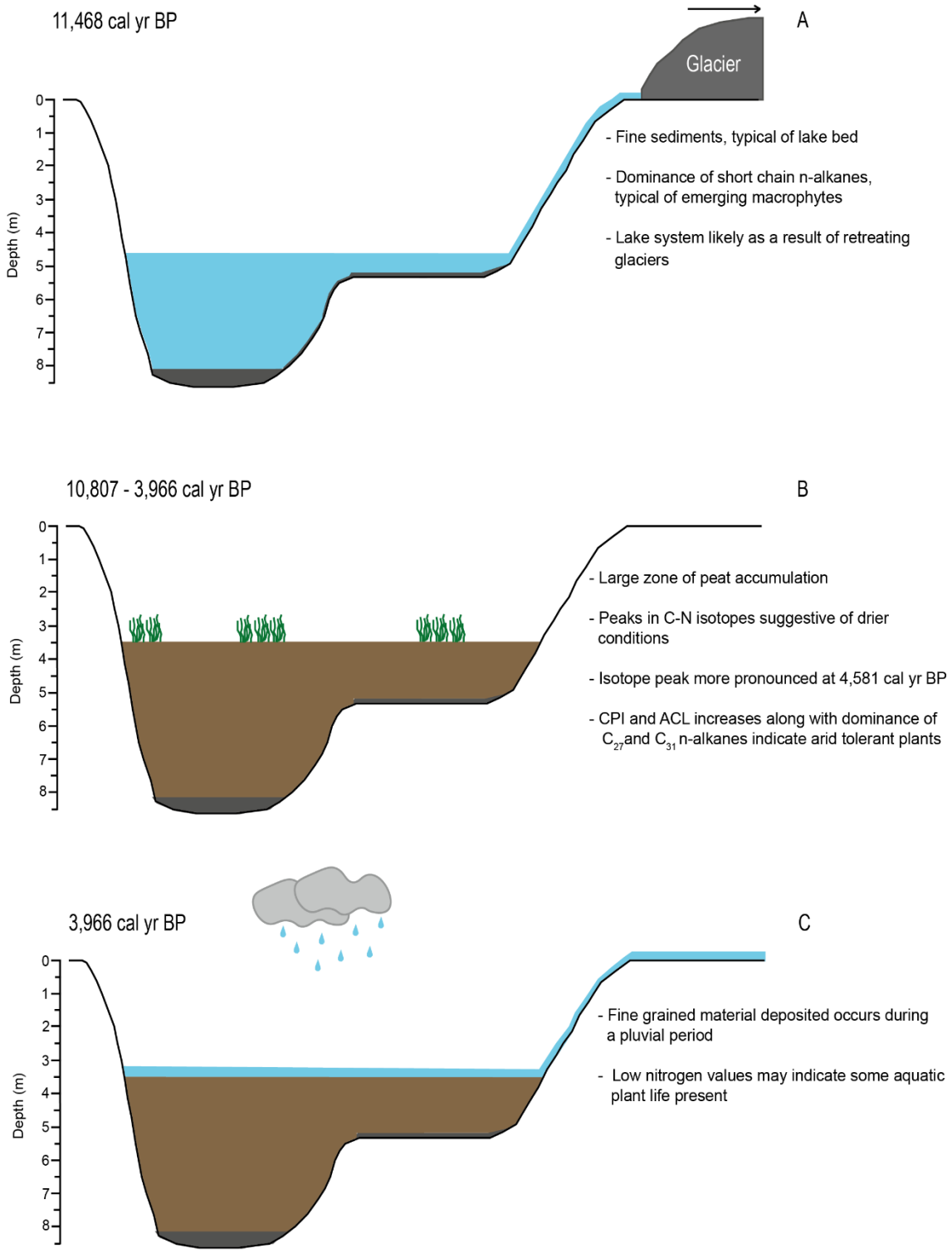

Figure 4.21: Schematic of the infilling of the Huarca basin. The lower portion of the basin represents the edge core location, the right hand side representing the central basin core.

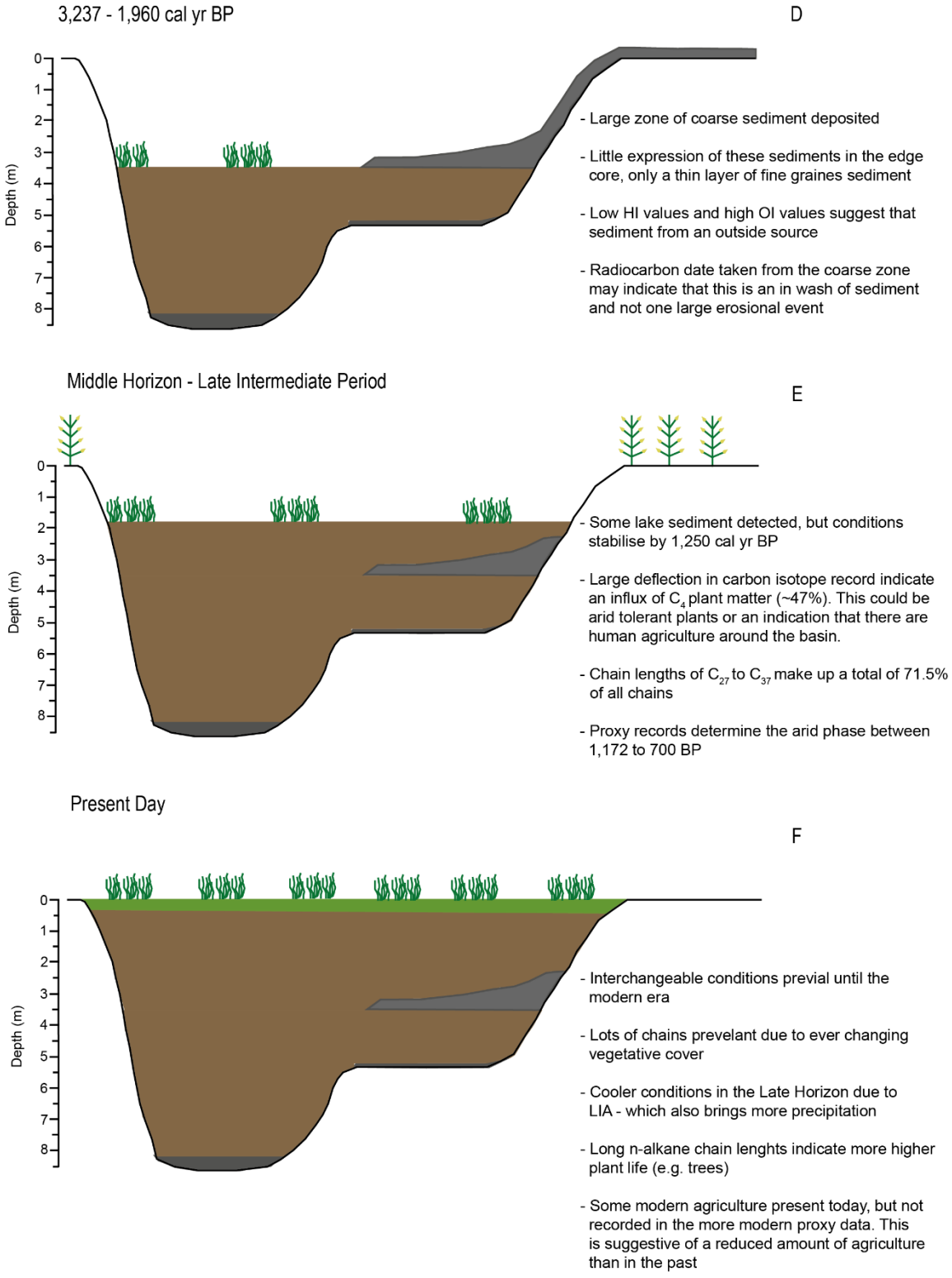

Figure 4.22: Schematic of the infilling of the Huarca basin. The lower portion of the basin represents the edge core location, the right hand side representing the central basin core.

wetness levels from ~569-609 cal yr BP during the beginning of the LIA. There is a rapid increase of mineral carbon ~475 cal yr BP, of around 2%, this mineral sediment must originate from the within the basin as there is no indication from the HI or OI values that this has been transported from another source (figure 4.14 point d). Therefore, this must indicate that this short-lived period is terrigenous input from possible erosional activity within the basin. Lower TOC% values continue into unit 20 (257 cal yr BP to ~1996AD), where there are continual in-washes of silt material in the modern-day soils. This may be representative of modern-day activity from around the basin, with the creation of Huarca village and the development of the modern agricultural systems which lead to increased erosional activity (Figure 4.22 F).

Basin Edge Core

The core gathered from closer to the edge of the Huarca basin may represent a deeper part of the basin than the core taken from closer to the central area. The sedimentary history is roughly the same and are likely an extension of the sediments expressed within the central basin core. Unlike the central basin core, there is not a large area that has coarse sands and unsorted clasts within it. Instead, this is expressed by 2 units of fine-grained material (units 26-28 - ~1,837-2,527 cal yr BP) that covers roughly 40cm with low LOI values of ~13%. There is then a further unit of organic matter accumulation (unit 27), that contains a large percentage of clays within it, this covers the same time frame as the rest of the low zone of low organic carbon (~1,026-1837 cal yr BP) (see figure 4.15 point a).

The sediments in units 33-36 (~6-211 cal yr BP), make up the more modern sedimentary units within the Huarca basin. The transition into unit 36 is within the limits of the LIA, and is marked by heightened OI values, in comparison to HI (see figure 4.15 point b). The increased silts and clays within this unit, suggests that these would have been brought into the basin from increased fluvial processes as a result of increased precipitation during the LIA (see central basin sedimentary history above), with the upper most units most likely from the increased human activity around the basin.

Geochemical History

Formative Period (3,000-8,000 cal yr BP)

The basin, during this time, is faithfully recording the vegetation changes within the basin, possibly as a result of the changing SASM and ITCZ – rather than directly recording precipitation changes due to these climate events. Evidence for this may be found in the *n*-alkane dataset, the lower samples identify that the basin is dominated by shorter chain *n*-alkanes chiefly that of C_{24} – which makes up 29.2% of the 370cm sample (6,774 ± 53 cal yr BP). This can be said for the 324cm sample, for which n-C_{24} makes up for a total of 28.3% of the total abundance (see figure 4.20). The percentage total of chains n-C_{21}-C_{26} in the first 2 samples is 62.9% and 61.0% respectively. This may be more indicative of an abundance of emerging macrophytes, which the carbon isotopes are recording. The comparative lack of chains n-C_{27}-C_{35} (28.1% at 370cm and 34.2% at 324cm) would also suggest that the plant

community is lacking in plants of a C_4 photosynthetic pathway and thus the basin is not recording changes in climate during this period.

The period between 7,000-5,000 BP is of significant interest for Peruvian studies, as it is a major aridity event coinciding with a low stand at Lake Titicaca (Seltzer et al., 1998). There is, a deterioration of both $\delta^{13}C$ and $\delta^{15}N$ values that move -2.1 per mil and -1.8 per mil, from the mean values (see figure 4.14), respectively before both curves enrich by 1.2 per mil and 6.1 per mil by ~6,158 cal yr BP – which may be indicative of an aridity gradient, which fit the period of aridity, although the values for the $\delta^{13}C$ do not indicate a large amount of arid tolerant plant mixing (~11%). The sigma errors associated with the age-depth model at this period, however, are quite large which makes it difficult to be accurate in pin-pointing the exact date of this event; but it would still occur during this mid-Holocene drought period.

A decrease of chains n-C_{21}-C_{26} (40.5%) and an increase in chains n-C_{27}-C_{35} (45.3%) creates a CPI increase to 3.1 (up from 1.7) and a slight increase to ACL; although the increased amount of shorter chained *n*-alkanes means ACL does not increase significantly. This shift in *n*-alkane abundance is mapped by a decrease of 4.9 per mil, from the mean value, in $\delta^{15}N$ values. This large deterioration of nitrogen values, along with the increased abundance of longer chained *n*-alkanes, may indicate an aridity gradient as a prior deviation of +3.6 per mil quickly declines to less positive values (e.g., Luo et al., 2018). There is also evidence from the carbon isotope curve, where values during this same period peak to -22.9‰ (a deviation of +3.1 per mil), at 4,581 ± 851 cal yr BP (see figure 4.14 point e) which indicate another period of aridity.

A rapid increase in CPI (3.1-5.2) and ACL (27.4-29.0) is derived from an increase in the abundance of the longer chained *n*-alkanes C_{27} to C_{35} which have a total abundance of 68.1% at 3,276 ± 397 cal yr BP. The vegetation changes at this time correlate to an increasing dust particulate matter as seen in the Huascarán sequence, as well as slightly increasing values in the $\delta^{18}O$ record at Huagapo cave (Thompson et al., 1995; Kanner et al., 2013). However, these records are more constrained at this period and so may not be exactly comparable to the shifts in the Huarca sequence. This would indicate that Huarca is recording vegetation that is tolerant to drier conditions. Cerro Llamoca also records that inorganic fraction and increased *Cyperaceae* pollen counts, from 3,100-2,900 cal yr BP, indicate that the climate was drier at this time. There is, however, no $\delta^{13}C$ values after this period so there is no observable peak to pinpoint if the abundance of longer chain alkanes is likely to be inputs from C_4 plants.

Middle Horizon – Wilkawain (1,050-1,250 cal yr BP)

A return to drier conditions is detected in the *n*-alkane abundances from 172cm (1,172 ± 150 cal yr BP), in the Central Basin core, with chain lengths n-C_{27}-C_{37} making up 76.4% of the total signature for the sample. The signature is dominated by C_{31} to C_{35} chain lengths, which are typical of arid tolerant plants, although the carbon isotopes in both parts of the basin do not reveal any aridity gradient during this time (see figure 4.20). This dominance of n-C_{27}-C_{37}

continues in the 160cm sample (1,081 ± 95 cal yr BP), which make up a total of 71.5% of the total abundance.

The $\delta^{13}C$ record records a deflection of +6.5 per mil from the recorded mean to -19.5‰, indicating a shift to arid conditions within the basin. This amelioration is a distinguishable shift from C_3 to C_4 plant communities with ~47% mixing of C_4 plant material at this depth. This return to drier conditions, in the Andes, is recorded in other records as occurring between 1,500 and 900 cal yr BP during the MCA (Bird et al., 2011b). The Huarca sequence has 2 *n*-alkane samples and the peak in $\delta^{13}C$ in this basin, during this time, that also add to the evidence of an increased dry/warm phase. Bird et al. (2011a) suggested that this period of drought is due to a considerable weakening of the SASM and linked this event with the MCA and northward positioning of the MCA, between 850-1,050 BP. With Schittek et al. (2015) linking sudden reductions in *Poaceae* pollen percentages and Mn/Fe ratios, affecting water regimes and vegetation cover of the Andean grasslands. They record that this period of extreme drought peaks ~1,050 BP and lasts until 700 BP, when grass pollen becomes more prevalent again. A second hypothesis for the large deflection in $\delta^{13}C$ values, could also come from agricultural practices. There is a suggestion from plant data, taken from a nearby maize field, that the samples at 160cm and 172cm could contain *n*-alkane signatures similar to that of Maize and Potato, the former producing $\delta^{13}C$ values that are between -15‰ and -10‰ (Szpak et al., 2012); with the bulk signal containing ~47% C_4 plant material, this isn't out of the realms of possibility for there to be agricultural practices during the MH. However, without definitive compound specific isotope analysis on these bulk *n*-alkane signatures, this project cannot be certain of this hypothesis. The drought period during the MH may have made it difficult for irrigation systems to keep up with water demand in the highlands, although evidence from Keushu (see figure 4.1, for location) suggests that irrigation canals fed from meltwater from Huandoy glacier would have still been in use during the MH and could have provided the water needed for agricultural practices (Herrera, 2007; Gerdau-Radonic and Herrera, 2010).

Late Intermediate Period (500-1,050 cal yr BP)

A *n*-alkane sample from the edge core, taken at 240cm (785 ± 267 cal yr BP), reveals changeable conditions in the basin with a mix of multiple chain lengths. The abundance of n-C_{16}-C_{20} are at the highest values in this part of the basin with a total of 9.1%, which affects the ACL bringing it to 28.0. The CPI, for this part of the basin, remains high due to the abundance of middle and longer chain *n*-alkanes which have an abundance of 36.0% and 47.5% respectively (see figure 4.20). The higher abundance of n-C_{16}-C_{20} *n*-alkanes, in the edge core, may indicate a presence of algae or cyanobacteria in the sediments which would mean the water table has risen sufficiently to accommodate them. The *n*-alkane signatures for the edge core 240cm sample also indicate a continued usage for agriculture, with similar signatures of maize and potato identified within the sample. This would suggest that the basin would have been used even after the decline of the Wari polity after the MH.

Similarly, the edge core 200cm sample (673 ± 105 cal yr BP) contains a *n*-alkane signature that is similar to that of containing potato and maize. This signature coincides with a peak in the edge $\delta^{13}C$ record of +2.1 per mil from the average, suggestive of increased mixing of C_4 material (~17%) (see figure 4.15 point b). The *n*-alkane abundance at this level is dominated by n-C_{27}-C_{35} chains, which make up a total of 74.9% of the total number of chains. There is no comparable peak in the central basin core, as there is another hiatus from large influx of unsorted clastic material during the early parts of the LIP record.

The central basin n-alkane sample at 76cm (572 ± 32), is recording another change in the plant communities from previous samples in this part of the basin. A sharp increase in chains n-C_{16}-C_{20} (2.2%-10.8%), decreases the CPI to 3.4 and slightly reduces ACL to 28.7. This event occurs within the LIA, a period of increased rainfall and cooler temperatures in the highlands. The LIA is also associated with glacial readvances likely as a result of southward displacement of the ITCZ (Bird et al., 2011a). At Huarca, this is also indicated by more negative $\delta^{13}C$ values as the bulk signal is identifying sources of C_3 plant material.

Late Horizon (418-500 cal yr BP)

Due to the short-lived nature of the LH, at Ancash, there are only a small number of samples associated with this horizon. There are 2 *n*-alkane samples for this horizon, central basin 40cm and edge core 150cm which are dated as 479 ± 39 cal yr BP and 470 ± 150 cal yr BP respectively. Both of these samples contain a large variety of chain lengths, but the most abundant is C_{31}. The edge core sample contains more chains that typify those from higher plants, such as trees, but this may be due to where the core is located rather than a large vegetative change. Due to the climatic pressures of the LIA, bringing in cooler temperatures, it is unlikely that there would have been any agriculture at these altitudes. As mentioned in section 4.4.1, any cooling of 1-2°C may have lowered the limit of arable agriculture by up to 400m (Cardich, 1985). $\delta^{13}C$ values for both records decrease by -0.7 per mil and -1.9 per mil for both the edge and central cores respectively.

Colonial Period to Present Day (0-418 cal yr BP)

Moving into the colonial period $\delta^{13}C$ values remain low for both areas of the basin and coincide with the lowest $\delta^{18}O$ values in the Huascarán sequence, during the height of the LIA (Thompson et al., 1995). The *n*-alkane sample at 116cm for the edge core (381 ± 50) reveals a mixed abundance of chain lengths, which influences the ACL increasing its value to 29.2. It is unlikely that there is any human occupation during this time, as the site at Keushu shows abandonment during the Colonial Period (Gerdau-Radonic and Herrera, 2010); thus, the dominance of n-C_{31} may be a signal of higher plants, such as trees, or from grass species on the bog surface rather than a signature of agricultural practices. This is similar to the signature found in the 12cm sample in the central basin core (257 ± 49 cal yr BP), where there is a mix of chain lengths, but is indicating the changes in plant communities at this time. The above samples still lie within the limits of the LIA and are therefore unlikely to be representative of arable agricultural sequences.

There is a definitive shift to negative $\delta^{15}N$ values, from 195 ± 133 cal yr BP, within the edge core record (see figure 4.15 point c). The deflection is mean decline of -6.74 per mil with low values continuing through until ~49 cal yr BP. The carbon isotope record for the same timeframe shows a slight deviation of -1.48 per mil before increasing to the mean value of -26.0‰ by ~49 BP. These negative values may indicate early use of nitrate rich fertilisers, for use in arable agriculture during the 1800s. Peru, during the 19th Century were one of the largest exporters of sodium nitrate (Melillo, 2012), so it is plausible that synthetic fertilisers could have been used (alongside the established guano fertiliser) during the 1800s. Previous studies have found that grain crops, such as maize, had lower $\delta^{15}N$ values than plants grown in the same soils with other natural fertilisers added into them (Yoneyama et al., 1990; Bateman et al., 2005).

$\delta^{13}C$ values for both cores become less negative towards the modern sediments, with the central basin and edge cores recording a mean increase of 1.8 per mil and 1.2 per mil by ~1990 AD, suggestive of a return to warm/dry conditions in the modern era. The signature for more modern *n*-alkanes can be observed in the 50cm edge core sample (~1960AD). The signature is potentially indicative of modern agricultural systems with similarities shown in the *n*-alkane abundances of potato, quinoa, and maize, which are still being farmed nearby today.

Environmental and Land-Use History

The NPP assemblage covers roughly the last 692 years BP, split into 4 zones and covers multiple cultural horizons. The identification of *Sporormiella* and other coprophilous fungal remains within the basin would suggest that Huarca has been used, in some form, throughout the last 692 years, by animals at the very least. The majority of zone 1 is made up of HdV-16a (*Byssothecium circinnans*), the fungus producing the HdV-16a ascospores prefer mesotrophic *Sphagnum* type peats coinciding with relatively dry periods (van Geel et al., 2006a). The HdV-16a ascospore counts decline towards the top of this zone, as conditions in the region start to deteriorate and precipitation starts to increase. The low counts of dung-related ascomycetes (17.8% of the assemblage), during the end of the MCA may reflect a pastoral use for the area, rather than large-scale human occupation.

HdV-16a does not appear in zone 2 (~385-377 cal yr BP), which indicates that Huarca may become too wet a habitat for it to occur. This zone occurs within the limits of the LIA, in the Andes, and occurs during a time of increased precipitation (as mentioned above). Coprophilous fungal spores start to increase in number, through this zone, although no spores of *Sporormiella* were identified – an important indicator of herbivory. In its place there are *Sordaria* type (HdV-55) spores (7.8%) and TM-H (17.1%), which may indicate that the basin is being used in for pastoral agriculture. Humans are within the basin area during this time, as indicated by the presence of HdV-351 (31%) (van Geel et al, 1981), which are most likely to be a mixture of colonial settlers and locals using the area for grazing large herbivores. This is further evidenced by the greater abundance of *Coniochaeta cf. ligniaria* (HdV-172, 13.9%), which occurs where there is a large density of herbivores (van Geel and Aproot, 2006). HdV-

172 is can also give an indication of open fen conditions, where the basin surface becomes wetter under increased precipitation during the LIA (as mentioned above). The reduced counts of *Discomycetes* (EMA-25) indicates a reduction of *Alnus* forestry in the area. Marcacocha records reduction in *Alnus* pollen around 500 BP, slightly earlier than at Huarca, which is attributed to forest clearances by the Spanish for a greater area for grazing pasture (Chepstow-Lusty et al., 2009; Handley, 2022).

Coprophilous fungal remains remain scattered throughout zone 3 (~309-108 cal yr BP), with low counts of *Sporormiella* identified (1%), although dung-related ascomycetes make up 28.8% of the total assemblage. However, the majority of these remains were identified within the first 4 samples (86-98cm) which could point towards a temporary abandonment of the basin from ~235 cal yr BP, during the colonial occupation of Peru, or at least a much-reduced usage of the basin. Further evidence of this may be found within the human disturbance indicator HdV-351, which also does not occur in any meaningful number after 94cm – with >1% identified in the upper parts of the zone. Climatic conditions during this time, may not have been favourable for large-scale agriculture, at this altitude. HdV-16a counts start to increase again at the beginning of zone 4 (~78 cal yr BP), indicating a return to relatively drier conditions at the end of the LIA – which increase through the zone to a maximum at 62cm (~49 cal yr BP). *Sporormiella*, *Sordaria* (HdV-55) and *Podospora* (HdV-368) type fungal spores are identified in large numbers through zone 4, indicative of an increased use of the basin into the modern day. HdV-351 is also identified in large numbers, giving further evidence to an increased human and animal use into the modern era.

KEY POINTS IN CHAPTER

- Huarca sedimentation has been accumulating for ~11,468 cal yr BP in the Central basin and ~11,480 in the Edge of the basin – roughly at the same period. Accumulation of sediments possibly occurred due to retreat of ice at the end of the last glaciation.
- Isotope signals show a drying signal and changes in plant communities after retreating glaciers, between 8,000 – 3,000 BP in the beginning of the Holocene.
- Sedimentary evidence suggests that Huarca may have become an open lake for a short time, during a pluvial phase between 3,877-3,966 cal yr BP, after a long period of aridity during the mid-Holocene.
- Large influx of sediment in the Central Basin core is mapped by a shorter section of clays and silts in the Edge core (units 26-28 - ~1,837-2,527 cal yr BP). The large sediment influx, in the central core may have originated from glacial meltwater entering the basin approaching the MCA, as temperatures increased.
- Large deflections in the isotope record, from the central basin, are mapped by dominance of long chain *n*-alkanes between 1,172-1,081 cal yr BP. Two hypotheses arise from this: 1) This is due to arid conditions towards the end of the MH during the MCA or 2) this is an agricultural signal as there is a mixing of ~47% of C_4 plant material. It is possible that this is a mixture of both, as meltwater from retreating glaciers could provide the necessary volume of water for irrigation.
- *n*-Alkane abundances from the Edge core, during the LH, suggest a change in plant community to emerging macrophytes and a greater number of woody species. This is due to the wetter climates during pluvial phases of the LIA (which is also recorded in the isotope curves). The *n*-alkanes would also be suggesting a change to agro-forestry rather than crop agriculture, as there is also a suggestion of lower temperatures during the LIA.
- Evidence from NPPs and *n*-alkanes to suggest that there was a reduced use of the basin during the early stages Colonial Period, but this again changes at some point into the 19th Century.
- Radiocarbon dating programme reveals that there are large age differences between the bulk and plant ages of the same depth sample, which seems to be greater with depth. Evidence from Rock-Eval pyrolysis to suggest that this is due to presence of ‘old carbon’ sediment sources.

5. Antaycocha

5.1 Introduction

Chapter 5 sets out the results and analyses from the Antaycocha sequence, Chillón Valley. The first section focusses on the main archaeological history of the region, as a way of introducing the history of the wider archaeological zonation. This is followed by a brief section of the methodology (more can be found in Chapter 3), which covers the main field methods as well as the radiocarbon chronology. A full description of the results follows this, including the sedimentology, inorganic and organic geochemistry, and the palaeoecological analysis. Finally, the results are discussed to allow for interpretations to be made about the history of the basin and the human interactions that might have occurred.

5.1.1 Regional Archaeology

The regional archaeology of the Chillón Valley has been broken down into three main zones (following the classification of Dillehay, 1977 and also set out in the PhD thesis of Handley, 2022), which are the lower valley (0-600m a.s.l) which is the most intensely farmed zone, middle valley (600-2000m a.s.l) being within the *Yungas zone* (500-1000m) this was especially important for the Inca, who implemented specialist workforces to cultivate the plants located here; and also the upper valley (2000-4000m a.s.l).

Lower Valley

The first recorded developments were recorded as early as 4,450 cal yr BP, which were only mere villages distributed along the lower river valleys (Cohen, 1978). It wasn't until ~3,900 cal yr BP that the first large-scale settlement of Chuquitanta, was recorded – which lasted until ~3,750 cal yr BP. According to Cohen (1978), the site itself may have developed due to its location within the wider expanses of the Chillón river allowing for the development of early agricultural systems for the growth of a variety of food and textile crops.

The first independent settlements expanded and developed further during these formative years, into the Early Intermediate Period (EIP) (2,150-1,300 cal yr BP for the Chillón Valley) through a system of inter-site trading and communication with nearby villages and towns (Jennings and Craig, 2001). During the latter stages of the EIP, the Lima culture developed and dominated the Chillón and other neighbouring coastal valley, such as the Ancón and Chancay – based on the distributions of Lima style pottery remains found in these sites (Mauricio, 2018). The Lima culture is accredited with advancements in agricultural practices, utilising both agricultural terrace systems and 'sunken fields', with evidence for this found in the nearby coastal valleys (Shoobridge, 2003; Kalicki, 2014). This advancement allowed for some rapid population growth through to the beginning stages of the Middle Horizon (MH) (1,750-1,300 cal yr BP) and has been attributed to a series of, well documented, El Niño events that transpired during this time; which affected much of the Peruvian coastland areas (Moseley et al, 2008; Beresford-Jones et al., 2009; Mauricio, 2014; Palacios et al., 2014). It is likely that

the higher river flows, and increased ground water levels, caused by these El Niño events would have played a vital role in the population nucleation of larger settlements and expansion of Lima polity, based on the expansion of the agricultural systems (Mauricio, 2014).

During the latter stages of the Lima culture, into the MH, newer types of architecture started to appear that is characterised by influences from Wari iconography (Segura Llanos, 2001). Surprisingly, however, there are very few Wari sites on the central coast of Peru except for some poorly understood orthogonal structures of Socos in the Chillón Valley (Jennings., 2006b, Kalicki, 2014). The subsequent population decline, in the MH, in the coastal valleys have been linked to intense droughts followed by large scale rainfall due to increased ENSO activity along the coast (Flores, 2019). The Lower Valley appears to be disconnected from the larger empire states of the MH and the LH – again there is little evidence for any LH archaeology within the coastal valley sites (Dillehay, 1977). There are, however, two sites within the Lower Valley of the Chillón that show some influence of Inca reconstructions commonly referred to as Tambo Inca and Collique. The site of Tambo Inca includes a series of remodelled enclosures and some remaining high-walled corridors on a strategic hilltop locale, leading to a suggestion that it had some minor administrative responsibility (Dillehay, 1977). Similarly, the site at Collique sits upon a vantage point overlooking a vast amount of the Chillón, allowing for the occupants to control the transportation route through the valley (Dillehay, 1977).

Middle Valley

The middle valley has been occupied from the EIP through until the Colonial era (c.2120-129 cal yr BP). One such site is that of Huancayo Alto, which lies ~50km inland, on the south bank of the river. It is comprised of a variety of residential areas, which would have housed the common and elite classes, and was built up over many years of occupation (Dillehay, 1977). On an adjacent hill there are vast amounts of storage units, which extend ~450m up the hillside, these were guarded by several controlling walls that would have also served as entranceways to these units and drying terraces (Dillehay, 1977). These findings support the contention that the agricultural practises, in the valley, likely produced an excess and that the distribution was accessed and controlled by a limited number of individuals (Dillehay, 1977).

During the LIP and LH, the populations took advantage of the Inca expansion through the valley, to press into the reaches of the lowlands for development; in complete contrast to earlier horizons which saw expansion and development up into the valley, with the emergence of the Lima state and pressure from coastal settlers (Flores, 2019). During this same period, the region between the coast and the highlands became an economically and culturally diverse region and acted as a developmental region for transhumance, in a time that is often described a period of endemic war dominated by local warlords (Covey, 2008b; Kalicki, 2014).

Upper Valley

The final study region is the steppe-sierra zone of the upper valley which, unlike the middle and lower valleys, did not have a permanent settlement until the LIP. However, in a similar way to the lower and middle valleys there are few remains of any Wari ceramic material or other representation of Wari culture, in the part of the valley either. The morphology of the upper parts of the valley, with its steep walls and rocky soils do not provide a suitable terrain for the earlier agricultural practices to be carried out. This may have been the contributing factor for less permanent settlements being the norm until the LIP. The later civilisations such as the Inca, who had the capabilities and the resources to occupy the highland territories, created vast swathes of terraced systems along the steep banks of the upper valley, to provide the agricultural space needed to feed its growing empire (Silva, 1996; Handley, 2022).

Through the LH, there are increasing number of archaeological sites the further up the valley as evidenced at Puramarca, Cantamarca, Huancuna, Huamantanga, Huayuncancha and Colli (Dillehay, 1977). These sites may have been placed strategically in order to control the access routes through the valley and may represent some other administrative roles, such as delegation of water control or of other local economic transactions (Dillehay, 1977). For example, the sites of Caballo Blanco and Lucana were both located near to major canal confluences and would have provided the main source of water for irrigation for the agricultural terraces built by the Inca (Dillehay, 1977).

Cantamarca is arguably one of the more important sites in the Chillón Valley, which is situated on a hilltop above the town of Canta above the wetland sites of Antaycocha and Torococha (Handley, 2022). The wider Cantamarca archaeological zone had been occupied from the early phases of the Chancay culture, during the Lima Period (1950-1300 cal yr BP), through to at least the Colonial period (418-129 cal yr BP) (Farfán, 1988; 1995; 2011). There is evidence to suggest that there was a more ephemeral settlement from at least the LIP onwards, with little data to suggest that there was a continuous settlement throughout its history (Handley, 2022). There is, however, a vast amount of Incan influence visible at the site with presence of murals, walls, storage houses, columns, and building styles (Farfán, 2011). The Cantamarca zone would have enabled the Incan populace to engage in a range of economic activities, revolving around the waterways and nearby lagoons (Farfán, 2000; 2011). Canals and other water features have been identified around the archaeological zone, allowing for the diversion and control of water around the area (Handley, 2022). Sources of water, thereby water control and access, was an important feature for pre-Columbian settlements, in the highlands, and remains as such today – revealed through the management of the water systems in pre-history and in modern management systems.

5.2 Study Area and Site Description

The basin at Antaycocha (11°26'33.60"S 76°35'9.69"W) is located near to the village of Canta at 3,601m a.s.l. The site itself consists of an infilled basin, which is dammed at one end: limiting

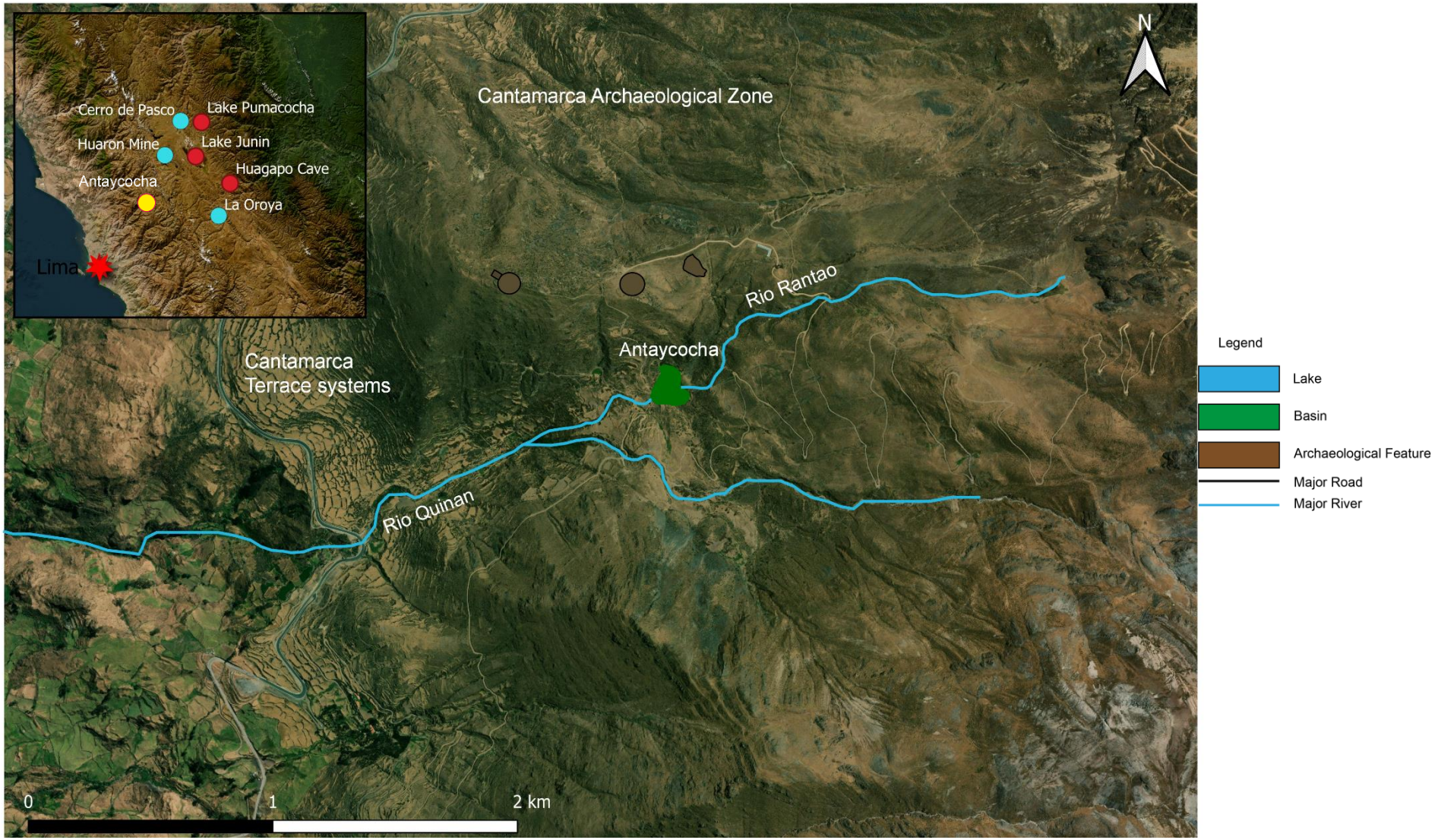

Figure 5.1: Map of the basin of Antaycocha, within the Cantamarca Archaeological Zone. Terrace systems can be found on thee left hand side of the image, with some archaeological features on the hill, to the north of the map. Inset is the location of the basin in relation to major quaternary records in Peru, as well as the major mines that are mentioned in the text. Map created in QGIS using the ESRI satellite plug-in.

the flow of water out of the basin. The dam is thought to be of Late-Intermediate in origin (C. Farfan, pers. comm.), but there is no concrete evidence to support this yet. The wall has a height of around 3m (see figures 5.1 and 5.2), but the material recovered was over 6m in depth – suggesting that this may have been put in place to manage the water table for irrigation through the valley or for water storage. Water enters the basin through a small stream, of relatively high velocity, towards the rear end of the basin and exits again over the wall into a smaller wetland named Torococha. The main vegetation types around the mire consist of grasses and mosses, with reeds towards the centre of the basin. The surrounding slopes are home to a variety of relic terraces that may have been used for agriculture and water transport through the valley. There may have been some camelid herding on these terraces also, as there are some corrals in the immediate area of the basin itself. Some of the terraces are heavily eroded in places and there is no evidence of any modern-day agricultural systems being undertaken on them. There are a variety of other structures around the basin, all indicating that the site has been occupied for multiple periods, ranging from the Late Intermediate Period to the Late Horizon and possibly through to the Colonial era.

5.3 Methodology

For the main methods used at Huarca, please see the methodology section (Chapter 3). Some of the original sample number codes for this site appear as “CAN-X” as the labels were identified as “Cantamarca”, adopting it name from the wider Cantamarca archaeological zone. It was after further discussions with Carlos Farfán, that the name Antaycocha was discovered and adopted for the basin for all future work.

5.3.1 Field Methods

The sampling site for the Antaycocha basin was decided in 2018, reaching a maximum depth of 5.97m (see Handley, 2022). The core was gathered near to the edge of the wetland with the dam, as this allowed the capture of proxies on the outflow of the basin while also allowing the best access to the site itself. The middle of the basin was under too much water, and the dense vegetation made it too difficult to try and gather any core material. The same area was cored again during the 2019 season, where three replicate cores of ~6m each (maximum depth reached was 6.1m) were gathered using a Russian peat corer. This was the full depth of the basin at the coring location, but the basin is likely to be deeper closer to the centre of the lagoon. There is only one previous quaternary study on this site from Handley (2022), but none that cover the geochemical techniques used in this project.

Figure 5.2: Photograph of the Antaycocha basin. Red arrow marks the location of relic terrace systems in the background. The blue arrow marks the location of a wall, thought to be of Inca origins. Photograph by Stuart Black.

5.4 Results

5.4.1 Sedimentary Analysis

There were 3 replicate cores gathered in 2019, with a maximum depth reached of 6.1m in core 2. In total, there are 44 separate units for the Antaycocha sequence which are described below (also see figure 5.4) and mostly comprise of fine lake sediments with detrital plant material found throughout. Unit 1 (557–610cm) contains some banded sedimentation that is primarily made up of coarse sands, indicating that this is the base of the lake system that would have existed before the infilling. The LOI here is at its lowest here (see figure 5.4) (6.5%), which correlates given the nature of the type of sediment. This continues into unit 2 (537-557cm), which is a continuation of the below unit – but the banding has ceased. At 537cm, there is a transition to more lake sediments with detrital herbaceous material identified within. LOI levels remain low, even at this depth, with values of 17.2%. There is a sharp contact into unit 3 (521-537cm), where there are some identifiable lenses of more herbaceous material. Unit 4 (508-521cm) is likely a continuation of some of this herbaceous material, but the nature of the sediment reveals that the water table has risen again, to deposit more fine-grained sediments. TOC% values peak at 28.9% towards the top of this unit, before returning to 20.8% towards the transition to unit 5. Unit 4 also has some evidence of banding, which given the resolution of the dating programme could mean that they are seasonal laminae. This banding continues into unit 5 (490-508cm) with some increase in plant macrofossils at the top of the unit, although a little increase in LOI values (25.5%).

Unit 6 (478-490cm) comprises of pale lake sediments with little plant macrofossils contained within it, which is overlain by a thick unit of clays (unit 7 – 452-478cm). This unit contains a greater abundance of plant macrofossils. Units 8-12 (395-452cm) the sequence primarily consists of lake sediments, with varying amounts of plant material contained within them. There appears to be more iron rich material found in the sediments between 412-415cm, with a small decrease in LOI values from 28.5% to 24.9%. There are more banded structures in unit 13 (378-395cm), where more silt and clays are input alongside the detrital material. Units 14 to 19 (330-378cm) contain more silts and clays, in place of the plant macrofossils, but there is no evidence of any banded structures within these units. There is, however, an irregular upper contact from unit 13 to 14 which could be a representation of erosional processes. LOI values remain relatively stable within these units, staying between 28.2% and 27.9% through all these units. Plant material appear in greater abundance towards the top of unit 19, but these are more detritus than large macrofossils.

Large plant macrofossil appear unit 20 (321-330cm), before making way for finer lake sediments again in unit 21 and 22. Banded structures are identified again in unit 23 (275-301cm) these layers, however, are only identified in one of the cores in the Antaycocha sequence. They also appear thicker than the layers identified further down the core; given the thickness and how few there are the bands may be separate units and not laminated segments. They could also be contamination from other sedimentary units as a result of the

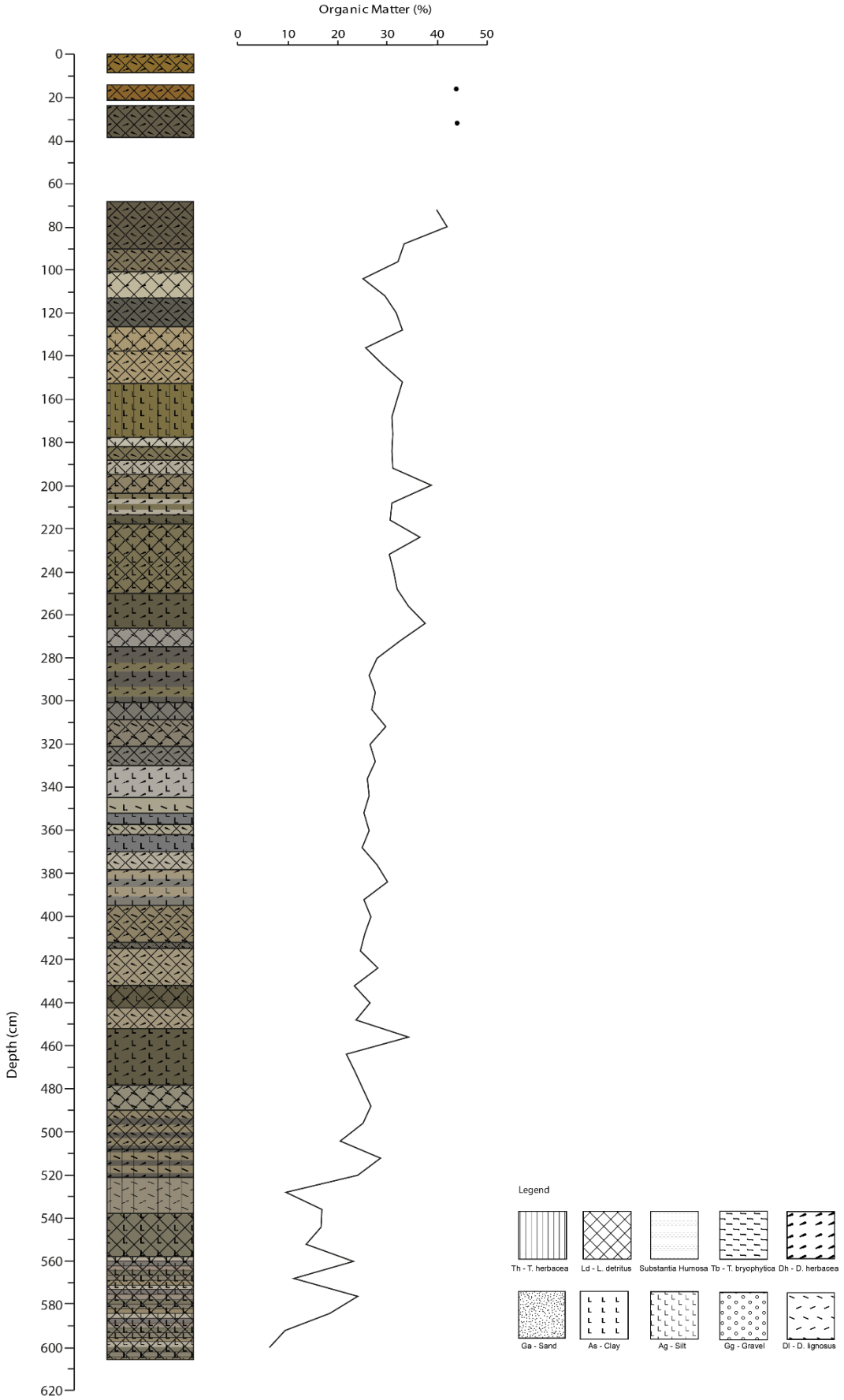

Figure 5.4: Stratigraphic log of the Antaycocha sequence with the Loss on Ignition (LOI) values expressed on the right-hand axis

coring methods. Lake sediment units 24 and 25 (250-275cm) contain increasing amounts of organic material within them, with LOI values increasing from 33.0% to 37.9% at the top of unit 25, where there are large grass and sedge macrofossils identified. Unit 25 is overlain by thick layers of clays and silts with some herbaceous organic material present (units 26 and 27, 214-250cm). However, LOI values drop to 32.3% towards the top of this unit as the organic matter becomes less prevalent, into the unit above. Unit 28 (204-214cm) is another continuation of banded structures, that appear in all cores in the sequence. These are all ~5mm and it is plausible that they could be annually laminated, given the rate of sedimentation at this basin.

Units 29 to 35 (153-204cm) all contain lake sediment type sediments, with some silt material through them. There is little plant material in these units, except for within unit 30 which appears to have a greater abundance of rootlets and some sedge material contained within it. TOC% values remain at around 31% through these units but rise to 39.1% in unit 30 – with the increase in plant matter. Despite the presence of reeds through unit 36 (137-153cm) LOI values decrease from 33.4% to 26.0%, possibly due to the prevalence of finer grained material. LOI values do increase in unit 37 (126-137cm), with a peak of 33.4% in LOI values recorded at 128cm. This peak deteriorates as organic matter becomes less abundant, and lake sediments more prevalent again, in units 38 and 39 (101-126cm as the basin moves into the modern age. A white precipitate is identified around some of the material in unit 39, but this has yet to be identified. Units 40 to 44 represent the top of the basin and the modern age of the sequence, as these ages are well into the post-bomb modelled radiocarbon ages. Some of the sediment was not retrieved here, and is missing from the sequence, but it would have most likely matched the surrounding sedimentary units of organic rich lake sediments.

5.4.2 Radiocarbon dating

There are currently 5 radiocarbon dates for this sequence, taken from the Antaycocha basin core selected from the 2018 core (See Table 5.1 below). The modelled ages and the radiocarbon samples can be found in the appendix. Where possible plant macrofossils were selected and sent to be dated (these made up 3 of the 5 samples), where there were not enough plant material bulk organic lake sediments were submitted instead. The basal radiocarbon age was revealed to be between 2,853 – 2,763 cal yr BP (95% confidence range), with the modelled age for the base of the core believed to be 2,920 ± 50 cal yr BP at 6.1m. The majority of the core has accumulated within the last 515 years, as a radiocarbon date from 5.5m suggests an age range of 537 – 496 cal yr BP. This has resulted in a large sediment accumulation rate, resulting in high precision analysis of the sediments.

Table 5.1: Results from the radiocarbon dating programme from Antaycocha

Lab No.	Sample ID	Sample Depth (cm)	Radiocarbon Age BP	Calibrated Date Cal yr. BP (95% confidence)	$\delta^{13}C$ ‰	Material Dated
SUERC-92957	CAN-2-88	88-89	n/a Modern Date	AD 1957-1988	-27.7	Bulk Organic Sediment
SUERC-92958	CAN-5-300	300-301	366±37	469-310	-24.4	Picked Sedge Material
SUERC-92959	CAN-7-504	504-505	413±37	524-451	-26.2	Picked Sedge Material
SUERC-97576 (GU57263)	CAN-8-550	550-551	475±26	537-496	-25	Picked Sedge Material
SUERC-97577 (GU57264)	CAN-10-590	590-591	2,714±26	2855-2759	-25.5	Bulk Organic Sediment

The purpose of carrying out this programme was to ascertain the age of the sequence, but to also try and ratify the age of the wall that has dammed the basin – as this is the most likely cause of the high sedimentation rate at the site. With a well constrained age model for the basin the project can make comparisons to existing terrestrial, marine, speleothem, and ice core records which span the length of the cultural horizons. One of the dates (SUERC-92957) returned a 129% modern reading and was therefore calibrated using the Bomb21NH1 curve (Hua et al., 2021). The rest of the dates were calibrated using the current IntCal20 radiocarbon curve (Reimer et al., 2020) using OxCal 4.4 (Bronk Ramsey, 2009a). All of the dates gave a good agreement with the model (>60% (see Bronk Ramsey, 2009)) and were all kept within the model (see figure 5.5). The use of IntCal20 and Bomb21NH1 were used in this study region as the results of using a mixed curve or the southern hemisphere equivalents, produced negligible differences when used in the construction of the age-depth model.

5.4.2.1 Note on the radiocarbon dating programme

The original radiocarbon dating programme was designed to give an age to the basal sediments and the start of organic matter accumulation (SUERC-97576 and SUERC-97577). The other dates were sampled at depths that gave the most amount of organic material (as the basin has low amount of organic matter). One date was taken at 300cm, as this is the depth of the base of the wall, at the top end of the basin (See figure 5.2). It was hypothesised that the wall may have been of Middle Horizon age, and thus adding a radiocarbon date at this depth would reveal its true age. A sample taken close to the top of the core was also taken, to give information on the age of the top sediments.

The radiocarbon dated material are all well constrained, with the majority of the model showing small date margins as modelled by OxCal. Where there are large margins are at the base of the core, with the largest range at ±947 years. This is not a big issue for this site, as the time

period for this modelled age would have had no humans within the landscape – which this study has particular interest in. It does, however, pose a problem when making comparisons to other records, as these modelled ages are during a time of changeable conditions in the Peruvian Andes.

5.4.3 Bulk Organic Geochemistry

The bulk geochemistry at Antaycocha has remained relatively very stable throughout much of its history, as shown through the Rock-Eval6 pyrolysis (see Figure 5.7). T_{MAX} remains high throughout the sequence, hovering around 400°C for much of the sequence. It is only towards the more modern sediments, where the sequence becomes more organic rich (~AD 1970) that the T_{MAX} rapidly declines to 280°C. TOC% and T_{MAX} curves have a more direct relationship at this site, where T_{MAX} remain higher the TOC% values remain low – due to the type of sediment that is found at Antaycocha. As alluded to in the previous section, TOC% values begin around the 1% mark, at the beginning of the sequence, as an abundance of sands can be found at this depth, which then increase to 4.6% at 2,778 ± 640 cal yr BP. Both HI and OI fluctuate at this lower section but, with the in-washing of sediments remaining relatively constant, the HI:OI ratio favours OI through much of the sequence. Both TOC% and HI values decrease at ~605 cal yr BP to low values, with TOC% remaining at 1-2% until 506 ± 34 cal yr BP. HI rapidly fluctuates between 141 and 189mg HC/TOC before reaching a low of 115mg HC/TOC at 506 ± 34 BP.

A small peak in TOC% values at 7.1%, is met by a rapidly decrease in values which stay at ~3.5% for ~14 years, before a two-step increase to 5.5% and then to 7.1%. At a similar stage, the HI:OI ratio is almost equal (476 ± 34 cal yr BP), potentially as a result of an increase of organic sediments from within the basin – as water levels decrease to allow for these sediments to accumulate. Both TOC% and HI values track one another as both curves rapidly decrease again to low values from 459 to 446 cal yr BP. Values in HI steadily increase, and map onto the increase in OI values, whilst TOC% values remain at a constant level. TOC% values rapidly increase again, to 7.0%, as it tracks more organic matter sources input into the basin from 371 ± 45 cal yr BP. TOC steadily increases from this point forwards, into the more modern sediments. The HI:OI ratio starts to favour HI in these modern sediments, from ~AD 1920, as more organic sediments have started to accumulate on the basin surface. The water table has decreased significantly enough for this to happen, but there is some observable fluctuation through the top 1m of the core.

5.4.3.1 Rock-Eval pyrolysis and PCA testing

Statistical analysis of the Rock-eval dataset was conducted using Principle Component Analysis (PCA) in order to identify potential OM sources and controls of thermal degradation of that OM. The results of the PCA test reveal that PC1 is mainly influenced by parameters that are controlled by thermal processes of degradation, or those samples that contain more hydrogen poor labile OM i.e., high values of OI and T_{MAX}. These samples often are of an allochthonous origin and therefore do not originate from within the basin itself.

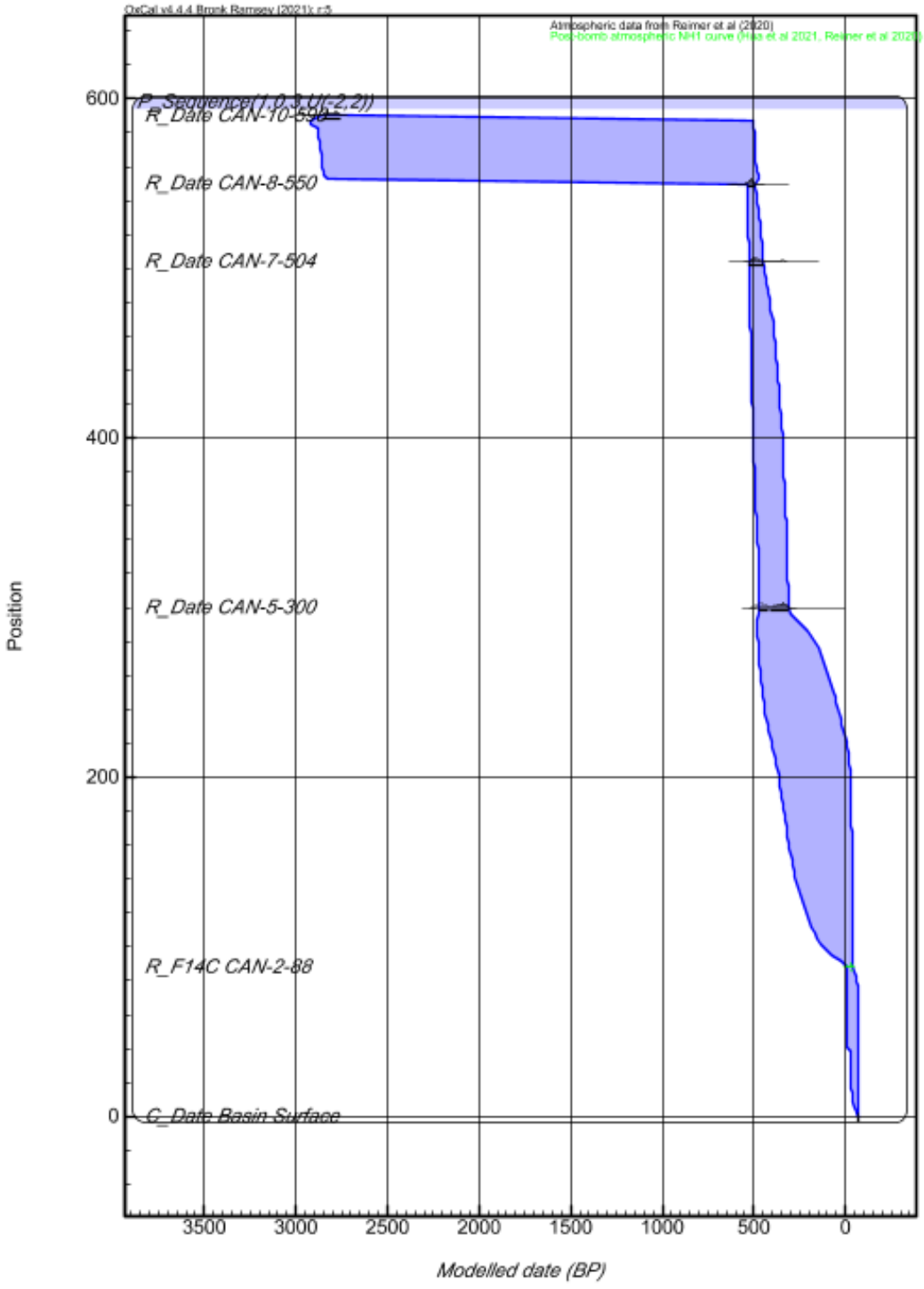

Figure 5.5: Results from the radiocarbon dating programme at Antaycocha. The "CAN-X" identifiers are due to using the name 'Cantamarca' from the wider archaeological zone.

This can be seen within in figure 5.6a with most samples plotting within the zone circled in blue. The parameters of the Rock-Eval within this zone are those mainly used to indicate sediments that have undergone more aerobic decay and are likely to have been transported into the basin by other means. The samples plotting towards PC1 are those samples that are terrigenous inputs, with the sediments originating from within the basin itself. Only a handful of samples plot towards PC2, which are those defined as organic productivity and are therefore more hydrogenous and seem to not have undergone aerobic decay.

The PCA plots can further be enhanced by adding in elemental components from XRF datasets (figure 5.6b). Here the metals identify further sources of sediment input. The elements Ti, Zr, K, Rb, Tb, Sr, Nb and Si all plot against PC1 – and are suggestive of terrigenous sediment transport within the basin. With P, Al, Zn, Ca, As, Mo, Y, Cu, Ag, and Cd all plotting against PC3, seemingly these elements are of an aeolian origin and are results of atmospheric pollutants. With the addition of the elemental data the TOC, PC, RC, and HI parameters now plot against PC2 along with Fe which indicate that Fe is related to organic productivity within the basin. The conclusion here is while the Rock-Eval dataset can unpick sources of OM from within a dataset, adding in other elemental data can help strengthen results further and may give further insights into sources of OM; for example, terrigenous vs transported matter.

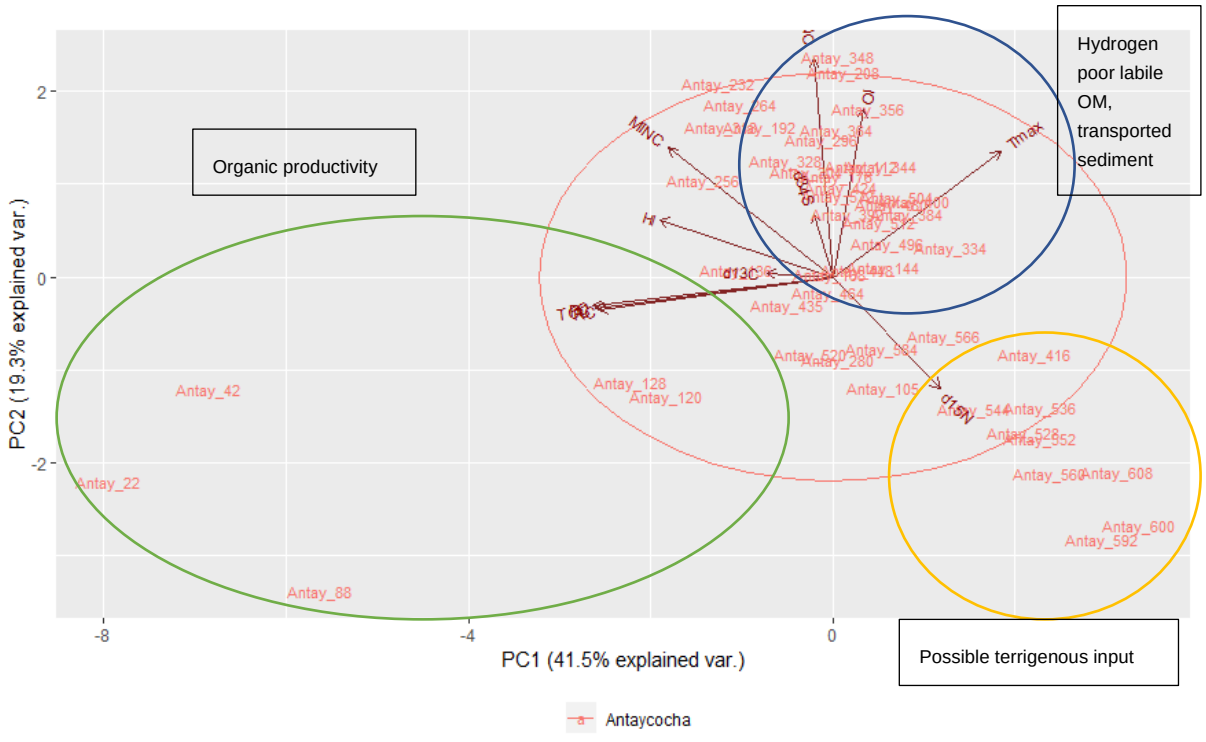

Figure 5.6a: PCA plot from Antaycocha, without the elemental data, illustrating the PC1 and PC2 groupings

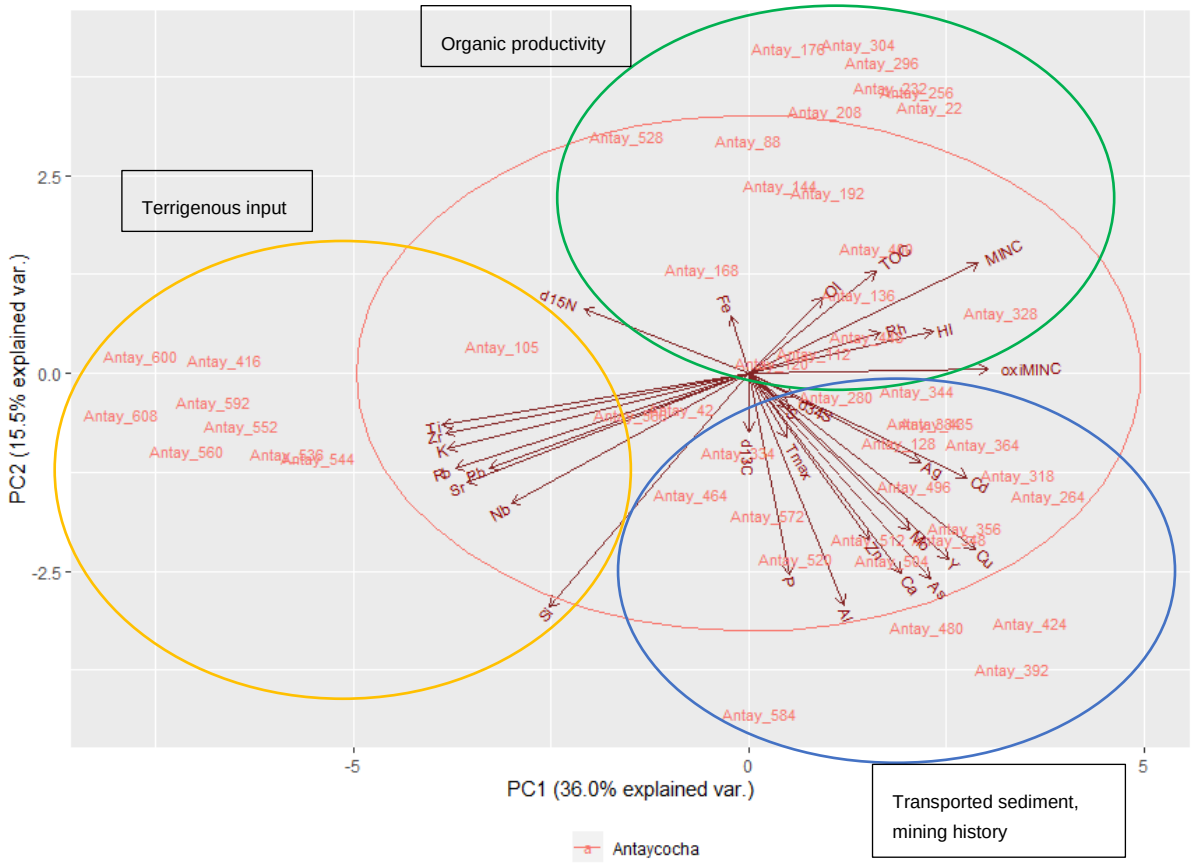

Figure 5.6b: PCA plot from Antaycocha, with the elemental data, illustrating the PC1 and PC2 groupings

5.4.4 Isotope Geochemistry

Both the $\delta^{13}C$ and $\delta^{15}N$ curves begin with very enriched values, at the base of the core, with nitrogen values increasing by 12.7 per mil (from the average) (see Figure 5.7) at 2,855 ± 600 cal yr BP, before rapidly a rapid decline only sees a +0.08 per mill increase by 2,778 ± 640 cal yr BP. Meanwhile, the carbon signal remains enriched for a longer having a mean increased value between 3-6 per mill between 2,903 and 605 cal yr BP and small increases occurring by 510 cal yr BP. These early nitrogen and carbon peaks are generally typical of an open water system, dominated by aquatic-based plants. $\delta^{34}S$ curve does not see an early enrichment peak, when compared to the other isotope curves, instead remains around -20.7‰ until a rapid enrichment of 10.3 per mil at 518 cal yr BP – around the same time as increased values in the carbon curve. A second peak, in all isotope curves, can be observed, at 506 cal yr BP. Shifts of +2.5 per mil in $\delta^{13}C$, +4.1 per mil in $\delta^{15}N$ and +27.4 per mil for $\delta^{34}S$; however, these peaks are all short-lived and quickly fall back to less positive values (see Figure 5.7)

Following this, isotope values steadily decline again in all analysed elements until 488 ± 27 cal yr BP where both $\delta^{13}C$ and $\delta^{34}S$ curves see an amelioration of +2.9 per mil and +12.2 per mil for both carbon and sulfur respectively, by 485 ± 29 cal yr BP. There is not any similar response identified within the nitrogen isotope curve during this period. Values for carbon and sulfur become depleted by 462 ± 39 cal yr BP, with $\delta^{13}C$ values deviating from the mean by –

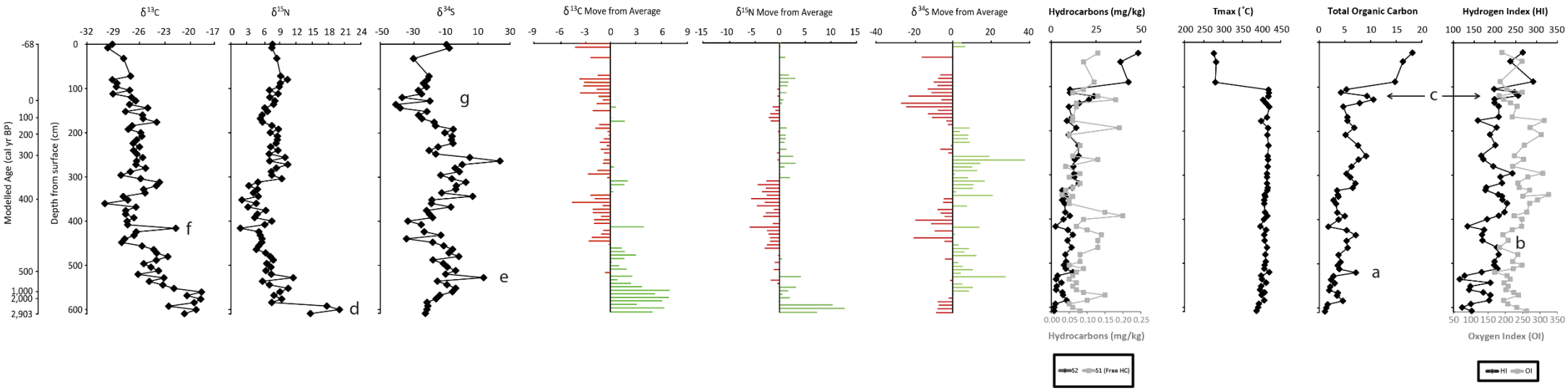

Figure 5.7: Isotope and Rock-Eval6 curves for the Antaycocha Basin, by the depth from the basin surface. Modelled ages are on an axis in calibrated years before present (cal yr BP), the top of the core appears as -68 years for 2018AD.

2.1 per mil with $\delta^{34}S$ values declining by -20.1 per mil. A fourth peak in the carbon record from of +3.9 per mil, at 446 ± 42 cal yr BP, is mapped by a mean decrease in nitrogen values of -5.8 per mil – unfortunately there is no sulfur isotopes recorded at this depth. This is generally typical of an arid event within the study region, where nitrogen values may increase before an arid event before quickly deteriorating to more negative values (e.g., Luo et al., 2018). This is another short-lived event, before both records decrease and increase in values respectively. The trend to less positive values then continues in the nitrogen and carbon curves, between 466 and 391 cal yr BP; before a mean increase of +1.9 per mil recorded in $\delta^{13}C$ and +1.9 per mil in $\delta^{15}N$ ~360 cal yr BP. During the same period, $\delta^{34}S$ values continue to climb, before a large mean increase of 37.5 per mil at 321 ± 89 cal yr BP (see Figure 5.7), the values then fluctuate between -19.9‰ and -6.09‰ in the next ~100 years. Carbon and nitrogen isotope values remain constant between 338-183 cal yr BP, with sulfur remaining in a similar state between 240-183 cal yr BP. There is then a shift to very negative $\delta^{34}S$ values, reaching -40.4‰ by AD 1919 and only increasing to -7.5‰ by the present day. The $\delta^{13}C$ and $\delta^{15}N$ signatures seem to have an inverse relationship, between 125 BP to AD 1984, where there is a shift to more negative $\delta^{13}C$ and more positive $\delta^{15}N$, until after AD 1984 where both records deteriorate to the present day.

5.4.5 pXRF

The pXRF method analysis a large range of trace elements within a sediment profile. This project will only discuss a select few elements that show the best correlations with one another; the elements can be found in Figure 5.8 below. There is an early lead (Pb) peak, at the base of the sequence of 252ppm whilst phosphorous (P), arsenic (As), iron (Fe), and aluminium (Al) also show some background readings. There are very little recorded readings for sulfur (S), copper (Cu) or zinc (Zn) at the same depth. Peaks P (288 to 672ppm), As (61ppm to 263ppm), Cu (166ppm to 840ppm), Zn (1846ppm to 8489ppm) and Al (15981ppm to 22465ppm) are mainly short-lived, however and quickly decrease by 552cm. S, Fe, Pb and Al, during this same period, all stay at relatively the same level with no major changes or increase slightly over time to 536cm. A major decrease to all elements occurs at 528cm with all shown elements decreasing in value during this time. Cu, however, undergoes a continued period of low values between 560cm and 528cm with all values between 50-100ppm.

A secondary peak can be identified in P (303-391ppm), S (6167-11740ppm), Fe (27487-49403ppm) and Zn (2391-4947ppm) at 435cm, where the other elemental data show a more steadily increase. At 424cm a peak in As (243-370ppm), Cu (573-1880ppm) and Al (21188-27338ppm), lag other elements in terms of peak area during the late Inca period. These rapid peaks decline shortly after, at 416cm, aside from Pb which shows a peak of 145ppm – an increase of 101ppm at this depth. This decrease in values for P, S, As and Cu is short lived however, with values for all these elements peaking again by 392cm.

The elemental data fluctuates between 392cm and 318cm for all datapoints, before another sharp decline in all elemental data at 304cm. Increasing counts in P (226-414ppm), Fe (8418-

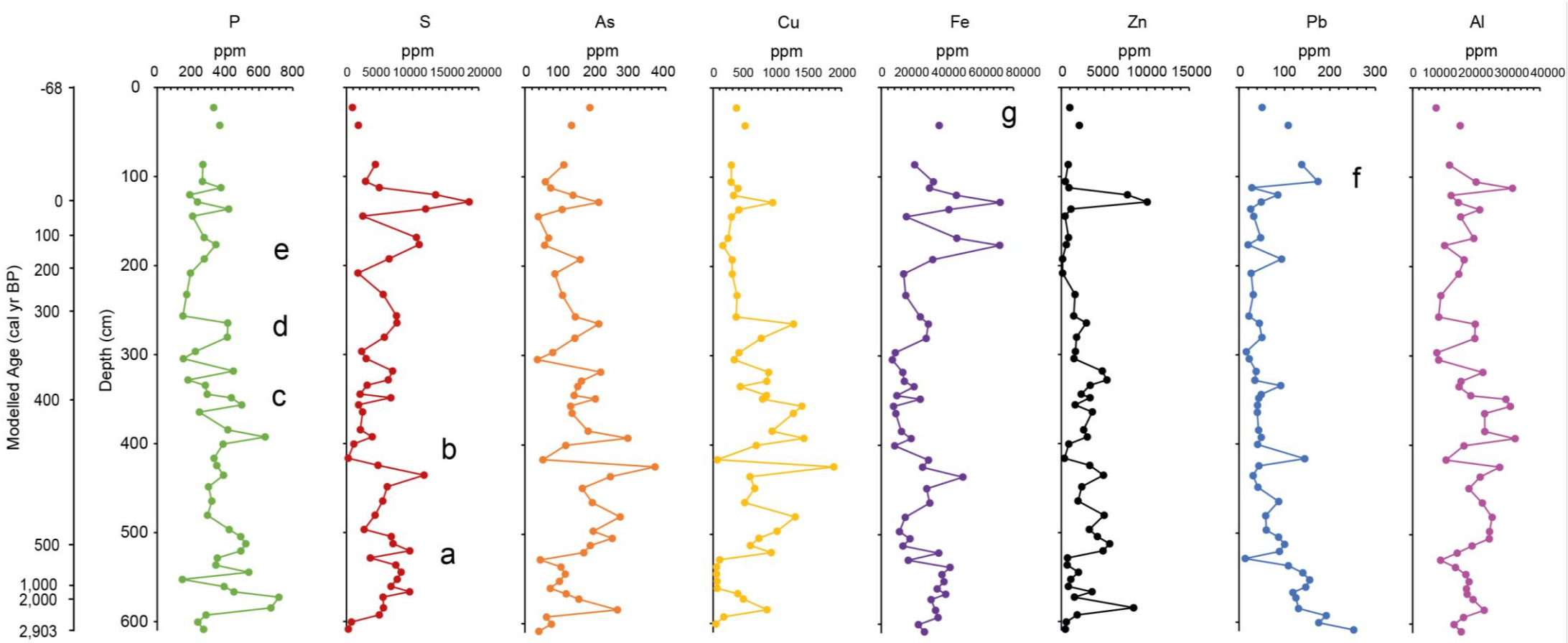

Figure 5.8: Elemental data from the pXRF analysis, for the Antaycocha basin. Elements shown are phosphorous (P), sulfur (S), arsenic (As), copper (Cu), iron (Fe), zinc (Zn), lead (Pb) and Aluminium (Al). Modelled ages are shown on the left hand side from the radiocarbon dating programme in calibrated years before present (cal yr BP), with -68 years denoting 2018AD.

27127ppm), Pb (23-50ppm) and Al (7597-19530ppm) all occur at 280cm and hold their levels 264cm when the other elements hit a peak: As (210ppm), Cu (1252ppm), Zn (2953ppm). Levels decrease slightly over time before peaks in As (85-157ppm) and Pb (27-93ppm) occur at 192cm, whilst other elements are still increasing reaching a peak at 176cm: P (346ppm), S (10996ppm) and Fe (71734ppm). The only element to see a decrease at this depth is Al. All values for the elements decrease at 144cm before increasing in value again shortly afterwards. P reaches a peak earlier in the sequence at 136cm (209-422ppm), with all other values, except Al (which shows a decrease) reaching a maximum at 128cm: S (11990-18556ppm), As (106-210pm), Cu (399-928ppm), Fe (40877-71934ppm), Zn (1124-10087), Pb (49-85ppm). These peaks then decrease rapidly, except for both Pb and Al which both have observable increases at 105cm. There are two other data points for all elements at the top of the sequence, but due to the disturbed nature of the core, these appear separate from the rest of the curve. Only As and Fe increase in value at the top of the core, the nature of the Fe increase is so vast (in excess of 200,000ppm) that it is not shown on figure 5, in order to accurately show the fluctuations in detail.

5.4.6 non-Pollen Palynomorphs

The NPP samples were collected, at regular intervals, during periods of changeable conditions identified within the geochemical analysis of the core material. The areas considered where were it was assumed there had been some significant environmental changes, and shifts within the plant communities, identified by the isotopic and Rock-Eval analyses. The full diagram can be found in Figure 5.9.

Zone 1 (520-544cm) (503-512 cal yr BP)

The most dominant taxa identified, in zone 1, is EMA-92 which makes up 16.9% of the total assemblage. It is represented by very low counts in the first two samples, in this zone, but is identified in greater number at the top of the zone. Other important taxa in the Other Fungal Remains (OFR) assemblage that have been identified in this zone are: HdV-170 (Cyanophyceae / *Rivularia*- type) (7.7%), HdV-121 (6.7%), HdV-351 (6.7%), HdV-1018b (*Spegazzinia tessarthra*) (5.6%), HdV-1022 (5.6%) and HdV-1035a (*Paraphaeosphaeria cf. michotii*) (4.1%). Coprophilous fungal remains only account for 25.6% of the total assemblage of zone 1, with *Sporormiella* (HdV-113) being identified most often (6.7%). It was, however, only observed in relatively high amounts in the first two samples of this zone, with only 1 spore found at 528cm – no spores were identified at 520cm. Other identifiable dung-related ascomycetes in zone 1 were sporadic throughout the zone but are as follows: HdV-55 (*Sordaria* type) (3.6%), TM-6 (*Delitschia* type) (2.6%), TM-110 (*Podospora polysporus*) (2.6%), HdV-112 (*Cercophora*) (2.1%), HdV-172 (*Coniochaeta* type) (1.5%), HdV-368 (*Podospora* type) (1.5%), HdV-546 (*Trichodelitschia*) (1.5%), and TM-H (0.5%).

Zone 2 (264-288cm) (321-346 cal yr BP)

The second zone is dominated by the *Rivularia* type Cyanobacteria, which accounts for 32.1% of all the NPPs identified. HdV-1103 (*Glomus* sp.) (10.4%), HdV-28 (Spermatophore of

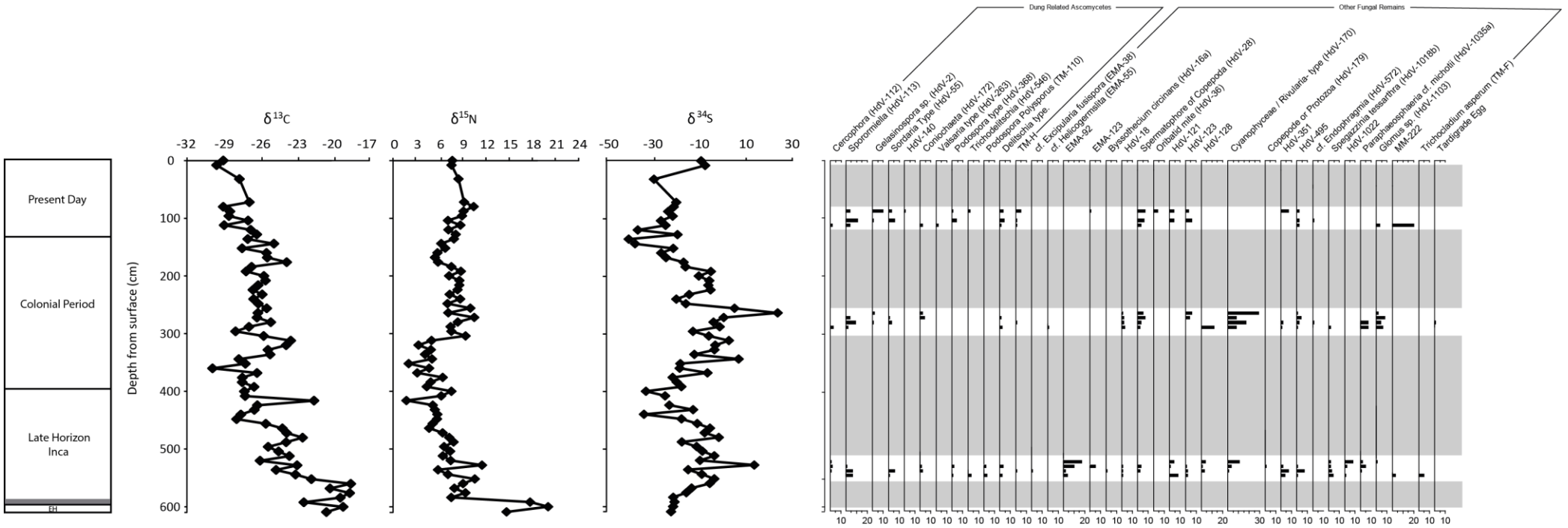

Figure 5.9: Synthesis diagram of the major isotopic curves with the identified NPPs, the grey bands denote areas that were not analysed

Copepoda) (7.3%), and HdV-1035a (7.3%), make up the other more abundant NPPs in this zone. The human marker HdV-351 dwindles in this zone, compared to the zones 1 and 3, with only a representation of 1.6% in zone 2. EMA-55 (*Helicogermslita*) and HdV-572 (*Endophragmia*) both only have 1 spore identified in this zone and must be used with caution when using in any environmental reconstructions. There is a distinct lack of dung-related ascomycetes, in zone 2, with only 18.1% of all taxa identified belonging to this group. *Sporormiella*, again, is the most prominent taxa of these coprophilous fungal species with 7.8% of the total number of spores. Again, however, *Sporormiella* does not appear in all of the samples and was not identified at 264cm – where there is a maxima in aquatic based taxa. The other coprophilous fungi identified in zone two are: HdV-172 (3.1%), HdV-55 (2.1%), HdV-112 (*Cercophora*) (1.6%), HdV-2 (*Gelasinospora* sp.) (1.6%), and TM-H (0.5%). Again these fungal spores appear sporadically throughout the zone, there is not one sample where coprophilous fungal spores are found in greater number, than the others.

Zone 3 (88-112cm) (AD 1980 – AD 1960)

The final NPP zone is taken from the more modern sediments, located near to deflections in the isotope records. OFR and coprophilous remains are almost equal in number with 52.4% and 47.6% respectively. The OFR assemblage mainly consists of MM-222 (14.0%), although this only appears at the base of this zone and was not identified in the other samples. HdV-28 (11.2%) appears more consistently through this zone and is present in all samples in this zone. HdV-351 (4.9%) is identified at the top of the zone only. There is also evidence of Oribatid mites in the top of this zone and accounts for 2.8% of the assemblage. The rest of the OFR include HdV-123 (6.3%), HdV-121 (5.6%), HdV-495 (4.2%), HdV-1103 (2.1%) and HdV-572 (0.7%). *Sporormiella* has been identified in all samples in zone 3 and accounts for 13.3% of the total assemblage and 27.9% of the coprophilous fungal remains in this zone. Dung ascomycetes have been identified more regularly in zone 3, in comparison to the other 2 zones. HdV-2 (7.7%), HdV-55 (6.3%), TM-6 (5.6%), TM-H (4.9%), HdV-368 (3.5%), HdV-112 (1.4%), HdV-172 (1.4%), HdV-263 (1.4%), HdV-546 (1.4%) and HdV-140 (0.7%) make up the remaining assemblage of dung fungi.

5.4.7 n-Alkane signatures

n-Alkanes for Antaycocha are dominated by longer chain lengths (n-C_{27}-C_{31}) (see figures 5.8 to 5.11), with a high Carbon Preference Index (CPI) throughout the sequence. The CPI remains between 5.2 and 10.9, which are not typical of samples that have any contamination from oil sources or from fossil carbon (Bray and Evans, 1961; Eglinton and Hamilton, 1967). There is a large variety of chain lengths through the sequence, which is represented by the fluctuations in the Average Chain Length (ACL) (see Figure 5.9). After early decline in ACL and CPI, these values increase again down the core first peaking at 412cm. This sample depth has an almost equal percentage of n-C_{29} and n-C_{31} chain lengths (~25% of each) with chains of C_{27} and C_{33} also prevalent. Shorter chain lengths are present throughout the sequence, but

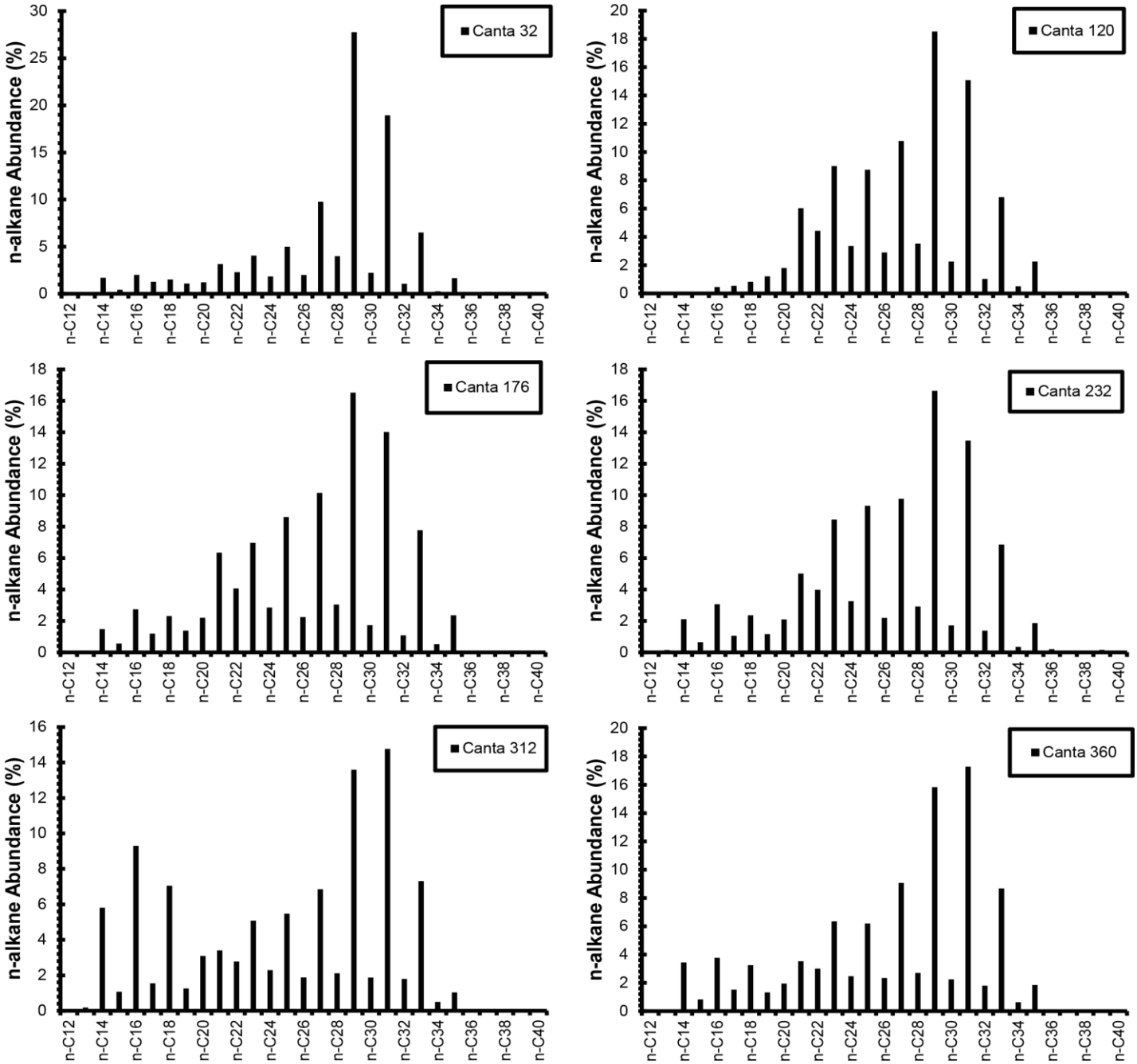

Figure 5.9: n-Alkane profiles for sample depths 32cm to 360cm for the Antaycocha basin. All chain lengths are as a total abundance of the sample.

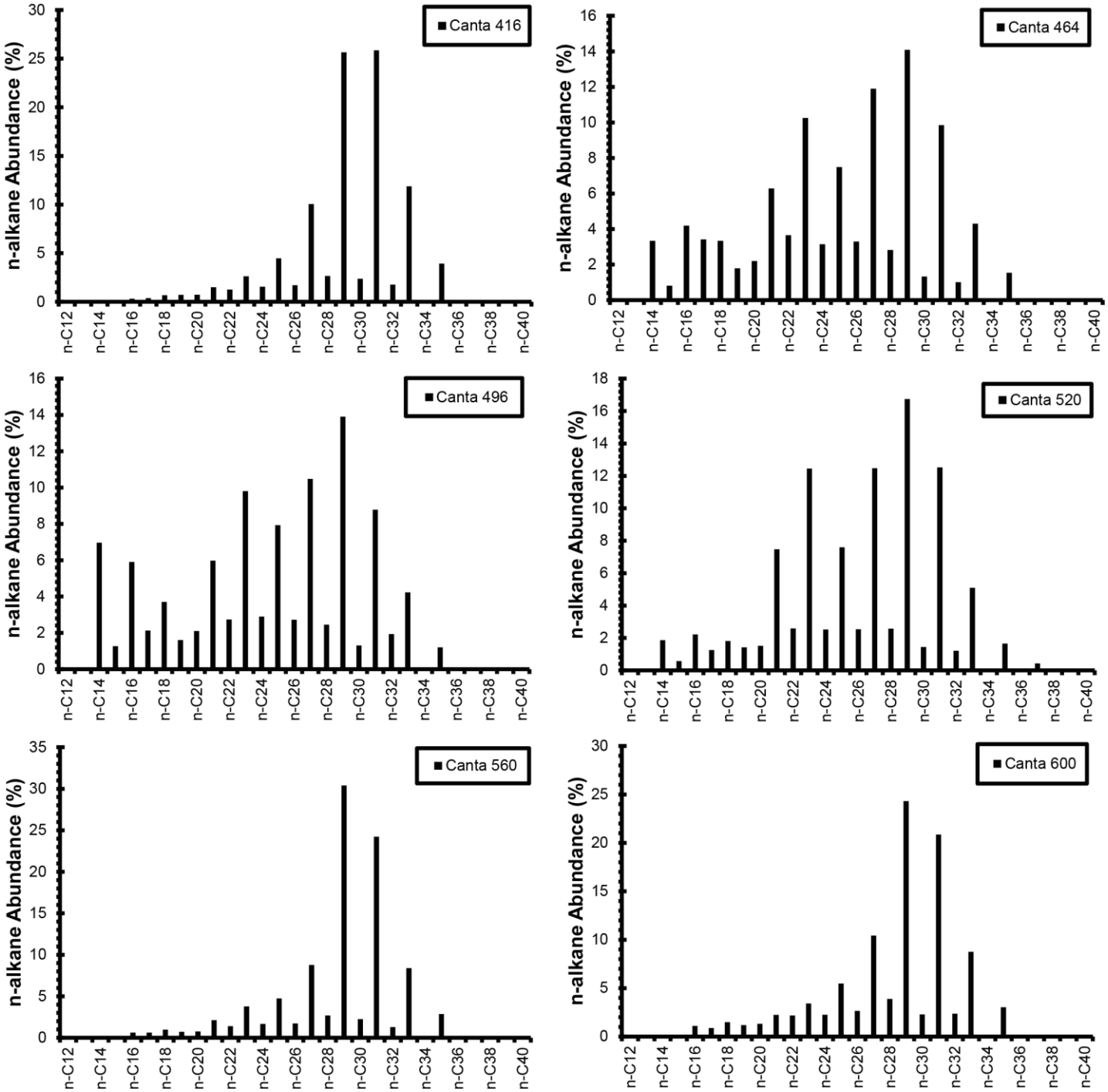

Figure 5.10: n-Alkane profiles for sample depths 416cm to 600cm for the Antaycocha basin. All chain lengths are as a total abundance of the sample.

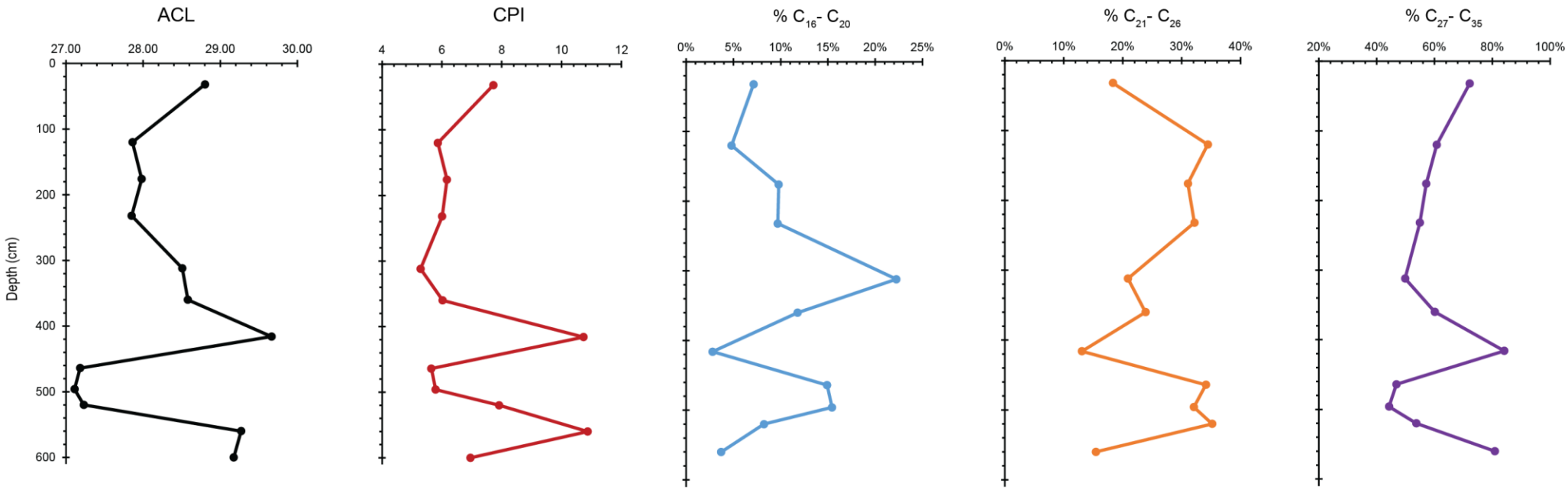

Figure 5.11: n-Alkane measurements for Average Chain Length (ACL) (Black), Carbon Preference Index (CPI) (Red), % abundance of chains C_{16}-C_{20} (Blue), % abundance of chains C_{21}-C_{26} (Orange), and % abundance of chains C_{27}-C_{35} (Purple) for the Antaycocha basin.

what is striking is the percentage of alkanes with chains of C_{14} to C_{18} which peak in the samples at 312cm, 464cm, 496cm and 520cm; the latter three having a profound impact upon the ACL and CPI, whereas the 312cm sample ACL and CPI values remain high, due to the relative amounts of n-C_{27}-C_{31} alkanes within the signatures. The samples where the ACL and CPI drop to their lowest values, show an increase in chain lengths of n-C_{21}-C_{26}, which then are not observed in the lowest sediments in any great abundance. Samples 560cm and 600cm are dominated by n-C_{29} and n-C_{31} chains, which account for over 50% of the chain lengths in both samples, owing for their high ACL and CPI values.

5.4.8 Interpretation of Paleoenvironmental Data

Sedimentary History

The organic matter of the basal sediments is very low, which corresponds to the large unit of sands and silts at the base of the sequence, with little presence of any plant material recorded. The bottom 60cm corresponds to 515-2,903 cal yr BP, with a large proportion of this time covering the EH and EIP. It is likely that the there would not have been a permanent settlement, during this time, and that the sediments here are likely a representation of the natural basin with little interference from any other human processes. There may have also been a higher velocity of water flow through the basin, during this period, as there are few observable plant remains identified at these depths (figure 5.12 A).

Within the age model, there are 4cm of sediment that denote the MH (564-567cm; 886-1,209 cal yr BP) and is within the transition from unit 1 into unit 2; the rate of sedimentation here is low and is modelled at 0.0198cm per year. This may be as a result of the lack of any MH civilisation involvement, as there is a distinct lack of any Wari-style ceramic finds at the upper Chillón Valley and none found in the Cantamarca archaeological zone (Farfán, 2011; Handley, 2022). A second hypothesis may be as a result of decreased amounts of precipitation entering the basin during the Medieval Climate Anomaly (MCA) (~650-1,050 cal yr BP) and the resulting climate stability (Bird et al, 2011). This may have led to less surface run-off from the surrounding slopes transporting a decreased sediment load into the basin.

Sediment accumulation rates start to accelerate at 551cm from 0.0286cm to 2.03cm per year by 547cm (516-512 cal yr BP), at a time where TOC% values begin to show an increasing trend (Figure 5.7 point a). This increase in organic carbon, reflects the increase in the detrital plant material present within the sediments and points towards more favourable conditions in the local area that are conducive for plant growth. The vast increase in sedimentation may reflect anthropogenic modification of the basin and 516 cal yr BP may be the point at which the basin wall was constructed. This is further backed up as this date coincides with the approximate known date for Inca occupation of Cantamarca (Farfán, 2011). There is also evidence, in the surrounding hills, that there are corrals and other evidence of Inca occupation (see figure 5.1) This wall would have increased the capacity of the natural basin, as the wall is over 3m in height, potentially allowing for sufficient volumes of water storage for domestic

consumption, cultivation, and water transport. The dam construction also coincides with the onset of the Little Ice Age (LIA) and the resulting decline in climatic conditions. From the latter stages of the LIP and through the LH, the Peruvian palaeoclimatic records show an increase in precipitation levels (Kanner et al., 2013; Apaéstegui et al., 2014). Farfán (2011) also comments on the construction of a host of reservoirs, in the area surrounding the Antaycocha basin, but these may have been built as a response to the increase in rainfall to capture it and prevent its run-off (Handley, 2022).

The increase in sedimentation rate brings an increase in organic carbon, as shown by the TOC%. Units 5 through to 9 (498-457 cal yr BP), show an increasing trend of TOC% values, rising from 3.6% at the base of unit 5, peaking at 7.1% at the top contact of unit 9. There is a transitionary point, identified in the HI:OI ratio, where both are almost equal at 464cm (476 cal yr BP) (Figure 5.7 point b). This may indicate that the sediment is from an autochthonous origin, in contrast to much of the sequence, and may represent the ongoing management of the basin as a location of water storage. TOC% values decrease rapidly after unit 9, to 1.7% at 416cm within unit 10 (~446 cal yr BP). This trough coincides with a low in HI values in the basin, as well as a decreased lithic load in the Quelccaya dust flux records (Thompson et al., 1992, 2013). This may correspond to weakened El Niño events, therefore a lack of sediment is likely to be available to be in-washed into the basin, causing these lower values.

TOC% values start to increase again from 400cm and reach a peak of 6.5% by 328cm (units 12 to 19) (434-378 cal yr BP), which occurs during a time of increased precipitation during the LIA (Bird et al., 2011b). This would have increased the flow of the stream entering the basin, bringing with it more minerogenic material as run-off from the surrounding hills. It is also possible that this period correlates with increased SASM activity, recorded during the LIA, as there is an increased lithic input in the Lima marine record during this same period (Rein et al., 2004; 2005). TOC% values continue to rise in units 20 to 25 (250-330cm) (380-298 cal yr BP) as more herbaceous material is deposited within the basin, suggesting a lowering of the water table has occurred. These dates correspond to the Spanish occupation of Peru and may have occurred as the site has become abandoned and the basin not managed so that peat formation could occur. This also coincides with a slower accumulation of sediment, which drops to $0.793cm^{-1}$ at 300cm (~357 cal yr BP) slowing to $0.542cm^{-1}$ by 250cm (~298 cal yr BP), allowing for the accumulation of herbaceous material in a lower energy environment.

A final change in sedimentary environment can be observed towards the top of the Antaycocha sequence. The first of these changes occurs at 120cm (~1951 AD), where there is a switch with the HI:OI ratio favours the HI. This also occurs at a point where the TOC% starts to decline, and relates to a strong La Niña event covered in the Multivariate ENSO Index (MEI) (Wolter and Timlin, 2011) (Figure 5.7 point c). During these conditions, the coastal regions usually see very dry conditions with increased precipitation in the highlands. The data observed here would typify that there is very little sediment availability from weakened ENSO flooding. Another event at 88cm (~1980 AD) is recorded, but with elevated TOC% values

(14.8%). The MEI records an elevated time of El Niño activity, which would normally entail increased precipitation into the coastal regions; with the highlands experiencing an increase in drier conditions. This does mean, however, that the Antaycocha basin is sensitive enough to pick up these rapid climatic oscillations, due to the nature of its rapid sediment accumulation rates.

Geochemical History

There is an early peak in $\delta^{15}N$, of +20.1‰ (~2,855 cal yr BP), which typifies that of aquatic based plants. This is further evidenced by the presence of short-chained *n*-alkane fractions of n-C_{16} to n-C_{20}, which are often characterised by algae, phytoplankton, and submerged plant matter (Kai et al., 2019) (Figure 5.7 point d). The $\delta^{13}C$ and the n-C_{27}-C_{35} chain dominant signals from the geochemistry are also typical of a C_4 plant input signal, with an observable Pb peak in the pXRF at 600-608cm this could point towards a period of aridity within the surrounding areas of the basin, with arid tolerant taxa in the surrounding hill slopes. The $\delta^{13}C$ signal remains enriched at -18.6‰ at 560cm (~605 cal yr BP), during the latter stages of the LIP. This could potentially reflect an early agricultural peak, however this is most likely an extension of the arid tolerant plants, such as cacti, surrounding the landscape. This is also reflected in the *n*-alkane abundance at the same sample depth, which is dominated by chain lengths C_{27} and C_{35} – which amount of 80.8% of the total number of chains identified in this sample (Figure 5.10).

A first peak in each of the isotope records is observed at ~506 cal yr BP, with a large deflection in the $\delta^{34}S$ and $\delta^{15}N$ records identified, there is a smaller enrichment peak in the carbon isotope record, but this is less comparable to the other two curves (Figure 5.7 point e). This is met by an inverse relationship in the pXRF data with sulfur, arsenic, copper, lead, aluminium and zinc values all dropping during this time (Figure 5.8 point a). The date denotes the early Inca period and would have been a time of building large-scale waterways through the highlands, as well as agricultural terraces and settlements – such as the one at Cantamarca. The pXRF signal at this time points towards less sediment availability within the basin, possibly due to the construction of the new highland settlements and management of the basin. The enriched $\delta^{34}S$ signal, is likely due to an increased amount of cyanobacteria discovered at the sample depths and not likely from any natural enriching. Evidence from the *n*-alkanes reveals that there is a decreased ACL, from an increased abundance of short-chain alkanes of C_{14}-C_{20} which would likely be of an algal/planktonic origin (Cranwell; 1984; Cranwell et al., 1987; Kai, et al., 2019). More than likely the basin, during the early LH, would have been eutrophic with large algal blooms present from stagnant water (Figure 5.12 B).

Values for $\delta^{34}S$ become increasingly more depleted after the initial peak, possibly as a result of bacterial sulfate reduction under anoxic conditions (Canfield and Des Marais, 1991; Habicht and Canfield, 1997) indicative of continuing water stagnation. The algal *n*-alkane signatures continue in samples at 496cm and 464cm, which drive the CPI and ACL to low values – typifying the continued eutrophication of the basin during the early Incan period. This could be

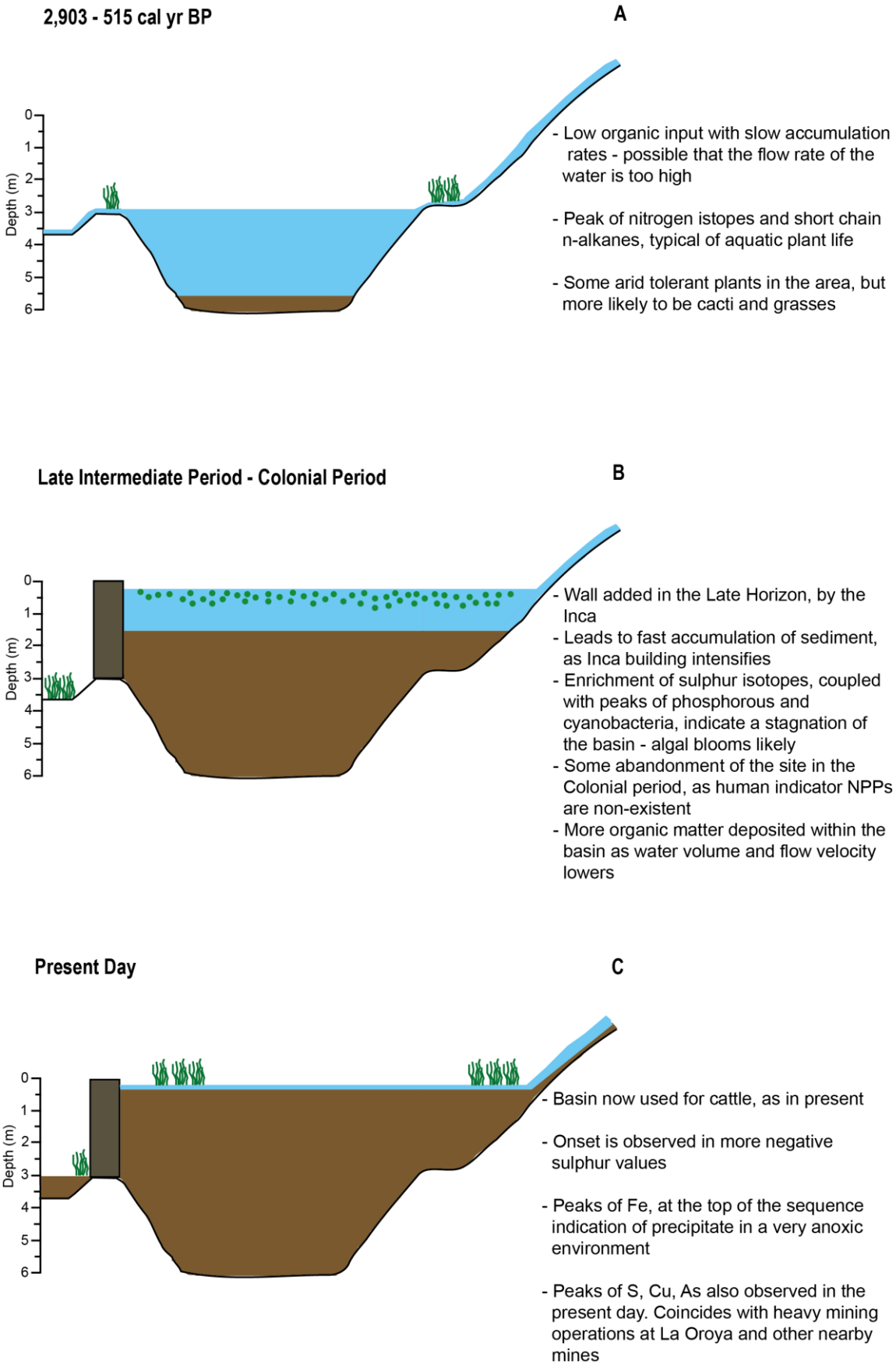

Figure 5.12: Schematic of the infilling of the Antaycocha basin

due to the construction of the dam, forcing the lake water to become more stagnant as water flow is impeded out of the basin, for water storage, or by way of defecation from increased herbivory (figure 5.12 B).

A secondary enrichment in the $\delta^{13}C$, at 446 ± 46 cal yr BP, is mapped by a deterioration in $\delta^{15}N$ values as well as decreasing metal loads in the pXRF counts(Figure 5.7 point f, and Figure 5.8 point b). This is generally typical of an arid event within the study region, where nitrogen values may increase before an arid event before quickly deteriorating to more negative values (e.g., Luo et al., 2018). The event is broadly correlated to a period of weakened ENSO activity in the area (see section above), and therefore there would have been less sediment load available to be in-washed into the basin. Further evidence is provided by the *n*-alkane signatures for 416cm, whereby there is a return of a n-C_{27}-C_{35} dominance (accounting for 84.1% of the total abundance), which also increases the CPI and ACL values. This is more likely reflecting arid tolerant taxa in the basin, rather than any agricultural practises ongoing in the immediate area. However, the Inca understood the importance of food storage throughout the highlands. Storehouses, or Collcas, were commonplace across much of the Inca agricultural systems (Reyes-Knoche, 2012), and can be seen across much of the Cantamarca archaeological zone proximal to the Antaycocha basin, (see figure 5.1) which was occupied by the Inca during the LH (Farfan, 2011). It is not without reason that this could also be a sign of agriculture at Antaycocha.

The area between 272-400cm (330-434 cal yr BP) is characterised by comparatively low $\delta^{15}N$ values, to the rest of the sequence, with a steady increase in $\delta^{34}S$ values; with the latter becoming increasing more positive. *n*-Alkane signatures reveal that there is an increasing abundance of shorter chains, similar to that of the sediments below it. This, then, is likely to be another representation of algal blooming, with several peaks in phosphorous identified at 392cm, 356cm, 318cm and 280cm in this zone (Figure 5.8 point c, Figure 5.12 B). The latter two depths date into the Colonial occupation of Peru and the basin did not likely have any occupation during this time and may have been largely abandoned. These short-lived fluctuations, in the isotopic and metal records, are likely a representation more natural occurrences in the basin rather than from any human land management. It is shortly after this period that the $\delta^{34}S$ record reaches its maximal value of +22.8‰ (321 ± 89 cal yr BP), where a large influx phosphorous also occurs – again typical of an algal bloom event (Figure 5.8 point d). Other elements peak at a similar time, which indicate an increased sediment load, this this then means that there is more sediment transport to the basin via run-off from increased precipitation.

From 150cm (~1850 AD), there is a distinct shift to very depleted $\delta^{34}S$ values. It appears that, during the republic era, the basin may have been repurposed for pastoral agriculture of large herbivores such as cattle, sheep, and some camelids. There is little evidence from the carbon isotope sequence to suggest any much C_4 input from large scale crop agriculture, returning to the surrounding landscape but there might have been some local usage elsewhere. There are

still cattle using the basin in modern times, using the basin as a watering hole which will have an impact upon the tropic status of the lake; further evidenced by peaks of P and enriched values of N, through the Republic era, which is largely typical of livestock production systems (Biagini and Lazzaroni, 2018) (Figure 5.7 point g, Figure 5.8 point e). Towards the end of the sequence, there are large peaks detected in S, Cu, As, Fe and Zn ~1930AD. This points towards environmental impacts from smelting activity from nearby mines in the Junín region, such as that of La Oroya which started smelting operations in 1922 (Reif et al., 1989; Reuer et al., 2012) (Figure 5.1). Arsenic, in the form of arsenic trioxide is a major component of the emissions from copper and zinc smelting operations and may make up most of this transported material (Reif et al., 1989). The large peaks in Pb from ~1950 AD, that steadily decrease into the present day, could be due to leaded gasoline, which was still in use in Peru until 2004 (Eichler et al., 2015) (figure 5.8 point f). Fe has two data points at the top of the core, with the latter recording at 204,192ppm which is a 582% increase from the previous recorded point. This must mean that pH of the water within the basin has been changed due to human interference. From the sulfur profile, the basin must have been highly anoxic and for iron precipitates to form (possibly that of goethite) at Antaycocha the pH must be high (Majzlan et al., 2006) (figure 5.8 point g).

Environmental and Land-Use History

The NPP assemblage covers the last ~500 years BP, in 3 zones, and the samples taken within the LH (Inca), Colonial Period and the Present Day. The identification of *Sporormiella*, as well as other coprophilous fungal remains, was present within all 3 zones in reasonable percentages. This would mean that the basin has been utilised in some form, from the Late Horizon onwards. Zone 1 consists mainly of open water taxa, from its OFR assemblage with EMA-92, HdV-170 and HdV-28 accounting for a large proportion of the identifiable spores. EMA-92 is an excellent indicator species of open fen conditions and is an indicator species of the *Phragmites* plant itself (Prager et al., 2012) – again indicative of open water conditions. The presence of Copepoda (including spermatophores) at these depths would also typify that the basin, during the early LH (503-512 cal yr BP), might have been open and potentially stagnant (Kuhry, 1997; Prager, 2012) (figure 5.12 B). The eutrophic conditions are further evidenced by the appearance of HdV-170, a type of cyanobacteria common in blue-green algal blooms (van Geel et al., 1989).

These eutrophic conditions may have been caused by the presence of animals and humans within the landscape. The radiocarbon dating programme puts this zone within the early stages of the Inca Empire, during the LH, a time of heavy Incan influence in the immediate area of the Cantamarca zone (archaeological features shown in figure 5.1). The coprophilous fungal remains that have been detected within this lower zone account for 22.6% of the total assemblage suggesting that herbivores, most likely to be camelids, were using the basin in some way – possibly as a source of drinking water. The presence *Sporormiella* typifies herbivory and has been used as a proxy for the detection of large herbivores within the

landscape and has proven to be useful in that regard in many studies (Davis and Shafer 2006; Etienne et al., 2013; Chepstow-Lusty et al., 2019). *Sporormiella* has a low height spore release that is not conducive to long-distance dispersal (Davis and Shafer, 2006) and is therefore only found locally to its source again making it a more ideal indicator of herbivory within the Antaycocha basin. *Cercophora* and *Sordaria* type fungal remains have also been detected, but in lower numbers, which may also represent camelids within the basin. Given the presence of the dung related taxa it must be assumed that there would have been camelids present within the local area, therefore the resulting defecation entering the basin waters driving the eutrophication processes (as discussed above). The coprophilous fungal assemblage coincides with a presence of the human disturbance indicators of *Glomus* and HdV-351 – although the former is only present in very limited counts. This coincides with the archaeological literature which suggests that there was a large influx of Inca influence in the upper valley of the Chillón, with the construction of waterways and agricultural terraces evident during the LH (Farfán, 2011) (agricultural terrace systems seen in figure 5.1). There are some signs of possible agriculture with the inclusion of HdV-1018b spores, which are indicative of monocotyledonous plants that are common in some cultigens. This interpretation, however, could be misleading and must be used with some caution as HdV-1018b can also be an identifier of common grass species (van Geel et al., 2011)

A similar pattern of eutrophic conditions can be found during zone 2, within the Colonial Period (within 321-346 cal yr BP), where there is an observable peak in the *Rivularia* type cyanobacteria, with a large influx occurring at the top of this zone. This is seemingly after a change in conditions from more mesotrophic-like conditions, indicated by a peak of HdV-128 at the beginning of this zone. The basin remains open water, with remains of HdV-28 being identified in most of the samples. The presence of *Sporormiella* and other dung ascomycetes is likely a representation of a mixture of camelids and old-world large herbivores, such as cattle and sheep, which were introduced into Peru during the 17th Century (Chepstow-Lusty et al., 2007). The dung fungal spore assemblage is lessened in this zone, however, indicating a decreased use of the basin. The occurrence of *Glomus* during this period is typical of an increase in catchment disturbance and landscape erosional processes and occurs at a time where there is a greater volume of sediment accumulation over a relatively short period of time.

The modern-day sediments of the final zone reveal more human activity around the basin, when compared to that of the past. The increase in coprophilous fungal spores, of all types, signals an increase in herbivory around the basin in the 20th Century. There is also a limited number of Oribatid Mites identified within the top sediments, which may indicate a presence of large herbivores within the basin. These were likely kept within the corrals surrounding the site, with the dung-related ascomycetes being washed into the basin rather than being directly deposited into the wetland from use as a source of drinking water. The water table, in the modern day, is shallower than it would have been in the past. This is evident with the increase in HdV-121, which is indicative of temporary drying up of the wetland surfaces, especially in the late summer (Kuhry, 1997).

KEY POINTS IN CHAPTER

- Sediment accumulation, at the coring location, began between 2,954-2,855 cal yr BP, during a pluvial phase following the mid-Holocene drought period. Sediment accumulation likely began earlier, towards the centre of the basin but water level increase allowed for lake sediment build up to occur during this time.
- Evidence from *n*-alkanes and a $\delta^{13}C$ peak of -18.6‰ from 605 cal yr BP, suggest that there could have been early agricultural practices in the upper valley. Radiocarbon errors are still quite large, so it is hard to say how accurate this is. Therefore, could be identifying continued dry period in the latter stages of the LIP, as coincides with less negative values in the $\delta^{18}O$ records at Huagapo and Pumacocha.
- Geochronological and sedimentological evidence suggest that a constructed wall that dams the basin could be aged between 512-516 cal yr BP, during the late LIP and the early LH. This coincides with the earliest known occupation of the Inca into Cantamarca. Wall was possibly built due to heavier precipitation, so water levels in the basin could rise for irrigation of the highlands.
- Damming of the wall caused water to stagnate within the basin. Evidenced by the observation of cyanobacteria in the NPP record, which is also influencing the $\delta^{34}S$ record – creating large deflections to more positive values.
- *n*-Alkanes and NPPs give evidence that the basin water level was sufficient enough to be used as a source of drinking water for herbivores (and possibly humans). Coprophilous fungal remains identified in LH, Colonial and Republic eras.
- Geochemical and palaeoecological evidence suggests that some abandonment of the highlands during the Colonial Period. Elemental data suggest some periods of reduced metallurgy, which quickly intensifies as new methods employed from the old-world.
- Antaycocha basin able to record short-lived climatic events, such as ENSO variations. Rock-Eval evidence to suggest that at least two periods of ENSO variability recorded in the sediments, but maybe more records shown.
- Elemental data recording evidence of past metallurgy in the highlands, but also recent processes such as that of smelting in the early 1930s and the introduction of leaded fuels, which were then banned in the 2000s – which can be observed with a reduced peak in Pb.
- Modern day interference of the basin has caused pH imbalance to occur. Basin during the 2000s must have been very anoxic, the pH change must have been very high for Fe precipitates to form (potentially goethite).

6. Discussions

6.1 Introduction

This chapter will explore the key findings from the previous chapters and consider these within the wider quaternary context, drawing upon the previously published research from the Andes region. This projects overall aim was to reconstruct the impact of pre-historic and historic agropastoral land use and climate change upon the environment of the Peruvian Andes. The study used some novel methods, chiefly that of Rock-Eval pyrolysis which hasn't been utilised on sedimentary sequences in South America, in order to add to the pool of information on the palaeoenvironments of Peru. This project has been able to illustrate the nature and the timing of human and environment interactions throughout much of the late-Holocene but has also shown that the intermontane basins are sensitive to the regional climatic changes, that are documented throughout much of the Andes. The types of human interactions, with their lived environment, has been varied and has included creation of agricultural terraces, irrigation systems, and dams but also includes camelid herding, crop cultivation and mining/smelting. The extent of each of these represent adaptations to climatic changes as well as advancements in each of the cultural horizons. To pull the sites together, the discussion will focus mainly on the time periods that cover the cultural horizons as the individual results chapters cover the time periods beyond that.

6.2 Inter-site comparisons

The original site selection for Huarca and Antaycocha was based on the fact that these sites sit within two separate climatic zones, *Quechua* and *Suni* zones respectfully. This has enabled this study to understand how humans might have interacted with these sites, in relation to one another and the use of these basins for agricultural activity.

6.2.1 Formative Period

The records are not comparable for much of the study period, as much of the modelled ages for Antaycocha are from the Late Horizon (LH) onwards. We also know that there wouldn't have been any permanent settlement, at this site, until the LH. This doesn't mean that the sites are not comparable, as they are. This study has shown that the sediments at Antaycocha would have started to accumulate between 2,954 and 2,855 cal yr BP during a pluvial period following the mid-Holocene drought, which lasted between 7,000 to 5,000 cal yr BP. Each of these basins has its own set of environmental and geomorphological controls for sediment accumulation, but it is interesting to note that each of these basins started to accumulate sediment within a similar time frame of one another. Huarca, however, formed in the early-Holocene but there is evidence to suggest that there was an open water system during this pluvial period between 3,877-3,966 cal yr BP, as a response to the wetter climate. It is

plausible that the sediments at Antaycocha were being deposited much earlier than this, towards the centre of the basin, but due to the increased rainfall it would have been possible that an increase in lake level would have meant that the edge of the basin would have started to accumulate sediments later in the Holocene.

The PCA data (see chapter 5, figure 5.6a,b), for Antaycocha, would suggest that the basal sediments are likely controlled by erosional processes and are being washed into the basin, from the slopes above. This is due to the points plotting towards the terrigenous elements such as Pb, Ti, Sr. This, therefore, would have likely been transported into the basin from the run-off from increased precipitation during the Formative period. The isotope curves for the Huarca Central Basin show an anti-phase relationship with the established sites during the Formative Period, due to the record picking up changes in plant communities, rather than the overall climate signal at the time (for more information refer to chapter 4).

6.2.2 Middle Horizon

The MH is a time of aridity within the Central Andes, however the expression of the sediments at Antaycocha is revealed to be only 6cm; with the cores at Huarca showing 32cm and 56cm for the edge and central basin cores respectively. A reduction in the amount of precipitation, in the Andes, would have a profound impact on the amount of sediment deposition. This can be found in the PCA plots for Antaycocha and Huarca, with the sole MH datapoint “Antay_566” plotting towards PC1, away from the indicators of organic sedimentation (see chapters 4 and 5 for more information on these PCA plots). This would indicate therefore that there would have been less sediment availability from within the basin itself and may have come from the dry valley slopes as aeolian transported sediment. This low rate of sediment accumulation could be as a result of the aridity experienced across Peru. The lowering of the water levels, at Antaycocha, may have exposed the area of coring and so there wouldn’t have been any sediment accumulation at this time. One other hypothesis is that there might have been some clearing of sediment, as the wall was constructed, although there needs to be more effective sedimentary analysis to conclude this point.

6.2.3 Late Intermediate period

The LIP is a period of interchangeable conditions within both of these basins. There are markers of more aquatic vegetative matter recorded in Antaycocha and Huarca. A *n*-alkane sample from the Huarca edge core from 785 ± 267 cal yr BP with 9.1% abundance of n-C_{16}-C_{20} chain lengths would indicate more algal life from wetter climatic conditions. There is also some evidence that there was continued use of the basins, in the form of arable agriculture. Huarca *n*-alkane abundances, at 673 ± 105 cal yr BP contain signatures that are similar to quinoa, potato and maize (see appendices for the specific plant abundance information). The abundance of n-C_{27}-C_{35} chains would also give evidence to continued cultivation through the latter half of the LIP, with 74.9% of the total number of *n*-alkane signature made up of C_{27}-C_{35}. At Antaycocha these similar signals are present at ~605 cal yr BP. Here there is a large $\delta^{13}C$

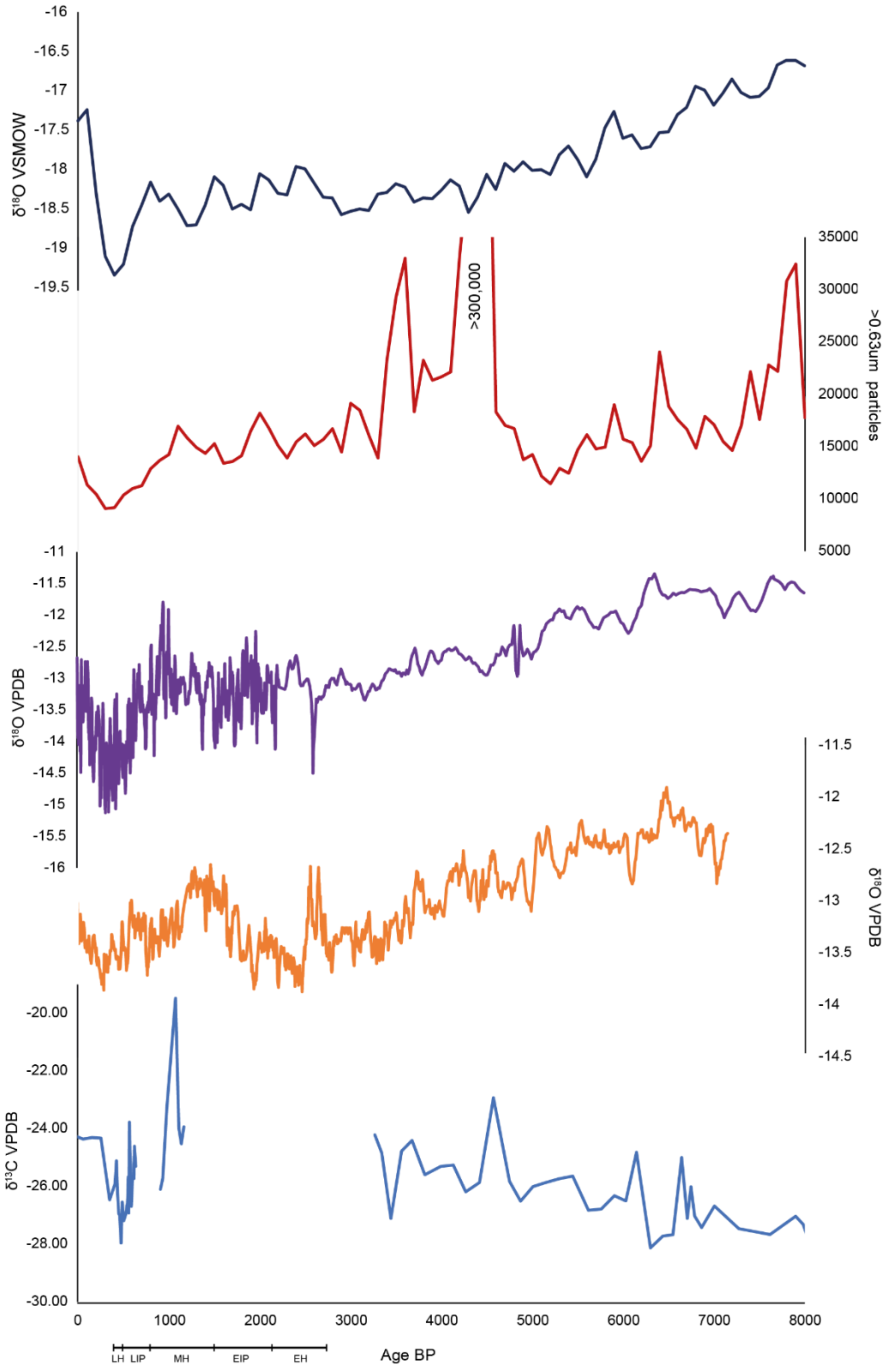

Figure 6.1: Comparative figure for the major Quaternary records over the last 8,000 years BP. Dark Blue: Huascarán δ18O. Red: Huascarán terrigenous dust (Thompson et al., 1995) Purple: Lake Pumacocha δ18O (Bird et al., 2011b). Orange: Huagapo Cave δ18O (Kanner et al., 2013). Light Blue: Huarca Central Basin $\delta^{13}C$ (this study).

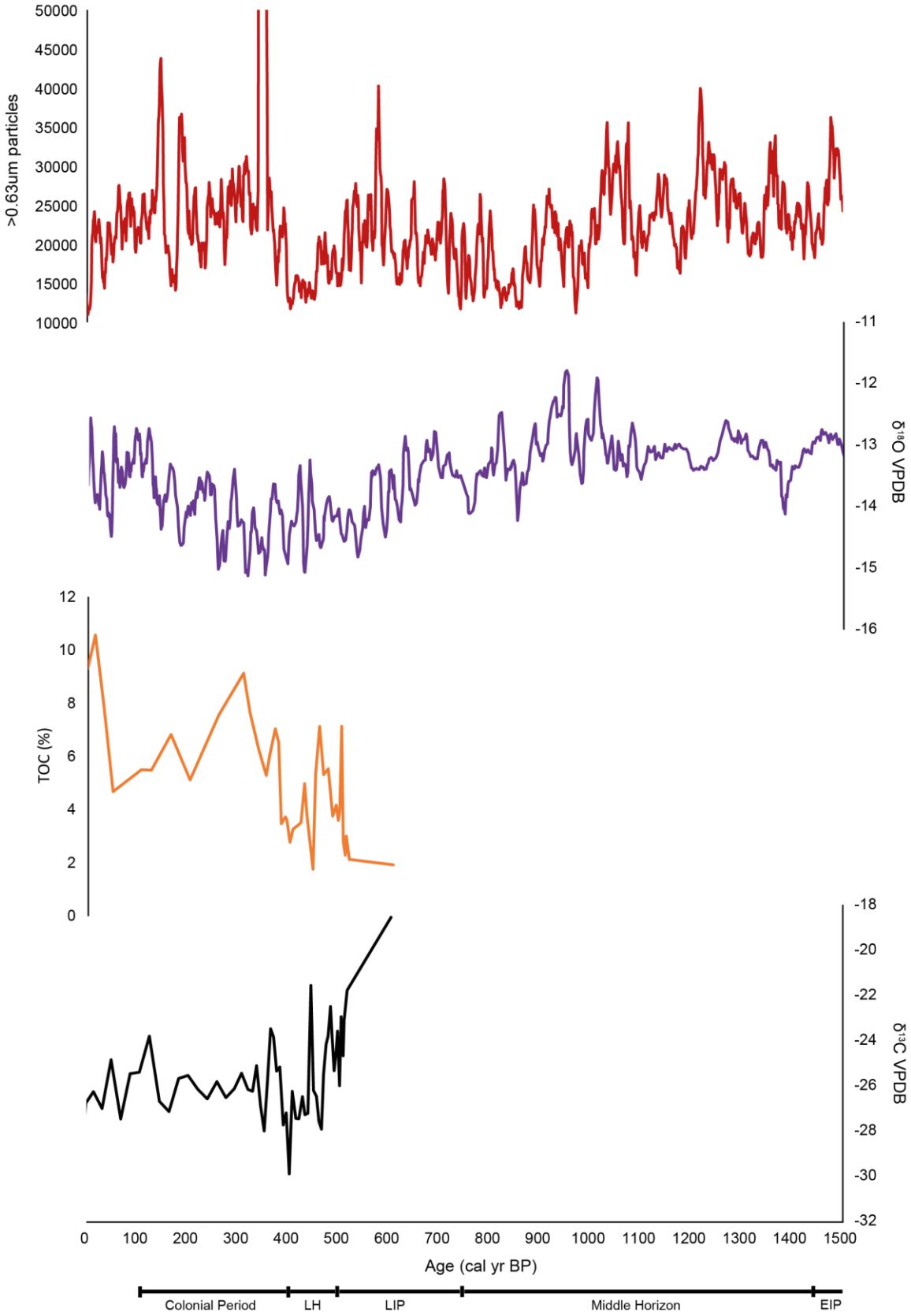

Figure 6.2: A comparative diagram of established quaternary studies. Quelccaya dust flux record (Thompson et al., 1992; 2013) (red), Lake Pumacocha d^{18}O record (Bird, 2011) (purple) and Antaycocha TOC% (Orange) and d^{13}C isotope curve (black) (both this study).

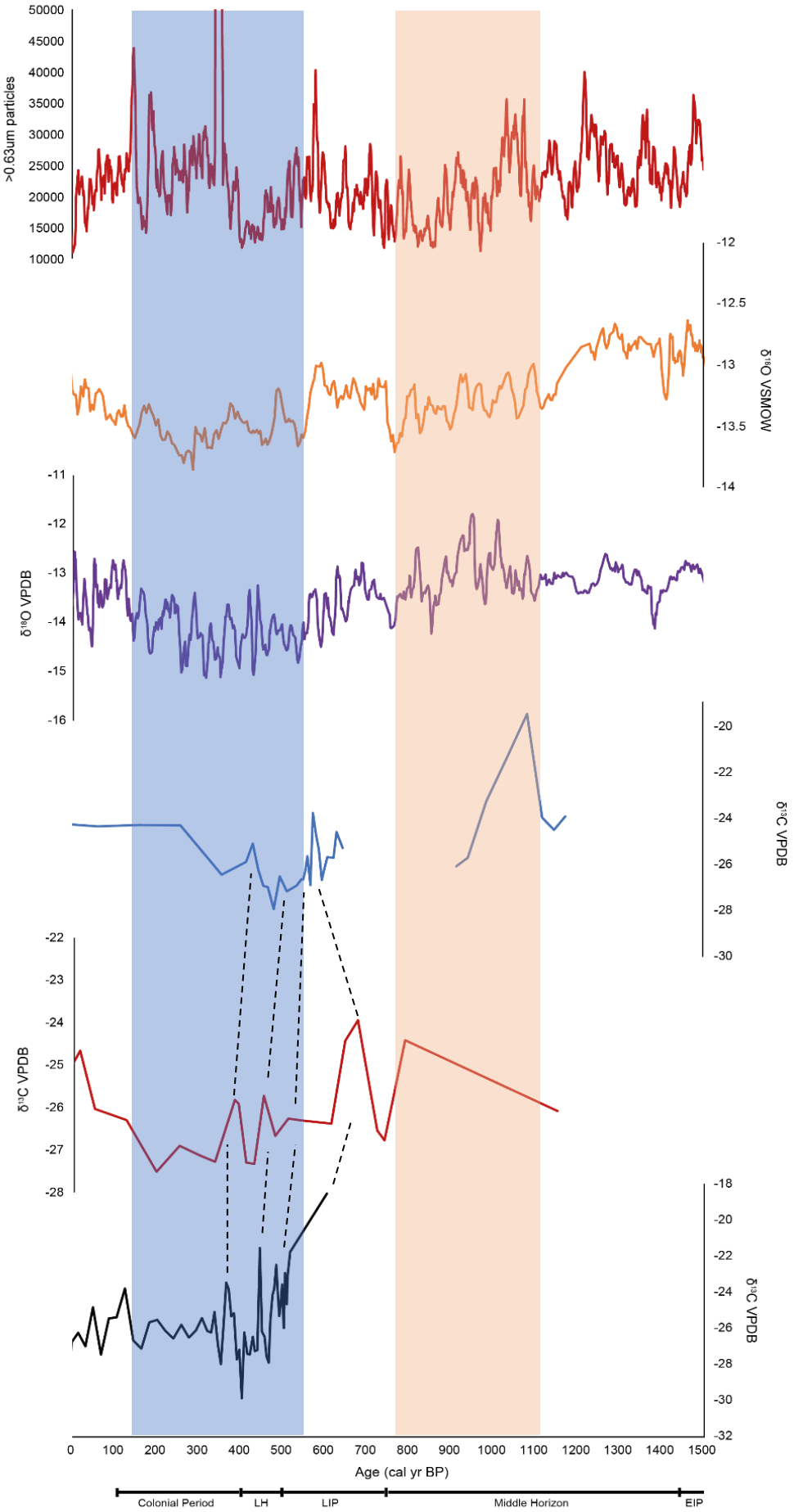

Figure 6.3: Comparative figure of key Peruvian sites of Quelccaya dust flux (Thompson et al., 1992, 2013) (Red), Huagapo Cave speleothem (Kanner et al., 2013) (Orange), Lake Pumacocha (Bird et al., 2011b) (Purple), Huarca Central Basin core (Light Blue), Huarca Edge core (Red) and Antaycocha (Black). The Andean cultural timeline can be found on the bottom axis. The blue bar is the approximate time scale of the Little Ice Age (LIA) with the Orange representative of the Medieval climate Anomaly (MCA). Dotted lines are approximate matching of shifts in each of the new palaeoclimate records.

peak of -18.6‰ with 80.6% of n-C_{27}-C_{35} chain lengths within the signature, suggestive of some usage of the basin well into the LIP.

6.2.4 Late Horizon

The LH for both of these records show wetter climatic conditions (see figure 6.1 and 6.2) from a period of changeability, shown by depleted $\delta^{13}C$ values during the transition from the LIP. These conditions also coincide with the Inca occupation of Peru. This intensification of human activity can be seen in the building of the wall, at Antaycocha, as well as the human markers within the NPP assemblage (inclusive of coprophilous fungal spores). It is difficult to pin-point the exact age of the wall itself, but the geochronological and sedimentological evidence (set out in chapter 5) puts the median age bracket between 512-516 cal yr BP.

What is interesting, that during the LH (and for much of the LIA), is that both the Huarca and Antaycocha basins are recording broadly similar processes albeit with some differences in timings. The oscillations in the geochemistry (see figure 6.3) are reflecting the broad climatic conditions that affect much of the Andes, such as the LIA. Antaycocha, however, is potentially sensitive to the short-lived effects of ENSO variability. The TOC% values (see chapter 5) as well as the fluctuations in the $\delta^{13}C$ record coincide with that of reduced lithic load in the Quelccaya dust flux record, which corresponds to a period of weakened ENSO activity. The offset in timings of more negative $\delta^{13}C$ values, with that of the Huarca basin, may be due to the Antaycocha sequence recording ENSO signatures with the Huarca basin recording the broader climatic regimes.

6.2.4 Colonial Period to Present

A reduction of human activity, with the arrival of the Spanish, is well documented at both of the study sites and across the central Andes region. There are observable reductions in all of the pXRF data at Antaycocha, as well as a single PCA point of ‘Antay_364’ which plots close to the mineral sedimentology vectors (see chapter 5). This reduction in human presence, at Huarca, is identified by an *n*-alkane sample at 381 ± 50 containing a mix of chain lengths as a result of lessened agricultural activity. The NPP record at Huarca also has an identifiable lack of human disturbance indicators, including the main coprophilous fungi between 377-385 cal yr BP. This is similar for the Antaycocha basin, which records lessened numbers of key indicators of disturbance between 321-346 cal yr BP. What this is likely suggesting is that both basins are being utilised for pastoral agriculture, either for camelids or for old world domesticates such as cattle or sheep, which were introduced into Peru around this time (Chepstow-Lusty et al., 2009).

The beginning of the Republic era sediments for both sites reveals a more reduced usage than in previous horizons. At Antaycocha, there is a distinct shift in the $\delta^{34}S$ record with more negative values (see chapter 5 for more information), indicating that the basin may have been repurposed as a watering hole for camelids and large herbivores, much as it is being used in the present day; further evidenced by increased phosphorous values in the pXRF data. There

is however, evidence of a return to crop rotation during the latter half of the Republic era. $\delta^{15}N$ values from 195 ± 133 cal yr BP within the edge core record show a mean deflection of -6.74‰ with low values continuing through until ~49 cal yr BP; possibly indicating early use of nitrate rich fertilisers along farming communities within the Huarca village.

6.3 Formative to Early Intermediate Period (8,000 – 1,450 cal yr BP)

During the early to md-Holocene, at Huarca, there is a distinctive anti-phasic relationship with the more established quaternary records Huascarán, Lake Pumacocha and Huagapo Cave (Thompson et al., 1995; Bird et al., 2011b; Kanner et al., 2013), between ~3,000-8,000 BP (See figure 6.1). This is most likely recording changes in vegetation communities within the basin environment, rather than recording changes in the SASM and ITCZ as the above records have faithfully been recording. The period between 7,000 and 5,000 BP is also of importance for Peru. Here we can observe that the above are enriched in $\delta^{18}O$ between 7,000-5,000 BP, which is indicative of aridity for Peru. During this time there is also a low stand in at Lake Titicaca from 7,500-5,000 BP, inferred from seismic profiles of the lake (Seltzer et al.,1998). There is also evidence, in the Huarca record, that suggests this site fits well with these records. Information derived from the carbon isotope curve, where values peak to -22.9‰ (a deviation of +3.1 per mil), at 4,581 ± 851 cal yr BP. The median age for this $\delta^{13}C$ peak, corresponds to a large flux of insoluble dust content in the Huascarán ice-core record, as well as peaks in As counts in the Cerro Llamoca peat sequence, which typify a peak in aridity from 4,500-4,400 cal yr BP (Thompson et al., 1995; Schittek et al., 2015). There is, however, a large margin of error modelled for this age in the Huarca basin, thus the events may not match.

There is a short period of time, following on from the mid-Holocene drought period, between 3,877-3,966 cal yr BP, which is suggestive of an open water system, at Huarca. This pluvial period is well documented in sites across the Andes, with identifiable decreases in $\delta^{18}O$ values within the Huagapo and lake Pumacocha records, alongside recorded lake level increases at Titicaca, Marcacocha, and Huaypo, as well as some glacial readvancement at Quelccaya (Abbott et al., 1997; Thompson et al., 2000, 2013; Chepstow-Lusty et al., 2003; Bird et al., 2011; Sublette-Mosblech et al., 2012; Kanner et al., 2013)(see figure 6.1 and 6.3). This pluvial period relates well to the accumulation of sediment at the base of the Antaycocha sequence, between 2,954 and 2,855 cal yr BP, suggestive of an increasing water table.

A major period of sedimentation in the Huarca sequence, between 1,948 and 1,081, corresponds to major societal development of the region and the beginning of continuous occupation of sites including Keushu during the beginning of the Recuay cultural phase (Herrera, 2007; Handley, 2022). This period also coincides with increased run-off records from the Peruvian coast (Rein et al., 2004, 2005), El Junco (Conroy et al., 2008) which infer periods of increased rainfall between 2,000-1,500 BP. This perhaps might have been a time of increased pastoralism within the highlands surrounding the Huarca basin as well as increased settlement building and expansionist ideals.

6.4 Middle Horizon (1,450-850 cal yr BP)

The inception of the MH is marked by a period of aridity, that is recorded in many of the established records across the Peruvian Andes. As previously described, this period is due to the Southern Hemisphere expression of the MCA and a weakening of the SASM, as well as a more northerly positioning of the ITCZ (Haug et al., 2001; Bird et al., 2011a, b; Vuille et al., 2012). This period of aridity may have had a knock-on effect with the sedimentation rate within the sites at Huarca and Antaycocha. The sedimentary sequences, during this time are only expressed by 6cm at the Antaycocha sequence, with 32cm of the Huarca edge core and 56cm for the middle basin core. This reduction in precipitation, as stated previously, would have led to a limited amount of surface run off and a decrease in the sediment load entering the basin.

A reduction of water levels was also recorded at lakes Titicaca and Marcacocha (Abbott et al., 1997; Chepstow-Lusty et al., 2003), but both of these records have continuous records throughout the MH. This suggests, therefore, that the smaller sites of Huarca and Antaycocha are sensitive to regional climate variability and reduction of precipitation related to the MCA. This is potentially highly significant to the wider community as it means there are 2 more sites that are recording major climatic events, in the Andean region. Given that the sedimentation rates are low during the MH this could indicate that a drying out of the wetland areas and may have had huge consequences on the cultures living close to the basins during this time. A reduction in the water levels would have meant that there would have been less water availability for pasture and crop rotations during a time of increased imperial expansion (Handley, 2022). The geochemical signal is only detected within the Huarca central basin core first by a switch in *n*-alkane distributions at 1,172 ± 150 cal yr BP, where a 76.4% abundance of n-C_{27}-C_{37} chain lengths dominate the sequence, which typify those of arid tolerant plants. This continues into a sample at 1,081 ± 95 cal yr BP with a total of 71.5% of the sample made up of chains n-C_{27}-C_{37}. There is also a large deviation of +6.5 per mil. recorded in the carbon isotope record (peak of -19.5‰), which is comparable to many other records for the Andes (see figure 6.1) (also refer back to chapter 4 for more information). This peak in the central basin record correlates well with peaks in $\delta^{18}O$ values in the Huagapo and Pumacocha sequences, as well as sudden reductions in *Poaceae* and Mn/Fe ratios in the Cerro Llamoca peatland record (Bird et al., 2011b; Kanner et al., 2013; Schittek et al., 2015). The timing of this arid period is particularly important in the Andes, as it also relates to the demise of the MH empire states of the Wari and the Tiwanaku towards the end of the horizon, which has been linked to this long-term drought (Binford et al., 1997; Weiss 2016).

Another hypothesis for the large isotope deflection could be the intensification of agriculture during the MH. The isotope signals reveal that there is a ~47% mixing of C_4 plants, which could be from arid tolerant plants but also from cultivars. *n*-Alkane abundances from the samples between 1,081 – 1,172 cal yr BP reveal a similarity between those found in maize and potato – which are important cultivated plants throughout much of the Andes even today. There is evidence at Chinqnajota, in the Chicha-Soras valley, with the presence of carbonised

maize within MH deposits (Meddens and Branch, 2010). Evidence from Keushu, which is above the basin at Huarca (see chapter 4, figure 4.1), also suggests that the irrigation systems fed from meltwater from the Huandoy glacier were in use during the MH and would have been able to feed agricultural systems during periods of drought, showing that communities through the Andes would have been able to adapt to their practices depending on the overall environment to keep up with crop demands.

6.5 Late Intermediate Period (850-512 cal yr BP)

The results from the montane basins reveal changeable conditions during the LIP, with *n*-alkane samples from the Huarca edge core from 785 ± 267 cal yr BP with 9.1% abundance of n-C_{16}-C_{20} chain lengths pertaining to algal/planktonic matter and submerged plant life (Cranwell, 1984; Cranwell et al., 1987; Kai et al., 2019). The median age for this sample is slightly earlier than increased flooding events recorded in the 106KL lithic record located off the coast of Lima (Rein et al., 2004, 2005), but occurs roughly at a similar time of increased *Poaceae* coverage in the Cerro Llamoca record (Schittek et al., 2015), which would indicate increasing amounts of surface run-off from a greater volume of precipitation occurring throughout the Andes. The same *n*-alkane signatures also contain a similarity with maize, and some other cultivars, which indicate a continued use of the basin for agricultural practices despite the decline of the Wari empire after the MH. This preference for maize agriculture was also identified at Marcacocha, also during the LIP with an increase in *Zea mays* pollen grains discovered within the sediments (Chepstow-Lusty et al., 2009). The reasonable percentages of coprophilous fungal remains around the Huarca basin, during this period, would also seem to suggest a continued use for the basin during the LIP after the demise of the Wari empire and would seem to confirm a nucleation of settlements during the LIP.

Similar *n*-alkane signals can be observed within the Huarca and at Antaycocha, continuing further into the LIP. The former at 673 ± 105 cal yr BP contains a sample with abundances like that of quinoa, potato and maize with the edge core signalling a $\delta^{13}C$ increase of +2.1‰ from the average. The abundance of n-C_{27}-C_{35} chains would also give evidence to continued cultivation through the latter half of the LIP, with 74.9% of the total number of *n*-alkane signature made up of C_{27}-C_{35}. At Antaycocha ~605 cal yr BP, there is a large enrichment peak in the $\delta^{13}C$ record of -18.6‰ with 80.6% of n-C_{27}-C_{35} chain lengths within the signature. This too could be an early sign of agriculture within the upper reaches of the Chillón valley, at a similar time there is agricultural practices in Ancash, but due to the large uncertainties within the age model it is hard to be completely accurate. This therefore could possibly be identifiying to continued dry periods in the latter stages of the LIP, with less negative $\delta^{18}O$ values in the Huagapo and Pumacocha sequences between ~800-600BP (Bird et al., 2011b; Kanner et al., 2013) (figure 6.3).

Towards the end of the LIP the Huarca basin starts to pick up a trend of increasing precipitation, which is recorded in other Andean records. Abundance of *n*-alkanes shifts, at 572 ± 32, to the shorter chain lengths of n-C_{16}-C_{20} with these chains accounting for 10.8% of

the total signal. This occurs at a similar time of reduced dust volume and more negative $\delta^{18}O$ values within the Huascarán ice-core sequence (Thompson et al., 1995), a likely representation of the onset of the LIA in the Andes. This time is also important to note as it is within the boundaries of major terrace reconstruction in the Chicha-Soras valley between 550-750 cal yr BP, which may be reflecting socio-economic changes in the face of climate change (Kemp et al., 2006; Branch et al., 2007, Handley, 2022).

6.6 Late Horizon (512-418 cal yr BP)

With the transition to the LH the changeable conditions in the Andes continue. $\delta^{13}C$ values for Antaycocha and Huarca become more depleted through the transition of the LIP and LH, as $\delta^{18}O$ values at Huascarán, Quelccaya, Pumacocha and Huagapo become more negative as a result of the onset of the LIA (see figure 6.3) (Thompson et al., 1995, 2000, 2013; Bird et al., 2011b; Kanner et al., 2013). This also coincides with increased human activity around the Antaycocha basin, as identified in the NPP assemblage, with the appearance of *Sporormiella* amongst other dung-related ascomycetes. This intensification can also be found with the construction of a wall which dams one end of the Antaycocha basin, which coincides with the approximate timing of the arrival of the Inca to the site of Cantamarca (Farfán, 2011). With the intensification of the SASM, during the LIA, and increased precipitation that occurred during this period it is likely that the creation of the dam was likely to create a reservoir for water storage as a response to climatic conditions of the time. Whereas in the Ancash region, the water technologies already existed throughout much of the province with canals, silt dams, irrigation networks etc. having been constructed much earlier in the MH (Lane, 2009).

Throughout the early stages of the LH human activity would intensify, as the Inca empire expanded into much of South America. This can be seen in each of the study sites, with samples occurring around 500BP plotting towards the inorganic fractions in the PCA plots. This can be seen more so at Antaycocha, where the added values from the pXRF data shows that increasing metal loads from Cu, As, An and Pb are likely sources of early mining peaks, which fit with other records of increased metallurgical indicators as seen in Pb rises from intensification of metallurgy in Laguna Pirhuacocha (Cooke et al., 2008). This pXRF data does fluctuate in the early stages of the LH at Antaycocha, which suggest that there is differing amounts of sediment availability within the basin possibly due to management of the basin and construction of new highland settlements around the Cantamarca zone. Evidence for the basin management can also be found within the $\delta^{34}S$ curve, NPP, and *n*-alkane samples for the LH from Antaycocha. The *n*-alkanes between 503 and 476 cal yr BP have between 8.2% and 15.4% n-C_{16}-C_{20} chain lengths, which are indicative of algal life, with the NPPs confirming that this is due to the presence of cyanobacteria, which is driving the more positive $\delta^{34}S$ values (refer back to Chapter 5 for further information). All these factors are due to the fact that the basin has been managed by the damming of the water which, in turn, is creating a stagnation of the reservoir – a knock on effect of population growth and the need for increased water management through the highlands.

There is a secondary peak in $\delta^{13}C$ values observed at Antaycocha at 446 ± 42 cal yr BP which is offset from a similar peak in the Huarca central basin record by some 130 years (see figure 6.3). This could be due to regional differences in vegetation in the records during this time. *n*-alkane samples taken from Antaycocha reveal that increased amounts of n-C_{29}-C_{33} may infer an agricultural signal from around the basin. The Inca knew the importance of storing food as surplus, for leaner times, with storehouses commonplace among Inca settlements. These can also be found proximal to the Antaycocha basin, at the Cantamarca settlement which was occupied by the Inca during the LH (Farfan, 2011). This seems to be a similarity with Huarca where two *n*-alkane samples at 479 ± 39 cal yr BP and 470 ± 150 cal yr BP contain a dominance of C_{31}, but less negative $\delta^{13}C$ values, which could relate to an increased amount of forest taxa in the Ancash province instead. This is supported by increasing amounts of Alder populations at Lake Pacucha and Marcacocha during the LH (Chepstow-Lusty et al., 2009; Sublette-Mosblech et al., 2012). The expansion of the forest taxa is likely a response to wetter and colder conditions during the LIA, and therefore probably encouraged by the Inca to increase lumber resources for building materials to support their empire expansion (Hughes, 1999).

6.7 Colonial Period to Present Day (418 cal yr BP onwards)

A reduction in the human activity with the arrival of the Spanish is well documented across South America (e.g. Bush et al., 2007a, b; Chepstow-Lusty et al., 2009), with the basins of Huarca and Antaycocha also recording diminished land-use during this time. As mentioned above, there is a reduction in the pXRF data, along with other sedimentary evidence. There is evidence that this mining does intensify again, later in this period, with peaks in Cu, As, Fe, Zn, S, and P by 394 ± 46 cal yr BP detected in the Antaycocha basin. This fits with the beginning of Spanish mining practices from other documented sites across the Andes (Nriagu, 1994; Cooke et al., 2008, 2009).

There is evidence to suggest that the climate during the Colonial Period was significantly wetter than the periods preceding it. The occurrence of *Glomus* at Antaycocha, as well as samples occurring nearer to the zone of increased minerogenic input from the PCA dataset, suggest increased erosion likely as a result of a greater volume of water entering the basin. The timing of this also coincides with decreased $\delta^{13}C$ values (at 403 ± 75 cal yr BP), in the Antaycocha basin, which are offset from the lowest values in the Huarca central basin by ~79 years, but are mapped by a slight deviation in the edge core of -1.3‰ (see figure 6.3). This fits with the timing of more negative $\delta^{18}O$ values in the Pumacocha record as well as a reduced volume of lithics within the Quelccaya sequence (Thompson et al., 2000, 2013; Bird et al., 2011b). There is some contention in the literature about the origin and cause of the increased precipitation during the Colonial Period, but it has been linked to increasing SASM intensity as a result of cooler Atlantic SSTs, increased ENSO activity and positional changes in the ITCZ (Rein et al., 2005; Thompson et al., 2013; Kanner et al., 2013, Handley, 2022).

Of particular interest to this project are the interactions between humans and environment and how this can be tracked and used for the future. The site of Antaycocha may give the best view of these interactions, as it has accumulated such a vast amount of sediment over a short amount of time – enabling this study to undertake analyses at a fine resolution. The basin itself is westerly facing, which is beneficial for detecting possible ENSO activity in the Andes. Towards the top of the sequence, the Rock-Eval pyrolysis method detects a 'switch' in the HI:OI ratio, which starts to favour the HI. This also coincides with a decline in TOC% values, as more minerogenic sediments enter the basin. Samples 'Antay_120' and 'Antay_128' both plot towards PC2 within the PCA data, away from the oxygen rich lake sediments that are commonplace in the sequence. These samples broadly correlate with a large Niña event covered in the Multivariate ENSO Index (MEI) during 1950-1951 (Wolter and Timlin, 2011). Similarly, another event placed at 88cm shows more pronounced values along the base of PC2 (see figure 6.6), with similarly elevated HI values, correlates with a strong El Niño event of 1982-1983; this is key information in the use of Rock-Eval for modern sedimentation, if this can be used to detect key ENSO horizons.

It is also worth noting that due to the sedimentation rate at Antaycocha, it is also possible to detect key pollutants in modern sediments. Large peaks in the pXRF data detected in S, Cu, As, Fe, and Zn, date to the 1930s. This points towards the environmental impacts from smelting activity from nearby mines, such as that of La Oroya which started smelting operations in 1922 (Reif et al., 1989; Reuer et al., 2012). Arsenic peaks are possibly due to emissions of arsenic trioxide, a major component of copper and zinc smelting. This has major connotations for human, animal, and environmental health and could be tracked along the Andes region to be used in environmental studies. Mining pollution released into the environment can enter food chains and can persist in the environment, potentially causing harm to large populations in the Andes (Custodio et al., 2020). It stands to reason that these intermontane basins are incredibly sensitive to human interference due to climate changes, as we have also seen at Huarca with the changes in plant community and farming regimes. Further investigations into similar sites, across the Andes, must be undertaken to better understand human-climate-environment interactions throughout the region.

6.8 Summary of Discussion

The data above has demonstrated that the basins in this project are highly resilient to periods of abrupt climatic changes, and they show broadly the same correlations with other established sites across the Andes. These upland wetland systems have also shown that they're highly important resources in preserving the long-term palaeoenvironmental histories and human-land use interactions, which can act as a precursor for current and future environmental change. These results have also shown that the basins are responding to the overarching climate patterns, at roughly the same time.

Of particular significance is the finding that the basin at Antaycocha seems to be sensitive enough to preserve the rapid onset of ENSO cycles. It's location on the western side of the

Andes chain means it is well placed to detect the cyclicity of the events. It is unfortunate, however, that this study did not recover the top sediments due to their unconsolidated nature. This means that this study could not detect any of the more modern ENSO events such as those in 1991-92, 1997-98 and 2002-03. Collecting sediment cores from similar sites, along the Andes western flank, would be beneficial in understanding if they too record these large ENSO events.

It would be beneficial to further the palaeoclimate knowledge of South America, if other mid-elevation records were collected to understand how these sites are interconnected and to further enhance out knowledge of human-environment interactions.

7. Conclusions and Recommendations for Future Work

The overall aim of this thesis was to reconstruct the impact of prehistoric and historic agro-pastoral land-use and climate change on the environment of the Peruvian Andes, and to try and evaluate the interactions between humans and the environment. The research questions primarily focussed on identifying periods of intense agro-pastoral land-use and the relationships between them and climatic changes, using a range of proxy methods. There was also a set of research questions aimed around testing methodologies to see whether they were sensitive enough to pick up short-term changes in climate and environment.

The importance of utilising intermontane basins for the reconstruction of Holocene climate, and to evaluate human-environment interactions has been demonstrated using a multi-proxy analysis of two basins situated in the Ancash and Lima regions of Peru. The multi-proxy approach combining inorganic (stable isotopes, pXRF) and organic (Rock-Eval, *n*-alkanes) geochemistry alongside palaeoecology (in the form of NPP analysis), integrated with published palaeoclimatic data has provided evidence that there has been a number of environmental responses to climatic variability (in precipitation and temperature) that has had an impact upon the cultural regimes in the highlands of Peru, who have also shown to have adapted to periods of climate change through the Holocene.

The project had a set of research questions and objectives that it set out to achieve, which can be found in Chapter 1, but are also summarised below.

To determine the relationship between cultural change and agro-pastoral land-use in the Peruvian Andes during the Late Holocene.

a. What do the new (this study) and published palaeoenvironmental records tell us about agro-pastoral land-use change?

Large $\delta^{13}C$ and $\delta^{15}N$ deflections in the Huarca sequence at 1,081 ± 95 cal yr BP, during the MH, is consistent with the wider literature and fits well within the dates for arid/warm conditions during the MCA. Data from the *n*-alkanes suggest that from 1,172 ± 150 cal yr BP communities around the Huarca basin may have been undertaking arable agricultural practices, with signatures sharing similarities with quinoa, potato, and maize – three major cultivars in the Andes. Irrigation systems fed from meltwater from the Nevado Huandoy may have been able to keep up with the necessary demand.

b. Is there a relationship between cultural change and agro-pastoral land-use change?

Evidence to suggest that there was some abandonment or reduced human interactions within both Huarca and Antaycocha basins during the LIP and Colonial Period. This may have been due to both the onset of climatic changes (wetter conditions at the end of the MH into the LIP) and societal reorganisation (decline of MH empires into the LIP and Spanish invasion into the Colonial Period). This can be identified with changes in NPP counts (less human disturbance spores and coprophilous fungi) as well as changes in plant communities as identified by the *n*-alkanes and isotope signals.

c. Did past climate change drive any of the agro-pastoral land-use changes observed?

Research has revealed that during wetter and cooler conditions, during the LIA, that there was a possible switch in agricultural practices. *n*-Alkane distributions from Huarca suggest a change from C_4 plants such as maize and potato being farmed, to more abundances of woody plant material during the LH. This suggests a change to agro-forestry from more traditional practices.

To determine the relationship between climate change and environmental change in the Peruvian Andes during the Late Holocene.

a. What do the new (this study) and published palaeoenvironmental records tell us about environmental change?

Both records are highly sensitive to periods of increased precipitation, as can be observed during the LIA. Huarca and Antaycocha both correlate with the wider literature, with lower $\delta^{13}C$ values during times of peak precipitation where more negative $\delta^{18}O$ values are recorded in Huagapo and Lake Pumacocha.

Huarca has an anti-phasic relationship with the wider literature, between 8,000-3,000 BP, suggestive that it is recording changes in vegetation cover during a period of relative precipitation increase following the mid-Holocene drought period. Huarca is also sensitive enough to pick up large scale environmental changes, during long lasting drought observed in the MCA with a signal indicative of arid tolerant taxa.

Antaycocha, due to its positioning in the Chillon Valley, is sensitive enough to pick up short-term variability in climate due to ENSO. There are at least 2 major ENSO cycles identified in its record (1950s and 1980s) but there are potentially more within its record, spanning back into the cultural horizons.

To undertake organic geochemical analyses of all core materials to provide information on depositional processes and detailed sedimentological record.

a. Can the n-alkane data identify dietary information, by way of identifying chains of key cultivars (e.g. Zea Mays, Chenopodium quinoa, Oxalis tuberosa, Solanum tuberosum)?

There are several *n*-Alkane samples identified in the Huarca record, especially, that have abundances that have similarities with that of the main cultivars above, which would typify that there are agricultural practices within the basin. We must, however, use caution when only using the abundance charts, as these may not give the full story. Only with the compound specific isotopic signature are we able to identify the cultivars directly.

Evaluate the application of RockEval data for radiocarbon dating of palaeoenvironmental records.

Rock-Eval pyrolysis has the potential to be used, not only to identify sources of OM, but may be used to determine the presence of "old carbon". There are several parameters that are all influenced by thermal degradation of OM: OI, T_{MAX}, I- and R-index. The Rock-Eval suggests that the bulk humic ages may not be suitable for radiocarbon dating in the future as they are the most influenced by aerobic and thermal degradation over time. Plant ages may be less susceptible to this and must be considered going forward over bulk dates.

Evaluate the application of trace elemental data to quantify sources of sediment input

a. ***What are the timings of arid events, which lead to periods of greater sediment accumulation and what can this tell us about land-use changes?***

The sedimentation rates of Antaycocha mean that it is possible to undertake high resolution trace elemental history of the region. This has revealed periods of increased mining/smelting throughout the LH and Colonial periods, as well as recent history due to opening of large smelters from as recently as the 1930's. pXRF data can also be used to identify areas of peak sediment availability due to arid events, and vice versa, which can be related to ENSO variability.

The trace elemental data can give insights into terrigenous vs aeolian sediment and can help unpick sources of OM identified in the Rock-Eval methods, as identified by PCA testing.

2. ***To construct robust chronologies, for each of the identified field sites.***

    a. ***What are the timings of climatic and environmental changes, in relation to the cultural horizons and do they alter the current narrative?***

    b. ***How can all the new records (from this project) be combined temporally, and how do they fit in with established palaeo-records?***

Results of radiocarbon dating and sedimentological analyses from both Huarca and Antaycocha reveal that environmental changes took place during the transition between the Formative Period and Early Horizon, into a pluvial phase following arid conditions in the mid-Holocene. These wetter conditions allowed sediment accumulation to being at the far edges of the Antaycocha basin around 2,903 ± 29 cal yr BP, while the Huarca sediments accumulated much earlier open water conditions were observed in the sediments dating to

between 3,877-3,966 cal yr BP. This shows that both basins are sensitive to changes in the overarching hydrological systems of the time.

Evidence from geochronology, sedimentology and bulk organic geochemistry reveals an estimated age for a dam at Antaycocha basin to be between 516-512 cal yr BP. This puts it within the transition of the LIP and LH, coinciding with an approximate known age for occupation by the Inca. This is concurrent with deteriorating conditions, during the onset of the LIA, with the climate becoming increasingly wetter. The basin may have been dammed in order to raise the level of the water for storage, as a response to the change in climatic conditions.

This research has demonstrated the need for a greater amount of palaeoenvironmental archives within the Andean region, that covers the entirety of the Holocene. There are a great number of long records, that stretch far into the past but that do not ratify the short-term cultural horizons that contain information on human-climate interactions. There is evidence from this and some other records that past societies were able to create networks of agricultural and water systems to adapt to current climatic conditions, with varying levels of success. There is however, an ever-growing need for more knowledge to be able to fully understand the relationship between climate variability and pre-Hispanic societies. Below are recommendations for future work to provide further understanding of how humans have responded to climatic changes through the Holocene, as well as future work to provide further methodological advancements.

- There still remains a paucity of palaeoenvironmental data for the Andes region that covers the last 2,500 years, with a high enough resolution. Sites within intermontane basins offer a chance at studying environmental change at a high resolution over the time periods covering the cultural horizons, as shown in this study.

- There is also a need for sites proximal to archaeological sites or remains. Those next to settlements or agricultural terraces etc. will enable the development of improved inter regional comparisons of land-use and environmental change.

- The collection of multiple cores across a selected wetland/lake etc. The cores collected for this study were either at the edge or in the centre of the basin. Cores spread across a transect along a basin offer the chance to capture land-use markers, vegetational changes, human and animal biomarkers, and other proxy data in their entirety and would ensure that studies can accurately reconstruct past environmental/climatic changes. It would also help to resolve problems relating to the local dispersal of coprophilous fungal spores, such as *Sporormiella*, and would also capture signals derived from local sources of plant leaf waxes.

- The development of an extensive collection of *n*-alkanes from modern plants from the regions around the basins of interest. This would help to build a database to untangle inputs of local and regional inputs of leaf waxes into the basins. It would also mean that studies would also be able to identify agricultural signals from *n*-alkane abundances, from the creation of mixing models.

- The analysis of coprostanols would provide a greater understanding of past pastoralism and human activity within the basins. While the NPPs can give information on past herbivory, it does not give in-depth amounts of detail pertaining to population sizes or periods of abandonment etc. The faecal biomarkers may be able to provide a greater understanding of the role and importance of pastoral agriculture within the wider context of agricultural systems in the Andes. The information of human population sizes we could also infer from its data would also be useful to ascertain periods of population decline, such as at the end of the MH, and pin-point timings of nucleation of populations during the LIP.

- While there are a great number of radiocarbon dates on the sedimentary sequences in this study, there are still some areas that have large uncertainties associated with them. Additional ^{14}C dates, or ^{210}Pb dating, may be able to ratify some of these larger errors to provide a more detailed view of Holocene climate changes.

- There is also a need for ^{14}C dating of funerary remains from archaeological sites. There is growing evidence to suggest that the current ceramic stratigraphies are not robust enough. Radiocarbon dating remains from excavations to build robust chronologies would allow for more accurate correlations between land-use practices, social development, abandonment, climatic changes.

- While the Rock-Eval show promise at identifying sources of old carbon within sedimentary sequences and can be used well with radiocarbon methods, to provide insight on where best select material to be dated; there is a need for more samples to be taken where there are both ages on plant and humic ages that show a significant age difference between the two. The main hypothesis here is that the Rock-Eval is picking out old carbon within bulk sediment, where the age differences get larger the older the sediment age, due to the amount of time it has undergone thermal and aerobic degradation processes. There is also more work that needs to be done to understand these processes further, as gaps in the knowledge remain.

References

Abbott, M.B., Binford, M.W., Brenner, M. and Kelts, K.R., 1997a. A 3500 14C yr High-Resolution Record of Water-Level Changes in Lake Titicaca, Bolivia/Peru. Quaternary Research, 47, pp.169–180.

Abbott, M.B., Seltzer, G.O., Kelts, K.R. and Southon, J., 1997b. Holocene Paleohydrology of the Tropical Andes from Lake Records. Quaternary Research, 47, pp.70–80.

Abbott, P.M., Jensen, B.J.L., Lowe, D.J., Suzuki, T. and Veres, D., 2020. Crossing new frontiers: extending tephrochronology as a global geoscientific research tool. Journal of Quaternary Science, https://doi.org/10.1002/jqs.3184.

Adkins, J.F., Griffin, S., Kashgarian, M., Cheng, H., M Druffel, E.R., Boyle, E.A., Lawrence Edwards, R. and Shen, C.-C., 2002. Radiocarbon Dating of Deep-Sea Corals. Radiocarbon, 44(2), pp.567–580.

Adrian, R., O'Reilly, C.M., Zagarese, H., Baines, S.B., Hessen, D.O., Keller, W., Livingstone, D.M., Sommaruga, R., Straile, D. and Van Donk, E., 2009. Lakes as sentinels of climate change. Limnology and oceanography, 54(6part2), pp.2283–2297.

Aguilar Díaz, M., 2019. Paisajes políticos y ushnu en el orden social y espacial de Choquerecuay, s. XV-XVI. Journal of Andean Archaeology, 39(1), pp.1–30. https://doi.org/10.1080/00776297.2018.1557871.

Apaéstegui, J., Cruz, F.W., Sifeddine, A., Vuille, M., Espinoza, J.C., Guyot, J.L., Khodri, M., Strikis, N., Santos, R. v., Cheng, H., Edwards, L., Carvalho, E. and Santini, W., 2014. Hydroclimate variability of the northwestern Amazon Basin near the Andean foothills of Peru related to the South American Monsoon System during the last 1600 years. Climate of the Past, 10(6), pp.1967–1981. https://doi.org/10.5194/cp-10-1967-2014.

Apaéstegui, J., Cruz, F.W., Vuille, M., Fohlmeister, J., Espinoza, J.C., Sifeddine, A., Strikis, N., Guyot, J.L., Ventura, R., Cheng, H. and Edwards, R.L., 2018. Precipitation changes over the eastern Bolivian Andes inferred from speleothem (δ18O) records for the last 1400 years. Earth and Planetary Science Letters, 494, pp.124–134. https://doi.org/10.1016/j.epsl.2018.04.048.

Aptroot, A. and van Geel, B., 2006. Fungi of the colon of the Yukagir Mammoth and from stratigraphically related permafrost samples. Review of Palaeobotany and Palynology, 141(1–2), pp.225–230. https://doi.org/10.1016/j.revpalbo.2005.04.006.

Arkush, E. and Tung, T.A., 2013. Patterns of War in the Andes from the Archaic to the Late Horizon: Insights from Settlement Patterns and Cranial Trauma. Journal of Archaeological Research, https://doi.org/10.1007/s10814-013-9065-1.

Aron, P.G., Poulsen, C.J., Fiorella, R.P., Levin, N.E., Acosta, R.P., Yanites, B.J. and Cassel, E.J., 2021. Variability and Controls on δ18O, d-excess, and∆′ 17O in Southern Peruvian Precipitation. Journal of Geophysical Research: Atmospheres, 126(23), p.e2020JD034009.

Aylor, D.E., 2002. Settling speed of corn (Zea mays) pollen. [online] Aerosol Science, Available at: <www.elsevier.com/locate/jaerosci>.

Baker, P.A., Fritz, S.C., Garland, J. and Ekdahl, E., 2005. Holocene hydrologic variation at Lake Titicaca, Bolivia/Peru, and its relationship to North Atlantic climate variation. Journal of Quaternary Science, 20(7–8), pp.655–662. https://doi.org/10.1002/jqs.987.

Bateman, A.S. and Kelly, S.D., 2007. Fertilizer nitrogen isotope signatures. Isotopes in Environmental and Health Studies, 43(3), pp.237–247. https://doi.org/10.1080/10256010701550732.

Bateman, A.S., Kelly, S.D. and Jickells, T.D., 2005. Nitrogen isotope relationships between crops and fertilizer: implications for using nitrogen isotope analysis as an indicator of agricultural regime. Journal of agricultural and food chemistry, 53(14), pp.5760–5765.

Bell, M.A. and Blais, J.M., 2021. Paleolimnology in support of archeology: a review of past investigations and a proposed framework for future study design. Journal of Paleolimnology, https://doi.org/10.1007/s10933-020-00156-8.

Bengtsson, L. and Enell, M., 1986. Chemical analysis. Handbook of Holocene Palaeoecology and Palaeohydrology. Wiley & Sons, Chichester.

Beresford-Jones, D., Lewis, H. and Boreham, S., 2009. Linking cultural and environmental change in Peruvian prehistory: Geomorphological survey of the Samaca Basin, Lower Ica Valley, Peru. Catena, 78(3), pp.234–249. https://doi.org/10.1016/j.catena.2008.12.010.

Bernabé, J., 2017. The Inca Route to the Huaylas. A Study of Inca Roads in Pampa de Pampas, Choquerecuay, Department of Ancash, Peru. Boletin del Museo Chileno de Arte Precolombino, 22(2), pp.47–63.

Biagini, D. and Lazzaroni, C., 2018. Eutrophication risk arising from intensive dairy cattle rearing systems and assessment of the potential effect of mitigation strategies. Agriculture, Ecosystems and Environment, 266, pp.76–83. https://doi.org/10.1016/j.agee.2018.07.026.

Binford, M.W., Kolata, A.L., Brenner, M., Janusek, J.W., Seddon, M.T., Abbott, M. and Curtis, J.H., 1997. Climate Variation and the Rise and Fall of an Andean Civilization. Quaternary Research, 47, pp.235–248.

Bird, B.W., Abbott, M.B., Rodbell, D.T. and Vuille, M., 2011a. Holocene tropical South American hydroclimate revealed from a decadally resolved lake sediment δ18O record. Earth and Planetary Science Letters, 310(3–4), pp.192–202. https://doi.org/10.1016/j.epsl.2011.08.040.

Bird, B.W., Abbott, M.B., Vuille, M., Rodbell, D.T., Stansell, N.D. and Rosenmeier, M.F., 2011b. A 2,300-year-long annually resolved record. PNAS, 108(21), pp.8583–8588.

Bishop, K.G., 2017. Re-approaching palaeodiet in the Andes Use and application of sulphur isotope analysis in reconstructing Peruvian palaeodiet. COMPASS, 1(1), pp.42–65.

Blaauw, M., Christen, J.A., Bennett, K.D. and Reimer, P.J., 2018. Double the dates and go for Bayes — Impacts of model choice, dating density and quality on chronologies. Quaternary Science Reviews, 188, pp.58–66. https://doi.org/10.1016/j.quascirev.2018.03.032.

Bradley, R.S., Vuille, M., Hardy, D. and Thompson, L.G., 2003. Low latitude ice cores record Pacific sea surface temperatures. Geophysical Research Letters, 30(4).

Branch, N.P., Kemp, R.A., Silva, B., Meddens, F.M., Williams, A., Kendall, A. and Pomacanchari, C.V., 2007. Testing the sustainability and sensitivity to climatic change of terrace agricultural systems in the Peruvian Andes: a pilot study. Journal of Archaeological Science, 34(1), pp.1–9. https://doi.org/10.1016/j.jas.2006.03.011.

Bray, E.E. and Evans, D., 1961. Distribution of n-paraffins as a clue to recognition of source beds. Geochemica et Cosmochimica Acta, 22, pp.2–15.

van Breukelen, M.R., Vonhof, H.B., Hellstrom, J.C., Wester, W.C.G. and Kroon, D., 2008. Fossil dripwater in stalagmites reveals Holocene temperature and rainfall variation in Amazonia. Earth and Planetary Science Letters, 275(1–2), pp.54–60. https://doi.org/10.1016/j.epsl.2008.07.060.

Van Breukelen, M.R., Vonhof, H.B., Hellstrom, J.C., Wester, W.C.G. and Kroon, D., 2008. Fossil dripwater in stalagmites reveals Holocene temperature and rainfall variation in Amazonia. Earth and Planetary Science Letters, 275(1–2), pp.54–60.

Bronk Ramsey, C., 2009a. Bayesian Analysis of Radiocarbon Dates. Radiocarbon, 51(1), pp.337–360.

Bronk Ramsey, C., 2009b. Dealing with Outliers and Offsets in Radiocarbon Dating. Radiocarbon, 51, pp.1023–1045.

Bruins, H.J. and van der Plicht, J., 2005. Desert settlement through the Iron Age. The Bible and Radiocarbon Dating, p.349.

Burger, R.L., 1981. The Radiocarbon Evidence for the Temporal Priority of. American Antiquity, 46(3), pp.592–602.

Burger, R.L., 1985. Archaeological Investigations at Huaricoto, Ancash, Peru: 1978–1979. National Geographic Society Research Reports, 19, pp.119–127.

Bush, M.B., Silman, M.R. and Listopad, C.M.C.S., 2007. A regional study of Holocene climate change and human occupation in Peruvian Amazonia. In: Journal of Biogeography. pp.1342–1356. https://doi.org/10.1111/j.1365-2699.2007.01704.x.

Bush, M.B., Silman, M.R., de Toledo, M.B., Listopad, C., Gosling, W.D., Williams, C., de Oliveira, P.E. and Krisel, C., 2007. Holocene fire and occupation in Amazonia: records from two lake districts. Philosophical Transactions of the Royal Society B: Biological Sciences, 362(1478), pp.209–218.

Bustamante, M.G., Cruz, F.W., Vuille, M., Apaéstegui, J., Strikis, N., Panizo, G., Novello, F. v., Deininger, M., Sifeddine, A., Cheng, H., Moquet, J.S., Guyot, J.L., Santos, R. v., Segura, H. and Edwards, R.L., 2016. Holocene changes in monsoon precipitation in the Andes of NE Peru based on δ18O speleothem records. Quaternary Science Reviews, 146, pp.274–287. https://doi.org/10.1016/j.quascirev.2016.05.023.

Cadwallader, L., Beresford-Jones, D.G., Sturt, F.C., Pullen, A.G. and Arce Torres, S., 2018. Doubts about How the Middle Horizon Collapsed (ca. A.D. 1000) and Other Insights from the Looted Cemeteries of the Lower Ica Valley, South Coast of Peru. Journal of Field Archaeology, 43(4), pp.316–331. https://doi.org/10.1080/00934690.2018.1464306.

Cai, W., McPhaden, M.J., Grimm, A.M., Rodrigues, R.R., Taschetto, A.S., Garreaud, R.D., Dewitte, B., Poveda, G., Ham, Y.G., Santoso, A., Ng, B., Anderson, W., Wang, G., Geng, T., Jo, H.S., Marengo, J.A., Alves, L.M., Osman, M., Li, S., Wu, L., Karamperidou, C., Takahashi, K. and Vera, C., 2020. Climate impacts of the El Niño–Southern Oscillation on South America. Nature Reviews Earth and Environment, https://doi.org/10.1038/s43017-020-0040-3.

Canfield, D.E. and Marais, D.J. des, 1991. Aerobic Sulfate Reduction in Microbial Mats. Science, [online] 251(5000), pp.1471–1473. Available at: <https://www.science.org>.

Cardich, A., 1985. The fluctuating upper limits of cultivation in the central Andes and their impact on Peruvian prehistory. Advances in World Archaeology, 4, pp.293–333.

Cardozo, A.Y.V., Gomes, D.F., da Silva, E.M., Duque, S.R.E., Rangel, J.O.C., Sifeddine, A., Turcq, B. and Albuquerque, A.L.S., 2014. Holocene paleolimnological reconstruction of a high altitude Colombian tropical lake. Palaeogeography, Palaeoclimatology, Palaeoecology, 415, pp.127–136. https://doi.org/10.1016/j.palaeo.2014.03.013.

Carrie, J., Sanei, H. and Stern, G., 2012. Standardisation of Rock–Eval pyrolysis for the analysis of recent sediments and soils. Organic Geochemistry, 46, pp.38–53.

Carter, J.F. and Barwick, V.J., 2011. Good practice guide for isotope ratio mass spectrometry. FIRMS Network, 48.

Catalan, J., Pla-Rabés, S., Wolfe, A.P., Smol, J.P., Rühland, K.M., Anderson, N.J., Kopáček, J., Stuchlík, E., Schmidt, R. and Koinig, K.A., 2013. Global change revealed by palaeolimnological records from remote lakes: a review. Journal of Paleolimnology, 49, pp.513–535.

Chapdelaine, C., 2011. Recent Advances in Moche Archaeology. Journal of Archaeological Research, 19(2), pp.191–231. https://doi.org/10.1007/s10814-010-9046-6.

Chappell, J. and Polach, A., 1972. Some Effects of Partial Recrystallisation on 14C Dating Late Pleistocene Corals and Molluscs. Quaternary Research, 2, pp.244–252.

Cheng, H., Lawrence Edwards, R., Shen, C.C., Polyak, V.J., Asmerom, Y., Woodhead, J., Hellstrom, J., Wang, Y., Kong, X., Spötl, C., Wang, X. and Calvin Alexander, E., 2013a. Improvements in 230Th dating, 230Th and 234U half-life values, and U-Th isotopic measurements by multi-collector inductively coupled plasma mass spectrometry. Earth and Planetary Science Letters, 371–372, pp.82–91. https://doi.org/10.1016/j.epsl.2013.04.006.

Cheng, H., Sinha, A., Cruz, F.W., Wang, X., Edwards, R.L., D'Horta, F.M., Ribas, C.C., Vuille, M., Stott, L.D. and Auler, A.S., 2013b. Climate change patterns in Amazonia and biodiversity. Nature Communications, 4. https://doi.org/10.1038/ncomms2415.

Chepstow-Lusty, A., Frogley, M.R., Bauer, B.S., Bush, M.B. and Herrera, A.T., 2003. A late Holocene record of arid events from the Cuzco region, Peru. Journal of Quaternary Science, 18(6), pp.491–502. https://doi.org/10.1002/jqs.770.

Chepstow-Lusty, A.J., Frogley, M.R. and Baker, A.S., 2019. Comparison of Sporormiella dung fungal spores and oribatid mites as indicators of large herbivore presence: evidence from the Cuzco region of Peru. Journal of Archaeological Science, 102, pp.61–70. https://doi.org/10.1016/j.jas.2018.12.006.

Chepstow-Lusty, A.J., Frogley, M.R., Bauer, B.S., Leng, M.J., Boessenkool, K.P., Carcaillet, C., Ali, A.A. and Gioda, A., 2009. Putting the rise of the Inca Empire within a climatic and land management context. [online] Clim. Past, Available at: <www.clim-past.net/5/375/2009/>.

Chepstow-Lusty, A.J., Frogley, M.R., Bauer, B.S., Leng, M.J., Cundy, A.B., Boessenkool, K.P. and Gioda, A., 2007. Evaluating socio-economic change in the Andes using oribatid mite abundances as indicators of domestic animal densities. Journal of Archaeological Science, 34(7), pp.1178–1186. https://doi.org/10.1016/j.jas.2006.12.023.

Cobeñas, G., Thouret, J.C., Bonadonna, C. and Boivin, P., 2012. The c.2030yr BP Plinian eruption of El Misti volcano, Peru: Eruption dynamics and hazard implications. Journal of Volcanology and Geothermal Research, 241–242, pp.105–120. https://doi.org/10.1016/j.jvolgeores.2012.06.006.

Cohen, M.N., 1978. Archaeological plant remains from the central coast of Peru. Ñawpa Pacha, 16(1), pp.23–50.

Conroy, J.L., Overpeck, J.T., Cole, J.E., Shanahan, T.M. and Steinitz-Kannan, M., 2008. Holocene changes in eastern tropical Pacific climate inferred from a Galápagos lake sediment record. Quaternary Science Reviews, 27(11–12), pp.1166–1180. https://doi.org/10.1016/j.quascirev.2008.02.015.

Cooke, C.A., Abbott, M.B. and Wolfe, A.P., 2008. Late-Holocene atmospheric lead deposition in the Peruvian and Bolivian Andes. Holocene, 18(2), pp.353–359. https://doi.org/10.1177/0959683607085134.

Cooke, C.A., Wolfe, A.P. and Hobbs, W.O., 2009. Lake-sediment geochemistry reveals 1400 years of evolving extractive metallurgy at Cerro de Pasco, Peruvian Andes. Geology, 37(11), pp.1019–1022. https://doi.org/10.1130/G30276A.1.

Covey, R.A., 2008. Multiregional perspectives on the archaeology of the andes during the Late Intermediate period (c. A.D. 1000-1400). Journal of Archaeological Research, 16(3), pp.287–338. https://doi.org/10.1007/s10814-008-9021-7.

Cranwell, P.A., 1984. Alkyl esters, mid chain ketones and fatty acids in late glacial and postglacial lacustrine sediments. Organic geochemistry, 6, pp.115–124.

Cranwell, P.A., Eglinton, G. and Robinson, N., 1987. Lipids of aquatic organisms as potential contributors to lacustrine sediments—II. Organic Geochemistry, 11(6), pp.513–527.

Cross, S.L., Baker, P.A., Seltzer, G.O., Fritz, S.C. and Dunbar, R.B., 2000. A new estimate of the Holocene lowstand level of Lake Titicaca, central Andes, and implications for tropical palaeohydrology. The Holocene, 10(1), pp.21–32.

Custodio, M., Cuadrado, W., Peñaloza, R., Montalvo, R., Ochoa, S. and Quispe, J., 2020. Human risk from exposure to heavy metals and arsenic in water from rivers with mining influence in the Central Andes of Peru. Water (Switzerland), 12(7). https://doi.org/10.3390/w12071946.

Davis, M.E. and Thompson, L.G., 2006. An Andean ice-core record of a Middle Holocene mega-drought in North Africa and Asia. Annals of Glaciology, 43, pp.34–41.

Davis, O.K. and Shafer, D.S., 2006. Sporormiella fungal spores, a palynological means of detecting herbivore density. Palaeogeography, Palaeoclimatology, Palaeoecology, 237(1), pp.40–50. https://doi.org/10.1016/j.palaeo.2005.11.028.

Deininger, M., Ward, B.M., Novello, V.F. and Cruz, F.W., 2019. Late Quaternary variations in the South American monsoon system as inferred by speleothems—New perspectives using the SISAL database. Quaternary, 2(1), p.6.

Denevan, W.M., 1976. The aboriginal population of Amazonia. The native population of the Americas in, 1492, pp.205–234.

Derda, M., Chmielewski, A.G. and Licki, J., 2006. Stable isotopes of sulphur in investigating pollution sources. Environment Protection Engineering, [online] 32(3), pp.63–68. Available at: <https://www.researchgate.net/publication/271440965>.

Dillehay, T.D., 1977. Tawantinsuyu integration of the chillon valley, peru:A case of inca geo-political mastery. Journal of Field Archaeology, 4(4), pp.397–405. https://doi.org/10.1179/009346977791490159.

Dunbar, R.B., Wellington, G.M., Colgan, M.W. and Glynn, P.W., 1994. Eastern Pacific sea surface temperature since 1600 A.D.' The d18O record of climate variability in Galapagos corals. PALEOCEANOGRAPHY, 9(2), pp.291–315.

Eglinton, G. and Hamilton, R.J., 1963. The distribution of alkanes. In: T. Swaine, ed. Chemical Plant Taxonomoy. pp.87–217.

Eglinton, T.I. and Eglinton, G., 2008. Molecular proxies for paleoclimatology. Earth and Planetary Science Letters, 275(1–2), pp.1–16. https://doi.org/10.1016/j.epsl.2008.07.012.

Eichler, A., Gramlich, G., Kellerhals, T., Tobler, L. and Schwikowski, M., 2015. Pb pollution from leaded gasoline in South America in the context of a 2000-year metallurgical history. Science Advances, 1(2). https://doi.org/10.1126/sciadv.1400196.

Ekdahl, E.J., Fritz, S.C., Baker, P.A., Rigsby, C.A. and Coley, K., 2008. Holocene multidecadal- to millennial-scale hydrologic variability on the South American Altiplano. Holocene, 18(6), pp.867–876. https://doi.org/10.1177/0959683608093524.

Etienne, D., Wilhelm, B., Sabatier, P., Reyss, J.L. and Arnaud, F., 2013. Influence of sample location and livestock numbers on Sporormiella concentrations and accumulation rates in surface sediments of Lake Allos, French Alps. Journal of Paleolimnology, 49(2), pp.117–127. https://doi.org/10.1007/s10933-012-9646-x.

Farfán, C., 1995. Asentamientos prehispánicos de la cuenca alta del Chillón. Gaceta Arqueológica Andina, 24, pp.31–61.

Farfán, C., 2011. Arquitectura prehispánica de Cantamarca-Canta.

Farrington, J.W., Davis, A.C., Sulanowski, J., McCaffrey, M.A., McCarthy, M., Clifford, C.H., Dickinson, P. and Volkman, J.K., 1988. Biogeochemistry of lipids in surface sediments of the Peru upwelling area at 15 S. Organic Geochemistry, 13(4–6), pp.607–617.

Feakins, S.J., Bentley, L.P., Salinas, N., Shenkin, A., Blonder, B., Goldsmith, G.R., Ponton, C., Arvin, L.J., Wu, M.S., Peters, T., West, A.J., Martin, R.E., Enquist, B.J., Asner, G.P. and Malhi, Y., 2016a. Plant leaf wax biomarkers capture gradients in hydrogen isotopes of precipitation from the Andes and Amazon. Geochimica et Cosmochimica Acta, 182, pp.155–172. https://doi.org/10.1016/j.gca.2016.03.018.

Feakins, S.J., Peters, T., Wu, M.S., Shenkin, A., Salinas, N., Girardin, C.A.J., Bentley, L.P., Blonder, B., Enquist, B.J., Martin, R.E., Asner, G.P. and Malhi, Y., 2016b. Production of leaf wax n-alkanes across a tropical forest elevation transect. Organic Geochemistry, 100, pp.89–100. https://doi.org/10.1016/j.orggeochem.2016.07.004.

Finucane, B.C., Valdez, E.J., Calderon, I.P., Pomacanchari, C.V., Valdez, L.M. and O'Connell, T., 2007. The End of Empire: New Radiocarbon Dates from the Ayacucho Valley, Peru, and their Implications for the Collapse of the Wari State. Radiocarbon, 49(2), pp.579–592.

Flohr, P., Fleitmann, D., Matthews, R., Matthews, W. and Black, S., 2016. Evidence of resilience to past climate change in Southwest Asia: Early farming communities and the 9.2 and 8.2 ka events. Quaternary Science Reviews, 136, pp.23–39. https://doi.org/10.1016/j.quascirev.2015.06.022.

Flores, G.M., 2019. The cultural trajectory of the Central Peruvian Coast, the territory and its people in the valleys of pre-Hispanic Lima. In: A companion to early modern Lima. Brill. pp.25–45.

Fornace, K.L., Hughen, K.A., Shanahan, T.M., Fritz, S.C., Baker, P.A. and Sylva, S.P., 2014. A 60,000-year record of hydrologic variability in the Central Andes from the hydrogen isotopic composition of leaf waxes in Lake Titicaca sediments. Earth and Planetary Science Letters, 408, pp.263–271. https://doi.org/10.1016/j.epsl.2014.10.024.

Fritz, S.C., Baker, P.A., Dwyer, G.S., Lowenstein, T.K., Seltzer, G.O., Rigsby, C.A., Ku, T. and Luo, S., 2001. A 160,000-Year Record of Tropical Climate Variability From Salar de Uyuni, Bolivia. In: AGU Fall Meeting Abstracts. pp.PP22A-0509.

Fritz, S.C., Baker, P.A., Seltzer, G.O., Ballantyne, A., Tapia, P., Cheng, H. and Edwards, R.L., 2007. Quaternary glaciation and hydrologic variation in the South American tropics as reconstructed from the Lake Titicaca drilling project. Quaternary Research, 68(3), pp.410–420. https://doi.org/10.1016/j.yqres.2007.07.008.

Garcin, Y., Schefuß, E., Schwab, V.F., Garreta, V., Gleixner, G., Vincens, A., Todou, G., Séné, O., Onana, J.-M. and Achoundong, G., 2014. Reconstructing C3 and C4 vegetation cover using n-alkane carbon isotope ratios in recent lake sediments from Cameroon, Western Central Africa. Geochimica et Cosmochimica Acta, 142, pp.482–500.

Garreaud, R., Vuille, M. and Clement, A.C., 2003. The climate of the Altiplano: Observed current conditions and mechanisms of past changes. In: Palaeogeography, Palaeoclimatology, Palaeoecology. Elsevier B.V. pp.5–22. https://doi.org/10.1016/S0031-0182(03)00269-4.

Garreaud, R.D., Vuille, M., Compagnucci, R. and Marengo, J., 2009. Present-day South American climate. Palaeogeography, Palaeoclimatology, Palaeoecology, 281(3–4), pp.180–195. https://doi.org/10.1016/j.palaeo.2007.10.032.

van Geel, B., 1972. Palynology of a section from the raised peat bog ‘Wietmarscher moor ‘, with special reference to fungal remains. Acta Botanica Neerlandica, 21(3), pp.261–284.

van Geel, B., 2001. Non-pollen palynomorphs. In: J.P. Smol, H.J.B. Birks and W.M. Last, eds. Tracking environmental change using lake sediments. Springer. pp.99–119.

van Geel, B., Bohncke, S.J.P. and Dee, H., 1980. A palaeoecological study of an upper Late Glacial and Holocene sequence from “De Borchert”, The Netherlands. Review of palaeobotany and palynology, 31, pp.367–448.

van Geel, B., Coope, G.R. and van der Hammen, T., 1989. Palaeoecology and stratigraphy of the Lateglacial type section at Usselo (The Netherlands). Review of palaeobotany and palynology, 60(1–2), pp.25–129.

van Geel, B., Gelorini, V., Lyaruu, A., Aptroot, A., Rucina, S., Marchant, R., Damsté, J.S.S. and Verschuren, D., 2011. Diversity and ecology of tropical African fungal spores from a 25,000-year palaeoenvironmental record in southeastern Kenya. Review of Palaeobotany and Palynology, 164(3–4), pp.174–190.

Gerdau-Radonic, K. and Herrera, A., 2010. Pourquoi fouiller des dépôts funéraires pillés? Deux exemples et quelques réponses de Keushu (Ancash, Pérou). Bulletins et Memoires de la Societe d'Anthropologie de Paris, 22(3–4), pp.145–156. https://doi.org/10.1007/s13219-010-0012-4.

Gijseghem, H. van, 2006. A Frontier Perspective on Paracas Society and Nasca Ethnogenesis. [online] Source: Latin American Antiquity, Available at: <https://www.jstor.org/stable/25063066>.

Grimm, A.M., 2003. The El Niño Impact on the Summer Monsoon in Brazil: Regional Processes versus Remote Influences. American Meteorological Society, 16, pp.263–280.

Grimm, A.M., Barros, V.R. and Doyle, M.E., 2000. Climate Variability in Southern South America Associated with El Niño and La Niña Events. American Meterological Society, 13, pp.35–58.

Grosjean, M., 2001. Mid-Holocene Climate in the South-Central Andes: Humid or Dry? Science, 292(5526), pp.2391–2391. https://doi.org/10.1126/science.292.5526.2391a.

Grosjean, M., van Leeuwen, J.F.N., van der Knaap, W.O., Geyh, M.A., Ammann, B., Tanner, W., Messerli, B., Nunez, L.A., Valero-Garces, ´˜b L and Veit, H., 2001. A 22,000 14 C year BP sediment and pollen record of climate ž / change from Laguna Miscanti 238S , northern Chile. [online] Global and Planetary Change, Available at: <www.elsevier.comrlocatergloplacha>.

Grosjean, M. and Veit, H., 2005. Water Resources in the Arid Mountains of the Atacama Desert (Northern Chile): Past Climate Changes and Modern Conflicts. Global Change and Mountain Regions, pp.93–104. https://doi.org/10.1007/1-4020-3508-x_10.

Habicht, K.S. and Canfield, D.E., 1997. Sulfur isotope fractionation during bacterial sulfate reduction in organic-rich sediments. Geochimica et Cosmochimica Acta, 61(24), pp.5351–5361.

Hansen, B.C.S., Seltzer, G.O. and Wright, H.E., 1994. Late Quaternary vegetational change in the central Peruvian Andes. Palaeogeography, Palaeoclimatology, Palaeoecology, 109, pp.263–285.

Hansen, B.C.S., Wright, H.E. and Bradbury, J.P., 1984. Pollen studies in the Junín area, central Peruvian Andes. Geological Society of America Bulletin, [online] 95, pp.1454–1465.

Available at: <https://pubs.geoscienceworld.org/gsa/gsabulletin/article-pdf/95/12/1454/3444965/i0016-7606-95-12-1454.pdf>.

Harsch, M.A., Hulme, P.E., McGlone, M.S. and Duncan, R.P., 2009. Are treelines advancing? A global meta-analysis of treeline response to climate warming. Ecology letters, 12(10), pp.1040–1049.

Haug, G.H., Hughen, K.A., Sigman, D.M., Peterson, L.C. and Röhl, U., 2001. Southward Migration of the Intertropical Convergence Zone through the Holocene. Science, 293(5533), pp.1304–1308.

Henderson, K.A., Thompson, L.G. and Lin, P.N., 1999. Recording of El Niño in ice core δ18O records from Nevado Huascarán, Peru. Journal of Geophysical Research Atmospheres, 104(D24), pp.31053–31065. https://doi.org/10.1029/1999JD900966.

Henke, L.M.K., Lambert, F.H. and Charman, D.J., 2017. Was the Little Ice Age more or less El Niño-like than the Medieval Climate Anomaly? Evidence from hydrological and temperature proxy data. Climate of the Past, 13(3), pp.267–301.

Herrera, A., 2007. Social landscapes and community identity: the social organisation of space in the north-central Andes. In: A. Herrea, S. Kohring and S. Wynne-Jones, eds. Socialising Complexity: Structure, Interaction and Power in Archaeological Discourse. Oxbow Books. pp.161–185.

Holmgren, M. and Scheffer, M., 2001. El Niño as a window of opportunity for the restoration of degraded arid ecosystems. Ecosystems, 4(2), pp.151–159. https://doi.org/10.1007/s100210000065.

Hughes, J.D., 1999. Conservation in the Inca empire. Capitalism Nature Socialism, 10(4), pp.69–76.

Jansen, E., Overpeck, J., Briffa, K.R., Duplessy, J.-C., Joos, F., Masson-Delmotte, V., Olago, D., Otto-Bliesner, B., Richard Peltier, W., Rahmstorf, S., Ramesh, R., Barnola, J., Bauer, E., Brady, E., Jouzel, J., Mitchell, J., Overpeck, J., Briffa, K., Duplessy, J., Joos, F., Masson-Delmotte, V., Olago, D., Otto-Bliesner, B., Peltier, W., Rahmstorf, S., Ramesh, R., Raynaud, D., Rind, D., Solomina, O., Villalba, R., Zhang, D. and Qin, D., 2007. Paleoclimate. In: S. Soloman, D. Qin, M. Manning, Z. Chen, M. Marquis, M. Averyt, M. Tignor and H.L. Miller, eds. Climate Change 2007: The Physical Science Basis. Contribution of Working Group I to the Fourth Assessment Report of the Intergovernmental Panel on Climate Change. Cambridge: Cambridge University Press. pp.433–498.

Janusek, J.W., 2008. Ancient Tiwanaku. Cambridge University Press.

Jarosz, N., Loubet, B., Durand, B., McCartney, A., Foueillassar, X. and Huber, L., 2003. Field measurements of airborne concentration and deposition rate of maize pollen. Agricultural and Forest Meteorology, 119(1–2), pp.37–51. https://doi.org/10.1016/S0168-1923(03)00118-7.

Jennings, J., 2006. Understanding Middle Horizon Peru: hermeneutic spirals, interpretative traditions, and Wari administrative centers. Latin American Antiquity, 17(3), pp.265–285.

Jennings, J. and Craig, N., 2001. Politywide analysis and imperial political economy: The relationship between valley political complexity and administrative centers in the Wari Empire of the Central Andes. Journal of Anthropological Archaeology, 20(4), pp.479–502. https://doi.org/10.1006/jaar.2001.0385.

Jimenez, G., Cole, J.E., Thompson, D.M. and Tudhope, A.W., 2018. Northern Galápagos corals reveal twentieth century warming in the eastern tropical Pacific. Geophysical Research Letters, 45(4), pp.1981–1988.

Jowsey, P.C., 1966. An improved peat sampler. New phytologist, 65(2), pp.245–248.

Kahmen, A., Schefuß, E. and Sachse, D., 2013. Leaf water deuterium enrichment shapes leaf wax n-alkane dD values of angiosperm plants I: Experimental evidence and mechanistic insights. Geochemica et Cosmochimica Acta, [online] 111, pp.39–49. Available at: <http://dx.doi.org/10.10>.

Kai, N., Naiang, W., Xiaonan, L., Zhuolun, L., Jiaqi, S., Ran, A. and Lvlv, Z., 2019. A grain size and n-alkanes record of Holocene environmental evolution from a groundwater recharge lake in Badain Jaran Desert, Northwestern China. Holocene, 29(6), pp.1045–1058. https://doi.org/10.1177/0959683619831430.

Kalicki, P., 2014. Model of Interregional Contacts Between Highland and Coastal Groups in Late Pre-Columbian Periods in the Lomas of the Central Coast of PEru. Contributions in New World Archaeology, 6, pp.83–110.

Kanner, L.C., Burns, S.J., Cheng, H. and Edwards, R.L., 2012. High-latitude forcing of the South American summer monsoon during the last glacial. Science, 335(6068), pp.570–573. https://doi.org/10.1126/science.1213397.

Kanner, L.C., Burns, S.J., Cheng, H., Edwards, R.L. and Vuille, M., 2013. High-resolution variability of the South American summer monsoon over the last seven millennia: Insights from a speleothem record from the central Peruvian Andes. Quaternary Science Reviews, 75, pp.1–10. https://doi.org/10.1016/j.quascirev.2013.05.008.

Kemp, R., Branch, N., Silva, B., Meddens, F., Williams, A., Kendall, A. and Vivanco, C., 2006. Pedosedimentary, cultural and environmental significance of paleosols within pre-hispanic agricultural terraces in the southern Peruvian Andes. Quaternary International, 158(1), pp.13–22.

Kinaston, R., Bedford, S., Richards, M., Hawkins, S., Gray, A., Jaouen, K., Valentin, F. and Buckley, H., 2014. Diet and human mobility from the lapita to the early historic period on Uripiv Island, Northeast Malakula, Vanuatu. PLoS ONE, 9(8). https://doi.org/10.1371/journal.pone.0104071.

Knüsel, S., Ginot, P., Schotterer, U., Schwikowski, M., Gäggeler, H.W., Francou, B., Petit, J.R., Simoes, J.C. and Taupin, J.-D., 2003. Dating of two nearby ice cores from the Illimani, Bolivia. Journal of Geophysical Research: Atmospheres, 108(D6).

Knutson, D.W., Buddemeier, R.W. and Smith, S. v, 1972. Coral chronometers: seasonal growth bands in reef corals. Science, 177(4045), pp.270–272.

Könitzer, S.F., Stephenson, M.H., Davies, S.J., Vane, C.H. and Leng, M.J., 2016. Significance of sedimentary organic matter input for shale gas generation potential of Mississippian Mudstones, Widmerpool Gulf, UK. Review of Palaeobotany and Palynology, 224, pp.146–168. https://doi.org/10.1016/j.revpalbo.2015.10.003.

Kuentz, A., Ledru, M.P. and Thouret, J.C., 2012. Environmental changes in the highlands of the western Andean Cordillera, southern Peru, during the Holocene. Holocene, 22(11), pp.1215–1226. https://doi.org/10.1177/0959683611409772.

Kuhry, P., 1997. The palaeoecology of a treed bog in western boreal Canada: a study based on microfossils, macrofossils and physico-chemical properties. Review of Palaeobotany and Palynology, 96(1–2), pp.183–224.

Lacey, J.H., Francke, A., Leng, M.J., Vane, C.H. and Wagner, B., 2015. A high-resolution Late Glacial to Holocene record of environmental change in the Mediterranean from Lake Ohrid (Macedonia/Albania). International Journal of Earth Sciences, 104(6), pp.1623–1638. https://doi.org/10.1007/s00531-014-1033-6.

Lacey, J.H., Leng, M.J., Vane, C.H., Radbourne, A.D., Yang, H. and Ryves, D.B., 2018. Assessing human impact on Rostherne Mere, UK, using the geochemistry of organic matter. Anthropocene, 21, pp.52–65. https://doi.org/10.1016/j.ancene.2018.02.002.

Lamy, F., Hebbeln, D., Ro, U. and Wefer, G., 2001. Holocene rainfall variability in southern Chile: a marine record of latitudinal shifts of the Southern Westerlies. Earth and Planetary Science Letters, [online] 185, pp.369–382. Available at: <www.elsevier.com/locate/epsl>.

Lane, K., 2009. Engineered highlands: The social organization of water in the ancient north-central Andes (AD 1000-1480). World Archaeology, 41(1), pp.169–190. https://doi.org/10.1080/00438240802655245.

Lau, G., 2002. Feasting and Ancestor Veneration at Chinchawas, North Highlands of Ancash, Peru. Latin american Antiquity, 13(3), pp.279–304.

Lau, G., 2012a. Intercultural Relations in Northern Peru: The Northern Central Highlands During the Middle Horizon. BOLETÍN DE ARQUEOLOGÍA PUCP, 16, pp.23–52.

Lau, G., 2016. An archaeology of Ancash: Stones, ruins and communities in Andean Peru. Routledge.

Lau, G.F., 2001. The ancient community of Chinchawas: economy and ceremony in the north highlands of Peru. Yale University.

Lau, G.F., 2004. The recuay culture of Peru's North-Central Highlands: A reappraisal of chronology and its implications. Journal of Field Archaeology, https://doi.org/10.1179/jfa.2004.29.1-2.177.

Lau, G.F., 2005. Core-periphery relations in the Recuay hinterlands: economic interaction at Chinchawas, Pe. Antiquity, 79, pp.78–99.

Lau, G.F., 2007. Andean Past Animal Resources and Recuay Cultural Transformations at Chichawas (Ancash, Peru). Andean Past, 8, p.22.

Lau, G.F., 2011. Andean expressions: art and archaeology of the Recuay culture. University of Iowa Press.

Lau, G.F., 2012b. The First Millennium ad in North-Central Peru: Critical Perspectives on a Linguistic Prehistory. Proceedings of the British Academy, 173, pp.161–195.

Lau, K. and Zhou, J., 2003. Anomalies of the South American summer monsoon associated with the 1997–99 El Nino–Southern Oscillation. International Journal of Climatology: A Journal of the Royal Meteorological Society, 23(5), pp.529–539.

Liu, W., Yang, H., Wang, H., Yao, Y., Wang, Z. and Cao, Y., 2016. Influence of aquatic plants on the hydrogen isotope composition of sedimentary long-chain n-alkanes in the Lake Qinghai region, Qinghai-Tibet Plateau. Science China Earth Sciences, 59, pp.1368–1377.

Lough, J.M., 2010. Climate records from corals. Wiley interdisciplinary reviews: climate change, 1(3), pp.318–331.

Lowe, D.J., 2011. Tephrochronology and its application: A review. Quaternary Geochronology, https://doi.org/10.1016/j.quageo.2010.08.003.

Lüning, S., Gałka, M., Bamonte, F.P., Rodríguez, F.G. and Vahrenholt, F., 2019. The Medieval Climate Anomaly in South America. Quaternary International, 508, pp.70–87. https://doi.org/10.1016/j.quaint.2018.10.041.

Luo, W., Wang, X., Sardans, J., Wang, Z., Dijkstra, F.A., Lü, X.T., Peñuelas, J. and Han, X., 2018. Higher capability of C3 than C4 plants to use nitrogen inferred from nitrogen stable isotopes along an aridity gradient. Plant and Soil, 428(1–2), pp.93–103. https://doi.org/10.1007/s11104-018-3661-2.

Maasch, K.A., 2008. El Niño and interannual variability of climate in the Western Hemisphere. El Niño, Catastrophism, and Culture Change in Ancient America, pp.33–55.

Majzlan, J., Navrotsky, A., McCleskey, R.B. and Alpers, C.N., 2006. Thermodynamic properties and crystal structure refinement of ferricopiapite, coquimbite, rhomboclase, and Fe2(SO4)3(H2O)5. European Journal of Mineralogy, 18(2), pp.175–186. https://doi.org/10.1127/0935-1221/2006/0018-0175.

Mann, M.E., Zhang, Z., Rutherford, S., Bradley, R.S., Hughes, M.S., Shindell, D., Ammann, C., Faluvegi, G. and Ni, F., 2009. Global signatures and Dynamical Origins of the Little Ice

Age and Medieval Climate Anomaly. Science, 326(5957), pp.1256–1260. https://doi.org/10.1126/science.1177012.

Manning, S.W., Birch, J., Conger, M.A. and Sanft, S., 2020. Resolving time among non-stratified short-duration contexts on a radiocarbon plateau: Possibilities and challenges from the ad 1480-1630 example and Northeastern North America. In: Radiocarbon. Cambridge University Press. pp.1785–1807. https://doi.org/10.1017/RDC.2020.51.

Marchant, M., Hebbeln, D. and Wefer, G., 1999. High resolution planktic foraminiferal record of the last 13,300 years from the upwelling area off Chile. [online] Marine Geology, Available at: <www.elsevier.nlrlocatermargeo>.

Mark, S.Z., Abbott, M.B., Rodbell, D.T. and Moy, C.M., 2022. XRF analysis of Laguna Pallcacocha sediments yields new insights into Holocene El Niño development. Earth and Planetary Science Letters, 593. https://doi.org/10.1016/j.epsl.2022.117657.

Mauricio, A.C., 2018a. Reassessing the Impact of El Niño at the end of the early intermediate period from the perspective of the Lima culture. Ñawpa Pacha, 38(2), pp.203–231. https://doi.org/10.1080/00776297.2018.1511312.

Mauricio, A.C., 2018b. Reassessing the Impact of El Niño at the end of the early intermediate period from the perspective of the Lima culture. Ñawpa Pacha, 38(2), pp.203–231.

McConnaughey, T., 1989. 13C and 18O isotopic disequilibrium in biological carbonates: I. Patterns. Geochimica et Cosmochimica Acta, 53(1), pp.151–162.

McDermott, F., 2004. Palaeo-climate reconstruction from stable isotope variations in speleothems: a review. Quaternary Science Reviews, 23(7–8), pp.901–918.

McWhirt, A., Weindorf, D.C. and Zhu, Y., 2012. Rapid analysis of elemental concentrations in compost via portable X-ray fluorescence spectrometry. Compost Science & Utilization, 20(3), pp.185–193.

Meddens, F.M. and Branch, N., 2010. The Huari state, its use of ancestors, rural hinterland and agricultural infrastructure. In: J. Jenning, ed. Beyond Wari walls: Regional perspectives on Middle Horizon Peru. University of New Mexico Press. pp.155–170.

Menzel, D., 1959. The Inca Occupation of the South Coast of Peru. Southwestern Journal of Anthropology, [online] 15(2), pp.125–142. Available at: <https://about.jstor.org/terms>.

Mills, K., Schillereff, D., Saulnier-Talbot, É., Gell, P., Anderson, N.J., Arnaud, F., Dong, X., Jones, M., McGowan, S. and Massaferro, J., 2017. Deciphering long-term records of natural variability and human impact as recorded in lake sediments: a palaeolimnological puzzle. Wiley Interdisciplinary Reviews: Water, 4(2), p.e1195.

Moberg, A., Sonechkin, D.M., Holmgren, K., Datsenko, N.M. and Karlén, W., 2005. Highly variable Northern Hemisphere temperatures reconstructed from low-and high-resolution proxy data. Nature, 433(7026), pp.613–617.

Moreno, A., Giralt, S., Valero-Garcés, B., Sáez, A., Bao, R., Prego, R., Pueyo, J.J., González-Sampériz, P. and Taberner, C., 2007. A 14 kyr record of the tropical Andes: The Lago Chungará sequence (18°S, northern Chilean Altiplano). Quaternary International, 161(1), pp.4–21. https://doi.org/10.1016/j.quaint.2006.10.020.

Moser, K.A., Baron, J.S., Brahney, J., Oleksy, I.A., Saros, J.E., Hundey, E.J., Sadro, S.A., Kopáček, J., Sommaruga, R., Kainz, M.J., Strecker, A.L., Chandra, S., Walters, D.M., Preston, D.L., Michelutti, N., Lepori, F., Spaulding, S.A., Christianson, K.R., Melack, J.M. and Smol, J.P., 2019. Mountain lakes: Eyes on global environmental change. Global and Planetary Change, 178, pp.77–95. https://doi.org/10.1016/j.gloplacha.2019.04.001.

Newell, A.J., Vane, C.H., Sorensen, J.P.R., Moss-Hayes, V. and Gooddy, D.C., 2016. Long-term Holocene groundwater fluctuations in a chalk catchment: evidence from Rock-Eval pyrolysis of riparian peats. Hydrological Processes, 30(24), pp.4556–4567. https://doi.org/10.1002/hyp.10903.

Nordt, L.C., 2001. Stable Carbon and Oxygen Isotopes in Soils Applications for Archaeological Research. Earth Sciences and Archaeology, pp.419–448.

Novello, V.F., Cruz, F.W., McGlue, M.M., Wong, C.I., Ward, B.M., Vuille, M., Santos, R.A., Jaqueto, P., Pessenda, L.C.R. and Atorre, T., 2019. Vegetation and environmental changes in tropical South America from the last glacial to the Holocene documented by multiple cave sediment proxies. Earth and Planetary Science Letters, 524, p.115717.

Nriagu, J.O., 1994. Mercury pollution from the past mining of gold and silver in the Americas. The Science of the Total Environment, 149, pp.167–181.

Ogburn, D., Sillar, B. and Sierra, J.C., 2013. Evaluating effects of chemical weathering and surface contamination on the in situ provenance analysis of building stones in the Cuzco region of Peru with portable XRF. Journal of Archaeological Science, 40(4), pp.1823–1837. https://doi.org/10.1016/j.jas.2012.09.023.

Ogburn, D.E., 2012. Reconceiving the Chronology of the Inca Imperial Expansion. Radiocarbon, 54(2), pp.219–237.

Okumura, T., Kumon, F. and Tokuyama, H., 2021. Radiocarbon dating of precious corals off the southwest coast of kochi prefecture, southwest japan. Radiocarbon, 63(1), pp.195–212. https://doi.org/10.1017/RDC.2020.114.

Olsson, I.U., 2009. Radiocarbon Dating History: Early Days, Questions, and Problems Met. Radiocarbon, 51(1), pp.1–43.

Ordoñez, L., Vogel, H., Sebag, D., Ariztegui, D., Adatte, T., Russell, J.M., Kallmeyer, J., Vuillemin, A., Friese, A., Crowe, S.A., Bauer, K.W., Simister, R., Henny, C., Nomosatryo, S.

and Bijaksana, S., 2019. Empowering conventional Rock-Eval pyrolysis for organic matter characterization of the siderite-rich sediments of Lake Towuti (Indonesia) using End-Member Analysis. Organic Geochemistry, 134, pp.32–44. https://doi.org/10.1016/j.orggeochem.2019.05.002.

Palacios, J., Maquera, E. and Toledo, C., 2014. Tecnología hidráulica, ampliación de la frontera agrícola y asentamientos no monumentales durante la época Lima. Boletín de arqueología PUCP, (18), pp.59–80.

Parker, B.J. and Rodseth, L., 2005. Untaming the frontier in anthropology, archaeology, and history. University of Arizona Press.

Parsons, L.A., LeRoy, S., Overpeck, J.T., Bush, M., Cárdenes-Sandí, G.M. and Saleska, S., 2018. The Threat of Multi-Year Drought in Western Amazonia. Water Resources Research, 54(9), pp.5890–5904. https://doi.org/10.1029/2017WR021788.

Peinado, F.M., Ruano, S.M., González, M.G.B. and Molina, C.E., 2010. A rapid field procedure for screening trace elements in polluted soil using portable X-ray fluorescence (PXRF). Geoderma, 159(1–2), pp.76–82. https://doi.org/10.1016/j.geoderma.2010.06.019.

Powell, R.L. and Still, C.J., 2009. Biogeography of C3 and C4 vegetation in South America. Anais XIV Simpósio Brasileiro de Sensoriamento Remoto, pp.2935–2942.

Powell, R.L., Yoo, E.-H. and Still, C.J., 2012. Vegetation and soil carbon-13 isoscapes for South America: integrating remote sensing and ecosystem isotope measurements. Ecosphere, 3(11), pp.1–25.

Prager, A., Theuerkauf, M., Couwenberg, J., Barthelmes, A., Aptroot, A. and Joosten, H., 2012. Pollen and non-pollen palynomorphs as tools for identifying alder carr deposits: a surface sample study from NE-Germany. Review of Palaeobotany and Palynology, 186, pp.38–57.

Quilter, J., 2013. The ancient central Andes. Routledge.

Raia, A. and Cavalcanti, I.F.A., 2008. The life cycle of the South American monsoon system. Journal of Climate, 21(23), pp.6227–6246.

Ramirez, E., Hoffmann, G., Taupin, J.-D., Francou, B., Ribstein, P., Caillon, N., Ferron, F.A., Landais, A., Petit, J.R. and Pouyaud, B., 2003a. A new Andean deep ice core from Nevado Illimani (6350 m), Bolivia. Earth and Planetary Science Letters, 212(3–4), pp.337–350.

Ramirez, E., Hoffmann, G., Taupin, J.D., Francou, B., Ribstein, P., Caillon, N., Ferron, F.A., Landais, A., Petit, J.R., Pouyaud, B., Schotterer, U., Simoes, J.C. and Stievenard, M., 2003b. A new Andean deep ice core from Nevado Illimani (6350 m), Bolivia. Earth and Planetary Science Letters, 212(3–4), pp.337–350. https://doi.org/10.1016/S0012-821X(03)00240-1.

Raper, D. and Bush, M., 2009. A test of Sporormiella representation as a predictor of megaherbivore presence and abundance. Quaternary Research, 71(3), pp.490–496. https://doi.org/10.1016/j.yqres.2009.01.010.

Raynor, G.S., Ogden, E.C. and Hayes, J. v, 1972. Dispersion and Deposition of Corn Pollen from Experimental Sources. Agronomy Journal, 64, pp.420–427.

Reed, E. v., Thompson, D.M., Cole, J.E., Lough, J.M., Cantin, N.E., Cheung, A.H., Tudhope, A., Vetter, L., Jimenez, G. and Edwards, R.L., 2021. Impacts of Coral Growth on Geochemistry: Lessons From the Galápagos Islands. Paleoceanography and Paleoclimatology, 36(4). https://doi.org/10.1029/2020PA004051.

Reeder, M.S., Stow, D.A. v and Rothwell, R.G., 2002. Late Quaternary turbidite input into the east Mediterranean basin: new radiocarbon constraints on climate and sea-level control. Geological Society, London, Special Publications, 191(1), pp.267–278.

Reif, J.S., Ameghino, E. and Aaronson, M.J., 1989. Chronic Exposure of Sheep to a Zinc Smelter in Peru. Environmental Research, 49, pp.40–49.

Reimer, P.J., Austin, W.E.N., Bard, E., Bayliss, A., Blackwell, P.G., Bronk Ramsey, C., Butzin, M., Cheng, H., Edwards, R.L., Friedrich, M., Grootes, P.M., Guilderson, T.P., Hajdas, I., Heaton, T.J., Hogg, A.G., Hughen, K.A., Kromer, B., Manning, S.W., Muscheler, R., Palmer, J.G., Pearson, C., van der Plicht, J., Reimer, R.W., Richards, D.A., Scott, E.M., Southon, J.R., Turney, C.S.M., Wacker, L., Adolphi, F., Büntgen, U., Capano, M., Fahrni, S.M., Fogtmann-Schulz, A., Friedrich, R., Köhler, P., Kudsk, S., Miyake, F., Olsen, J., Reinig, F., Sakamoto, M., Sookdeo, A. and Talamo, S., 2020. The IntCal20 Northern Hemisphere Radiocarbon Age Calibration Curve (0-55 cal kBP). Radiocarbon, 62(4), pp.725–757. https://doi.org/10.1017/RDC.2020.41.

Rein, B., Lückge, A., Reinhardt, L., Sirocko, F., Wolf, A. and Dullo, W.C., 2005. El Niño variability off Peru during the last 20,000 years. Paleoceanography, 20(4). https://doi.org/10.1029/2004PA001099.

Rein, B., Lückge, A. and Sirocko, F., 2004. A major Holocene ENSO anomaly during the Medieval period. Geophysical Research Letters, 31(17). https://doi.org/10.1029/2004GL020161.

Reuer, M.K., Bower, N.W., Koball, J.H., Hinostroza, E., de la Torre Marcas, M.E., Surichaqui, J.A.H. and Echevarria, S., 2012. Lead, Arsenic, and Cadmium Contamination and Its Impact on Children's Health in La Oroya, Peru. ISRN Public Health, 2012, pp.1–12. https://doi.org/10.5402/2012/231458.

Reuter, J., Stott, L., Khider, D., Sinha, A., Cheng, H. and Edwards, R.L., 2009. A new perspective on the hydroclimate variability in northern South America during the Little Ice Age. Geophysical Research Letters, 36(21). https://doi.org/10.1029/2009GL041051.

Reyes-Knoche, A., 2012. Sustainable water supply in pre-Columbian civilizations in Ancient Peru and South America. Evolution of water supply through the millennia, pp.271–299.

Rodbell, D.T., Delman, E.M., Abbott, M.B., Besonen, M.T. and Tapia, P.M., 2014. The heavy metal contamination of Lake Junín National Reserve, Peru: An unintended consequence of the juxtaposition of hydroelectricity and mining. GSA Today, 24(8), pp.4–10. https://doi.org/10.1130/GSATG200A.1.

Rodbell, D.T., Seltzer, G.O., Anderson, D.M., Abbott, M.B., Enfield, D.B. and Newman, J.H., 1999. An ~15,000-Year Record of El Niño-Driven Alluviation in Southwestern Ecuador. Science, 283, pp.516–520.

Roosevelt, A.C., Lima Da Costa, M., Lopes Machado, C., Michab, M., Mercier, N., Valladas, H., Feathers, J., Barnett, W., Imazio Da Silveira, M., Henderson, A., Sliva, J., Chernoff, B., Reese, D.S., Holman, J.A., Toth, N. and Schick, K., 1996. Paleoindian Cave Dwellers in the Amazon: The Peopling of the Americas. Science, [online] 272(5260), pp.373–384. Available at: <http://science.sciencemag.org/>.

Rowe, H.D., Guilderson, T.P., Dunbar, R.B., Southon, J.R., Seltzer, G.O., Mucciarone, D.A., Fritz, S.C. and Baker, P.A., 2003. Late Quaternary lake-level changes constrained by radiocarbon and stable isotope studies on sediment cores from Lake Titicaca, South America. Global and Planetary Change, 38(3–4), pp.273–290. https://doi.org/10.1016/S0921-8181(03)00031-6.

Rowe, J.H., 1944. An introduction to the archaeology of Cuzco. The Museum.

Sandweiss, D.H., Maasch, K.A., Burger, R.L., Richardson III, J.B., Rollins, H.B. and Clement, A., 2001. Variation in Holocene El Niñ o frequencies: Climate records and cultural consequences in ancient Peru. [online] Geology, Available at: <https://pubs.geoscienceworld.org/gsa/geology/article-pdf/29/7/603/3521912/i0091-7613-29-7-603.pdf>.

Sandweiss, D.H., Richardson, J.B., Reitz, E.J., Rollins, H.B. and Maasch, K.A., 1996. Geoarchaeological Evidence from Peru for a 5000 Years B.P. Onset of El Nino. Science , [online] 273(5281), pp.1531–1533. Available at: <http://science.sciencemag.org/>.

Sapkota, A., Cheburkin, A.K., Bonani, G. and Shotyk, W., 2007. Six millennia of atmospheric dust deposition in southern South America (Isla Navarino, Chile). Holocene, 17(5), pp.561–572. https://doi.org/10.1177/0959683607078981.

Schiferl, J.D., Bush, M.B., Silman, M.R. and Urrego, D.H., 2018. Vegetation responses to late Holocene climate changes in an Andean forest. Quaternary Research (United States), 89(1), pp.60–74. https://doi.org/10.1017/qua.2017.64.

Schittek, K., Forbriger, M., Mächtle, B., Schäbitz, F., Wennrich, V., Reindel, M. and Eitel, B., 2015. Holocene environmental changes in the highlands of the southern Peruvian Andes

(14° S) and their impact on pre-Columbian cultures. Climate of the Past, 11(1), pp.27–44. https://doi.org/10.5194/cp-11-27-2015.

Schneider, J.K., Gagosian, R.B., Cochran, J.K. and Trull, T.W., 1983. Particle size distributions of n-alkanes and 210Pb in aerosols off the coast of Peru. Nature, 304, pp.429–432.

Schreiber, K.J., 1987. Conquest and Consolidation: A Comparison of the Wari and Inka Occupations of a Highland Peruvian Valley. American Antiquity, 52(2), pp.266–284.

Sebag, D., Disnar, J.-R., Guillet, B., di Giovanni, C., Verrecchia, E.P. and Durand, A., 2006. Monitoring organic matter dynamics in soil profiles by 'Rock-Eval pyrolysis': bulk characterization and quantification of degradation. European journal of soil science, 57(3), pp.344–355.

Sebag, D., Verrecchia, E.P., Cécillon, L., Adatte, T., Albrecht, R., Aubert, M., Bureau, F., Cailleau, G., Copard, Y., Decaens, T., Disnar, J.R., Hetényi, M., Nyilas, T. and Trombino, L., 2016. Dynamics of soil organic matter based on new Rock-Eval indices. Geoderma, 284, pp.185–203. https://doi.org/10.1016/j.geoderma.2016.08.025.

Segura, R. and Shimada, I., 2010. The Wari footprint on the central coast: a view from Cajamarquilla and Pachacamac. Beyond Wari Walls: Regional Perspectives on Middle Horizon, Peru, pp.113–135.

Seki, O., Nakatsuka, T., Shibata, H. and Kawamura, K., 2010. A compound-specific n-alkane δ13C and δD approach for assessing source and delivery processes of terrestrial organic matter within a forested watershed in northern Japan. Geochimica et Cosmochimica Acta, 74(2), pp.599–613.

Seltzer, G., Rodbell, D. and Burns, S., 2000. Isotopic evidence for late Quaternary climatic change. Geology, 28(1), pp.35–38.

Seltzer, G.O., BAker, P., Cross, S., Dunbar, R. and Fritz, S., 1998. High-resolution seismic reflection profiles from Lake Titicaca, Peru Bolivia Evidence for Holocene Aridity in the tropical Andes. Geology, 26(2), pp.167–170.

Shimada, I., Schaaf, C.B., Thompson, L.G. and Mosley, E., 1991. Cultural Impacts of Severe Droughts in the Prehistoric Andes: Application of a 1,500-Year Ice Core Precipitation Record. World Archaeology, 22(3), pp.247–270.

Sigl, M., Jenk, T.M., Kellerhals, T., Szidat, S., Ga¨ggeler, H.W., Ga¨ggeler, G., Wacker, L., Synal, H.-A., Boutron, C., Barbante, C., Gabrieli, J. and Schwikowski, M., 2009. Instruments and Methods Towards radiocarbon dating of ice cores. Journal of Glaciology, [online] 55(194), pp.985–996. https://doi.org/10.7892/boris.36171.

Sikes, E.L., Uhle, M.E., Nodder, S.D. and Howard, M.E., 2009. Sources of organic matter in a coastal marine environment: Evidence from n-alkanes and their δ13C distributions in the

Hauraki Gulf, New Zealand. Marine Chemistry, 113(3–4), pp.149–163. https://doi.org/10.1016/j.marchem.2008.12.003.

Silva, J.E., 1996. Prehistoric settlement patterns in the Chillón river valley, Peru. University of Michigan.

Silverman, H., 1994. The Archaeological Identification of an Ancient Peruvian Pilgrimage Center. World Archaeology, 26(1), pp.1–18.

Slowakiewicz, M., Tucker, M.E., Vane, C.H., Harding, R., Collins, A. and Pancost, R.D., 2015. SHALE-GAS POTENTIAL OF THE MID-CARBONIFEROUS BOWLAND-HODDER UNIT IN THE CLEVELAND BASIN (YORKSHIRE), CENTRAL BRITAIN. Journal of Petroleum Geology, [online] 38(1), pp.59–76. Available at: <www.jpg.co.uk>.

Smith, B.N. and Epsten, S., 1971. Two Categories of 13C/12C Ratios for Higher Plants. Plant Physiol., 47, pp.380–384.

Solis, R.S., Haas, J. and Creamer, W., 2001. Dating Caral, a Preceramic Site in the Supe Valley on the Central Coast of Peru. Science, [online] 292, pp.723–726. Available at: <http://science.sciencemag.org/>.

Stansell, N.D., Rodbell, D.T., Licciardi, J.M., Sedlak, C.M., Schweinsberg, A.D., Huss, E.G., Delgado, G.M., Zimmerman, S.H. and Finkel, R.C., 2015. Late glacial and Holocene glacier fluctuations at Nevado Huaguruncho in the eastern cordillera of the Peruvian Andes. Geology, 43(8), pp.747–750.

Stern, C., de Porras, M.E. and Maldonado, A., 2015. Tephrochronology of the upper Río Cisnes valley (44 S), southern Chile. Andean Geology, 42(2), pp.173–189.

Stroup, J.S., Kelly, M.A., Lowell, T. v., Smith, C.A., Beal, S.A., Landis, J.D. and Tapia, P.M., 2015. Late Holocene fluctuations of Quelccaya Ice Cap, Peru, registered by nearby lake sediments. Journal of Quaternary Science, 30(8), pp.830–840. https://doi.org/10.1002/jqs.2821.

Sublette Mosblech, N.A., Chepstow-Lusty, A., Valencia, B.G. and Bush, M.B., 2012. Anthropogenic control of late-Holocene landscapes in the Cuzco region, Peru. Holocene, 22(12), pp.1361–1372. https://doi.org/10.1177/0959683612449760.

Sutter, R.C. and Sharratt, N., 2010. Continuity and Transformation During the Terminal Middle Horizon (A.D. 950-1150): A Bioarchaeological Assessment of Tumilaca Origins Within the Middle Moquegua Valley, Peru. [online] Source: Latin American Antiquity, Available at: <https://www.jstor.org/stable/25766979?seq=1&cid=pdf-reference#references_tab_contents>.

Szpak, P., Millaire, J.F., White, C.D. and Longstaffe, F.J., 2012. Influence of seabird guano and camelid dung fertilization on the nitrogen isotopic composition of field-grown maize (Zea mays). Journal of Archaeological Science, 39(12), pp.3721–3740. https://doi.org/10.1016/j.jas.2012.06.035.

Tantaleán, H. and Pérez, C., 2003. Pueblo Viejo. Un centro administrativo inca en el Callejón de Huaylas. Arqueo logía de la sierra de Ancash. Propuestas y perspectivas. B. Ibarra, Ed, pp.445–456.

Taylor, R.E., Stuiver, M. and Reimer, P.J., 1996. Development and extension of the calibration of the radiocarbon time scale: archaeological applications. Quaternary Science Reviews, 15(7), pp.655–668.

Tello, J.C. and Xesspe, T.M., 1959. Paracas. Institute of Andean Research.

Thomas, C.L., Jansen, B., Van Loon, E.E. and Wiesenberg, G.L.B., 2021. Transformation of n-alkanes from plant to soil: a review. SOIL, https://doi.org/10.5194/soil-7-785-2021.

Thompson, G., Kolata, A.I. and Weiss, H., 2017. Twelfth Century AD. Climate, Environment and the Tiwanaku State. Megadrought and Collapse: From early agriculture to Angkor, pp.231–246.

Thompson, L.G., 2000. Ice core evidence for climate change in the Tropics: implications for our future. Quaternary Science Reviews, 19, pp.19–35.

Thompson, L.G., Davis, M.E., Mosley-Thompson, E. and Liu, K.B., 1988. Pre-Incan agricultural activity recorded in dust layers in two tropical ice cores. Nature, 336(6201), pp.763–765. https://doi.org/10.1038/336763a0.

Thompson, L.G., Davis, M.E., Mosley-Thompson, E., Sowers, T.A., Henderson, K.A., Zagorodnov, V.S., Lin, P.-N., Mikhalenko, V.N., Campen, R.K. and Bolzan, J.F., 1998. A 25,000-year tropical climate history from Bolivian ice cores. Science, 282(5395), pp.1858–1864.

Thompson, L.G., Mosley-Thompson, E., Davis, M.E., Lin, P.-N., Henderson, K.A., Cole-Dai, J., Bolzan, J.F. and Liu, K.-B., 1995. Late Glacial Stage and Holocene Tropical Ice Core Records from Huascaran, Peru. Science, [online] 269(5220), pp.46–50. Available at: <http://science.sciencemag.org/>.

Thompson, L.G., Mosley-Thompson, E., Davis, M.E., Zagorodnov, V.S., Howat, I.M., Mikhalenko, V.N. and Lin, P.N., 2013. Annually resolved ice core records of tropical climate variability over the past ~1800 years. Science, https://doi.org/10.1126/science.1234210.

Thompson, L.G., Mosley-Thompson, E., Henderson, K.A. and G, T.L., 2000. Ice-core palaeoclimate records in tropical South America since the Last Glacial Maximum. Journal of Quaternary Science, 15(4), pp.377–394.

Thompson, L.G., Mosley-Thompson, E. and Thompson, P.A., 1992. Reconstructing interannual climate variability from tropical and subtropical ice-core records. In: H.F. Diaz and V. Markgraf, eds. El Nino historical and paleoclimatic aspects of the Southern Oscillation. Cambridge University Press. pp.295–322.

Thouret, J.-C., Juvigné, E., Marino, J., Moscol, M., Legeley-Padovani, A., Loutsch, I., Dávila, J., Lamadon, S. and Rivera, M., 2002. Late Pleistocene and Holocene Tephrostratigraphy and Chronology in Southern Peru. Andes, pp.215–239.

Troels-Smith, J., 1955. Karakterisering af løse jordarter. Danmarks Geologiske Undersøgelse IV. Række, 3(10), pp.1–73.

Trust, B.A. and Fry, B., 1992. Stable sulphur isotopes in plants: a review. Plant, Cell and Environment, 15, pp.1105–1110.

Tudhope, A.W., Chilcott, C.P., Mcculloch, M.T., Cook, E.R., Chappell, J., Ellam, R.M., Lea, D.W., Lough, J.M. and Shimmield, G.B., 2001. Variability in the El Niño-Southern Oscillation Through a Glacial-Interglacial Cycle. Science, [online] 291(5508), pp.1511–1517. Available at: <http://science.sciencemag.org/>.

Unkel, I., Kromer, B., Wacker, L. and Wagner, G., 2007. A Chronology of the Pre-Columbian Paracas and Nasca Cultures in South Peru Based on AMS 14C Dating. Radiocarbon, [online] 49(2), pp.551–564. https://doi.org/10.2458/azu_js_rc.49.2953.

Unkel, I., Reindel, M., Gorbahn, H., Isla Cuadrado, J., Kromer, B. and Sossna, V., 2012. A comprehensive numerical chronology for the pre-Columbian cultures of the Palpa valleys, south coast of Peru. Journal of Archaeological Science, 39(7), pp.2294–2303. https://doi.org/10.1016/j.jas.2012.02.021.

Urrego, D.H., Bush, M.B. and Silman, M.R., 2010. A long history of cloud and forest migration from Lake Consuelo, Peru. Quaternary Research, 73(2), pp.364–373. https://doi.org/10.1016/j.yqres.2009.10.005.

Vaughn, K.J. and van Gijseghem, H., 2007. A compositional perspective on the origins of the ‘Nasca cult’ at Cahuachi. Journal of Archaeological Science, 34(5), pp.814–822. https://doi.org/10.1016/j.jas.2006.08.008.

Veit, H., 1996. Southern Westerlies during the Holocene deduced from geomorphological and pedological studies in the Norte Chico, Northern Chile (27-33°S). Palaeogeography, Palaeoclimatology, Palaeoecology, 123, pp.107–119.

Vimeux, F., Ginot, P., Schwikowski, M., Vuille, M., Hoffmann, G., Thompson, L.G. and Schotterer, U., 2009. Climate variability during the last 1000 years inferred from Andean ice cores: A review of methodology and recent results. Palaeogeography, Palaeoclimatology, Palaeoecology, 281(3–4), pp.229–241. https://doi.org/10.1016/j.palaeo.2008.03.054.

Vuille, M., Burns, S.J., Taylor, B.L., Cruz, F.W., Bird, B.W., Abbott, M.B., Kanner, L.C., Cheng, H. and Novello, V.F., 2012. A review of the South American monsoon history as recorded in stable isotopic proxies over the past two millennia. Climate of the Past, https://doi.org/10.5194/cp-8-1309-2012.

Vuille, M. and Werner, M., 2005. Stable isotopes in precipitation recording South American summer monsoon and ENSO variability: observations and model results. Climate Dynamics, 25, pp.401–413.

Wang, X., Auler, A.S., Edwards, R.L., Cheng, H., Cristalli, P.S., Smart, P.L., Richards, D.A. and Shen, C.-C., 2004. Wet periods in northeastern Brazil over the past 210 kyr linked to distant climate anomalies. Nature, 432(7018), pp.740–743.

Wang, X., Auler, A.S., Edwards, R.L., Cheng, H., Ito, E., Wang, Y., Kong, X. and Solheid, M., 2007. Millennial-scale precipitation changes in southern Brazil over the past 90,000 years. Geophysical Research Letters, 34(23).

Weide, D.M., Fritz, S.C., Hastorf, C.A., Bruno, M.C., Baker, P.A., Guedron, S. and Salenbien, W., 2017. A ~6000 yr diatom record of mid- to late Holocene fluctuations in the level of Lago Wiñaymarca, Lake Titicaca (Peru/Bolivia). Quaternary Research (United States), 88(2), pp.179–192. https://doi.org/10.1017/qua.2017.49.

Weiss, H., 2016. Global megadrought, societal collapse and resilience at 4.2-3.9 ka BP across the Mediterranean and west Asia. Past Global Change Magazine, 24(2), pp.62–63. https://doi.org/10.22498/pages.24.2.55.

Wendt, K.A., Li, X. and Edwards, R.L., 2021. Uranium-thorium dating of speleothems. Elements, 17(2), pp.87–92. https://doi.org/10.2138/GSELEMENTS.17.2.87.

Whitney, B.S., Mayle, F.E., Punyasena, S.W., Fitzpatrick, K.A., Burn, M.J., Guillen, R., Chavez, E., Mann, D., Pennington, R.T. and Metcalfe, S.E., 2011. A 45kyr palaeoclimate record from the lowland interior of tropical South America. Palaeogeography, Palaeoclimatology, Palaeoecology, 307(1–4), pp.177–192. https://doi.org/10.1016/j.palaeo.2011.05.012.

Williams, P.R., 2002. Rethinking disaster-induced collapse in the demise of the Andean highland states: Wari and Tiwanaku. World Archaeology, 33(3), pp.361–374. https://doi.org/10.1080/00438240120107422.

Wolter, K. and Timlin, M.S., 2011. El Niño/Southern Oscillation behaviour since 1871 as diagnosed in an extended multivariate ENSO index (MEI.ext). International Journal of Climatology, 31(7), pp.1074–1087. https://doi.org/10.1002/joc.2336.

Woods, A., Rodbell, D.T., Abbott, M.B., Hatfield, R.G., Chen, C.Y., Lehmann, S.B., McGee, D., Weidhaas, N.C., Tapia, P.M. and Valero-Garcés, B.L., 2020. Andean drought and glacial retreat tied to Greenland warming during the last glacial period. Nature communications, 11(1), pp.1–7.

Yoneyama, T., Kouno, K. and Yazaki, J., 1990. Variation of natural 15N abundance of crops and soils in Japan with special reference to the effect of soil conditions and fertilizer application. Soil Science and Plant Nutrition, 36(4), pp.667–675.

Appendices

A link has been created for the data and radiocarbon application submission to be viewed. You can find this below:
https://www.dropbox.com/sh/bujgjovjt1khe56/AAD7SsKmEwym6YBIU0OEuXnea?dl=0